

Regioselective Synthesis of Polysaccharide-based Polyelectrolytes

Shu Liu

Dissertation submitted to the faculty of the Virginia Polytechnic Institute and State
University in partial fulfillment of the requirements for the degree of

Doctor of Philosophy

In

Chemistry

Kevin J. Edgar, Chair

S. Richard Turner, Co-Chair

Alan R. Esker

Maren Roman

Nov. 18, 2015

Blacksburg, VA

Keywords: polysaccharides, polysaccharide derivatives, regioselective synthesis,
polyelectrolytes, Staudinger reactions

Copyright © 2017, Shu Liu

Regioselective Synthesis of Polysaccharide-based Polyelectrolytes

Shu Liu

Abstract

Polysaccharides are one of the most abundant and diverse families of natural polymers, and have an incredibly wide range of natural functions including structural reinforcement, energy storage, aqueous rheology modification, and communication and identity. Application of native polysaccharides like cellulose as sustainable materials is limited by some inherent drawbacks such as insolubility in common solvents including water, and poor dimensional stability. To increase their functionality and utility, researchers have sought to tailor the chemical and physical properties of cellulose and other polysaccharides using a variety of chemical modification techniques, resulting in a number of important, useful commercial derivatives.

Because of their greater biocompatibility and biodegradability, and low immunogenicity, naturally derived cationic polymers including cationic polysaccharide derivatives are very attractive candidates for biomedical applications, due to the fact that they are capable of binding with anionic biomolecules, such as nucleic acids and certain proteins, via electrostatic interactions. However, there are relatively few practical synthetic methods reported for their preparation. We demonstrated a useful and efficient strategy for cationic polysaccharide salt preparation by reaction of 6-bromo-6-deoxypolysaccharides such as 6-bromo-6-deoxycellulose esters with pyridine or 1-methylimidazole exclusively at the C-6

position, resulting in high degrees of substitution (DSs). These permanently cationic polysaccharide derivatives have been demonstrated to dissolve readily in water, and bind strongly with a hydrophilic and anionic surface. Availability of these cationic polysaccharides will facilitate structure-property relationship studies for biomedical uses including drug delivery and bioelectronics applications. We also extended the chemistry, reacting 6-imidazo-6-deoxycellulose with propane sultone, leading to a new synthetic pathway to zwitterionic cellulose derivatives.

In addition to cationic and zwitterionic derivatives, we found a simple, efficient route to carboxyl-containing polysaccharide derivatives from curdlan esters via regioselective ring-opening reactions catalyzed by triphenylphosphine (Ph₃P) under mild conditions. Curdlan, a polysaccharide used by the food industry and in biomedical applications, was employed as starting material for preparing these carboxyl-containing derivatives by a reaction sequence of bromination, azide displacement and ring-opening reaction with cyclic anhydrides, affording high conversions. These modification techniques have been demonstrated to display essentially complete regio- and chemo-selectivity at C-6. These novel polysaccharide-based materials starting from abundant and inexpensive curdlan are promising for some applications such as amorphous solid dispersion (ASD) oral drug delivery.

General Audience Abstract

Polysaccharides are chains of natural sugars. They constitute one of the most abundant and diverse families of natural polymers (polymers are chains of small molecules, and polysaccharides are a class of polymers), and in nature polysaccharides play an incredibly wide range of functions such as structural reinforcement, energy storage, changing the viscosity of solutions of things in water, and communication. Cellulose, a polymer comprising long chains of linked glucose molecules, may be the most abundant natural polysaccharide on earth. Application of native cellulose as a sustainable material is limited by its inability to dissolve in water or commonly used organic solvents, poor dimensional stability, inability to melt and flow when heated, and the fact that it degrades when exposed to the environment. In order to increase its functionality and utility, a number of research groups have tried to tailor the chemical and physical properties of things made from cellulose (cellulose “derivatives”) using various chemical modification techniques, resulting in some important, useful commercial cellulose derivatives. The Edgar group, in the recent years has developed a series of new techniques to synthesize various cellulose derivatives for effective oral drug delivery. We have demonstrated that these cellulose derivatives are capable of preventing drugs from forming insoluble crystals, meanwhile protecting the drugs from the harsh environment of the stomach. As a result, these formulations based on cellulose derivatives enhance the solubility of drugs in the digestive tract, and the ability of the drug to permeate to the blood stream, thereby enhance distribution to the parts of the body where it is needed, is enhanced as well. Cellulose- and other polysaccharide-based polyelectrolytes are very attractive candidates for biomedical

and therapeutical applications. However, currently, the set of commercially available cellulose derivatives is limited in number and diversity, and contains no positively charged derivatives.

This dissertation focuses on the development of new ways to make charged polysaccharide derivatives using chemical modification of cellulose, cellulose esters, and other polysaccharides. Unlike conventional methods which require harsh reaction conditions or metal catalysts, the new approaches in this dissertation offer simple and efficient ways to make a wide variety of charged derivatives of cellulose or other polysaccharides under mild conditions. Availability of these polysaccharide-based charged polymers will help us design more useful, economical materials for biomedical, pharmaceutical, and other applications including gene or drug delivery, oral delivery of potent and selective protein drugs, agricultural applications, and coatings.

Dedication

To my beloved wife

Acknowledgments

This dissertation would not be finished without the support and help from many people who are gratefully acknowledged here.

First and foremost, I would like to thank my advisor Dr. Kevin Edgar, for his contributions of time, knowledge, patience and concern. Without his encouragement and support, I could not complete this dissertation. He is always encouraging, motivating and enlightening. His expertise in polysaccharide chemistry and other various subjects are the major reasons that I could complete a productive work in the past four years. Moreover, it is appreciated that he always patiently and kindly advised me or discussed with me, when I had questions or met difficulties.

My gratitude is also extended to my committee members, Dr. Roman, Dr. Turner and Dr. Esker for guiding my research and helping me learn new knowledge in organic chemistry, physical chemistry and polymer science. In addition, I wish to give big thanks to everyone in our lovely and joyful group: Dr. Xueyan Zheng, Dr. Joyann Marks, Dr. Xiangtao Meng, Dr. Cigdem Arca, Dr. Yifan Dong, Brittany Nichols, Chengzhe Gao, Junyi Chen, Diana Novo and Brady Hall. They provided assistance to me when I worked in the group. They were willing to share their valuable experience on research with me, and helped me practice oral presentations again and again. Finally, I would like to thank my family and friends, especially my wife. Without their support and care, I could not complete this dissertation.

Attribution

Three colleagues aided with sample characterization and another colleague aided with writing and research behind three of my chapters presented as part of this dissertation. A brief description of their contributions is included here.

Chapter 2: Dr. Kevin J. Edgar, currently a professor of Sustainable Biomaterials at Virginia Tech, served as corresponding author on this paper (*Biomacromolecules* **2015**, *16*, 2556–2571.) and helped edit writing.

Chapter 3: Jianzhao Liu, currently a Ph.D. candidate of Chemistry at Virginia Tech, served as a co-author on this paper (*Biomacromolecules* **2016**, *17*, 503–513.) and helped characterize some samples with SPR and AFM. Dr. Alan R. Esker, currently a professor of Chemistry at Virginia Tech, served as a co-author on this paper and helped analyze experimental data, and gave suggestions for writing. Dr. Kevin J. Edgar, currently a professor of Sustainable Biomaterials at Virginia Tech, served as corresponding author on this paper and helped discuss experimental data and edit writing.

Chapter 4: Dr. Kevin J. Edgar, currently a professor of Sustainable Biomaterials at Virginia Tech, served as corresponding author on this paper (*Carbohydrate Polymers* **2017**, *162*, 1–9.) and helped discuss experimental results and edit drafts.

Chapter 5: Laura I. Mosquera-Giraldo, currently a Ph.D. candidate of Industrial and Physical Pharmacy at Purdue University, measured nucleation induction times for samples. Chengzhe Gao, currently a M.S. student of Chemistry at Virginia Tech, helped test solubility of samples. Dr. Kevin J. Edgar, currently a professor of Sustainable Biomaterials at Virginia Tech, gave suggestions for writing and helped analyze and discuss experimental results.

Chapter 6: Dr. Ruoran Zhang, currently a postdoctoral researcher at National Renewable Energy Lab, served as an author on this paper (*Carbohydrate Polymers* **2017**, *171*, 1–8.) for some curdlan synthesis experimental data. Dr. Kevin J. Edgar, currently a professor of Sustainable Biomaterials at Virginia Tech, served as corresponding author on this paper and helped discuss experimental data, and edited writing.

Table of Contents

Abstract.....	II
General Audience Abstract.....	III
Dedication.....	VI
Acknowledgments.....	VII
Attribution.....	VIII
Table of Contents.....	X
Chapter 1. Dissertation Review	1
Chapter 2. Literature Review: Staudinger Reactions for Selective Functionalization of Polysaccharides.....	4
2.1 Abstract	4
2.2 Introduction	4
2.3 Staudinger reactions	8
2.3.1 Staudinger reduction.....	8
2.3.2 Staudinger ligation.....	10
2.3.2 Traceless Staudinger ligation	13
2.4 Applications of Staudinger reactions to polysaccharide functionalization	15
2.4.1 Aminated polysaccharide preparation via Staudinger reduction.....	15
2.4.2 Bioconjugate preparation via Staudinger ligation	28
2.5 Conclusions and future perspectives	40
2.6 Acknowledgement.....	42
2.7 References	43
Chapter 3. An Efficient, Regioselective Pathway to Cationic and Zwitterionic <i>N</i> -Heterocyclic Cellulose Ionomers.....	54
3.1 Abstract	54
3.2 Introduction	55
3.3 Materials and methods	58
3.3.1 Materials.....	58
3.3.2 Measurements.....	59
3.3.3 Regioselective bromination and acetylation of MCC	61
	X

3.3.4 Synthesis of 6-pyridinio-6-deoxy-2,3-di- <i>O</i> -acetyl-cellulose (6-PyrCA)	61
3.3.5 Synthesis of 6-(1-methyl-3-imidazolyl)-6-deoxy-2,3-di- <i>O</i> -acetyl-cellulose (6-MeIMCA)	62
3.3.6 Syntheses of 6-imidazolyl-6-deoxy-2,3-di- <i>O</i> -acetyl-cellulose (6-IMCA) and 6-(1-(3-sulfopropyl)-3-imidazolyl)-6-deoxy-2,3-di- <i>O</i> -acetyl-cellulose (6-SPrIMCA)	63
3.3.7 Self-assembled monolayer (SAM) preparation and surface plasmon resonance (SPR)	64
3.4 Results and discussion.....	65
3.4.1 6-Bromo-6-deoxy-2,3-di- <i>O</i> -acetyl-cellulose.....	66
3.4.2 Cationic <i>N</i> -heterocyclic cellulose derivatives	67
3.4.3 Thermal stability of cationic <i>N</i> -heterocyclic cellulose derivatives	77
3.4.4 Adsorption of cationic <i>N</i> -heterocyclic cellulose derivatives onto SAM-COOH surfaces	78
3.4.5 6-Imidazolyl-6-deoxy-2,3-di- <i>O</i> -acetyl-cellulose and 6-(1-(3-sulfopropyl)-3-imidazolyl)-6-deoxy-2,3-di- <i>O</i> -acetyl-cellulose.....	84
3.5 Conclusions	87
3.6 Supporting information	89
3.7 Acknowledgement.....	102
3.8 References	103
Chapter 4. Water-soluble Co-polyelectrolytes by Selective Modification of Cellulose Esters.....	109
4.1 Abstract	109
4.2 Introduction	110
4.3 Materials and methods	113
4.3.1 Materials.....	113
4.3.2 Measurements.....	114
4.3.3 Perpropionylation of CA320S.....	115
4.3.4 Regioselective bromination of CA320S.....	116
4.3.5 Synthesis of (6-azido-6-deoxy)- <i>co</i> -(6- <i>O</i> -acetyl)-CA320S (6-N ₃ CA320S)....	116
4.3.6 Synthesis of (6-pyridinio-6-deoxy)- <i>co</i> -(6- <i>O</i> -acetyl)-CA320S (6-PyrCA320S)	117
4.3.7 Synthesis of (6-(1-methyl-3-imidazolyl)-6-deoxy)- <i>co</i> -(6- <i>O</i> -acetyl)-CA320S (6-MeIMCA 320S).....	118
4.3.8 One pot synthesis of 6-MeIMCA320S.....	118

4.3.9 Synthesis of (6-imidazolyl-6-deoxy)- <i>co</i> -(6- <i>O</i> -acetyl)-CA320S (6-IMCA320S) and quaternization of 6-IMCA320S	119
4.4 Results and discussion.....	120
4.4.1 6-BrCA320S.....	122
4.4.2 Azide displacement	124
4.4.3 Cationic copolymer electrolytes (6-PyrCA320S and 6-MeIMCA320S) derived from 6-BrCA320S	125
4.4.4 One-Pot synthesis of 6-MeIMCA320S	127
4.4.5 6-IMCA320S and quaternization of 6-IMCA320S	128
4.4.6 Water solubility and zeta potential of 6-PyrCA320S and 6-MeIMCA320S..	132
4.5 Conclusions	133
4.6 Supporting information	135
4.7 Acknowledgements	145
4.8 References	145
Chapter 5. Selective Synthesis of Curdlan ω -Carboxyamides by Staudinger Ylide Nucleophilic Ring-opening.....	152
5.1 Abstract	152
5.2 Introduction	153
5.3 Materials and methods	156
5.3.1 Materials.....	156
5.3.2 Measurements.....	157
5.3.3 Synthesis of 6-bromo-6-deoxy-curdlan.....	158
5.3.4 Syntheses of 6-azido-6-deoxy-curdlan and 6-azido-6-deoxy-2,4-di- <i>O</i> -acetyl-curdlan	159
5.3.5 Synthesis of 6- ω -carboxypropionamido-6-deoxy-2,4-di- <i>O</i> -acetyl-curdlan ...	160
5.3.6 Synthesis of 6- ω -carboxybutyramido-6-deoxy-2,4-di- <i>O</i> -acetyl-curdlan	160
5.3.7 Nucleation induction time measurements	161
5.4 Results and discussion.....	162
5.4.1 Synthesis of 6-azido-6-deoxycurdlan via 6-bromo-6-deoxycurdlan.....	163
5.4.2 Synthesis of 6- ω -carboxypropionamido-6-deoxy-2,4-di- <i>O</i> -acetyl-curdlan ...	166
5.4.3 Synthesis of 6- ω -carboxybutyramido-6-deoxy-2,4-di- <i>O</i> -acetyl-curdlan	169

5.4.4 Crystallization inhibition properties of 6- ω -carboxypropionamido-6-deoxy-2,4-di- <i>O</i> -acetyl-curdlan and 6- ω -carboxybutyramido-6-deoxy-2,4-di- <i>O</i> -acetyl-curdlan.....	172
5.5 Conclusions	174
5.6 Supporting information	176
5.7 Acknowledgements	185
5.8 References	185
Chapter 6. Efficient Synthesis of Secondary Amines by Reductive Amination of Curdlan Staudinger Ylides.....	190
6.1 Abstract	190
6.3 Materials and methods	194
6.3.1 Materials	194
6.3.2 Measurements.....	195
6.3.4 Synthesis of 6-azido-6-deoxycurdlan.....	196
6.3.5 Synthesis of 6-azido-6-deoxy-2,4-di- <i>O</i> -acyl-curdlan.....	196
6.3.6 Syntheses of (6-amino- <i>N</i> -benzylidene/4-nitrobenzylidene/4-chlorobenzylidene/2-pyridinylmethylene)-6-deoxy-2,4-di- <i>O</i> -acetyl-curdlands	197
6.3.7 Synthesis of 6-amino- <i>N</i> -benzyl-6-deoxy-2,4-di- <i>O</i> -acetyl-curdlan	199
6.3.8 Synthesis of 6-amino- <i>N</i> -benzyl-6-deoxy-2,4-di- <i>O</i> -acetyl-curdlan by one-pot reductive amination via Staudinger ylide	200
6.3.9 Synthesis of 6-amino- <i>N</i> -benzyl-6-deoxycurdlan by one-pot reductive amination via Staudinger ylide.....	201
6.4 Results and discussion.....	201
6.4.1 Synthesis of 6-amino- <i>N</i> -benzylidene-6-deoxy-2,4-di- <i>O</i> -acyl-curdlan.....	202
6.4.2 Borohydride reduction of 6-amino- <i>N</i> -benzylidene-6-deoxy-2,4-di- <i>O</i> -acetyl-curdlan	208
6.4.3 One-pot reductive amination via Staudinger ylide.....	210
6.5 Conclusions	212
6.6 Supporting information	214
6.7 Acknowledgements	227
6.8 References	227
Chapter 7. Summary and Future Work.....	232

7.1 Syntheses of 6-pyridinio-6-deoxy-2,3-di-O-acetyl-cellulose (6-PyrCA), 6-(1-methyl-3-imidazolio)-6-deoxy-2,3-di-O-acetyl-cellulose (6-MeIMCA) and 6-(1-(3-sulfopropyl)-3-imidazolio)-6-deoxy-2,3-di-O-acetyl-cellulose (6-SPrIMCA)	232
7.2 Syntheses of water-soluble co-polyelectrolytes from commercial cellulose esters by selective modification	233
7.3 Syntheses of carboxyl-containing curdlan derivatives via regioselective ring- opening modifications.....	235
7.4 Syntheses of iminated and aminated curdlan derivatives from a Staudinger ylide	236
7.5 Proposed future work	236
7.6 References	238

Chapter 1. Dissertation Review

Sustainable materials based on natural polysaccharides have great popularity because of declining reserves of fossil fuels, global climate change, and energy and materials security. Polysaccharides, perhaps the most abundant organic polymer family on earth, constitute a large family of polymers made up of cyclic carbohydrate units, joined together through ketal or more typically acetal linkages between a hydroxyl group of one carbohydrate monosaccharide and the aldehyde or ketone group of the next monosaccharide, with the loss of one molecule of water for each linkage. Polysaccharides have in nature a variety of functions such as structural component, energy storage, aqueous rheology modification, and identity and communication. Due to their abundance, relatively low cost, renewability and biodegradability, polysaccharide materials are promising for use in areas as diverse as textiles, composite materials, drug delivery, and personal care. Billions of kilograms of polysaccharides and their derivatives are sold annually and used for numerous applications.

We demonstrated a useful and efficient strategy for preparing polysaccharide-based polyelectrolytes including cationic, zwitterionic and carboxyl-containing derivatives, from cellulose and curdlan esters by a series of regioselective reactions at the C-6 position, resulting in high DS. These modifications can be carried out with essentially perfect regio- and chemo-selectivity, and the new methodology constitutes a synthesis of novel polyelectrolytes starting from uncharged, commercial, inexpensive polysaccharide esters. These cationic polysaccharide derivatives have great potential for biomedical applications

including complexation of poly(nucleic acids) for delivery to cell nuclei, delivery of anionic drugs, and epithelial tight junction opening for oral protein delivery.

My doctoral research work in this dissertation presents a complete study on the synthesis of a series of polyelectrolytes derivatives substituted at the less hindered C-6 position for potential biomedical applications such as tight junction opening and drug delivery. Detailed spectroscopic and property analyses of those derivatives are described as well.

Chapter 2 reviews recent investigations that exploit chemical modifications such as chlorination, bromination, azide displacement and Staudinger-related reactions for effectively altering physical and chemical properties of polysaccharides in order to make them more diversely applicable.

Chapter 3 presents the synthesis of cationic polysaccharides by reaction of 6-bromo-6-deoxypolysaccharides such as 6-bromo-6-deoxycellulose esters with pyridine or 1-methylimidazole exclusively at the C-6 position, resulting in high degrees of substitution. These permanently cationic polysaccharide derivatives have been demonstrated to dissolve readily in water, and bind strongly with a hydrophilic and anionic surface. In addition, we further extended this chemistry, and reported a zwitterionic cellulose derivative by reacting 6-imidazolo-6-deoxycellulose with 1,3-propane sultone.

Chapter 4 describes the preparation of cellulose-based sustainable materials for advanced technologies, by applying phosphine-catalyzed bromination and subsequent aromatic

amine displacements to commercial cellulose esters. A commercial cellulose acetate with high DS(OH), cellulose acetate (DS(Ac) = 1.78) was selected as substrate for phosphine-catalyzed bromination, and was further functionalized by azide and aromatic amine displacements, resulting in cellulose-based *N*-containing copolymers such as polyelectrolytes.

Chapter 5 presents a simple and efficient pathway for synthesizing ω -carboxamide polysaccharide derivatives from curdlan esters via regioselective ring-opening reactions catalyzed by triphenylphosphine (Ph₃P). Curdlan, a polysaccharide used for food industry and biomedical applications, was selected as starting material for synthesizing carboxyl-containing derivatives by a reaction sequence of regioselective bromination, azide displacement, Staudinger reduction to the iminophosphorane ylide, and ring-opening reaction with cyclic anhydrides, affording high reaction conversions.

Chapter 6 reports a new approach to regioselectively substituted iminated/aminated curdlan derivatives from a Staudinger ylide. 6-Azido-6-deoxy-2,4-di-*O*-acyl-curdlan was reacted with Ph₃P, affording a highly nucleophilic iminophosphorane, which can be used to prepare 6-imino curdlans by reaction with several aromatic aldehydes, and 6-monoalkylamino curdlans by reductive amination with aromatic aldehydes in the presence of NaBH₃CN.

Chapter 7 summarizes the research results for Chapters 2-6 in this dissertation and discusses future work.

Chapter 2. Literature Review: Staudinger Reactions for Selective Functionalization of Polysaccharides

Liu S.; Edgar, K. J. *Biomacromolecules* **2015**, *16*, 2556–2571. Used with permission of American Chemical Society, 2015.

2.1 Abstract

Staudinger reactions are frequently highly chemoselective, and can occur under very mild conditions, so are attractive methods for efficient functionalization of polysaccharides. This review describes recent investigations that exploit Staudinger related reactions to effectively alter physical and chemical properties of polysaccharides, in order to make them more diversely applicable. Staudinger-related reactions, such as Staudinger reduction, Staudinger ligation, and traceless Staudinger ligation comprise a powerful family of techniques enabling preparation of a wide range of polysaccharide derivatives with excellent chemoselectivity, and the potential for excellent regioselectivity when combined with other methods. The remarkably mild conditions of the Staudinger reactions, combined with the abiotic nature of the azide group, make these reactions exceptionally attractive for modification of intact biological entities including living cells.

2.2 Introduction

Polysaccharides are a remarkably diverse, abundant family of natural polymers that perform an equally diverse assortment of natural functions including structural

reinforcement, energy storage, modification of aqueous rheology, and communication. Polysaccharides are ubiquitous: for example, cellulose, starch, hemicellulose and pectin originate primarily from plants, chitosan is mainly extracted from crustacean shells, and alginate is an important component of algae and a product of certain bacteria.^{1,2} Due to their structural and functional diversity, abundance, relatively low cost, renewable nature, and biodegradability, polysaccharide-based materials are promising for use in areas as diverse as textiles, personal care, drug delivery, and composite materials.³⁻⁵ Native polysaccharides, however, have some inherent drawbacks that limit their application. For example, although billions of kilograms of cellulose and their derivatives are sold annually and used for numerous applications, cellulose itself is difficult to apply more widely due in part to its insolubility in common solvents, poor dimensional stability, hydrophilicity, and lack of thermoplasticity.^{3,6}

Appending functional groups with new properties onto polysaccharide backbones through chemical modification is an effective way to overcome those drawbacks. If designed properly, the new derivative will preserve for the most part the desirable intrinsic properties of the natural polysaccharide.⁶ After the first chemical modification of cellulose was carried out in 1848 by Schönbein to generate cellulose nitrate, which was then used to produce the first thermoplastic polymeric material named celluloid at the Hyatt Manufacturing Company^{7,8}, chemical modification was subsequently employed to prepare various cellulose derivatives such as cellulose acetate, cellulose acetate propionate, cellulose acetate butyrate, methyl cellulose, carboxymethyl cellulose and hydroxyalkyl celluloses. So far, a variety of techniques have been demonstrated to be applicable for

effective functionalization of polysaccharides such as esterification, etherification, and reaction with isocyanates. However, most of the commonly used techniques are based principally upon reactions between nucleophiles and electrophiles, and thus cannot readily be carried out in biological systems that contain a large and diverse assortment of competing electrophiles and nucleophiles.⁹

In order to be able to better exploit the great diversity of natural, sustainable polysaccharides, we need to expand our synthetic toolkit. There is particular need for methods that are more regioselective, and more chemoselective; every polysaccharide possesses multiple functional groups (including alcohol, amine, and carboxylic acid groups, for example). Often there are multiple groups of the same type (very often alcohols), which are chemically non-equivalent, differ slightly in inherent reactivity, and all of which are relatively unreactive compared to equivalent groups on small molecules. The low reactivity usually requires more aggressive reaction conditions (temperature, duration, equivalents of reagent, powerful catalysts) which are not conducive to selectivity. Hence achieving regio- and chemoselectivity is a huge challenge in polysaccharide chemistry; these challenges must be surmounted if polysaccharide chemists are to reach their goal of designing polysaccharide derivatives precisely to deliver desired performance.

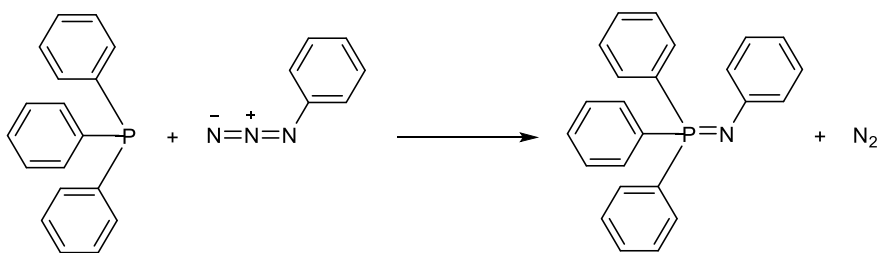
Several chemistries have been more recently applied to polysaccharide derivatization to help achieve these selectivity goals, including approaches like highly selective protection and deprotection (e.g. using trityl or hexyldimethylsilyl moieties)¹⁰⁻²¹, oxidation at the primary alcohol groups²²⁻²⁶, regioselective deacylation with tetraalkylammonium fluorides

or hydroxides^{4,27-29}, and olefin metathesis chemistry.³⁰⁻³² Among these more recent approaches, Staudinger chemistry stands out, for reasons of efficiency and mild nature upon which we elaborate in this review. Compared to other functionalization techniques, Staudinger reactions between azides and phosphines are also more suitable for biological systems, due to the fact that azide groups are absent in almost all organisms and naturally occurring compounds, and to the fact that azides only undergo reactions with a very limited number of functional group types.³³ In comparison to an amide linkage accomplished via amine related techniques such as classical peptide chemistry, azides are highly and selectively reactive to phosphines via Staudinger ligation and traceless Staudinger ligation, and azide dependent Staudinger reactions can avoid undesired side reactions that often occur between amines and other compounds in classical amide formations. In addition, due to its small size, the azide group can be introduced easily into biological samples and results in no significant increase in molecular size.³³ No need of catalyst is another attribute of Staudinger reactions, and does make Staudinger reactions preferred in biological systems, whereas the highly efficient and selective “Click Chemistry” reported by Sharpless *et al.*^{34,35} is a copper(I)-catalyzed azide-alkyne cycloaddition that is not favored for some biomedical applications such as cell encapsulation. It is, therefore, of particular interest to review Staudinger reactions between azides and phosphines and their use for selective functionalization of polysaccharides. This review covers recent studies that employed Staudinger related reactions, including Staudinger reduction, Staudinger ligation and traceless Staudinger ligation, for selective functionalization of illustrative polysaccharides for a variety of biomedical and pharmaceutical applications.

2.3 Staudinger reactions

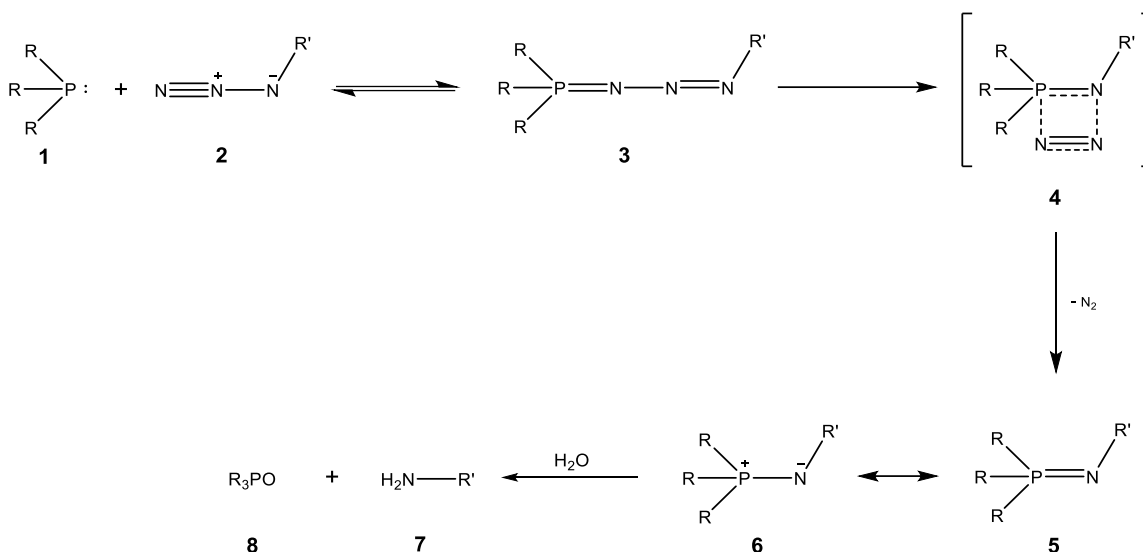
2.3.1 Staudinger reduction

In 1919, Staudinger and Meyer reported a reaction in which an azide reacts with a triaryl phosphine to generate an iminophosphorane almost quantitatively, with the loss of one molecule of nitrogen (Scheme 2.1).³⁶ This reaction proceeds under mild conditions, without formation of any byproducts besides N₂.



Scheme 2.1. Staudinger reaction between a triphenylphosphine and an azide-functionalized benzene.

In recent decades, investigators have attempted to probe in depth the mechanism of this reaction.³⁷⁻³⁹ As Scheme 2.2 shows, in a primary imination reaction triaryl phosphine (**1**) and azide (**2**) react to form a phosphazide (**3**) which decomposes during the reaction with the loss of nitrogen. The rate of the formation of phosphazide is controlled only by the inductive effects of the groups attached to the phosphorus atom and the azide, and not by steric factors. Phosphazides (**3**) are stable at room temperature in organic solvents if substituents are present that delocalize the positive charge on the phosphorus atom and/or provide steric shielding of the phosphorus atom. The final form of iminophosphorane (represented by **5** or **6**) and the loss of nitrogen are achieved via a 4-membered-ring transition state (**4**) with retention of the original configuration at phosphorus.

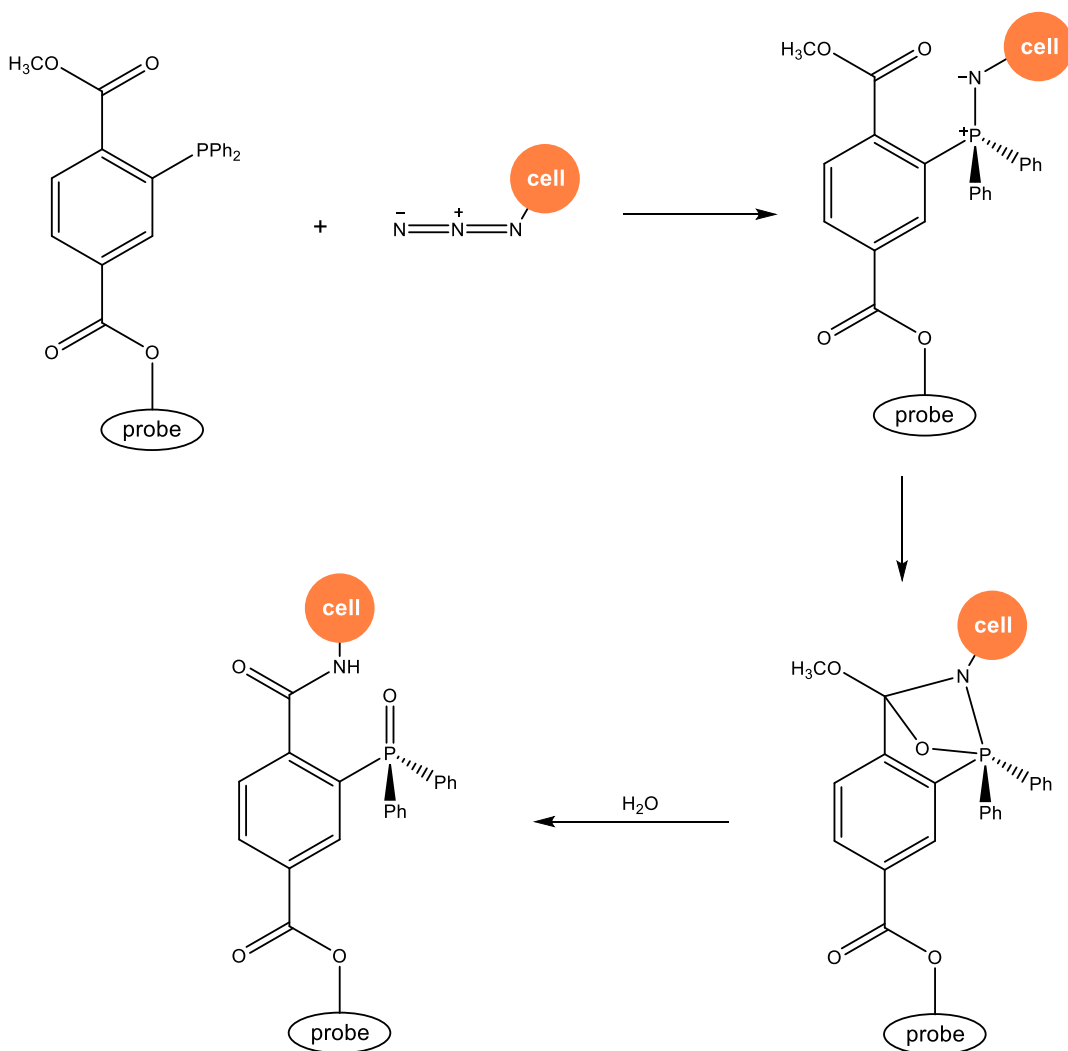


Scheme 2.2. Mechanism of Staudinger reaction between a phosphine and an azide and hydrolysis of iminophosphorane. Adapted with permission from Köhn, M.; Breinbauer, R. *Angew. Chem. Int. Ed.* **2004**, *43*, 3106-3116. Copyright 2004 Wiley-VCH Verlag GmbH & Co. KGaA, Weinheim.

The iminophosphorane possesses a highly nucleophilic negatively charged nitrogen atom. If the reaction is carried out in an aqueous solvent, the iminophosphorane (represented by **5** or **6**) is hydrolyzed rapidly to generate a primary amine (**7**) and phosphine (V) oxide (**8**). This reaction is the so-called Staudinger reduction that is frequently used to convert azides into amines. Since the iminophosphorane is so highly nucleophilic, it can react with a wide range of electrophiles. For example, Staudinger and co-workers also discovered that iminophosphorane can react not only with water to form amines, but also with aldehydes and ketones to form imines.⁴⁰ More recently, less reactive carbonyl electrophiles including amides and esters have been shown to react with iminophosphoranes, especially if the electrophiles react with iminophosphoranes in an intramolecular fashion.³³

2.3.2 Staudinger Ligation

In 2000, Saxon and Bertozzi introduced Staudinger ligation as a mild reaction between two truly bioorthogonal functionalities for the metabolic engineering of cell surfaces.⁴¹ As described above, the amine and phosphine oxide are formed in an aqueous environment by hydrolyzing the aza-ylide. Based upon previous studies, Bertozzi *et al.* prepared a ligand in which an electrophilic trap like an ester moiety is attached to the phosphine, and can capture the nucleophilic aza-ylide by intramolecular cyclization (Scheme 2.3). This reaction would result in formation of a stable amide bond before the competing aza-ylide hydrolysis occurs. Through standard esterifications or amidations, the phosphine-containing ligand is reacted with the probe to form a conjugate, which can then undergo Staudinger ligation in aqueous solution with the azide.



Scheme 2.3. Staudinger ligation for cell surface engineering. Adapted with permission from Köhn, M.; Breinbauer, R. *Angew. Chem. Int. Ed.* **2004**, *43*, 3106-3116. Copyright 2004 Wiley-VCH Verlag GmbH & Co. KGaA, Weinheim.

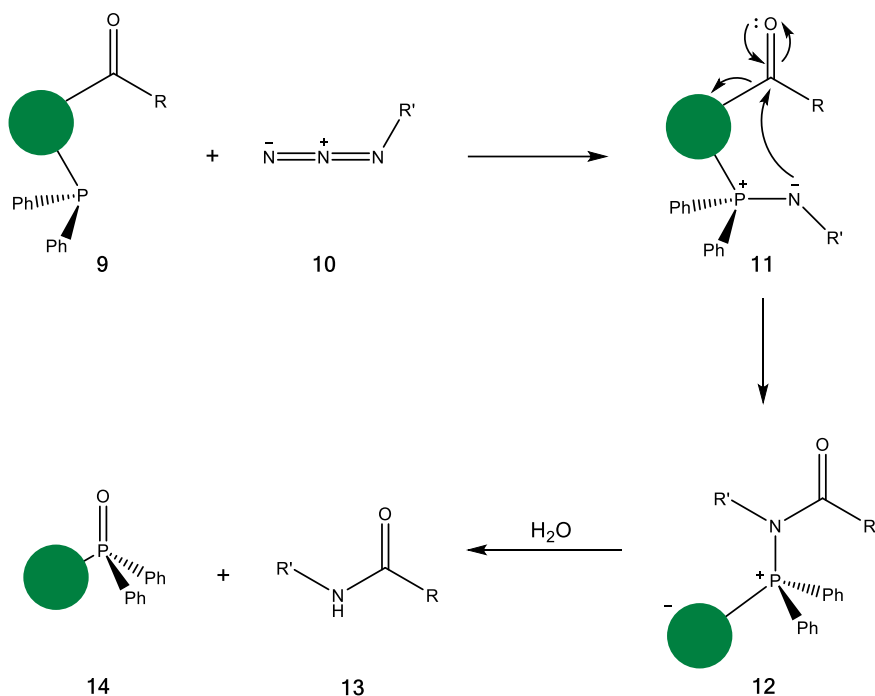
Saxon and Bertozzi employed Staudinger ligation as a mild reaction for the metabolic engineering of cell surfaces. They incubated mammalian cells with peracetylated azidoacetylmannosamine (Ac_4ManNAz), which was processed by the sialic acid biosynthetic pathway to produce azidoacetylsialic acid (Sia-NAz). Sia-NAz was then used

to form cell surface glycoconjugates.⁴¹ The azide groups on the cell surface are capable of linking with a phosphine probe, such as biotinylated phosphine⁴¹ or FLAG (Asp-Tyr-Lys-Asp-Asp-Asp-Asp-Lys) peptide-functionalized phosphine⁴², through Staudinger ligation. Such a probe, once attached to a glycoprotein on the cell surface, can be used for flow cytometry. More importantly, in comparison to conventional cell-surface ketone-hydrazine reactions, the cell-surface Staudinger ligation is superior due to the relatively high level of fluorescence generated, the abiotic nature of azides, the pH independence of the reaction, and the absence of side reactions.

In addition to cell surface engineering, chemical biologists have employed Staudinger ligations for bioconjugate preparation, in which a probe, such as a dye, label, or recognition motif, is attached to a biomolecule such as protein or nucleic acid. Bertozzi and co-workers successfully covalently coupled a fluorogenic coumarin phosphine dye to an azido-functionalized murine dihydrofolate reductase (mDHFR) via Staudinger ligation.⁴³ It is of particular interest to observe that the fluorogenic coumarin phosphine dye itself is not fluorescent, but can be activated by the azide through the Staudinger ligation. The resulting fluorescently labeled mDHFR could be directly observed, without Western blotting, washing or secondary labeling. Ju *et al.* have also reported using a fluorescein-modified phosphine to label an oligonucleotide, previously modified with an azido group at its 5' end, under Staudinger conditions to generate a fluorescein labeled oligonucleotide, which acts as a primer for producing fluorescent DNA extension fragments in a Sanger dideoxy sequencing reaction.⁴⁴

2.3.2 Traceless Staudinger Ligation

Shortly after their report of Staudinger ligation, Bertozzi and Raines modified the reaction by using a triaryl phosphine oxide moiety to act as a connector between the two coupling partners, and almost at the same time reported a more attractive ligation named traceless Staudinger ligation, in which the triaryl phosphine oxide moiety is cleaved by hydrolysis.⁴⁵⁻⁴⁸ In this reaction (Scheme 2.4), phosphines (**9**) such as 2-diphenylphosphanylphenol and diphenylphosphanylmethanethiol are acylated, then the phosphine moiety is reacted with an azide (**10**) to form an aza-ylide intermediate (**11**). The nucleophilic nitrogen atom of this intermediate attacks the carbonyl group, transferring the acyl from *O* or *S* to *N* and forming an amide (**12**). Finally, amides (**13**) and phosphine oxides (**14**) are produced by hydrolysis with water. The net result is reduction of the original azide to amine and ligation with the original acyl group to form an amide.

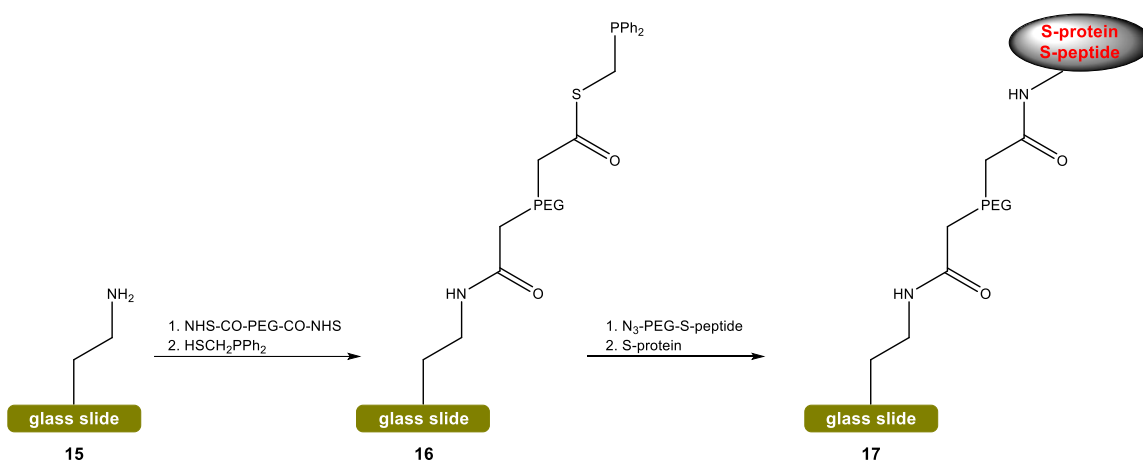


Scheme 2.4. Mechanism of traceless Staudinger ligation. Adapted with permission from Köhn, M.; Breinbauer, R. *Angew. Chem. Int. Ed.* **2004**, *43*, 3106-3116. Copyright 2004 Wiley-VCH Verlag GmbH & Co. KGaA, Weinheim.

Traceless Staudinger ligation has been employed as a peptide ligation reaction for total synthesis of proteins. Raines and co-workers reported that *N*-acetylglycine is capable of smoothly coupling with azido functionalized amino acids to give various dipeptides via traceless Staudinger ligations, affording very good yields and no epimerization.⁴⁵ Raines *et al.* also completed the total synthesis of ribonuclease A (RNase A) containing 124 amino acids by linking three fragments using traceless Staudinger ligations.⁴⁹

Due to its high chemoselectivity and the fact that phosphorus-containing moieties are not appended to the final product, traceless Staudinger ligation is favored as an immobilization

technique for protein microarray preparation. As Scheme 2.5 shows, Raines *et al.* covalently attached a thiol-containing phosphine (HSCH₂PPh₂) to an aminopropylsilane-functionalized glass slide (**15**) which was previously modified with a bifunctional polyethyleneglycol (PEG) spacer (NHS-CO-PEG-CO-NHS), resulting in a phosphanyl thioester formation (**16**) on the glass slide. Subsequently, an azide-functionalized S-peptide (residues 1-15 of RNase A) (N₃-PEG-S-peptide) was ligated to the slide via traceless Staudinger ligation.⁵⁰ The array was finally formed after incubation with S-protein (residues 21-124 of RNase A) (**17**), enabling assays based upon ribonucleolytic activity and immunostaining.



Scheme 2.5. Protein microarray prepared through traceless Staudinger ligation. Adapted with permission from Soellner, M. B.; Dickson, K. A.; Nilsson, B. L.; Raines, R. T. *J. Am. Chem. Soc.* **2003**, *125*, 11790–11791. Copyright 2003 American Chemical Society.

2.4 Applications of Staudinger reactions to polysaccharide functionalization

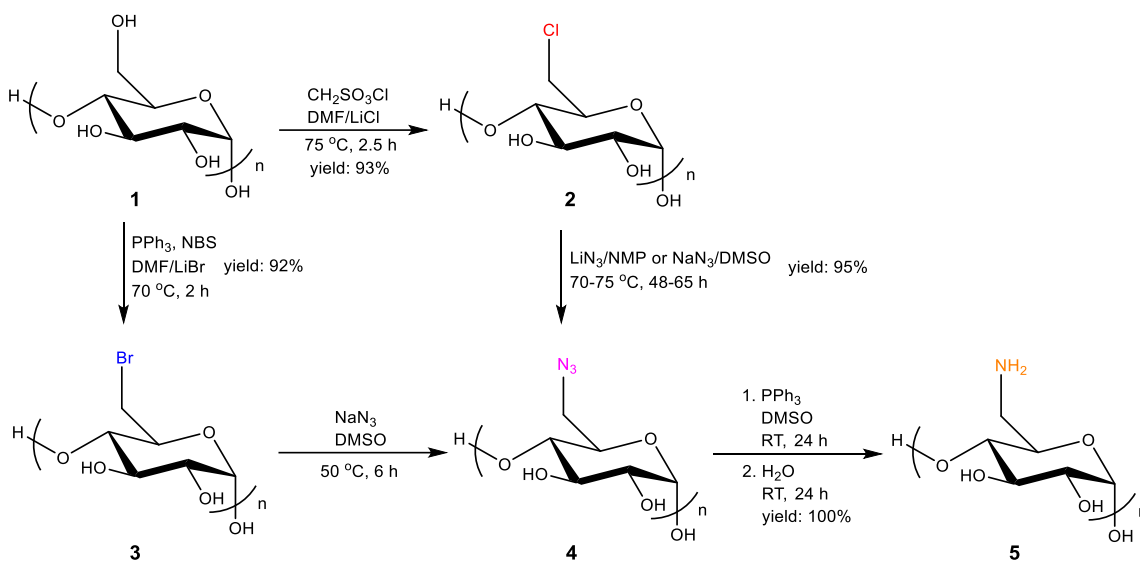
2.4.1 Aminated polysaccharide preparation via Staudinger reduction

Polysaccharides containing amine functional groups are of interest due to properties that may be beneficial to a wide range of biomedical and pharmaceutical applications. Natural amine-containing polysaccharides like chitosan are capable of electrostatically binding or encapsulating anionic compounds such as proteins and nucleic acids, and may act as delivery carriers that protect certain nucleic acids and proteins from enzymes in biological systems.⁵¹⁻⁵³ It has been reported that chitosan has potential to be a low toxicity carrier to deliver poly(nucleic acids) and anionic drugs as polyelectrolyte complexes for gene therapy.⁵⁴

To mimic the biomedical properties of chitosan and avoid potential issues with chitosan such as protein impurities and lack of structural control, polysaccharide chemists began to modify some neutral polysaccharides including cellulose, curdlan and pullulan with amino groups, via chemical attachment of amine-containing side chains to the polysaccharide backbone. It has been demonstrated that these modified polysaccharides were able to effectively encapsulate nucleic acids and improve the transfection efficiency into model cells.⁵⁵⁻⁶⁰ Amine groups can also be introduced into polysaccharides by a reaction sequence resulting in overall substitution of polysaccharide primary hydroxyl groups by an amine. This approach involves first tosylating or halogenating the polysaccharide, then reacting the resulting intermediate compound with an azide salt, and finally reducing the azide to an amine. Although these transformations involve more than one step, one of the merits of this approach is that all reactions are regioselective, preferentially occurring at primary hydroxyl groups, and thus result in regioselectively substituted aminated polysaccharide derivatives such as 6-amino-6-deoxy-cellulose.⁶¹ In the case of bromination, it can be

essentially perfectly regioselective for polysaccharides containing a free 6-hydroxymethylene group (e.g. cellulose, amylose, chitin).⁶²⁻⁶⁷

Among various azide reduction reactions, Staudinger reduction is one of the most useful approaches to introduce amine groups onto polysaccharides. The Kaplan group first prepared 6-amino-6-deoxy-amylose from amylose under Staudinger conditions.⁶⁸ As Scheme 2.6 shows, amylose (**1**) is a natural and mostly linear polysaccharide composed of D-glucopyranose residues linked via α -(1 \rightarrow 4)-glycosidic linkages.⁶⁹ Kaplan *et al.* directly halogenated amylose at the C-6 position either by using methanesulfonyl chloride in dimethylformamide (DMF)/lithium chloride (LiCl), resulting in 6-chloro-6-deoxy-amylose (**2**), or using PPh₃ and *N*-bromosuccinimide (NBS) in DMF/lithium bromide (LiBr), affording 6-bromo-6-deoxy-amylose (**3**). 6-Halo-6-deoxy-amyloses (**2** and **3**) were then converted to the corresponding 6-azido-6-deoxy-amylose (**4**) by quantitatively chloride or bromide displacement with an azide ion in dipolar aprotic media such as *N*-methyl-2-pyrrolidone (NMP) or dimethylsulfoxide (DMSO). Subsequent Staudinger reduction with PPh₃ in DMSO was employed to completely reduce the azide groups at room temperature, resulting in 6-amino-6-deoxy-amylose (**5**) in 100 % yield with 100% conversion. Moreover, it was found that the 6-amino-6-deoxy-amylose obtained from 6-chloro-6-deoxy-amylose has the same high amine degree of substitution (DS) as that obtained from 6-bromo-6-deoxy-amylose (displacement was quantitative).



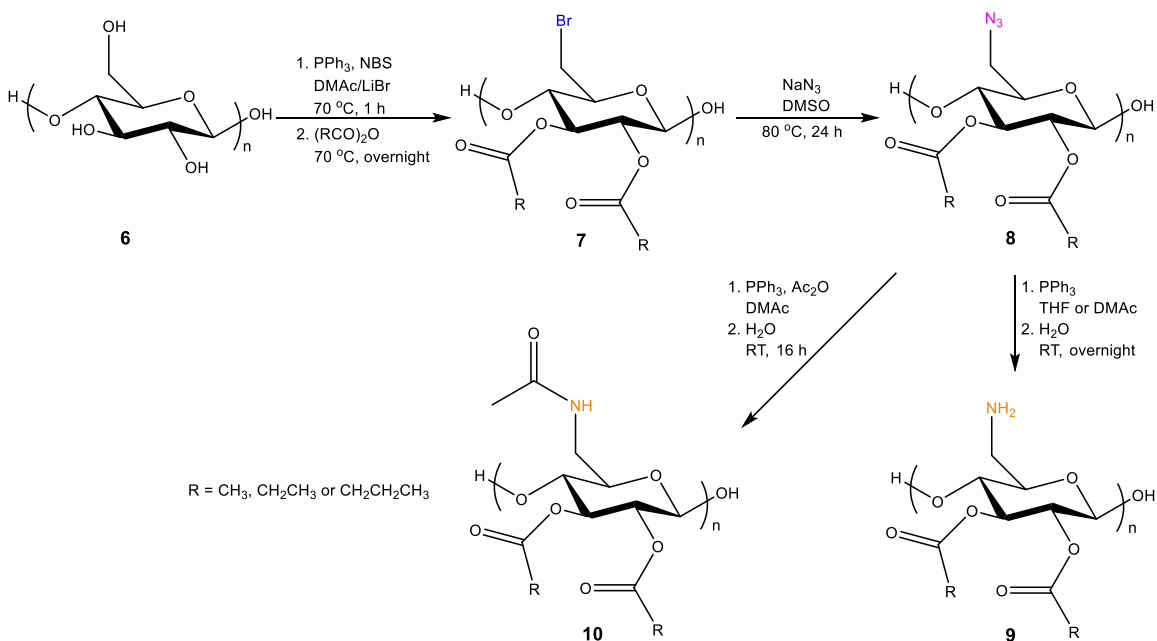
Scheme 2.6. Syntheses of 6-amino-6-deoxyamylose via Staudinger reduction. Adapted with permission from Cimecioglu, A. L.; Ball, D. H.; Kaplan, D. L.; Huang, S. H. *Macromolecules* **1994**, *27*, 2917–2922. Copyright 1994 American Chemical Society.

Aminated polysaccharides are often further modified to append other important functionality that can satisfy the requirements of specific biomedical applications. For example, additional modifications of aminated polysaccharides can alter the solubility in water or organic solvents, attach ligands for targeting a particular cell type, or improve the affinity for a particular encapsulated compound.⁷⁰⁻⁷² Most of these additional modifications involve esterification, due to the prevalence of hydroxyl groups along the polysaccharide backbone and the relatively mild conditions necessary for esterification. It is a problem to modify the hydroxyls of polysaccharides that bear both amino and hydroxyl groups, due to the higher nucleophilicity of amines. The *N*-phthaloyl protecting group has been used to protect chitosan amino groups, allowing selective esterification at the hydroxyl groups.⁷³ However, deprotection can be problematic; for example, phthalimide deprotection with

hydrazine could result in the cleavage of esters or other easily removable groups linked at the hydroxyl sites, and could cause chitosan molecular weight degradation. An alternative approach is to first acylate azide-containing polysaccharides, then chemoselectively reduce the azide to an amine. In this approach, the azide can act as a latent protected amine. It is potentially challenging to find a reducing reagent that can selectively reduce azide to amine, in the presence of readily reduced ester linkages. Commonly used reducing reagents like lithium aluminum hydride (LiAlH₄) can convert azide groups into amines, but also react with a variety of reducible functional groups including esters.^{74,75} A suitable reducing reagent for this selective transformation was lacking until Daly and Lee demonstrated the use of 1,3-propanedithiol to selectively reduce the azide moieties of 6-azido-6-deoxy-cellulose esters, while retaining the ester functionalities.⁷⁶ However, although 1,3-propanedithiol reduction results in the desired selectivity, only a small proportion of the azide groups were reduced to free amines.

In comparison to other azide reduction reactions, Staudinger reduction is the most suitable method for reducing azide to amine while retaining ester groups on polysaccharides, due to its high chemoselectivity and mild reaction conditions. The Edgar group first prepared 6-azido-6-deoxy-2,3-di-*O*-acyl-cellulose from cellulose, and successfully selectively reduced the azide groups through a Staudinger reduction.⁷⁷ Cellulose (**6**), one of the simplest polysaccharides, is a linear polymer consisting of single D-glucopyranose monosaccharides, with no branching or substituents in nature, composed of D-glucopyranose units with β -(1 \rightarrow 4)-anomeric linkages. Each anhydroglucose unit (AGU) possesses one primary hydroxyl group at the C-6 position and two secondary hydroxyl

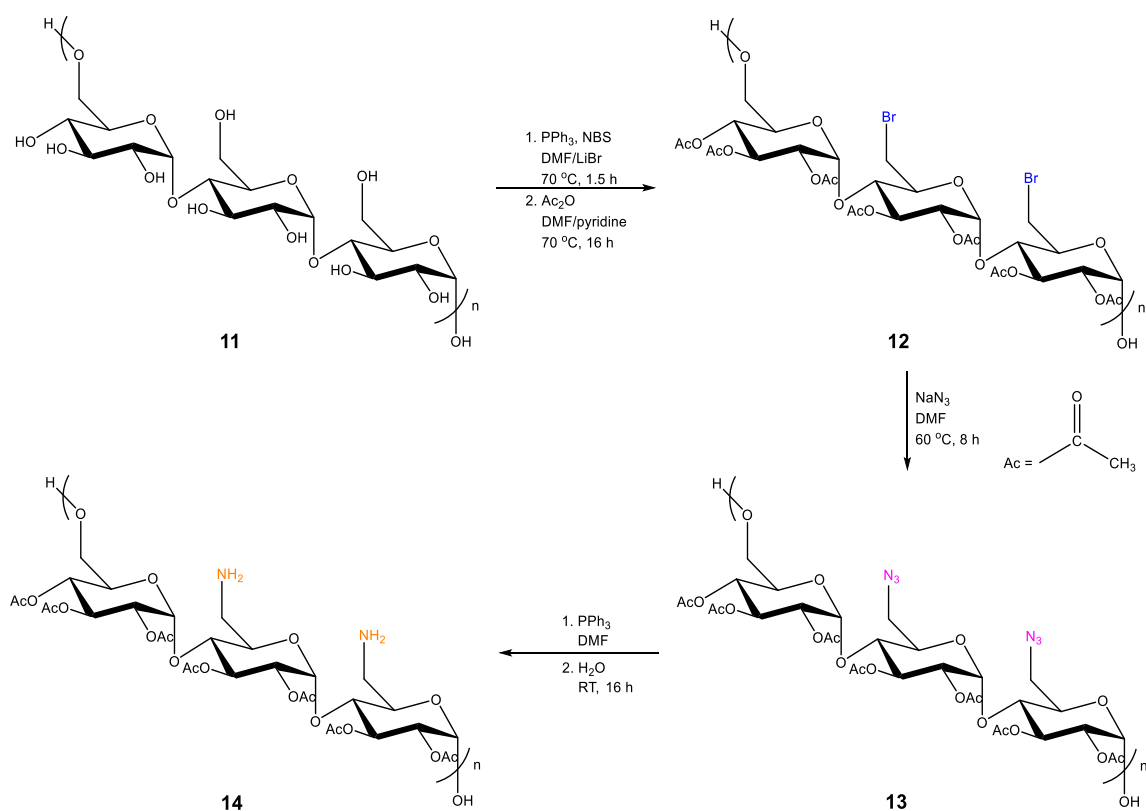
groups at the C-2 and C-3 positions. As Scheme 2.7 shows, Edgar *et al.* modified cellulose with PPh₃ and NBS in *N,N*-dimethylacetamide (DMAc)/LiBr, followed by peracylation, affording 6-bromo-6-deoxy-2,3-di-*O*-acyl-cellulose (**7**). The bromoester was then transformed to 6-azido-6-deoxy-2,3-di-*O*-acyl-cellulose (**8**) by quantitatively bromide displacement with azide ion in DMSO. The azide group at the C-6 position was finally converted into an amine in tetrahydrofuran (THF) or DMAc using a Staudinger reduction under mild conditions (room temperature and atmospheric pressure), in the presence of water, with little or no loss of esters at the C-2 and C-3 positions. The product, 6-amino-6-deoxy-2,3-di-*O*-acyl-cellulose (**9**), possesses a regioselectively substituted free amine and selectively acylated hydroxyl groups. This approach represents a substantial improvement over previous efforts to synthesize *O*-acyl-6-amino-cellulose derivatives, due to shorter reaction times and very high regioselectivity. It should be noted that, reminiscent of traceless Staudinger ligations, the anionic aminophosphorane ylide intermediate may tend to attack the ester carbonyls, causing acyl transfer to *N* to form an amide. Such acyl transfer reactions can be avoided by carrying out the Staudinger reduction in the presence of a carboxylic acid anhydride such as acetic anhydride; the anhydride reacts with the negatively charged nitrogen of the Staudinger ylide, thereby forming an amide (**10**) at C-6 whose acyl group may be either the same as those of the 2,3-*O*-esters, or different, depending on the choice of anhydride used. The ability to carry out Staudinger reduction successfully even in the presence of a reactive species like a carboxylic acid anhydride is striking evidence for its mild and chemoselective nature.



Scheme 2.7. Conversion of cellulose to 6-amino or amido-6-deoxycellulose esters.

After 6-amino-6-deoxycellulose derivative preparation using Staudinger reduction, Edgar *et al.* extended the use of Staudinger reduction to the bacterial exopolysaccharide pullulan.⁷⁸ As Scheme 2.8 shows, pullulan (**11**) is a linear polysaccharide of D-glucose monosaccharides, with exclusive α -linkages between the monosaccharides and no branching or substituents. Unlike those of amylose or cellulose, the repeating unit of pullulan is maltotriose trisaccharide, linked α -(1 \rightarrow 6), resulting in a 2:1 proportion of α -(1 \rightarrow 4) to α -(1 \rightarrow 6) linkages in the polysaccharide. They began the synthesis with regioselective bromination of pullulan at C-6 by reaction with NBS and PPh₃ in DMF/LiBr, producing 6-bromo-6-deoxy-pullulan. In contrast to the rigid rod, poorly soluble 6-bromo-6-deoxy-cellulose, brominated pullulan was found to have good organic solubility, and is thus a useful intermediate for further reactions. 6-Bromo-6-deoxy-pullulan esters (**12**) were obtained in a one-pot method (bromination/acylation in one pot) by peracylation of 6-

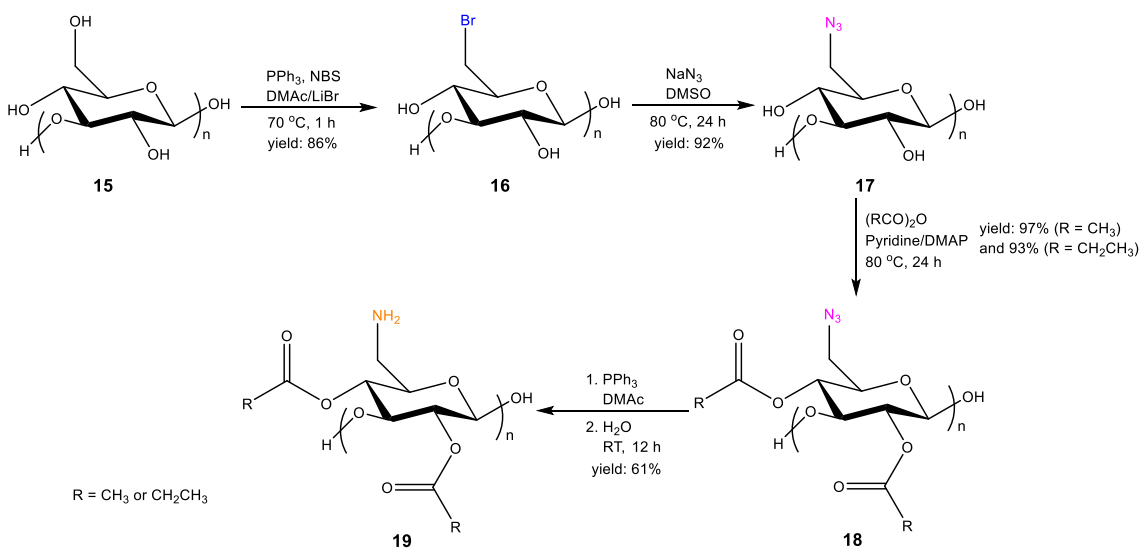
bromo-6-deoxy-pullulan with a carboxylic anhydride (e.g. acetic anhydride). Bromide from 6-bromo-6-deoxy-pullulan esters was displaced by azide, providing the corresponding 6-azido-6-deoxy-pullulan esters (**13**). Finally, the azide was efficiently and chemoselectively reduced to an amino group through Staudinger reduction in DMF at room temperature, resulting in 6-amino-6-deoxy-pullulan esters (**14**).



Scheme 2.8. Conversion of pullulan to 6-amino-6-deoxy-2,3,4-*O*-acetyl-pullulan.

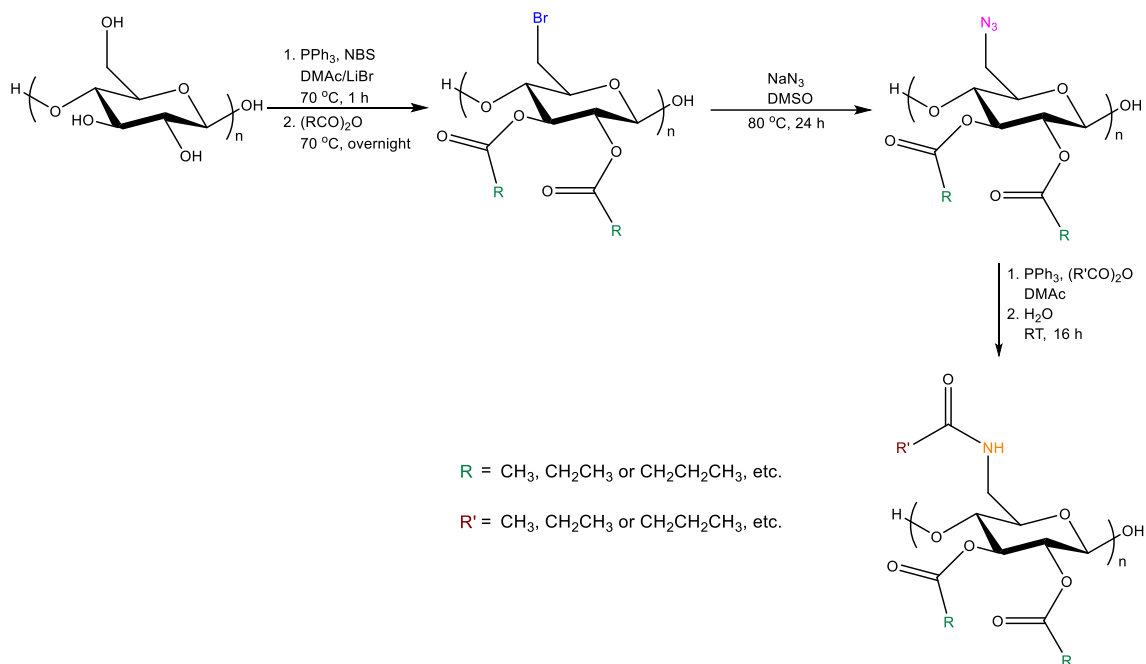
Furthermore, based on the success on cellulose and pullulan, Edgar *et al.* prepared *O*-acetylated 6-amino-6-deoxy-curdlan using a similar approach under Staudinger conditions.⁷⁹ Curdlan is a bacterial, helical polysaccharide generated from a mutant bacterium and was first discovered by Harada and co-workers in 1966.^{80,81} As Scheme 2.9 shows, curdlan (**15**)

is a linear homopolymer of D-glucose monosaccharides covalently bonded via β -(1 \rightarrow 3) linkages (Scheme 2.9).⁸² Edgar *et al.* brominated curdlan in DMAc/LiBr using PPh₃ and NBS, affording 6-bromo-6-deoxy-curdlan (**16**). Similar to 6-bromo-6-deoxy-pullulan, 6-bromo-6-deoxy-curdlan is soluble in common organic solvents. 6-Bromo-6-deoxy-curdlan was converted to the 6-azido derivative (**17**) by nucleophilic substitution with sodium azide (NaN₃), following with peracylation with carboxylic anhydride such as acetic anhydride or propionic anhydride in the presence of pyridine and 4-dimethylaminopyridine (DMAP). The product 6-azido-6-deoxy-2,3-di-*O*-acyl-curdlan (**18**) finally was chemoselectively and quantitatively reduced to 6-amino-6-deoxy-2,3-di-*O*-acyl-curdlan (**19**) under Staudinger conditions (PPh₃, H₂O, DMAc, room temperature), with no spectroscopic evidence of incompleteness or side reactions.

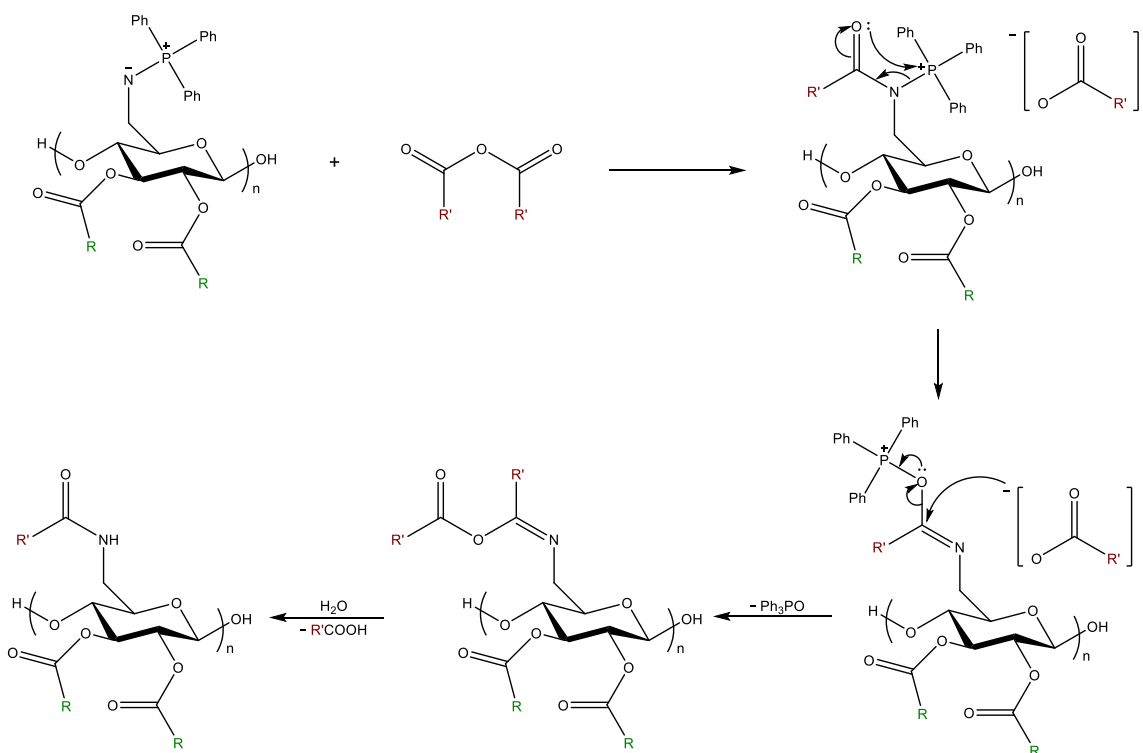


Scheme 2.9. Conversions of curdlan to 6-amino-6-deoxy-2,4-di-*O*-acyl-curdlan.

However, *O*-acylated 6-amino-6-deoxypolysaccharide derivatives of cellulose, pullulan and curdlan generally appeared to have poor solubility in both water and organic solvents. To enhance solubility for some specific biomedical applications, Edgar *et al.* reported a modified approach for the selective *N*-acylation of the aminated cellulose, providing an efficient and convenient route (only three isolations from natural cellulose, no protecting groups) for the synthesis of 6-amido-6-deoxycellulose-2,3-*O*-esters in which the acyl groups on *N*- and *O*- may be selected separately. As Schemes 2.10 and 2.11 show, the 6-azido-6-deoxy-2,3-di-*O*-acyl-cellulose was reduced by a Staudinger reduction under anhydrous conditions in the presence of carboxylic anhydrides, which afforded organic-soluble 6-amido-6-deoxy-2,3-di-*O*-acylcellulose derivatives with > 93% reaction conversion.⁷⁷ Again, remarkably the Staudinger conditions are so mild that even the highly reactive anhydrides were not consumed by the reducing agent, and thus were available for reaction with the aza-ylide intermediate as it formed. This modified approach was applied to curdlan and pullulan as well, and generated 6-amido-6-deoxy-2,3-di-*O*-acylcurdlan derivatives and 6-amido-6-deoxy-2,3,4-*O*-acylpullulan derivatives, respectively.^{78,79} More importantly, it has been demonstrated that the 6-amido-6-deoxy-2,3-di-*O*-acylpolysaccharide derivative has improved solubility in comparison with the 6-amino-6-deoxypolysaccharides and their *O*-esters.



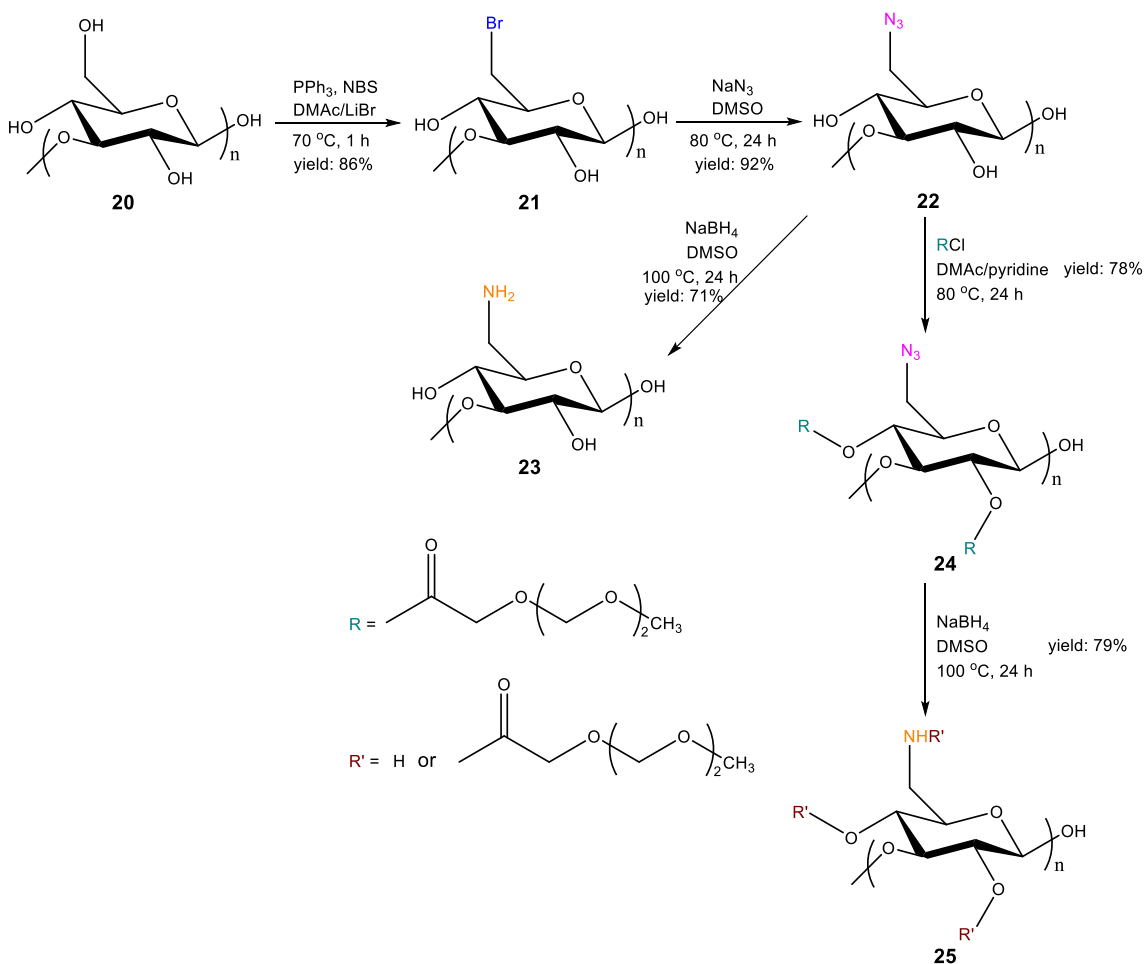
Scheme 2.10. Synthesis of 6-amido-6-deoxy-cellulose esters.



Scheme 2.11. Proposed mechanism for the *N*-acylation of 6-iminophosphorane-6-deoxy-cellulose esters.

Based upon previous studies of aminated polysaccharides prepared by Staudinger reductions, it has been observed that most of the 6-amino-6-deoxypolysaccharide derivatives so produced reductions exhibit poor water and organic solubility, probably due to small amounts of phosphine-containing residues and/or phosphine oxide byproduct. The poor solubility greatly limits the further use of these aminated polysaccharide derivatives. Therefore, a clean separation of product from phosphine-containing residual reagent and phosphine oxide byproduct is needed, to improve product solubility. Boons *et al.* used trimethylphosphine (PMe₃) instead of PPh₃ as a reductant, and employed Staudinger reduction for preparing a well-defined heparan sulfate hexasaccharide for investigation of structure-activity relationships.⁸³ As a consequence, the product from Staudinger reduction was easily isolated in pure form, due in part to the fact that gaseous PMe₃ possesses better solubility and is more easily removed than PPh₃. In another approach, in order to improve the solubility of 6-amino-6-deoxy-curdlan, the Edgar group recently reported a non-Staudinger protocol in which 6-azido-6-deoxy-curdlan was reduced by sodium borohydride (NaBH₄) under mild conditions, affording water-soluble aminated curdlan derivatives with very high regioselectivity.⁸⁴ As Scheme 2.12 shows, Edgar *et al.* brominated curdlan (**20**) using PPh₃ and NBS in DMAc/LiBr, and displaced the bromide using NaN₃ in DMSO, affording 6-azido-6-deoxy-curdlan (**22**). It is of particular interest to find that the final product 6-amino-6-deoxy-curdlan (**23**) (DS(NH₂) = 0.95) generated from 6-azido-6-deoxy-curdlan by NaBH₄ reduction exhibited good solubility in water and some common organic solvents, as opposed to the water insolubility observed for the Staudinger reduction product of the same azide. Based upon the successful transition from

6-azido to 6-amino through NaBH₄ reduction, the Edgar group further developed a similar method to yield another water-soluble curdlan derivative. After initial bromination of curdlan and azide displacement of the bromide, hydrophilic and non-charged 3,6,9-trioxodecanoate (TOD) groups appended by *O*-acylation at the C-2 and C-4 positions of curdlan in the presence of DMAc and pyridine, affording 6-azido-2,4-di-*O*-TOD-curdlan (**24**); the 6-azido group was then reduced to the 6-amine by NaBH₄. Additionally, it is interesting to find that upon NaBH₄ reduction of the 6-azido group to the 6-amine, TOD group migration occurred, along with concomitant reduction of residual ester groups, providing the *N*-TOD amide (**25**), which is also water soluble. Therefore, borohydride reduction can be a suitable method for preparing water-soluble aminocurdlan derivatives, since it involves no phosphine containing reagents or byproducts. However, this example also illustrates the disadvantages of borohydride reduction, since it is not sufficiently selective to reduce azides while preserving esters from reduction. In addition, it cannot be used in the presence of anhydrides, so the amines cannot be trapped *in situ* as amides; this inability thereby promotes *O* to *N* acyl migration. These water-soluble, regioselectively substituted curdlan derivatives are helpful for investigations of structure-property relationships for biomedical applications.

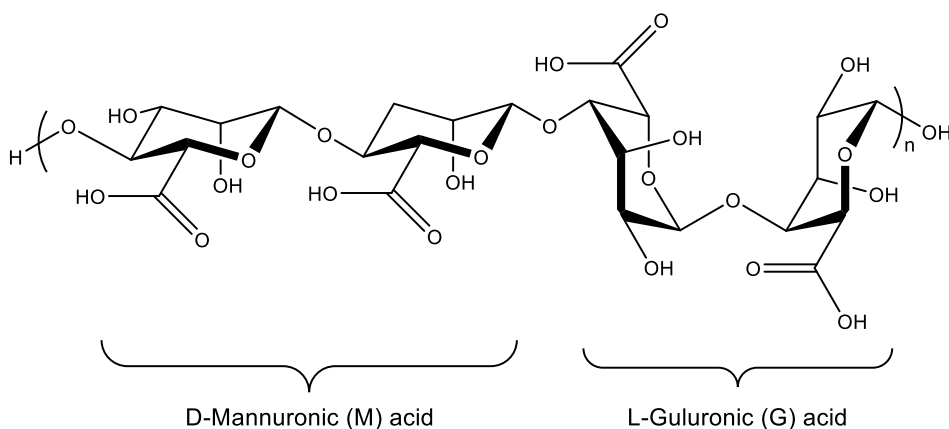


Scheme 2.12. Syntheses of 6-amino-6-deoxycurdlangs using NaBH₄.

2.4.2 Bioconjugate preparation via Staudinger ligation

Being biocompatible, efficient, chemoselective, and catalyst free, the recently introduced Staudinger ligation has been used for numerous biological applications, from cell surface modification to protein detection. However, compared to Staudinger reductions, there are few examples of Staudinger ligation for modifying polysaccharides other than alginate. Alginate, also known as alginic acid, is one of the most popular polysaccharides for biomedical applications, because of its desirable physiochemical properties and high biocompatibility. Alginate is a linear polysaccharide comprising D-mannuronic (M) and

L-guluronic (G) acids, with entirely β -(1 \rightarrow 4) linkages (Scheme 2.13). Each alginate monosaccharide possesses two secondary hydroxyl groups at C-2 and C-3, and one carboxyl group at C-6. Partial hydrolysis studies reveal that alginate is made up of blocks of M, blocks of G, and mixed M-G blocks. Particularly, alginate solutions are capable of forming hydrogels via ionic cross-linking with divalent cations such as Ca^{2+} or Ba^{2+} , and these cross-linked alginate hydrogels have been prepared in various sizes and shapes for diverse applications.⁸⁵ Notably this ability to gel under very mild conditions (neutral pH, room or physiological temperature) allows alginate to be used to encapsulate living cells, such as islets of Langerhans for treatment of Type 1 diabetes.⁸⁶ Alginate chemical modifications have been pursued for a variety of applications, since the carboxylic groups and hydroxyl groups in alginate provide sites for chemical modification.^{87,88} The most common motivation for alginate modification is to improve the durability of alginate hydrogels via covalent cross-linking of alginate chains, either independently of or in addition to ionic crosslinking.



Scheme 2.13. Molecular structure of alginate showing β -(1 \rightarrow 4) linkages.

To improve the stability of alginate hydrogels without losing their desirable properties, Stabler *et al.* used azide-functionalized alginate as a novel platform for the chemoselective crosslinking of complimentary agents via biologically favored Staudinger ligations.⁸⁹ As Figure 2.1 shows, in the presence of *N*-hydroxysuccinimide (NHS) and 1-ethyl-(dimethylaminopropyl)carbodiimide hydrochloride (EDC), alginate-PEG-azide (**28**) was prepared by conjugation between alginate carboxylic groups (**26**) and an amine group of a PEG whose other end had an azide end group (**27**), to afford a product which then formed hydrogel beads (**A**) with Ba²⁺ via ionic interactions. The azide groups of alginate-PEG-azide hydrogel beads (**A**) can also act as platforms for the covalent linkage of methyl-2-(diphenylphosphino)terephthalate (MDT)-functionalized bioactive or labeling agents via Staudinger ligation. Stabler *et al.* used an MDT-functionalized carboxyfluorescein agent (**29**) to conjugate with alginate-PEG-azide hydrogel beads (**A**) in Dulbecco's phosphate buffered saline (DPBS) at 37 °C via Staudinger ligation, resulting in up to 40% of the azide groups on alginate-PEG-azide (**28**) reacted with MDT groups on MDT-functionalized carboxyfluorescein agent (**29**). The resulting fluorescent hydrogel beads (**30** or **C**) studied by confocal microscopy exhibit good stability and have potential for use in *in vivo* monitoring. In addition, Stabler *et al.* used difunctional PEG polymers with complementary MDT groups (**31**) that are able to cross link with azide functionalized PEG-alginate (**29**) via Staudinger ligation, affording 9-12% of the azide groups were functionalized, suggesting that the resulting polymers (**32**) are capable of forming highly stable hydrogels (**B**) through strong covalent bonds.

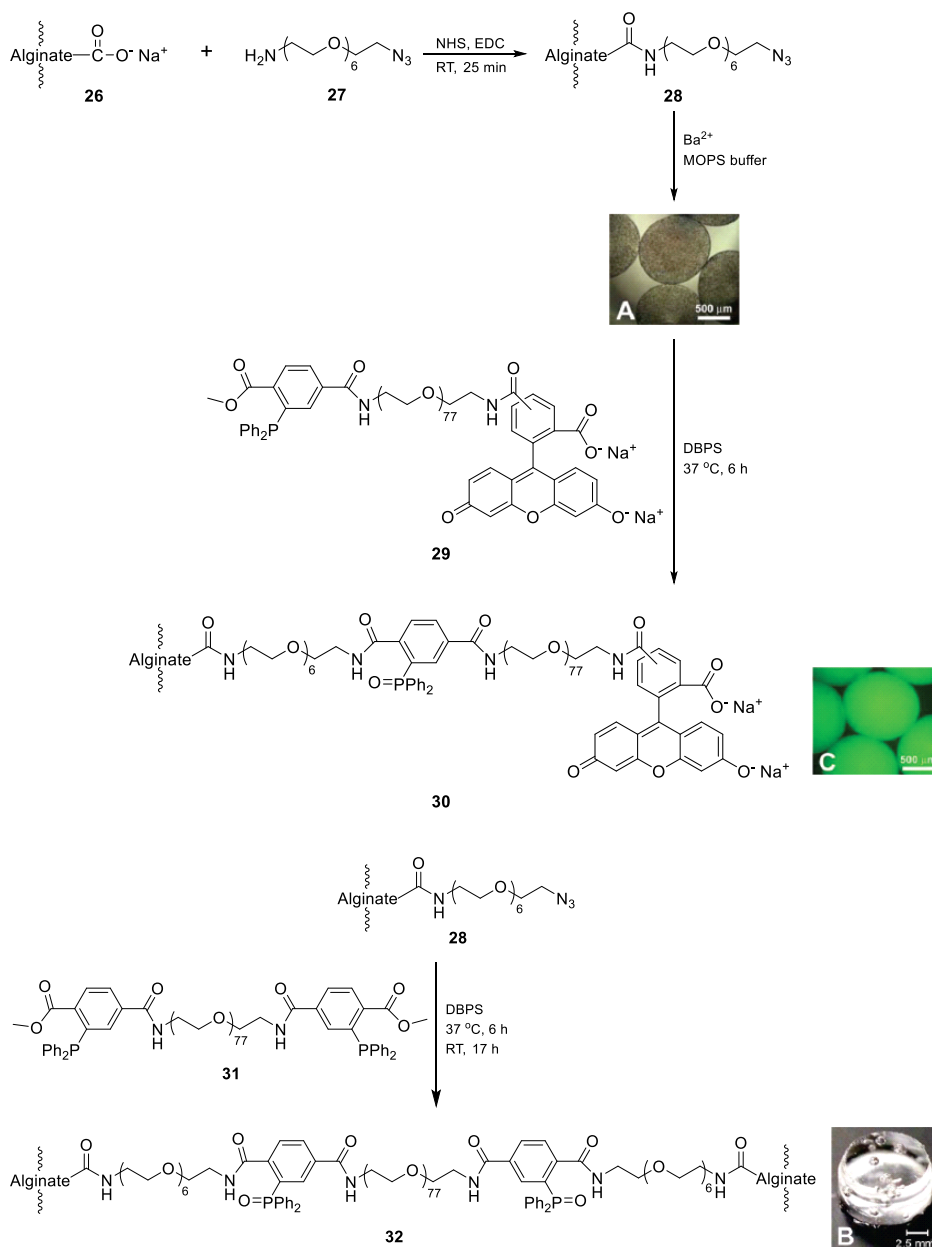


Figure 2.1. Alginate-PEG- N_3 can form gels via divalent ion (e.g., Ba^{2+}) cross-linking, or via incubation with MDT-PEG-MDT under Staudinger conditions. The gels formed with Ba^{2+} can be further functionalized with MDT-labeled agents like MDT-PEG-carboxyfluorescein. Adapted with permission from Gattás-Asfura, K. M.; Stabler, C. L. *Biomacromolecules* **2009**, *10*, 3122–3129. Copyright 2009 American Chemical Society.

After the report of alginate hydrogels modified by Staudinger ligation, Stabler and co-workers fabricated ionically and covalently crosslinked alginate-PEG microbeads for islet microencapsulations using ionic interaction and Staudinger ligation.⁹⁰ As Figure 2.2 shows, azide-functionalized alginate (**33**) and MDT-terminated PEG (**34**) were pre-incubated for 1 h and 15 min at 37 °C prior to Ba²⁺ addition. This pre-incubation allowed initially covalent linkage between azide-functionalized alginate and MDT-terminated PEG by Staudinger ligation, and avoided significant leakage of MDT-terminated PEG during crosslink between azide-functionalized alginate and Ba²⁺, resulting in pre-mixed alginate-PEG (**35**). After Ba²⁺ was added into pre-mixed alginate-PEG, ionically crosslinked alginate-PEG (**36**) was formed due to crosslink between Ba²⁺ and azide-functionalized alginate. The final ionically and covalently crosslinked alginate-PEG microbeads (**37**) were generated by further incubation between the two polymers through Staudinger ligation. The resulting crosslinked alginate-PEG microbeads exhibit greater resistance to osmotic swelling than conventional barium crosslinked alginate beads. Based upon diffusion and porosity studies, crosslinked alginate-PEG beads have permeability properties comparable to those of conventional barium crosslinked alginate beads. More importantly, crosslinked alginate-PEG beads exhibit excellent cellular compatibility with insulinoma cell lines, and rat and human pancreatic islets, where the viability and functional assessment of cells within crosslinked alginate-PEG beads are comparable with those of barium crosslinked alginate bead controls. Due to their enhanced stability and high cellular compatibility, the crosslinked alginate-PEG hydrogels prepared by Staudinger ligation are promising materials for a wide variety of tissue engineering applications.

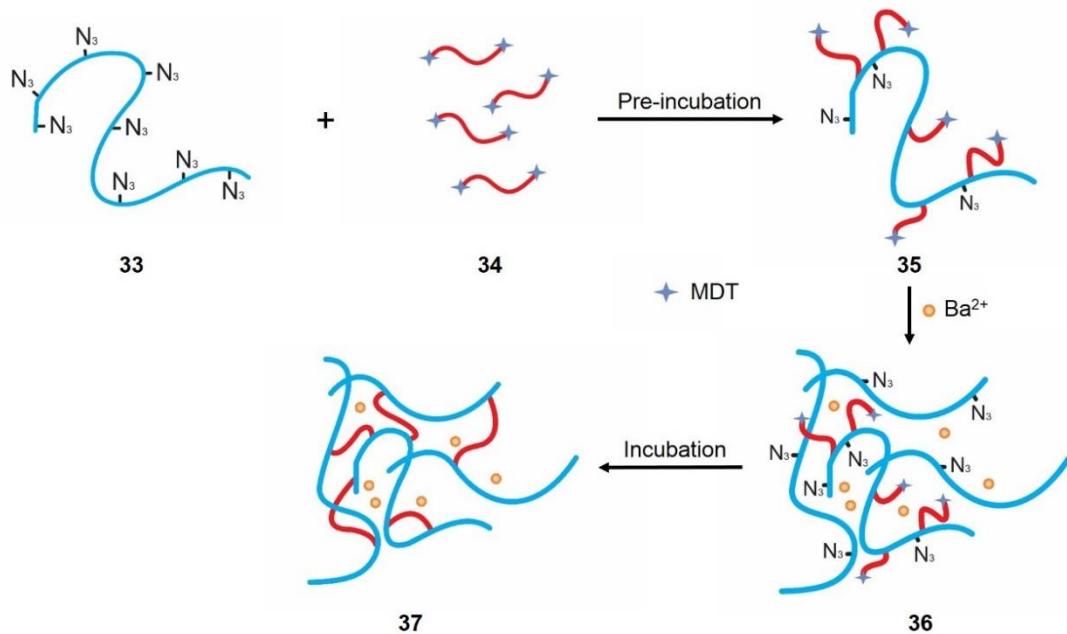


Figure 2.2. Crosslinked alginate-PEG microbead fabrication based upon Staudinger ligation and ionic interaction. Adapted from *Acta Biomater.* **2011**, 7, Hall, K. K.; Gattás-Asfura, K. M.; Stabler, C. L. Microencapsulation of islets within alginate/poly(ethylene glycol) gels cross-linked via Staudinger ligation, 614–624, Copyright 2011, with permission from Elsevier.

Stabler and co-workers also employed Staudinger ligation to fabricate hyperbranched, polymer-based, ultrathin capsules possessing bioorthogonal functionality and altered physiochemical properties.⁹¹ N_3 -PEG-NHS (**38**) was first covalently linked to amine groups on the surface of pancreatic islet cells at room temperature (Figure 2.3). Poly(amidoamine) (PAMAM) dendrimers (**39**) functionalized with phosphine-bearing MDT groups were then covalently bound to the pancreatic islet cells via Staudinger ligation between the azide and MDT moieties at 37 °C. Finally, hyperbranched alginate (**40**) functionalized with azide was coupled to the exposed MDT-functionalized PAMAM

coating, also via Staudinger ligation under similar conditions. Additional layers could be built via stepwise incubation of MDT-functionalized PAMAM and hyperbranched alginate azide, until the desired number of layers was achieved. This encapsulation of viable tissues through layer-by-layer polymer assembly offers a versatile platform for cell surface engineering, providing tailored properties, and could only be possible by use of a gentle, rapid, and chemospecific reaction like Staudinger ligation. Moreover, the hyperbranched polymers provide a highly functionalized surface for bioorthogonal conjugation of bioactive or labeling motifs. In addition, Stabler and co-workers used a similar approach to develop a polymeric material by coupling azide-functionalized alginates with phosphine functionalized 4-arm PEGs through Staudinger ligation.⁹² It has been demonstrated that the polymeric material can be used for preparing immunoprotective and ultrathin coatings on murine primary pancreatic islets, and the resulting non-toxic coatings provide significant protective effects in an allograft murine model.

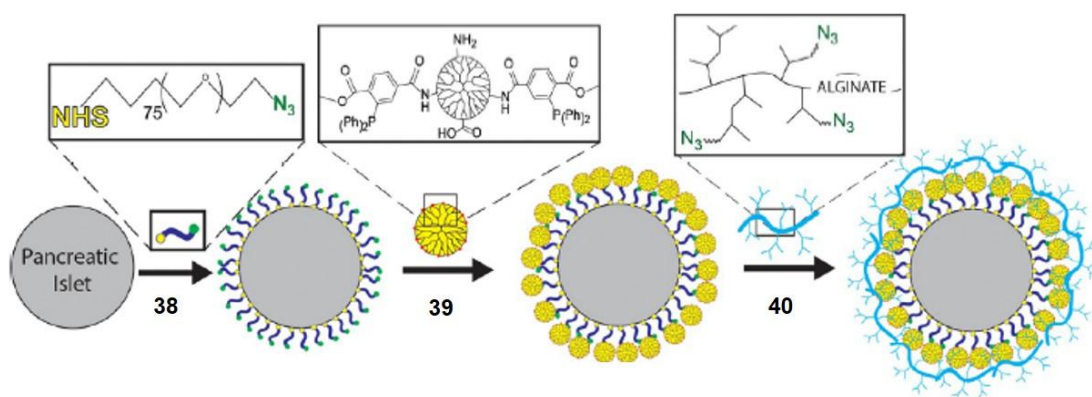
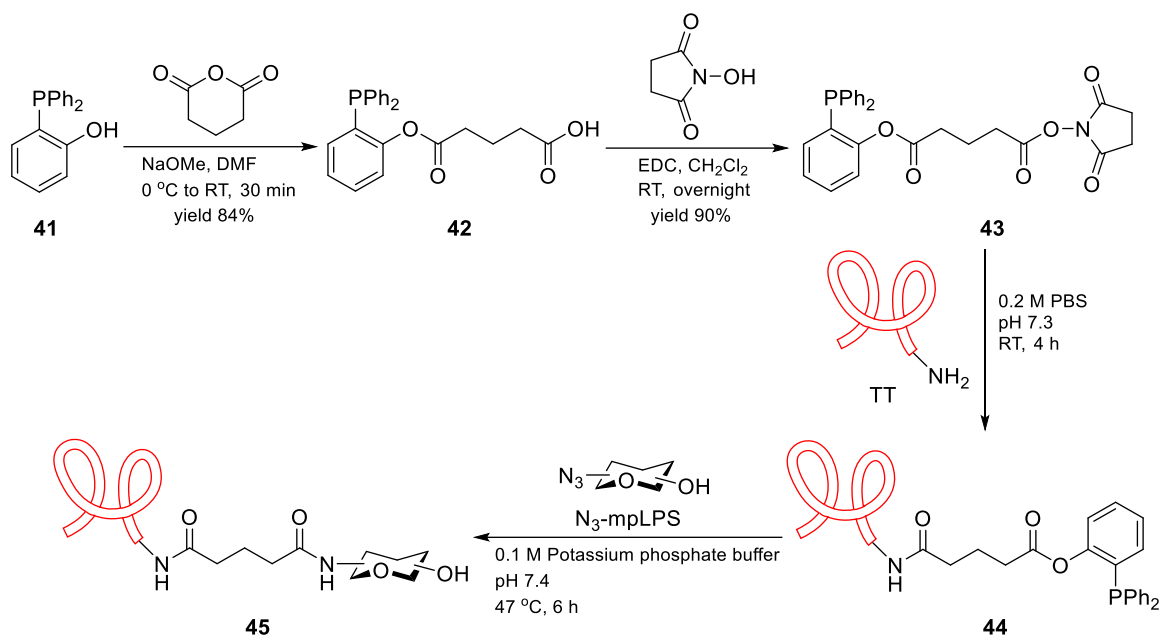


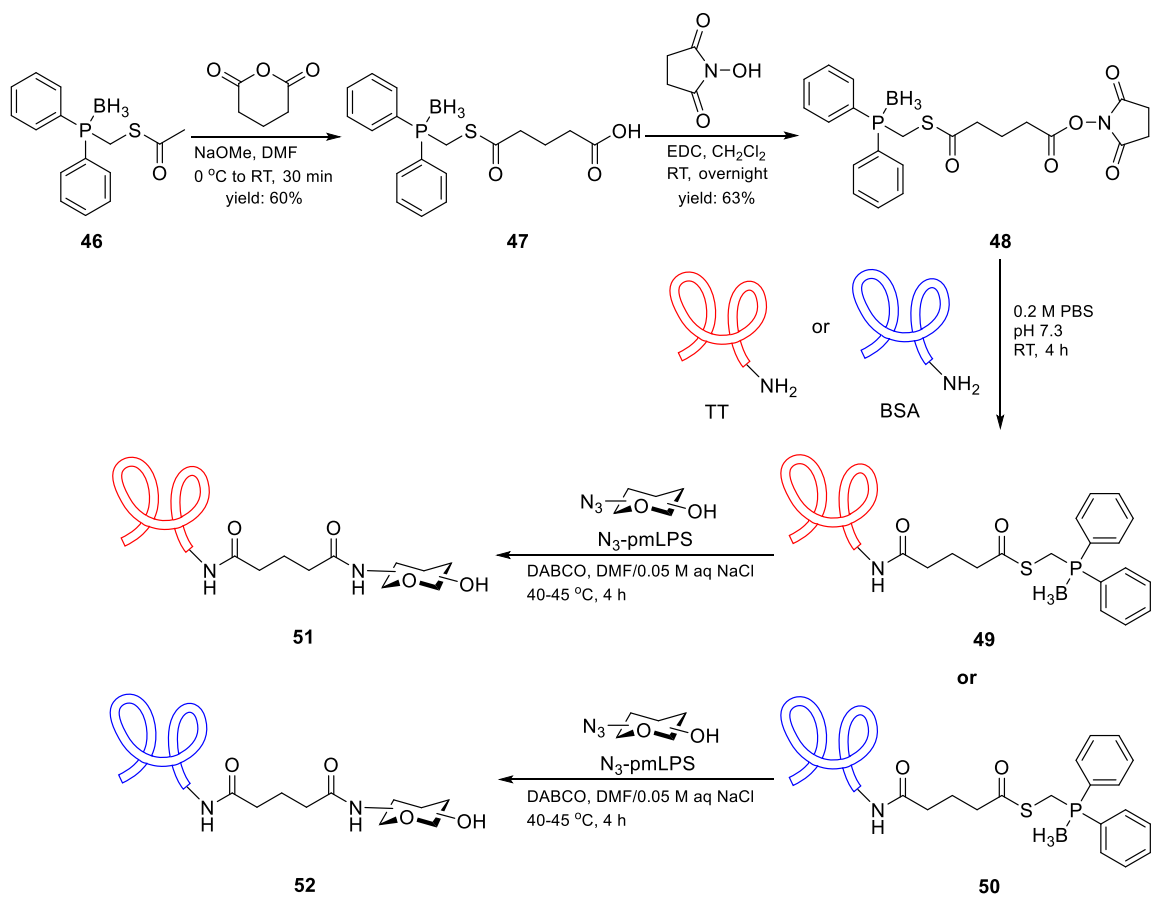
Figure 2.3. Ultrathin coating assembly on pancreatic islet cells through Staudinger ligation. Adapted with permission from Gattás-Asfura, K. M.; Stabler, C. L. *ACS Appl. Mater. Interfaces* 2013, 5, 9964–9974. Copyright 2013 American Chemical Society.

Traceless Staudinger ligation has been shown also to be a valuable tool for coupling polysaccharides to certain biomolecules. In recent decades, a number of glycoconjugates have been prepared and developed as potential anti-infectious and anti-cancer vaccines, and some of these have already been licensed as pharmaceuticals.⁹³ Since poly- or oligosaccharides are so extraordinarily complex, they often are highly useful for targeting only one organism or part of an organism with great precision. However, adjuvants are frequently necessary, since the poly/oligosaccharide portion alone does not elicit a sufficiently strong immune response. Proteins are far better at eliciting strong immune responses, hence one clear application of protein/saccharide conjugates. Although a number of other coupling reactions have been employed for covalently conjugating polysaccharides to certain proteins, there remained a need for a chemoselective and efficient reaction to provide well-defined conjugate structure, and enhance efficiency by reducing the need for excess of expensive and complex reagents. The rapid and selective traceless Staudinger ligation is a very attractive technique for biological chemists to conjugate polysaccharides with certain biomolecules. Traceless Staudinger ligation is a good choice for achieving a well-defined amide bond connection, since it is a highly selective reaction in which the phosphine is incorporated in the leaving group and not in the transferred acyl group. Wider use of traceless Staudinger ligations, however, is restricted by the difficulty in designing and synthesizing the phosphine for overcoming the two main limitations: competitive hydrolysis of the iminophosphorane intermediate and premature oxidation of the phosphorus atom.

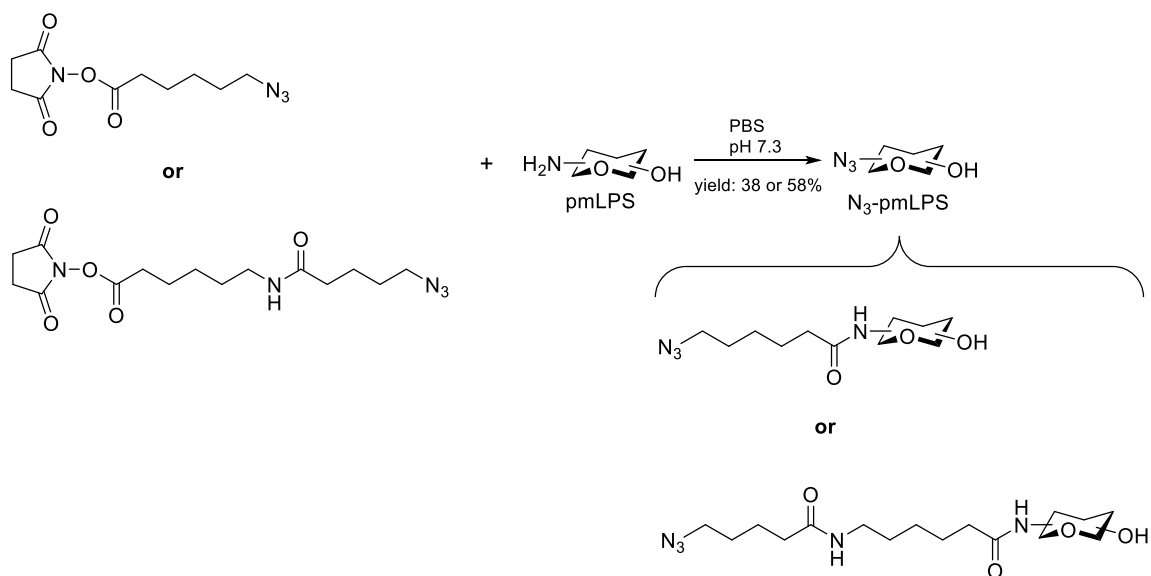
To further develop the utility of traceless Staudinger ligation for preparation of glycoconjugates, Mulard and co-workers designed two new phosphino-functionalized protein carriers to allow construction of potential glycoconjugate vaccines.⁹⁴ Initially, *o*-(diphenylphosphino)phenol (**41**, Scheme 2.14) and a borane protected phosphine (**46**, Scheme 2.15) were reacted with glutaric anhydride in DMF at 0 °C to room temperature, affording the corresponding carboxy-functionalized phosphines (**42**) and (**47**), respectively. To prepare them for traceless Staudinger ligation to prepare the glycoconjugates, both (**42**) and (**47**) were activated into their corresponding succinimide esters (**43** and **48**), respectively) in the presence of NHS and EDC. Succinimide ester (**43**) was further linked with tetanus toxoid (TT) in 0.2 M phosphate buffered saline (PBS), affording the phosphino-functionalized protein carrier (**44**), while the other succinimide ester (**48**) was further covalently associated with TT and bovine serum albumin (BSA) in 0.2 M PBS, resulting in the corresponding phosphino-functionalized protein carriers (**49**) and (**50**), respectively. Mulard *et al.* chose a polysaccharide moiety of the lipopolysaccharide (pmLPS) of *Vibrio cholerae* O1 serotype Inaba, a causative agent of cholera. This surface polysaccharide is the major target of human protective immune response against this disease. The researchers modified pmLPS by azide-functionalized succinimidyl esters to give the corresponding azido-containing pmLPS derivatives (N₃-pmLPS, Scheme 2.16) via amide bonding, and finally these azide-containing pmLPS derivatives were coupled with (**44**), (**49**), and (**50**) in potassium phosphate buffer or DMF containing DABCO and sodium chloride (NaCl) via traceless Staudinger ligation in good yields (between 52% and 83%), forming the corresponding glycoconjugates (**45**), (**51**), and (**52**), respectively.



Scheme 2.14. Synthesis of glycoconjugate from *o*-(diphenylphosphino)phenol. Adapted with permission from Grandjean, C.; Boutonnier, A.; Guerreiro, C.; Fournier, J.; Mulard, L. A. *J. Org. Chem.* **2005**, *70*, 7123–7132. Copyright 2005 American Chemical Society.



Scheme 2.15. Synthesis of glycoconjugates from a borane protected phosphine. Adapted with permission from Grandjean, C.; Boutonnier, A.; Guerreiro, C.; Fournier, J.; Mulard, L. A. *J. Org. Chem.* **2005**, *70*, 7123–7132. Copyright 2005 American Chemical Society.



Scheme 2.16. Synthesis of azido-containing polysaccharide derivatives. Adapted with permission from Grandjean, C.; Boutonnier, A.; Guerreiro, C.; Fournier, J.; Mulard, L. A. *J. Org. Chem.* **2005**, *70*, 7123–7132. Copyright 2005 American Chemical Society.

In addition to glycoconjugate syntheses, Mulard *et al.* assessed the antigenicity of these glycoconjugate derivatives by enzyme-linked immunosorbent assay (ELISA) inhibition assays, in order to indicate whether the functionality of the carbohydrate haptens was affected by conjugation. Their results revealed that all of these conjugates were capable of inhibiting the interaction between *V. cholera* O1 serotype Inaba LPS and the monoclonal antibody (mIgG) I-24-2, with some conjugates even exhibiting antigenicity equipotent to that of Inaba LPS, suggesting that both pmLPS derivatizations and traceless Staudinger ligations do not greatly affect the unique antigenic determinant recognized by mIgG I-24-2. This example is an excellent demonstration of the value of the unique combination of selectivity, efficiency, and mild reaction conditions available through Staudinger ligations.

2.5 Conclusions and future perspectives

Staudinger reduction offers an efficient way to selectively functionalize polysaccharides, resulting in regioselectively aminated polysaccharide derivatives that are partial structural analogs of natural, highly bioactive polysaccharides like glycosaminoglycans, and semi-synthetic chitosans, and therefore have promise for biomedical applications. This methodology has been used to prepare a series of 6-amino- and 6-amido-6-deoxypolysaccharide derivatives from native polysaccharides including cellulose, amylose, curdlan, pullulan, and others. In addition, Saxon and Bertozzi pioneered Staudinger ligation, which as we have discussed is a powerful technique for mild, chemoselective modification of polysaccharides, other more sensitive biomolecules, and even living cells. The application by polysaccharide chemists of Staudinger ligation to alginate modification promises to provide great benefits, complementing and enhancing the natural ability of alginates to gel under extremely mild conditions, enabling enhancement of alginate hydrogel durability, fluorescent labeling of alginate hydrogels, and the attachment of targeting moieties, to name just a few potential advantages. The further discovery by Bertozzi and Raines of traceless Staudinger ligation, in which the triaryl phosphine oxide moiety is cleaved by hydrolysis to end up as part of the leaving group rather than part of the conjugate, permits us to think even more about the exciting possibilities that can be realized by using traceless Staudinger ligation to label or otherwise modify the surfaces of living cells and other sensitive biomolecules. The promise of traceless Staudinger ligation is well illustrated by the examples we have presented of conjugation of oligo- or polysaccharide haptens to immunogenic protein carriers, providing a fully stable and biocompatible amide link between the haptens and protein carriers. These

bioconjugates combine the incredible targeting specificity available from polysaccharides with the strong immune response elicitation available from the protein portion of the conjugate, in a manner that is structurally very well defined thanks to the specificity and mild nature of the Staudinger ligation chemistry.

In the future, we believe that a greater variety of complex aminated polysaccharide derivatives will be available through the efficiency and selectivity of Staudinger reductions, in some cases in combination with other selective chemistries. There will be many more exciting synthetic possibilities created by the intermediacy of polysaccharide 6-deoxy-6-iminophosphorane ylides and their bromo precursors⁹⁵ through Staudinger-related reactions. These ylides contain remarkably nucleophilic, negatively charged nitrogen atoms, and the exploitation of these intermediates in polysaccharide chemistry is still in its infancy. Although there are still relatively few examples of Staudinger ligations in polysaccharide chemistry, a large number of researchers have successfully used Staudinger ligations in small molecule carbohydrate chemistry, for example to conjugate biological molecules with carbohydrates such glucose and mannose, and it has been demonstrated that those bioconjugates have great potential for use in applications such as biosensing and drug delivery. More of these carbohydrate methods will be imported for use in Staudinger ligation with polysaccharides.

Biomolecules such as peptides, proteins, and nuclei acids can in principle be conjugated with cellulose and other polysaccharides via Staudinger ligations. Since traceless Staudinger ligations are capable of providing a well-defined amide bond between two

moieties, it is promising to use this method for coupling azide functionalized polysaccharides with different bioactive probes to produce amide-functionalized polysaccharide derivatives possessing various bioactive, targeting, and other physicochemical properties. Further work should aim at designing and preparing phosphine linkers that are entirely stable toward oxidation for allowing intramolecular acylation in the absence of an organic co-solvent. Also, water-soluble phosphine-functionalized linkers for traceless Staudinger ligations are still needed, in order to make bioconjugates in aqueous environments.

Overall the intrinsic attractive properties and versatility of Staudinger reductions, ligations, traceless ligations, and other variants yet to be described and named are likely to make them important components of the synthetic arsenals of polysaccharide chemists, biomaterial developers, cell biologists, and a panoply of other scientists and engineers for many decades to come.

2.6 Acknowledgement

We gratefully acknowledge the Institute for Critical Technologies and Applied Science (ICTAS), Macromolecules and Interfaces Institute (MII) and Department of Sustainable Biomaterials at Virginia Tech for their financial, facilities, and educational support. We thank the USDA for partial support of this work through grant No. 2011-67009-20090.

2.7 References

1. Heinze, T. *Polysaccharides I: Structure, Characterisation and Use* Springer, Berlin, **2005**.
2. Severian, D. *Polysaccharides: Structural Diversity and Functional Versatility* Marcel Dekker, New York, **1998**.
3. Roy, D.; Semsarilar, M.; Guthrie, J. T.; Perrier, S. Cellulose modification by polymer grafting: a review. *Chem. Soc. Rev.* **2009**, *38*, 2046–2064.
4. Fox, S. C.; Li, B.; Xu, D.; Edgar, K. J. Regioselective esterification and etherification of cellulose: a review. *Biomacromolecules* **2011**, *12*, 1956–1972.
5. Zheng, X.; Gandour, R. D.; Edgar, K. J. Probing the mechanism of TBAF-catalyzed deacylation of cellulose esters. *Biomacromolecules* **2013**, *14*, 1388–1394.
6. Hebeish, A.; Guthrie, J. T. *The Chemistry and Technology of Cellulosic Copolymers* Springer-Verlag, Berlin, **1981**.
7. Nolte, P., Schonbein, C. F. *Gas, Wasser, Abwasser* **1999**, *79*, 819–823.
8. Hyatt, J. W. *US Patent 00232037*, **1880**.
9. Hang, H. C.; Bertozzi, C. R. Chemoselective approaches to glycoprotein assembly. *Acc. Chem. Res.* **2001**, *34*, 727–736.
10. Helferich, B.; Köster, H. Äther des triphenyl-carbinols mit cellulose und stärke. *Ber. Dtsch. Chem. Ges.* **1924**, *57*, 587–591.
11. Hearon, W. M.; Hiatt, G. D.; Fordyce, C. R. Cellulose trityl ether. *J. Am. Chem. Soc.* **1943**, *65*, 2449–2452.
12. Honeyman, J. Reactions of cellulose. Part I *J. Chem. Soc.* **1947**, 168–173.

13. Hall, D.M.; Horne, J. R. Model compounds of cellulose: Trityl ethers substituted exclusively at C-6 primary hydroxyls. *J. Appl. Polym. Sci.* **1973**, *17*, 2891–2896.
14. Heinze, T.; Röttig, K.; Nehls, I. Synthesis of 2,3-*O*-carboxymethylcellulose. *Macromol. Rapid Commun.* **1994**, *15*, 311–317.
15. Gomez, J. A. C.; Eler, U.; Klemm, D. 4-Methoxy substituted trityl groups in 6-*O* protection of cellulose: Homogeneous synthesis, characterization, detritylation. *Macromol. Chem. Phys.* **1996**, *197*, 953–964.
16. Klemm, D.; Stein, A. J. Silylated cellulose materials in design of supramolecular structures of ultrathin cellulose films. *Macromol. Sci., Pure Appl. Chem.* **1995**, *32*, 899–904.
17. Koschella, A.; Heinze, T.; Klemm, D. First synthesis of 3-*O*-functionalized cellulose ethers via 2,6-di-*O*-protected silyl cellulose. *Macromol. Biosci.* **2001**, *1*, 49–54.
18. Yin, X.; Koschella, A.; Heinze, T. Regioselectively oxidized 3-*O*-alkyl ethers of cellulose: synthesis and characterization. *React. Funct. Polym.* **2009**, *69*, 341–346.
19. Koschella, A.; Fenn, D.; Heinze, T. Water soluble 3-mono-*O*-ethyl cellulose: synthesis and characterization. *Polym. Bull.* **2006**, *57*, 33–41.
20. Heinze, T.; Pfeifer, A.; Sarbova, V.; Koschella, A. 3-*O*-propyl cellulose: Cellulose ether with exceptionally low flocculation temperature. *Polym. Bull.* **2010**, *66*, 1219–1229.
21. Petzold, K.; Klemm, D.; Heublein, B.; Burchard, W.; Savin, G. Investigations on structure of regioselectively functionalized celluloses in solution exemplified by using 3-*O*-alkyl ethers and light scattering. *Cellulose* **2004**, *11*, 177–193.

22. Isogai, A.; Kato, Y. Preparation of polyuronic acid from cellulose by TEMPO-mediated oxidation. *Cellulose* **1998**, *5*, 153–164.
23. Saito, T.; Kimura, S.; Nishiyama, Y.; Isogai, A. Cellulose nanofibers prepared by TEMPO-mediated oxidation of native cellulose. *Biomacromolecules* **2007**, *8*, 2485–2491.
24. Fukuzumi, H.; Saito, T.; Iwata, T.; Kumamoto, Y.; Isogai, A. Transparent and high gas barrier films of cellulose nanofibers prepared by TEMPO-mediated oxidation. *Biomacromolecules* **2009**, *10*, 162–165.
25. Saito, T.; Isogai, A. TEMPO-mediated oxidation of native cellulose. The effect of oxidation conditions on chemical and crystal structures of the water-insoluble fractions. *Biomacromolecules* **2004**, *5*, 1983–1989.
26. Bragd, P.L.; van Bekkum, H.; Besemer, A. C. TEMPO-mediated oxidation of polysaccharides: Survey of methods and applications. *Top. Catal.* **2004**, *27*, 49–66.
27. Xu, D.; Edgar, K. J. TBAF and cellulose esters: Unexpected deacylation with unexpected regioselectivity. *Biomacromolecules* **2012**, *13*, 299–303.
28. Zheng, X.; Gandour, R. D.; Edgar, K. J. TBAF-catalyzed deacylation of cellulose esters: Reactions scope and influence of reaction parameters. *Carbohydr. Polym.* **2013**, *98*, 692–698.
29. Zhang, R.; Zheng, X.; Kuang, J.; Edgar, K. J. Glycan esters deacylation by TBAOH or TBAF: Regioselectivity vs. polysaccharide structure. *Carbohydr. Polym.* **2014**, *113*, 159–165.

30. Meng, X; Matson, J. B.; Edgar, K. J. Olefin cross-metathesis as a source of polysaccharide derivatives: cellulose ω -carboxyalkanoates. *Biomacromolecules* **2014**, *15*, 177–187.
31. Meng, X; Matson, J. B.; Edgar, K. J. Olefin cross-metathesis, a mild, modular approach to functionalized cellulose esters. *Polym. Chem.* **2014**, *5*, 7021–7033.
32. Dong, Y.; Edgar, K. J. Imparting functional variety to cellulose esters via olefin cross-metathesis. *Polym. Chem.* **2015**, *6*, 3816–3827.
33. Köhn, M.; Breinbauer, R. The Staudinger ligation—a gift to chemical biology. *Angew. Chem. Int. Ed.* **2004**, *43*, 3106–3116.
34. Lewis, W. G.; Green, L. G.; Grynszpan, F.; Radic, Z.; Carlier, P. R.; Taylor, P.; Finn, M. G.; Sharpless, K. B. Click chemistry in situ: acetylcholinesterase as a reaction vessel for the selective assembly of a femtomolar inhibitor from an array of building blocks. *Angew. Chem. Int. Ed.* **2002**, *41*, 1053–1057.
35. Rostovtsev, V. V.; Freen, L. G.; Fokin, V. V.; Sharpless, K. B. A stepwise Huisgen cycloaddition process: Copper(I)-catalyzed regioselective “ligation” of azides and terminal alkynes. *Angew. Chem. Int. Ed.* **2002**, *41*, 2596–2599.
36. Staudinger, H.; Meyer, J. Über neue organische phosphorverbindungen III. Phosphinmethylenderivate und phosphinimine *Helv. Chim. Acta* **1919**, *2*, 635–646.
37. Gololobov, Y. G.; Zhmurova, I. N.; Kasukhin, L. F. Sixty years of Staudinger reaction. *Tetrahedron* **1981**, *37*, 437–472.
38. Gololobov, Y. G.; Kasukhin, L. F. Recent advances in the Staudinger reaction. *Tetrahedron* **1992**, *48*, 1353–1406.

39. Breinbauer, R.; Köhn, M. The Staudinger ligation—a gift to chemical biology. *Angew. Chem. Int. Ed.* **2004**, *43*, 3106–3116.
40. Staudinger, H.; Hauser, E. Über neue organische phosphorverbindungen IV phosphinimine *Helv. Chim. Acta* **1921**, *4*, 861–886.
41. Saxon, E.; Bertozzi, C. R. Cell surface engineering by a modified Staudinger reaction. *Science* **2000**, *287*, 2007–2010.
42. Luchansky, S. J.; Hang, H. C.; Saxon, E.; Grunwell, J. R.; Yu, C.; Dube, D. H.; Bertozzi, C. R. Constructing azide-labeled cell surfaces using polysaccharide biosynthetic pathway. *Meth. Enzymol.* **2003**, *362*, 249–272.
43. Lemieux, G. A.; de Graffenried, C. L.; Bertozzi, C. R. A fluorogenic dye activated by the Staudinger reaction. *J. Am. Chem. Soc.* **2003**, *125*, 4708–4709.
44. Wang, C. C.; Seo, T. S.; Li, Z.; Ruparel, H.; Ju, J. Site-specific fluorescent labeling of DNA using Staudinger ligation. *Bioconjugate Chem.* **2003**, *14*, 697–701.
45. Saxon, E.; Armstrong, J. I.; Bertozzi, C. R. A “traceless” Staudinger ligation for the chemoselective synthesis of amide bonds. *Org. Lett.* **2000**, *2*, 2141–2143.
46. Nilsson, B. L.; Kiessling, L. L.; Raines, R. T. Staudinger ligation: a peptide from a thioester and azide. *Org. Lett.* **2000**, *2*, 1939–1941.
47. Nilsson, B. L.; Kiessling, L. L.; Raines, R. T. High-yielding Staudinger ligation of a phosphinothioester and azide to form a peptide. *Org. Lett.* **2001**, *3*, 9–12.
48. Soellner, M. B.; Nilsson, B. L.; Raines, R. T. Staudinger ligation of α -azido acids retains stereochemistry. *J. Org. Chem.* **2002**, *67*, 4993–4996.
49. Nilsson, B. L.; Hondal, R. J.; Soellner, M. B.; Raines, R. T. Protein assembly by orthogonal chemical ligation methods. *J. Am. Chem. Soc.* **2003**, *125*, 5268–5269.

50. Soellner, M. B.; Dickson, K. A.; Nilsson, B. L.; Raines, R. T. Site-specific protein immobilization by Staudinger ligation. *J. Am. Chem. Soc.* **2003**, *125*, 11790–11791.
51. Dash, M.; Chiellini, F.; Ottenbrite, R. M.; Chiellini, E. Chitosan-a versatile semi-synthetic polymer in biomedical applications. *Prog. Polym. Sci.* **2011**, *36*, 981–1014.
52. Mao, S.; Sun, W.; Kissel, T. Chitosan-based formulations for delivery of DNA and siDNA. *Adv. Drug Delivery Rev.* **2010**, *62*, 12–27.
53. Kumar, M. N. V. R.; Muzzarelli, R. A. A.; Muzzarelli, C.; Sashiwa, H.; Domb, A. Chitosan chemistry and pharmaceutical perspectives. *J. Chem. Rev.* **2004**, *104*, 6017–6084.
54. Bowman, K.; Leong, K. W. Chitosan nanoparticles for oral drug and gene delivery. *Int. J. Nanomed.* **2006**, *1*, 117–128.
55. Thakor, D. K.; Teng, Y. D.; Tabata, Y. Neuronal gene delivery by negatively charged pullulan-spermine/DNA anioplexes. *Biomaterials* **2009**, *30*, 1815–1826.
56. Kanatani, I.; Ikai, T.; Okazaki, A.; Jo, J.; Yamamoto, M.; Imamura, M.; Kanematsu, A.; Yamamoto, S.; Ito, N.; Ogawa, O.; Tabata, Y. Efficient gene transfer by pullulan-spermine occurs through both clathrin-and raft/caveolae-dependent mechanism. *J. Controlled Release* **2006**, *116*, 75–82.
57. Jo, J.; Ikai, T.; Okazaki, A.; Yamamoto, M.; Hirano, Y.; Tabata, Y. Expression profile of plasmid DNA by spermine derivatives of pullulan with different extents of spermine introduced. *J. Controlled Release* **2007**, *118*, 389–398.
58. Thomsen, L. B.; Lichota, J.; Kim, K. S.; Moos, T. Gene delivery by pullulan derivatives in brain capillary endothelial cells for protein secretion. *J. Controlled Release* **2011**, *151*, 45–50.

59. Ikeda, M.; Hasegawa, T.; Numata, M.; Sugikawa, K.; Sakurai, K.; Fujiki, M.; Shinkai, S. In stantaneous inclusion of a polynucleotide and hydrophobic guest molecules into a helical core of cationic β -1,3-glucan polysaccharide. *J. Am. Chem. Soc.* **2007**, *129*, 3979–3988.
60. Song, Y.; Wang, H.; Zeng, X.; Sun, Y.; Zhang, X.; Zhou, J.; Zhang, L. Effect of molecular weight and degree of substitution of quaternized cellulose on the efficiency of gene transfection. *Bioconjugate Chem.* **2010**, *21*, 1271–1279.
61. Heinze, T.; Koschella, A.; Brackhagen, M.; Engelhardt, J.; Nachtkamp, K. Studies on non-natural deoxamomnium cellulose. *Macromol. Symp.* **2006**, *244*, 74–82.
62. Aoki, N.; Koganei, K.; Chang, H.S.; Furuhata, K.; Sakamoto, M. Gas chromatographic-mass spectrometric study of reactions of halodeoxycellulose with thiols in aqueous solutions. *Carbohydr. Polym.* **1995**, *27*, 13–21.
63. Aoki, N.; Furuhata, K.; Saegusa, Y.; Nakamura, S.; Sakamoto, M. Reaction of 6-bromo-6-deoxycellulose with thiols in lithium bromide-*N, N*-dimethylacetamide. *J. Appl. Polym. Sci.* **1996**, *61*, 1173–1185.
64. Aoki, N.; Fukushima, K.; Kurakata, H.; Sakamoto, M.; Furuhata, K. 6-Deoxy-6-mercaptocellulose and its *S*-substituted derivatives as sorbents for metal ions. *React. Funct. Polym.* **1999**, *42*, 223–233.
65. Saad, G. R.; Sakamoto, M.; Furuhata, K. Dielectric study of β -relaxation in some cellulosic substances. *Polym. Int.* **1996**, *41*, 293–299.
66. Saad, G. R.; Furuhata, K. Effect of substituents on dielectric β -relaxation in cellulose. *Polym. Int.* **1997**, *42*, 356–362.

67. Furuhashi, K.; Ikeda, H. Ionic cellulose derivatives: Synthesis of sodium 6-deoxycellulose-6-sulfonate with high degree of substitution. *React. Funct. Polym.* **1999**, *42*, 103–109.
68. Cimecioglu, A. L.; Ball, D. H.; Kaplan, D. L.; Huang, S. H. Preparation of amylose derivatives selectively modified at C-6. 6-amino-6-deoxyamylose. *Macromolecules* **1994**, *27*, 2917–2922.
69. Hizukuri, S.; Shirasaka, K.; Juliano, B. O. Phosphorus and amylose branching in rice starch granules. *Starch* **1983**, *35*, 348–350.
70. Zong, Z.; Kimura, Y.; Takahashi, M.; Yamane, H. Characterization of chemical and solid state structures of acylated chitosans. *Polymer* **2000**, *41*, 899–906.
71. Aktas, Y.; Yemisci, M.; Andrieux, K.; Güçlüoğlu, M.; Çakır, L.; Ediz, L.; Dönmez, D.; Münir, B.; Çakır, E.; Riguera, R.; Sargon, M. F.; Çelik, H. H.; Demir, A. S.; Hincal, A. A.; Dalkara, T.; Çapan, Y.; Couvreur, P. A nanomedicine transports a peptide caspase-3 inhibitor across the blood-brain barrier and provides neuroprotection. *Bioconjugate Chem.* **2005**, *16*, 1503–1511.
72. Miwa, A.; Ishibe, A.; Nakano, M.; Yamahira, T.; Itai, S.; Jinno, S.; Kawahara, H. Development of novel chitosan derivatives as micellar carrier of taxol. *Pharm. Res.* **1998**, *15*, 1844–1850.
73. Kurita, K.; Ikeda, H.; Yoshida, Y.; Shimojoh, M.; Harata, M. Chemoselective protection of the amino groups of chitosan by controlled phthaloylation: Facile preparation of a precursor useful for chemical modifications. *Biomacromolecules* **2001**, *3*, 1–4.

74. Liu, C.; Baumann, H. Exclusive and complete introduction of amino groups and their *N*-sulfo and *N*-carboxymethyl groups into the 6-position of cellulose without the use of protecting groups. *Carbohydr. Res.* **2002**, *337*, 1297–1307.
75. Teshirogi, T.; Yamamoto, H.; Sakamoto, M.; Tonami, H. Synthesis of 6-amino-6-deoxycellulose. *Sen'I Gakkaishi* **1979**, *35*, 525–529.
76. Daly, W. H.; Lee, S., *Peptide Graft Copolymers from Soluble Aminodeoxycellulose Acetate*. In *Water-Soluble Polymers*; Shalaby, S. W., McCormick, C. L., Butler, G. B., Eds.; American Chemical Society: Washington, DC, 1991; pp 189–200.
77. Fox, S. C.; Edgar, K. J. Staudinger reduction chemistry of cellulose: Synthesis of selectively *O*-acylated 6-amino-6-deoxy-cellulose. *Biomacromolecules* **2012**, *13*, 992–1001.
78. Pereira, J. M.; Edgar, K. J. Regioselective synthesis of 6-amino and 6-amido-6-deoxypullulans. *Cellulose* **2014**, *21*, 2379–2396.
79. Zhang, R.; Edgar, K.J. Synthesis of curdlan derivatives regioselectively modified at C-6: *O*-(*N*)-Acylated 6-amino-6-deoxycurdlan. *Carbohydr. Polym.* **2014**, *105*, 161–168.
80. Maeda, I.; Saito, H.; Masada, M.; Misaki, A.; Harada, T. Properties of gels formed by heat treatment of curdlan, a bacterial β -1,3 glucan. *Agric. Biol. Chem.* **1967**, *31*, 1184–1188.
81. Zhang, R.; Edgar, K. J. Properties, chemistry, and applications of the bioactive polysaccharide curdlan. *Biomacromolecules* **2014**, *15*, 1079–1096.
82. Kim, B.; Jung, I.; Kim, J.; Lee, J.-h.; Lee, I.; Lee, K. Curdlan gels as protein drug delivery vehicles. *Biotechnol. Lett.* **2000**, *22*, 1127–1130.

83. Arungundram, S.; Al-Mafraji, K.; Asong, J.; Leach, F. E.; Amster, I. J.; Venot, A.; Turnbull, J. E.; Boons, G. Modular synthesis of heparan sulfate oligosaccharides for structure-activity relationship studies. *J. Am. Chem. Soc.* **2005**, *131*, 17394–17405.
84. Zhang, R.; Edgar, K. J. Water-soluble aminocurdlan derivatives by chemoselective azide reduction using NaBH₄. *Carbohydr. Polym.* **2015**, *122*, 84–92.
85. Pawar, S. N.; Edgar, K. J. Chemical modification of alginates in organic solvent systems. *Biomacromolecules* **2011**, *12*, 4095–4103.
86. Darrabie, M. D.; Kendall, W. F.; Opara, E. C. Characteristics of poly-L-ornithine-coated alginate microcapsules. *Biomaterials* **2005**, *26*, 6846–6852.
87. Pawar, S. N.; Edgar, K. J. Alginate esters via chemoselective carboxyl group modification. *Carbohydr. Polym.* **2013**, *98*, 1288–1296.
88. Pawar, S. N.; Edgar, K. J. Alginate derivatization: a review of chemistry, properties and applications. *Biomaterials* **2012**, *33*, 3279–3305.
89. Gattás-Asfura, K. M.; Stabler, C. L. Chemoselective cross-linking and functionalization of alginate via Staudinger ligation. *Biomacromolecules* **2009**, *10*, 3122–3129.
90. Hall, K.K.; Gattás-Asfura, K.M.; Stabler, C.L. Microcapsulation of islets within alginate/poly(ethylene glycol) gels cross-linked via Staudinger ligation. *Acta Biomater.* **2011**, *7*, 614–624.
91. Gattás-Asfura, K. M.; Stabler, C. L. Bioorthogonal layer-by-layer encapsulation of pancreatic islets via hyperbranched polymers. *ACS Appl. Mater. Interfaces* **2013**, *5*, 9964–9974.

92. Rengifo, H. R.; Giraldo, J. A.; Labrada, I.; Stabler, C. L. Long-term survival of allograft murine islets coated via covalently stabilized polymers. *Adv. Healthcare Mater.* **2014**, *3*, 1061–1070.
93. Obbins, J. B.; Schneerson, R.; Anderson, P.; Smith, D. H. Prevention of systemic infections, especially Meningitis, caused by Haemophilus influenzae type b impact on public health and implications for other polysaccharide-based. *J. Am. Med. Assoc.* **1996**, *9*, 1181–1185.
94. Grandjean, C.; Boutonnier, A.; Guerreiro, C.; Fournier, J.; Mulard, L. A. On the preparation of carbohydrate-protein conjugates using the traceless Staudinger ligation. *J. Org. Chem.* **2005**, *70*, 7123–7132.
95. Zhang, R.; Liu, S.; Edgar, K. J. “Regioselective synthesis of cationic 6-(N, N, N-trialkylammonio)-6-deoxycurdlan derivatives” *Carbohydr. Polym.* **2016**, *136*, 474–484.

Chapter 3. An Efficient, Regioselective Pathway to Cationic and Zwitterionic *N*-Heterocyclic Cellulose Ionomers

Liu, S.; Liu, J.; Esker, A. R.; Edgar, K. J. *Biomacromolecules* **2016**, *17*, 503–513. Used with permission of American Chemical Society, 2016.

3.1 Abstract

Cationic derivatives of cellulose and other polysaccharides are attractive targets for biomedical applications due to their propensity for electrostatically binding with anionic biomolecules, such as nucleic acids and certain proteins. To date however, relatively few practical synthetic methods have been described for their preparation. Herein, we report a useful and efficient strategy for cationic cellulose ester salt preparation by the reaction of 6-bromo-6-deoxycellulose acetate with pyridine or 1-methylimidazole. Dimethyl sulfoxide solvent favored this displacement reaction to produce cationic cellulose acetate derivatives, resulting in high degrees of substitution (DS) exclusively at the C-6 position. These cationic cellulose derivatives bearing substantial, permanent positive charge exhibit surprising thermal stability, dissolve readily in water, and bind strongly with a hydrophilic and anionic surface, supporting their potential for a variety of applications such as permeation enhancement, mucoadhesion, and gene or drug delivery. Expanding upon this chemistry, we reacted a 6-imidazolyl-6-deoxycellulose derivative with 1,3-propane sultone

to demonstrate the potential for further elaboration to regioselectively substituted zwitterionic cellulose derivatives.

3.2 Introduction

Polymers bearing positive and/or negative charges, known as ionic polymers or ionomers, exhibit remarkable physical and chemical properties that may be exploited for various uses. Recently, ionomers, including polyelectrolytes¹⁻³ and polyzwitterions^{4,5}, have been extensively investigated for biomedical uses. For example, anionic polymers have been employed to form polyelectrolyte complexes through electrostatic interactions with cationic biomolecules including cationic drugs, basic peptides, and blood proteins, for therapeutic applications.^{6,7} Conversely, cationic polymers can bind electrostatically with anionic biomolecules including nucleic acids and certain proteins, producing polyelectrolyte complexes for gene and drug delivery, tissue engineering, and other therapeutic uses.⁸ It has been reported that cationic polymers are potentially effective vehicles for delivery of nucleic acids to the cell, since they effectively protect these anionic biomolecules from degradative enzymes and aid in transfection.^{9,10}

Naturally derived cationic polymers may in some cases be more attractive candidates for therapeutic uses than commonly investigated synthetic cationic polymers such as poly(ethyleneimine) (PEI) or poly[2-(*N,N*-dimethylamino)ethyl methacrylate] (PDMAEMA), because of their greater biocompatibility and biodegradability, and low immunogenicity.¹⁰ Chitosan is one of the most commonly used cationic polysaccharides. It is a semi-synthetic polymer, derived from the naturally occurring polysaccharide chitin.

Protonated chitosan is able to increase permeation of peptide drugs across mucosal epithelia, showing promise as an effective absorption enhancer in specific regions of the intestinal lumen.¹¹ Chitosan can encapsulate anionic nucleic acids or certain proteins via electrostatic interactions, protecting them from degradative enzymes.¹² Despite its promising properties as a vehicle for gene and drug delivery, the limited charge and solubility of chitosan at neutral pH, and the potential for protein contamination from the original crustacean shell source of the precursor chitin greatly affect its suitability. In order to overcome these limitations, researchers have sought to prepare superior derivatives of chitosan, as well as cationic derivatives of other polysaccharides. Peralkylation of chitosan amine groups affords quaternized ammonium derivatives bearing substantial permanent positive charge, that as a result have greater aqueous solubility across a wider range of pH. These *N*-quaternized chitosan derivatives show promising ability to enhance absorption of hydrophilic drugs by temporary opening of tight junctions between gastrointestinal enterocytes at pH values similar to those of the intestine (pH 6.4-7.5).¹¹ It has been reported that *N,N,N*-trimethyl chitosan chloride (TMC) acts as a permeation enhancer for the peptide drug buserelin and for mannitol across Caco-2-cell monolayers at neutral pH.¹³

In addition to cationic polysaccharides, zwitterionic polysaccharides are also of special interest. Some polysaccharides bear both basic amino groups and acidic carboxylate groups, and thus possess zwitterionic character at physiological pH. It has been reported that zwitterionic polysaccharides are capable of stimulating CD-4⁺ T-cell proliferation, after being presented via the MHC-II processing pathway.¹⁴⁻¹⁶ Some semisynthetic polyzwitterions prepared from naturally occurring polysaccharides possess potent

immunostimulatory activity; it has been demonstrated that structurally varied zwitterionic polysaccharides appear to stimulate distinct immunological responses.¹⁷⁻¹⁹ A zwitterionic polysaccharide was also reported to form a cancer vaccine candidate by conjugating with the carbohydrate hapten Tn.²⁰ Moreover, some mammalian glycoaminoglycans (GAGs) are members of the zwitterionic polysaccharide family, due to the fact that they are partly sulfated copolymers consisting of alternating glucosamine and uronic acid monosaccharides. These zwitterionic GAGs play important roles in biological systems. For example, it has been demonstrated that the adhesion of the malaria pathogen *P. falciparum* to placental cells is mediated by chondroitin sulfate.²¹

Our group has previously explored preparation of cationic polysaccharide derivatives. Compared with similar reactions of tosylated cellulose reported by other groups,²² employing trialkylamines as nucleophiles for S_N2 displacement of the primary alkyl bromides of 6-bromo-6-deoxyglycans, e.g. 6-bromo-6-deoxy-cellulose esters and 6-bromo-6-deoxy-curdlan, results in 6-(*N, N, N*-trialkylammonio)-6-deoxypolysaccharide derivatives with essentially complete chemoselectivity and regiocontrol.^{23,24} However, this body of work showed that trialkylamine nucleophilic bromide displacements of 6-bromo-6-deoxyglucans are quite difficult to drive to high reaction conversion. These publications presented the hypothesis that accumulating cationic charge along the glycan chain as displacement by trialkylamines proceeds is responsible for the poor conversion, and presented evidence in support of this hypothesis, including the fact that displacements with dialkylamines (in which case the tertiary amine product is not charged) under otherwise equivalent conditions proceed nearly to completion. Our previous work with curdlan also

indicated that displacement with more nucleophilic aromatic amines could be more favorable and lead to higher DS values,²⁴ but it was uncertain whether these results with the relatively soluble curdlan would translate to the more intractable cellulose. In this work, we hypothesize that nucleophilic displacements by aromatic amines such as pyridine or alkyl imidazoles will proceed to much higher degrees of substitution of 6-cationic substituents than is the case for tertiary aliphatic amines, because of the greater nucleophilicity of these aromatic amines, as well as their greater ability to disperse positive charge. If this hypothesis is correct, it could enable us to improve reaction efficiency and prepare cationic polysaccharides with the necessary properties, including charge density, for the biomedical applications mentioned above. Herein, we report our efforts to confirm this hypothesis by carrying out regioselective nucleophilic displacement on 6-bromo-6-deoxycellulose derivatives, using pyridine and imidazoles. In addition to confirming the hypothesis, we hoped that these methods would provide regioselectively substituted, water-soluble quaternary pyridinium and 1-methylimidazolium cellulose derivatives that would enable future structure-property experiments to determine their utility in gene delivery, tight junction opening, and other valuable applications. We planned to test their affinity for negatively charged molecules and surfaces by measuring adsorption to a hydrophilic, anionic surface using surface plasmon resonance (SPR). Moreover, we hoped to be able to test the ability to utilize aromatic amines synthesized by this general approach for further elaboration to poly(zwitterions).

3.3 Materials and methods

3.3.1 Materials

Microcrystalline cellulose (MCC, Avicel PH-101, Fluka, degree of polymerization (DP) = 80, measured by size exclusion chromatography of the per(phenylcarbamate) derivative²⁵) was dried under vacuum at 50 °C overnight before use. Lithium bromide (LiBr, Fisher) was dried under vacuum at 125 °C. *N*-Bromosuccinimide (NBS, 99%, Acros) was recrystallized from boiling water and dried for two days under reduced pressure over anhydrous calcium chloride. Triphenylphosphine (Ph₃P, Strem), acetic anhydride (Acros), pyridine (anhydrous, 99+%, AcroSeal), imidazole (Sigma-Aldrich 99+%), 1-methylimidazole (Sigma-Aldrich 99+%), 1,3-propane sultone (Aldrich, 99+%), 16-mercaptohexadecanoic acid (Sigma-Aldrich) and 1-hexadecanethiol (Sigma-Aldrich) were used as received. Ethanol and acetone were from Fisher Scientific, Pittsburgh, PA and used as received. *N,N*-Dimethylacetamide (DMAc, Fisher), *N,N*-dimethylformamide (DMF, Fisher) and dimethyl sulfoxide (DMSO, Acros) were kept over 4 Å molecular sieves under dry nitrogen until use. Regenerated cellulose dialysis tubing (3500 g/mol molecular weight cut-off (MWCO)) was from Fisher and used as received. SPR gold sensor (20 mm × 20 mm) was from Reichert Technologies Life Sciences and used as received. Ultrapure water (18.2 MΩ•cm, 25°C) was obtained from a Synergy UV (EMD Millipore, Billerica, MA).

3.3.2 Measurements

¹H, ¹³C NMR, HMBC and HSQC spectra were obtained on a Bruker AVANCE II 500 MHz spectrometer in DMSO-*d*₆ at room temperature or 50 °C. Infrared spectroscopic analyses of samples as pressed KBr pellets were obtained on a Thermo Electron Nicolet 8700 instrument using 64 scans and 4 cm⁻¹ resolution. Thermogravimetric analyses were performed on a Q500 Thermogravimetric analyzer, TGA (TA Instruments, DE, USA).

Approximately 5 mg of the sample was heated from 25°C to 600°C at a rate of 10°C/min under a continuous nitrogen flow at 60 mL/min. Modulated differential scanning calorimetry (MDSC) was conducted using a TA Instruments DSC Q2000. DSC data were obtained from -50 °C to 200 °C at heating rates of 20 °C/min under nitrogen. An atomic force microscope (MFP-3D-BIO, Asylum Research, Goleta, CA) was used in tapping mode to image adsorption on SPR sensor surfaces. Height images were obtained by a silicon tip (OMCL-AC160TS, Olympus Corp., Tokyo, Japan) under ambient conditions (22 °C, 50% humidity). The roughnesses of the samples were calculated based upon the root-mean-square (RMS) values of 5 μm × 5 μm scan areas. Carbon, nitrogen and bromine contents were performed by Micro Analysis Inc. using a Perkin Elmer 2400 II analyzer. Carbon and nitrogen contents were measured by flask combustion followed by ion chromatography, and bromine content was determined with a thermal conductivity detector. DS values were determined by means of ¹H NMR spectroscopy, according to the following equations, respectively.

$$DS_{Ac} = \frac{7I_{CH_3}}{3I_{cellulose\ backbone}}$$

$$DS_{Pyr^+} = \frac{7I_{CH-ring}}{5I_{cellulose\ backbone}}$$

$$DS_{IM} = \frac{7I_{CH-ring}}{3I_{cellulose\ backbone}}$$

$$DS_{MeIM^+} = \frac{7}{\frac{3I_{cellulose\ backbone+CH_3}}{I_{CH-ring}} - 3}$$

$$DS_{3\text{-sulfopropyl}} = \frac{7I_{\text{CH}_2\text{-z}}}{2(I_{\text{cellulose backbone+CH}_2\text{-x}} - I_{\text{CH}_2\text{-z}})}$$

3.3.3 Regioselective bromination and acetylation of MCC

The method of MCC dissolution in DMAc/LiBr was adapted from previous work.²⁶ The synthesis of 6-BrCA has been previously published.^{26,27} Briefly, Ph₃P (32.35 g, 4 equiv per anhydroglucose unit (AGU)) was dissolved in 100 mL of DMAc, while 21.95 g NBS (4 equiv per AGU) was dissolved in an additional 100 mL of DMAc. The Ph₃P solution was added dropwise to the MCC solution (5 g MCC in 200 mL DMAc/LiBr), followed by the dropwise addition of the NBS solution. The resulting solution was heated to 70 °C under nitrogen for 1 h. Acetic anhydride (10 equiv per AGU) was then added dropwise, and the resulting solution was stirred overnight at 70 °C. It was then cooled and added slowly to 4 L of a 50:50 (v/v) mixture of methanol and deionized water to precipitate the product, followed by filtration. The precipitate was then twice redissolved in acetone, followed by precipitation in ethanol, and then it was dried overnight in a vacuum oven at 50 °C. Yield: 87%. ¹H NMR (500 MHz, DMSO-*d*₆): 2.00-2.10 (O-(C=O)-CH₃), 3.30-5.40 (cellulose backbone). DS by ¹H NMR: DS(Ac) 2.05. Elemental analysis: %C 38.86, %H 4.33, %N Not Found, %Br 25.32; DS by elemental analysis: DS(Br) 0.98. Average molar mass of AGU, <M>_{6-BrCA} = 309 g/mol.

3.3.4 Synthesis of 6-pyridinio-6-deoxy-2,3-di-*O*-acetyl-cellulose (6-PyrCA)

In a 100 mL three-necked round-bottom flask, 6-BrCA (250 mg) was weighed and dissolved in 10 mL of DMSO. Pyridine (10-100 equiv per AGU) was added to the flask. The solution was heated to 80 °C for a selected time period under nitrogen while stirring.

The solution was transferred to dialysis tubing. After 3 days of dialysis against ethanol and 3 days of dialysis against deionized water, the solution was freeze-dried to yield 6-PyrCA. Data from experiment using 50 equiv pyridine at 80 °C in DMSO: Yield: 77%. ¹H NMR (500 MHz, DMSO-*d*₆): 1.75-2.25 (O-(C=O)-CH₃), 3.00-6.00 (cellulose backbone), 8.20 (N-CH=CH-CH), 8.65(N-CH=CH-CH), 9.04 (N-CH=CH-CH); ¹³C NMR (500 MHz, DMSO-*d*₆): 21.17 (O-(C=O)-CH₃), 60.12 (C-6), 60.15 (C-6'), 71.00-77.00 (C-2, C-3, C-4 and C-5), 98.18 (C-1), 99.67 (C-1'), 128.08 (N-CH=CH-CH), 146.21 (N-CH=CH-CH and N-CH=CH-CH), 169.90 (O-(C=O)-CH₃). DS by ¹H NMR: DS(Pyr⁺) 0.71. Elemental analysis: %C 45.88, %H 4.88, %N 2.86, %Br 15.25. DS by elemental analysis: DS(Pyr⁺) 0.73. Average molar mass of AGU, <M>_{6-PyrCA} = 308 g/mol.

3.3.5 Synthesis of 6-(1-methyl-3-imidazolyl)-6-deoxy-2,3-di-O-acetyl-cellulose (6-MeIMCA)

6-BrCA (250 mg) was dissolved in 10 mL of DMSO in a 100 mL three-necked round-bottom flask. 1-Methylimidazole (10-100 equiv per AGU) was added to the flask. The solution was heated to 80 °C and stirred for a selected time period under nitrogen. The cooled solution was transferred to dialysis tubing. After 3 days of dialysis against ethanol and 3 days of dialysis against deionized water, the solution was freeze-dried to yield 6-MeIMCA. Data from experiment using 10 equiv 1-methylimidazole at 80 °C in DMSO: Yield: 88%. ¹H NMR (500 MHz, DMSO-*d*₆): 1.75-2.25 (O-(C=O)-CH₃), 3.00-6.00 (cellulose backbone and N-CH₃), 7.83 (N-CH=CH-N-CH₃ and N-CH=CH-N-CH₃), 9.47 (N=CH-N-CH₃); ¹³C NMR (500 MHz, DMSO-*d*₆): 21.05 (O-(C=O)-CH₃), 36.10 (N-CH₃), 49.40 (C-6), 62.57 (C-6'), 71.00-77.00 (C-2, C-3, C-4 and C-5), 98.58 (C-1),

99.69 (C-1'), 123.42 (N-CH=CH-N-CH₃), 123.70 (N-CH=CH-N-CH₃), 137.71 (N=CH-N-CH₃), 169.82 (O-(C=O)-CH₃). DS by ¹H NMR: DS(MeIM⁺) 0.74. Elemental analysis: %C 41.32, %H 4.82, %N 5.25, %Br 14.26. DS by elemental analysis: DS(MeIM⁺) 0.70. Average molar mass of AGU, <M>_{6-MeIMCA} = 310 g/mol.

3.3.6 Syntheses of 6-imidazolyl-6-deoxy-2,3-di-O-acetyl-cellulose (6-IMCA) and 6-(1-(3-sulfopropyl)-3-imidazolyl)-6-deoxy-2,3-di-O-acetyl-cellulose (6-SPrIMCA)

Under nitrogen in a 100 mL three-necked round-bottom flask, 6-BrCA (250 mg) was dissolved in 10 mL of DMSO. Imidazole (50 equiv per AGU) was added to the flask and dissolved. The solution was heated to 80 °C for 48 h under nitrogen with mechanical stirring. The cooled reaction solution was added to dialysis tubing, followed by 3 days of dialysis against ethanol and 3 days of dialysis against deionized water. The retentate was finally freeze-dried to yield 6-IMCA. Yield: 75%. ¹H NMR (500 MHz, DMSO-*d*₆): 1.70-2.30 (O-(C=O)-CH₃), 3.00-6.00 (cellulose backbone), 7.70 (N-CH=CH-N), 7.74 (N-CH=CH-N), 9.08 (N-CH=N); ¹³C NMR (500 MHz, DMSO-*d*₆): 21.02 (O-(C=O)-CH₃), 46.88 (C-6), 62.56 (C-6'), 71.00-77.00 (C-2, C-3, C-4 and C-5), 98.36 (C-1), 99.66 (C-1'), 120.48 (N-CH=CH-N), 128.97 (N-CH=CH-N), 138.05 (N-CH=N), 169.87 (O-(C=O)-CH₃). DS by ¹H NMR: DS(IM) 0.74. Elemental analysis: %C 49.31, %H 5.15, %N 6.47. DS by elemental analysis: DS(IM) 0.72.

6-IMCA (100 mg) was dissolved in 5 mL of DMSO in a 25 mL three-necked round-bottom flask under nitrogen. Then 3 equiv per AGU of 1,3-propane sultone was added. The resulting solution was heated to 80 °C and stirred 20 h under nitrogen. The cooled solution

was transferred to dialysis tubing, followed by 3 days of dialysis against ethanol and 3 days of dialysis against deionized water. The resulting precipitate was collected by filtration, and then the sulfobetaine-containing product, 6-(1-(3-sulfopropyl)-3-imidazolio)-6-deoxy-2,3-di-*O*-acetyl-cellulose (6-SPrIMCA), was dried overnight in a vacuum oven at 50 °C. Yield: 67%. ¹H NMR (500 MHz, DMSO-*d*₆): 1.70-2.10 (O-(C=O)-CH₃ and N-CH₂-CH₂-CH₂-SO₃), 2.68 (N-CH₂-CH₂-CH₂-SO₃), 3.00-6.00 (cellulose backbone and N-CH₂-CH₂-CH₂-SO₃), 7.50-8.00 (N-CH=CH-N and N-CH=CH-N), 9.16 (N-CH=N). DS by ¹H NMR: DS(3-sulfopropyl) 0.43.

3.3.7 Self-assembled monolayer (SAM) preparation and surface plasmon resonance (SPR)

Square SPR gold sensors (20 mm × 20 mm) were loaded into an UV/Ozone Procleaner for 20 min, and were then placed face-up in a solution of 1:1:5 (v/v/v) hydrogen peroxide: ammonium hydroxide: ultrapure water. The solution was heated to boiling for at least 40 min. Then each sensor was rinsed with ultrapure water, and dried under nitrogen. The cleaned sensor slides were then placed in a 1 mM solution of 16-mercapto-hexadecanoic acid or 1-hexadecanethiol absolute ethanol for at least 24 h. The slide was then removed from the solution, rinsed with absolute ethanol to remove excess 16-mercapto-hexadecanoic acid, and dried with nitrogen. Finally, the SAM sensor slide was washed with ultrapure water and dried with nitrogen.

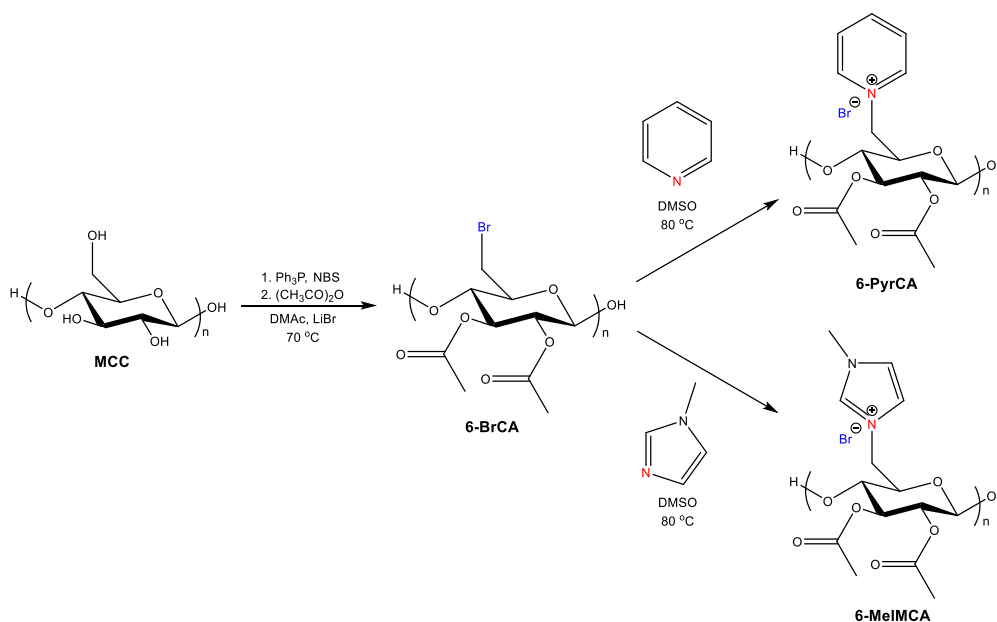
Cationic cellulose derivative adsorption onto SAM surfaces was investigated by SPR. The sensor slide with the desired film (bare gold, SAM-COOH, SAM-CH₃) was refractive

index-matched to the prism of a Reichert SR 7000 surface plasmon resonance refractometer with immersion oil. This SPR system used a laser diode with an emission wavelength of 780 nm. The flow cell was equipped with a Viton gasket (Dupont Dow Elastomers, LLC) and was mounted on top of the sensor slide. Solutions were pumped into the flow cell at a flow rate of 0.10 mL/min via Teflon tubing connected to a cartridge pump (Masterflex) at 20 °C. The pump was linked to a switch valve that made it possible to switch between the polymer solutions and ultrapure water without the introduction of air bubbles into the system. 6-PyrCA and 6-MeIMCA solutions were prepared from stock solutions by dilution with ultrapure water and were degassed before SPR experiments. Prior to data acquisition, gold or SAM-COOH surfaces were allowed to reach equilibrium swelling as ultrapure water was flowed through the system. Once a stable baseline was established, 6-PyrCA or 6-MeIMCA solution was pumped into the flow cell. Each solution flowed over the sensor until adsorption ceased and was followed by a switch to water via the solvent selection valve.

3.4 Results and Discussion

Synthesis of cationically substituted polysaccharide derivatives by direct displacement of 6-halo substituents by amines is a simple and appealing approach, particularly so because of the essentially complete regioselectivity for C-6 substitution of Furuhashi bromination²⁷. There is reason for concern about the potential of this approach however, since substitution could be limited by developing charge along the cellulose chain; at a certain point charge-charge repulsion of the cationic substituents may impede creation of additional positive charges. A similar phenomenon limits the achievable DS (in one pass) of carboxymethyl

groups (anionically charged) in the synthesis of carboxymethyl cellulose to approximately half of the theoretical maximum.²⁸ Other work in our laboratory has shown that displacement of 6-halides from derivatives of cellulose or curdlan by trialkylamines does indeed seem to be limited by developing cationic charge,^{23,24} and large reagent excesses and other measures were required to achieve high DS of the cationic substituents. On the other hand, aromatic amines are often better nucleophiles than trialkylamines because of reduced steric hindrance and other factors²⁹, and the resulting aromatic substituent on the quaternary ammonium salt should be better able to disperse positive charge, so we were hopeful that the direct approach might be particularly useful for aromatic amines.



Scheme 3.1. Reaction scheme for conversion of cellulose to cationic cellulose derivatives.

3.4.1 6-Bromo-6-deoxy-2,3-di-O-acetyl-cellulose

Using a reaction reported by Furuhashi et al.²⁷, cellulose can be directly brominated using Ph₃P and NBS with selectivity at C-6 that appears to be complete by spectroscopic and

monosaccharide analyses, affording 6-bromo-6-deoxycellulose. Acetylation of 6-bromo-6-deoxycellulose affords fully regioselectively substituted derivatives that exhibit good solubility in polar aprotic solvents such as DMSO, DMF or DMAc, and thus can be widely used to prepare other regioselectively substituted derivatives by displacement of the 6-bromo substituent.^{26,30,31} Using an adaptation of that reported procedure, we prepared 6-BrCA (Scheme 3.1), which was then dissolved in DMSO for further reactions with *N*-heterocyclic compounds. DS(Ac) of 6-BrCA was calculated by integration of the ¹H NMR spectrum (Figure 3.1) as 2.05, and thus DS(Br) was 0.95 by difference. DS(Br) calculated from elemental analysis was 0.98, showing good agreement between the two methods.

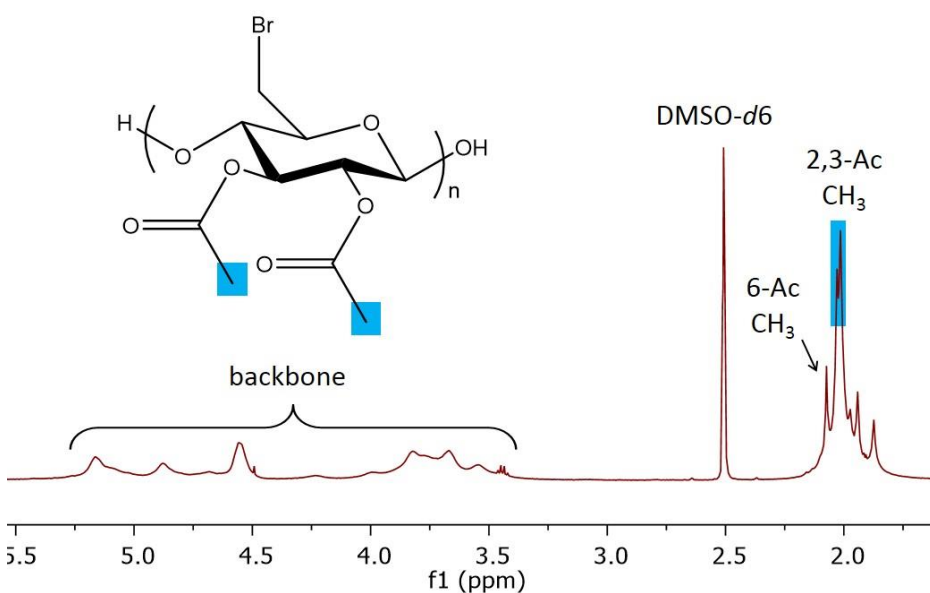


Figure 3.1. ¹H NMR spectrum of 6-bromo-6-deoxy-2,3-di-*O*-acetyl-cellulose (6-BrCA).

3.4.2 Cationic *N*-heterocyclic cellulose derivatives

Direct displacement of bromide from 6-BrCA was attempted with pyridine as a reagent in DMSO at 80 °C for 48 h (Scheme 3.1). Initially, we added 30 equiv pyridine per AGU to the 6-BrCA solution in DMSO. ¹H NMR spectroscopy confirmed that product identity was

as targeted, 6-PyrCA (Figure 3.2); new resonances at 8-10 ppm belong to the aromatic protons of the added pyridinium substituent. The ^{13}C NMR spectrum (see Supporting Information, Figure S3.1) supported this proposed product identity; for example the chemical shift for C-6 appeared at 50 ppm, shifted downfield from 32 ppm in the brominated starting material. No trace of the starting material brominated carbon remains in the product spectrum. A weak signal from an acetylated C-6 is evident at 62 ppm, due to a previously observed minor side reaction during the bromination step between the cellulose and the DMAc reaction solvent.²⁶ The FTIR spectra (see Supporting Information, Figure S3.3) demonstrate that compared to 6-BrCA, a weak C₆-N stretch at 1560 cm⁻¹ and an aromatic C-H bending absorption at 760 cm⁻¹ appear in the spectrum of 6-PyrCA, indicating successful pyridinium incorporation. In addition, the disappearance of the weak C-Br absorption at ca. 550 cm⁻¹ from the starting material spectrum supports the contention that most of the bromide was displaced by pyridine. A broad absorption present around 3500 cm⁻¹ suggests the presence of free hydroxyl groups, most likely resulting from moisture in the hygroscopic sample. Pyridine base could in theory catalyze the hydrolysis or deacetylation of some cellulose ester groups.³² However, DS(Ac) was measured by ^1H NMR to be 2.07, indicating that little or no deacetylation occurred during the S_N2 displacement. Compared to related displacements by trialkylamines,^{23,24} pyridine displacement appeared to be relatively clean and efficient, as we had hypothesized.

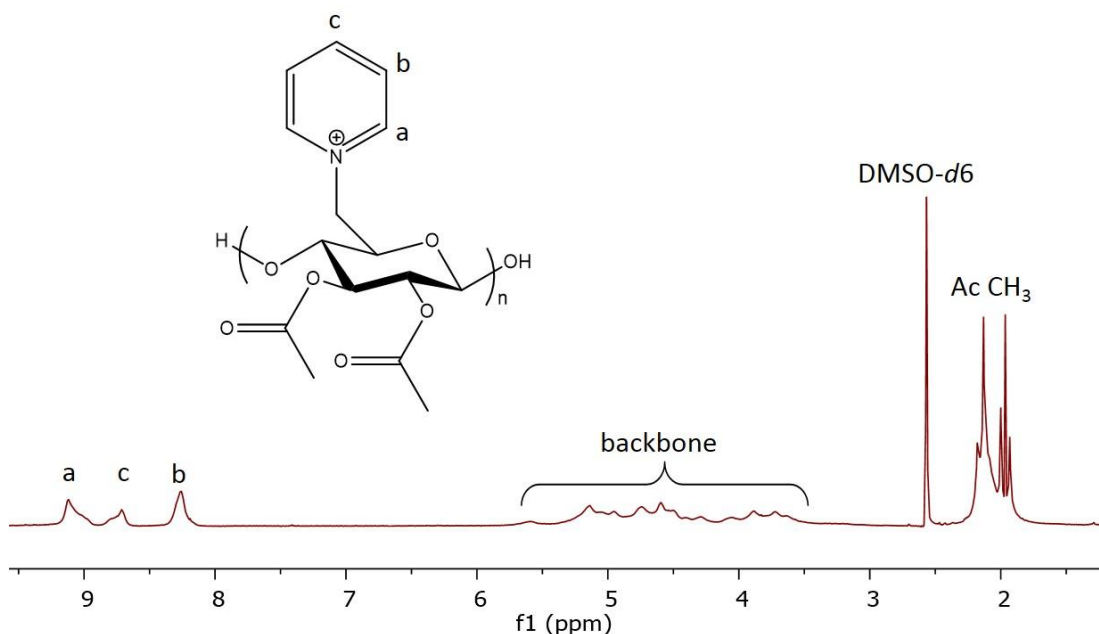


Figure 3.2. ^1H NMR spectrum of 6-pyridinio-6-deoxy-2,3-di-*O*-acetyl-cellulose (6-PyrCA).

With the success of pyridinium substitution, we wished to explore further the breadth of this synthesis of cationic cellulose derivatives using other *N*-heterocyclic compounds, in order to improve the reaction efficiency and obtain more highly charged cellulose esters. It is known that nucleophilicity is one of the important factors affecting the efficiency of $\text{S}_{\text{N}}2$ displacements³³, and the pK_{a} of pyridine is only moderately high at 5.2 (see Supporting Information, Table S3.1). Therefore, we thought that pyridine might not be an optimal nucleophile for the $\text{S}_{\text{N}}2$ displacement.³⁴ In order to improve reaction conversion, an *N*-heterocyclic compound with higher nucleophilicity is needed. 1-Methylimidazole, whose pK_{a} is 7.4 (see Supporting Information, Table S3.1), was deemed to be a promising candidate for this displacement reaction.

We attempted to synthesize 6-MeIMCA by a method analogous to that used for the pyridinium derivatives, reacting 6-BrCA with 1-methylimidazole in DMSO at 80 °C (Scheme 3.1). Initially 30 equiv 1-methylimidazole per AGU was employed. The ^1H NMR spectrum of the product (Figure 3.3) shows new resonances at 7.5 - 9.5 ppm, belonging to the aromatic protons of the 1-methylimidazolium substituent, and a sharp and strong peak at 4 ppm from the protons of the N-methyl group. The product ^{13}C NMR spectrum (see Supporting Information, Figure S3.2) shows a new resonance for the imidazolium-substituted C-6 at 50 ppm, and no trace of the brominated carbon (32 ppm) remains in the product spectrum. The weak signal at 62 ppm is from a small amount of C-6 acetylation from the side reaction with DMAc, as described for the pyridinium derivative. The FTIR spectrum (see Supporting Information, Figure S3.4) shows a C₆-N stretch at 1560 cm^{-1} and ester C=O stretch at 1761 cm^{-1} , indicating successful incorporation of 1-methylimidazolium, and suggesting retention of the 2, 3-*O*-ester groups. The absorption at ca. 3500 cm^{-1} is again likely from a small amount of moisture in the hygroscopic sample. The HMBC spectrum (Figure 3.4) shows that there is a correlation (blue circled) between the aromatic protons of the 1-methylimidazolium substituent (7.8 ppm) and C-6 (50 ppm), while no correlation between aromatic protons and other carbons on the cellulose backbone is found. The result from the HMBC spectrum supports the contention that the *N*-heterocyclic substitution is regioselective and occurs exclusively at C-6.

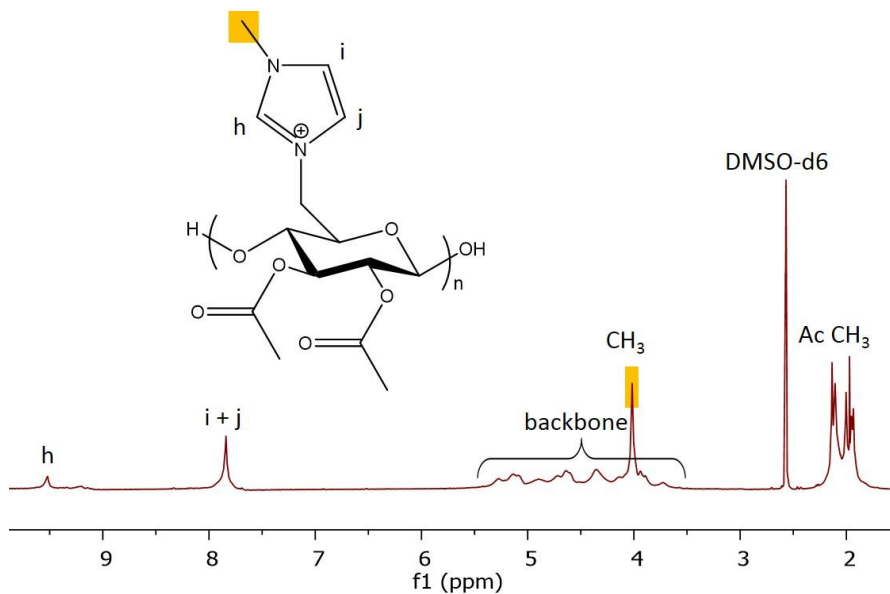


Figure 3.3. ^1H NMR spectrum of 6-(1-methyl-3-imidazolio)-6-deoxy-2,3-di-*O*-acetylcellulose (6-MeIMCA).

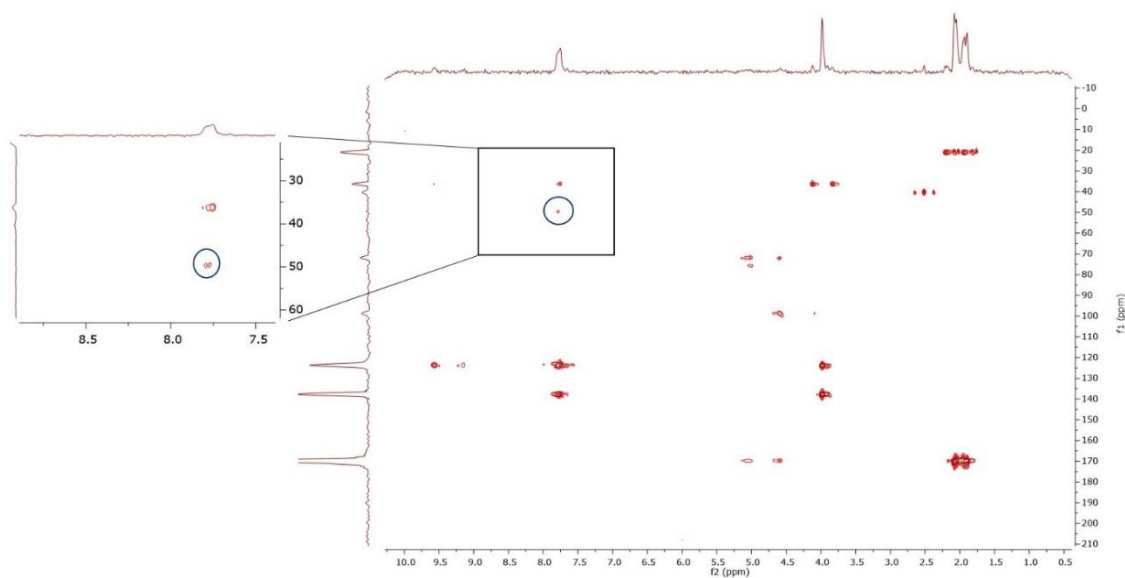


Figure 3.4. HMBC spectrum of 6-(1-methyl-3-imidazolio)-6-deoxy-2,3-di-*O*-acetylcellulose (6-MeIMCA).

We explored reaction conditions seeking those that would achieve near-complete displacement, while being as efficient as possible with regard to reagent use. If one or more of these derivatives proves to be effective in biomedical applications like gene delivery or tight junction opening, it would be undesirable from a toxicological perspective to allow the presence of residual unreacted alkyl bromide at C-6. First we examined the effect of the ratio of pyridine equiv/AGU (10 - 100) using an otherwise standardized set of conditions (6-BrCA in DMSO at 80 °C for 2 days), with product pyridinium DS calculated from ^1H NMR spectra. As expected the reaction conversion ($\text{DS}(\text{Pyr}^+)$) rises with increasing equivalents pyridine/AGU (Table 3.1), but $\text{DS}(\text{Pyr}^+)$ levels off around 0.70 as equiv. (pyridine) reaches 50/AGU. Therefore, we can conclude that $\text{DS}(\text{Pyr}^+) \sim 0.71$ or conversion $\sim 75\%$ is the upper limit for this reaction under these conditions. In comparison to trialkylamine displacement, the $\text{DS}(\text{Pyr}^+)$ is much higher than that of triethylammonium obtained by $\text{S}_{\text{N}}2$ substitution of the C-6 Br ($\text{DS} \sim 0.4$) under similar conditions.²³ We expect that the higher $\text{DS}(\text{Pyr}^+)$ obtained is due to the fact that the nucleophilic pyridine nitrogen atom is less sterically encumbered than that of triethylamine, and thus pyridine is able to more easily approach C-6 of 6-BrCA, affording high reaction efficiency, even though triethylamine is a stronger base than pyridine.³⁵ The greater ability of pyridinium to disperse positive charge may also contribute to the higher DS observed.

Table 3.1. Effect of equiv (Pyr⁺) on reaction with 6-bromo-6-deoxy-2,3-di-*O*-acetyl-cellulose*

Equivalent / AGU	DS(Pyr ⁺)	Conversion (%)
10	0.25	26
30	0.51	54
50	0.69	73
70	0.69	73
100	0.71	75

*DMSO solvent, 80 °C, conversion(%) = DS(Pyr⁺)/DS(Br) × 100% from ¹H NMR.

The relationship between equiv (10, 20, 30 or 40 per AGU) 1-methylimidazole and DS or reaction conversion was investigated in similar fashion as described for the pyridine reaction. In contrast to pyridine displacement, 1-methylimidazolium DS does not vary significantly with the molar excess of 1-methylimidazole, remaining around 0.79 (see Supporting Information, Table S3.2); 20 equiv 1-methylimidazole/AGU is enough to ensure maximum reaction conversion under these conditions, with no apparent deacylation as indicated by both ¹H NMR and FTIR spectra. The highest DS(MeIM⁺) obtained from 1-methylimidazole displacement is slightly higher than that of pyridinium, since 1-methylimidazole is a slightly better nucleophile than is pyridine.

Moreover, since partial cellulose degradation can occur under some conditions at 80 °C or higher,²⁵ it was important to understand the kinetics of pyridine or 1-methylimidazole

substitution, in order to avoid unnecessary DP loss and maintain high reaction efficiency. Initially, S_N2 reaction progress was monitored by a kinetic study in which 50 equiv Pyr/AGU reacted with 6-BrCA and the reaction product was isolated after predetermined times (12, 24, 36, 48, 60 and 72 hours) for ¹H NMR analysis (Table 2.2). After 12 h, DS(Pyr⁺) = 0.28 is obtained, increasing to the maximum of 0.71 by 48 h, and leveling off at that point; longer reaction time does not afford higher DS(Pyr⁺).

Table 3.2. Kinetic study of pyridine displacement on 6-bromo-6-deoxy-2,3-di-*O*-acetyl-cellulose*

Reaction time (h)	DS(Pyr ⁺)	Conversion (%)
12	0.28	29
24	0.49	52
36	0.60	63
48	0.71	75
60	0.71	75
72	0.73	77

*DMSO solvent at 80 °C, conversion(%) = DS(Pyr⁺)/DS(Br) × 100% from ¹H NMR.

A similar kinetic study was carried out to monitor 1-methylimidazole (10 equiv/AGU) substitution progress by ¹H NMR analysis (Table 3.3). Imidazolium substitution increases to 0.74 after 36 h, and levels off at ca. 0.79 after 48 h, slightly higher DS than for pyridine at the same reaction time (Table 3.2), even though a five-fold lower mole ratio of 1-methylimidazole was used than for pyridine.

Table 3.3. Kinetic study of 1-methylimidazole displacement on 6-bromo-6-deoxy-2,3-di-*O*-acetyl-cellulose*

Reaction time (h)	DS(MeIM ⁺)	Conversion (%)
12	0.41	43
24	0.62	65
36	0.74	78
48	0.79	83
60	0.79	83
72	0.79	83

*DMSO solvent at 80 °C, conversion (%) = DS(MeIM⁺)/DS(Br) × 100% from ¹H NMR.

The effect of solvent was also explored; other polar aprotic solvents, DMAc and DMF, were examined under otherwise identical conditions. DMSO afforded the highest conversion to DS(MeIM⁺) = 0.79, while in the other solvents lower DS values were obtained (0.74 and 0.68 in DMAc and DMF, respectively (Table 3.4)). We attempted unsuccessfully to determine molecular weights for 6-PyrCA and 6-MeIMCA by size exclusion chromatography (SEC) in DMAc, THF or DMF systems, observing considerable aggregation in each solvent system, confirmed by dynamic light scattering experiments. This sort of behavior has been previously observed for other polyelectrolytes upon attempted SEC analysis.³⁶ Solubility of the cationic derivatives is also important to their suitability in biomedical and other applications. Both 6-PyrCA and 6-MeIMCA were found to exhibit good solubility in common polar aprotic solvents such as DMSO and DMF.

Moreover, whereas the starting 6-BrCA is insoluble in water, the 6-Pyr- (DS 0.71) and 6-MeIM- (DS 0.79) derivatives are soluble in water (Figure 3.5), enhancing their potential for use in areas such as coatings, or gene or drug delivery.

Table 3.4. Solvent effects on 1-methylimidazole substitution*

Solvent	DS(MeIM ⁺)
DMSO	0.79
DMAc	0.74
DMF	0.68

*at 80 °C for 24 h

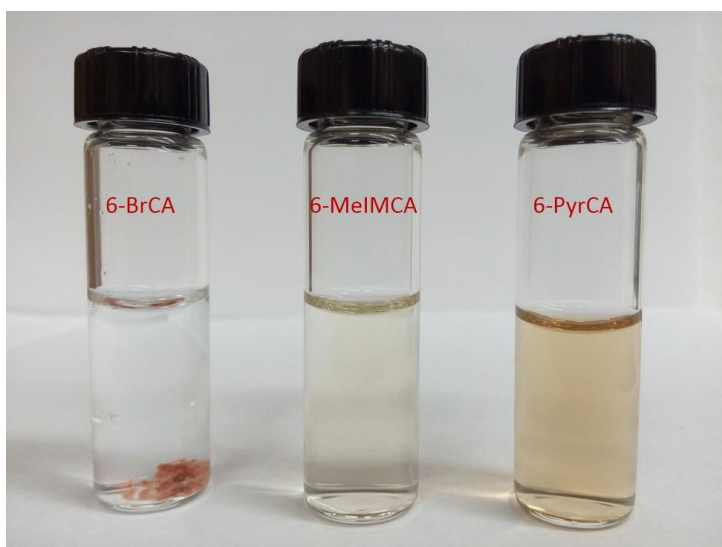


Figure 3.5. Comparison of water solubility among 6-bromo-deoxy-2,3-di-*O*-acetyl-cellulose, 6-(1-methyl-3-imidazolium)-6-deoxy-2,3-di-*O*-acetyl-cellulose (1 mg/mL) and 6-pyridinium-6-deoxy-2,3-di-*O*-acetyl-cellulose (1 mg/mL).

3.4.3 Thermal stability of cationic *N*-heterocyclic cellulose derivatives

Thermal stability is of interest for these ammonium-containing polymers, since quaternary ammonium compounds (e.g. tetraalkylammonium salts) can undergo Hofmann elimination reactions at high temperature.³⁷ Therefore, we investigated the thermal stability of 6-PyrCA and 6-MeIMCA using TGA. As Table 3.5 and Figure S3.5 (see Supporting Information) show, the degradation temperature (T_d) of 6-BrCA is 207 °C, while 6-PyrCA ($DS(Pyr^+) = 0.71$) and 6-MeIMCA ($DS(MeIM^+) = 0.79$) do not degrade until 250 °C. Moreover, three 6-PyrCA samples with different $DS(Pyr^+)$ (0.25, 0.51 and 0.71) were compared with regard to thermal stability. It was interesting to observe (Table 3.6) that degradation temperature (T_d) increases as $DS(Pyr^+)$ increases; the highest $DS(Pyr^+)$ (0.71) sample possesses the highest T_d (249 °C). This interesting and unexpected thermal stability is worthy of further mechanistic study, but in any case is encouraging with regard to potential use of 6-PyrCA and 6-MeIMCA as durable materials for specific applications at higher temperatures.

Table 3.5. Degradation temperatures of 6-bromo-deoxy-2,3-di-*O*-acetyl-cellulose (6-BrCA), 6-pyridinio-6-deoxy-2,3-di-*O*-acetyl-cellulose (6-PyrCA) and 6-(1-methyl-3-imidazolium)-6-deoxy-2,3-di-*O*-acetyl-cellulose (6-MeIMCA)

Derivatives	T_d (°C)
6-BrCA	207
6-PyrCA	249
6-MeIMCA	251

Table 3.6. Degradation temperatures of 6-pyridinio-6-deoxy-2,3-di-*O*-acetyl-cellulose (6-PyrCA) vs. DS(Pyr⁺)

DS(Pyr ⁺)	T _d (°C)
0.25	214
0.51	224
0.71	249

3.4.4 Adsorption of cationic *N*-heterocyclic cellulose derivatives onto SAM-COOH surfaces

Having developed synthetic access to cationic cellulose derivatives, it was important to quantify their interactions with anionic molecules and surfaces. As a preliminary investigation of their binding properties, we employed SPR to study the adsorption of these cationic cellulose derivatives onto a hydrophilic and anionic surface, gold functionalized by a self-assembled monolayer of 16-mercaptohexadecanoic acid (SAM-COOH). Ultrapure water was initially flowed over the SAM-COOH surfaces to reach equilibrium swelling. Once a stable baseline was established, 6-PyrCA or 6-MeIMCA aqueous solution was allowed to flow over the surface until adsorption ceased. Then the flowing solution was switched to ultrapure water for the removal of reversibly adsorbed cellulose derivative. A representative SPR curve for the adsorption of 1 mg/mL 6-PyrCA aqueous solution onto a SAM-COOH surface is provided in Figure 3.6. As Figure 3.6 shows, most of the adsorption was irreversible, as the majority of adsorbed cationic cellulose derivative remained attached to the SAM-COOH surface after the surface was rinsed with ultrapure

water. Moreover, the adsorption of 6-MeIMCA aqueous solution onto SAM-COOH monitored by SPR also exhibited a similarly high degree of irreversible binding. Thus, based upon these SPR results, it is demonstrated that 6-PyrCA and 6-MeIMCA are capable of binding strongly to hydrophilic and anionic molecules.

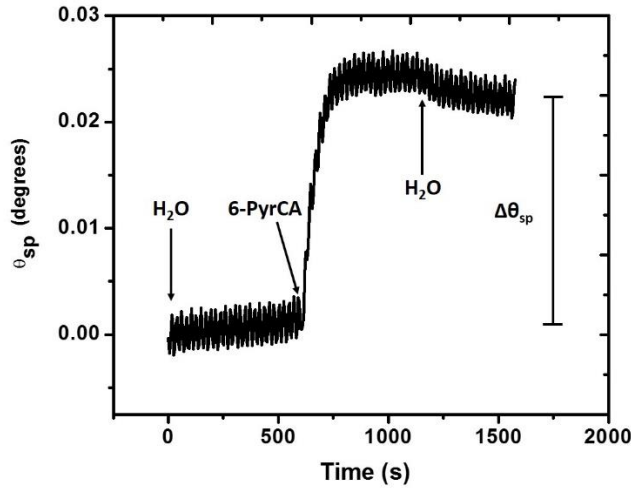


Figure 3.6. Representative SPR data for the adsorption of 1 mg/mL 6-PyrCA onto SAM-COOH surface. Label arrows indicate where a solution started flowing.

At least three parallel trials were carried out for $\Delta\theta_{sp}$ at each concentration and $\Delta\theta_{sp}$ was converted to surface concentration (Γ_{SPR}) using the formula of de Feijter et al.³⁸:

$$\Gamma_{SPR} = \frac{\Delta\theta_{sp}}{(d\theta/dL)} \frac{(n_f - n)}{(dn/dc)} \quad (1)$$

where n_f is the refractive index of the film (assumed to be 1.45), $n = 1.333$ is the refractive index of water, $(d\theta/dL) = 0.0039 \text{ deg} \cdot \text{\AA}^{-1}$ was obtained from Fresnel calculations, and $(dn/dc) = 0.146 \text{ mL/g}$.³⁹

Surface vs. bulk concentrations for 6-PyrCA and 6-MeIMCA adsorption onto SAM-COOH surfaces are shown in Figure 3.7. Irreversible adsorption of 6-PyrCA and 6-MeIMCA onto SAM-COOH surfaces plateaued at $\Gamma_{\text{SPR}} \sim 0.44 \text{ mg}\cdot\text{m}^{-2}$ and $0.47 \text{ mg}\cdot\text{m}^{-2}$, respectively. Values of Γ_{SPR} for adsorption of both 6-PyrCA and 6-MeIMCA are remarkably similar to calculated values for a flat cellulose monolayer ($\sim 0.45 \text{ mg}\cdot\text{m}^{-2}$, assuming an anhydroglucose cross-sectional area of $\sim 66 \text{ \AA}^2 \cdot \text{molecule}^{-1}$)⁴⁰. Adsorption onto bare gold and SAM-CH₃ surfaces was also investigated by SPR. Surface vs. bulk concentrations for 6-PyrCA and 6-MeIMCA adsorption onto bare gold surfaces are shown in Figure S10. Irreversible adsorption of 6-PyrCA and 6-MeIMCA onto bare gold surfaces plateaued at $\Gamma_{\text{SPR}} \sim 1.65 \text{ mg}\cdot\text{m}^{-2}$ and $1.55 \text{ mg}\cdot\text{m}^{-2}$, respectively. Wettabilities of different surfaces (bare gold, SAM-COOH and SAM-CH₃) were also studied by static water contact angles before and after 6-PyrCA or 6-MeIMCA adsorption (see Supporting Information, Table S3.3). In addition to SPR and contact angle measurements, the surface morphologies were studied by atomic force microscopy (AFM) (see Supporting Information, Figures S3.11 and S3.12). Comparisons of AFM images and RMS roughness values revealed no significant differences between 6-PyrCA or 6-MeIMCA adsorption onto the SAM-COOH surfaces. The AFM images after 6-PyrCA or 6-MeIMCA adsorbed onto SAM-COOH are consistent with a flat monolayer. In contrast, 6-PyrCA or 6-MeIMCA adsorbed onto bare gold surfaces as aggregates with an increase in the RMS roughness. Similar behavior was observed for 6-PyrCA and 6-MeIMCA adsorption onto SAM-CH₃ surfaces, although Γ_{SPR} for 1 mg/mL solutions were smaller than for adsorption onto gold (see Supporting Information, Figure S3.13). For SAM-CH₃ surfaces, dispersive interactions drive the adsorption, whereas gold surfaces have both dispersive interactions and image charge that

can enhance adsorption. The observation of aggregates for the SAM-CH₃ and gold surfaces indicates three-dimensional conformations of the polymers. In contrast, the adsorption of the highly charged polymers on the highly and oppositely charged surface avoids aggregate formation leading to quasi-two-dimensional conformations. Since both cellulose derivatives are highly charged, the likelihood of monolayer coverage is also examined in terms of current theories for polyelectrolyte adsorption and their predictions for theoretical surface concentrations (Γ).

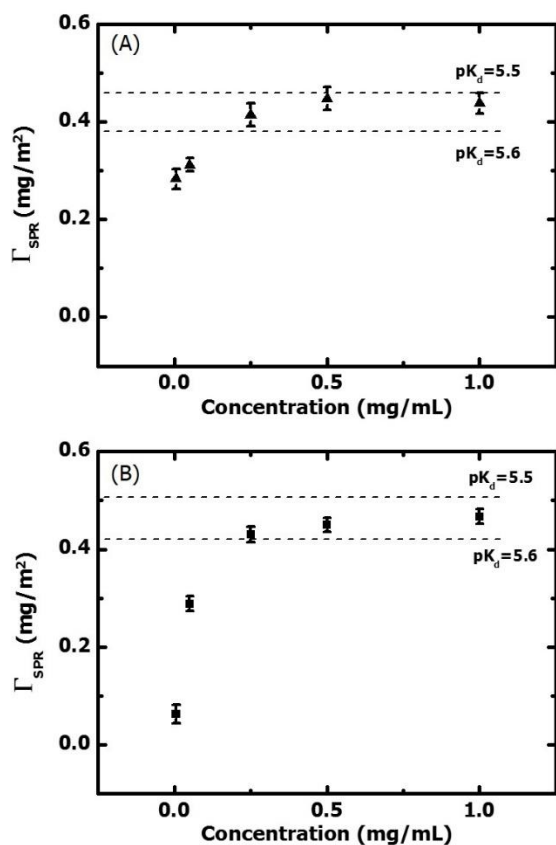


Figure 3.7. Surface vs. bulk concentrations for (A) 6-PyrCA and (B) 6-MeIMCA adsorption onto SAM-COOH surfaces at 20 °C. The dashed lines are theoretical surface concentrations for 6-PyrCA and 6-MeIMCA adsorbed on SAM-COOH at pK_a 5.5 and 5.6.

Based upon the scaling theory of polyelectrolyte adsorption at oppositely charged surfaces developed by Dobrynin et al.,⁴¹ at very low salt concentrations, two-dimensional (2D) adsorbed layers are formed due to the balance between chain entropy penalties and the energy gained through electrostatic attractions to the charged surface. Under these conditions, the 2D adsorbed polyelectrolyte neutralizes the oppositely charged SAM surface. Therefore, the surface charge density (σ) for SAM-COOH is equal to and opposite in sign to the charge density of the adsorbed cationic cellulose derivatives. In this limit:

$$\Gamma = M_{\text{blob}} \times n \quad (2)$$

where the equivalent molar mass per mole of charge $M_{\text{blob}} = \langle M \rangle / \text{DS}$ of the charged group (Pyr⁺ or MeIM⁺) and n , the moles of adsorbed charge per unit area is given as

$$n = \frac{|\sigma|}{e \times N_A} \quad (3)$$

where $|\sigma|$ represents the absolute value of the surface charge density of the SAM-COOH, e is the elementary charge and N_A is Avogadro's number.

Fears et al.⁴² published a model for σ for SAMs. The Henderson-Hasselbalch equation relates the bulk pH to the relative concentrations of the protonated (C_{COOH}) and deprotonated (C_{COO^-}) forms of the SAM-COOH molecules and their effective surface dissociation constant (K_d):

$$\text{pH} = \text{p}K_d + \log \left(\frac{C_{\text{COO}^-}}{C_{\text{COOH}}} \right) \quad (4)$$

Rearrangement of Equation 4 yields the fraction (f) of ionized molecules in the SAM-COOH:

$$f = \left(\frac{C_{\text{COO}^-}}{C_{\text{COOH}} + C_{\text{COO}^-}} \right) = \frac{10^{(\text{pH} - \text{pK}_d)}}{1 + 10^{(\text{pH} - \text{pK}_d)}} \quad (5)$$

The result of Equation 5 can be used to calculate σ :

$$\sigma = \frac{|z_i|fe}{A} = 0.749|z_i|f \quad (6)$$

where z_i is -1 for SAM-COOH, and $A = 21.4 \text{ \AA}^2/\text{alkanethiol chain}$ is the cross-sectional area for an alkanethiol-SAM chain formed on a gold (111) surface⁴³.

Application of Equations 2, 3, 5 and 6 to the adsorption of 6-PyrCA and 6-MeIMCA requires a value for the pK_d of the SAM-COOH. Literature values for pK_d vary widely (5.2-10.3) for SAM-COOH on the basis of technique and length of the hydrocarbon spacer between the gold surface and the COOH. However, many of the effective pK_d values for SAM-COOH are in a range of 5 to 6.⁴²⁻⁴⁴ Values of $\text{pK}_d = 5.5$ and 5.6 for SAM-COOH, in conjunction with the measured average pH values for 1 mg/mL 6-PyrCA and 6-MeIMCA, of 4.7 and 4.8, respectively, bracketed the plateau regions of Γ_{SPR} versus bulk concentration in Figure 7. These pK_d values correspond to $f = 0.14$, $\sigma = 0.10 \text{ C/m}^2$ and $\Gamma = 0.46 \text{ mg/m}^2$ ($\text{pK}_d = 5.5$, 6-PyrCA); $f = 0.17$, $\sigma = 0.12 \text{ C/m}^2$ and $\Gamma = 0.51 \text{ mg/m}^2$ ($\text{pK}_d = 5.5$, 6-MeIMCA); $f = 0.11$, $\sigma = 0.08 \text{ C/m}^2$ and $\Gamma = 0.38 \text{ mg/m}^2$ ($\text{pK}_d = 5.6$, 6-PyrCA); and $f = 0.14$, $\sigma = 0.10 \text{ C/m}^2$ and $\Gamma = 0.42 \text{ mg/m}^2$ ($\text{pK}_d = 5.6$, 6-MeIMCA). These values along with the experimentally Γ_{SPR} are reasonable and consistent with essentially monolayer adsorption

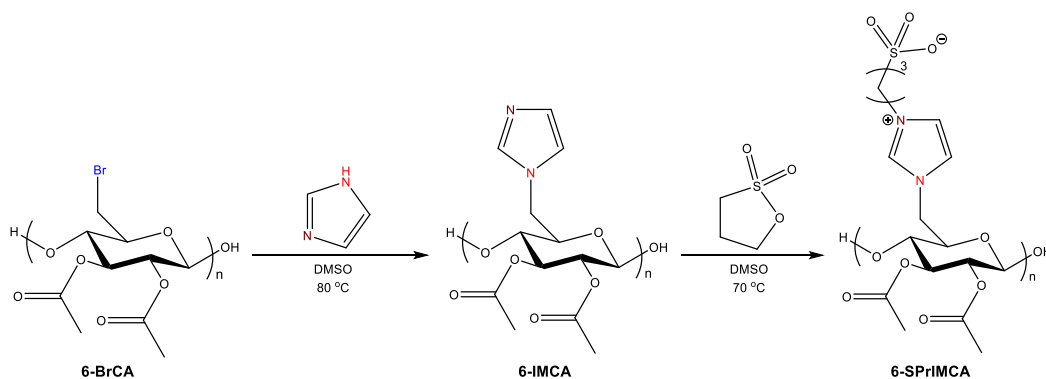
of 6-PyrCA and 6-MeIMCA on SAM-COOH via a charge neutralization mechanism in the low salt limit. This behavior is different from recent work in the literature⁴⁶⁻⁴⁸ for polysaccharide polyelectrolyte adsorption onto cellulose and other surfaces where ions such as Ca²⁺ and Na⁺ shift adsorption away from the low salt regime⁴¹ and afford thicker adsorbed polyelectrolyte layers because of charge screening.

3.4.5 6-Imidazolyl-6-deoxy-2,3-di-*O*-acetyl-cellulose and 6-(1-(3-sulfopropyl)-3-imidazolyl)-6-deoxy-2,3-di-*O*-acetyl-cellulose

The success of 1-methylimidazolium substitution led us to believe that a variety of imidazolium-containing cellulose derivatives could be prepared in similar fashion. It was of particular interest for us to explore the reaction between 6-BrCA and imidazole. Unlike 1-methylimidazole or other imidazolium compounds, imidazole contains two nucleophilic nitrogen atoms. If imidazole can be efficiently incorporated on cellulose via S_N2 reaction of one basic imidazole nitrogen displacing a C-6 bromide, the other basic nitrogen of imidazole could then be used as a nucleophile for further incorporation of other interesting functional groups. On the other hand, there was also the danger that this difunctional amine could cause crosslinking by further reaction of the second nucleophilic nitrogen with 6-halo-6-deoxy substituents on other cellulose chains.

To determine whether monosubstitution without crosslinking could be successful, excess imidazole was employed to react with 6-BrCA in DMSO at 80 °C for 48 h (Scheme 3.2). ¹H NMR spectroscopy (Figure 3.8) confirmed the identity of 6-IMCA; new resonances at 8-10 ppm belong to the aromatic protons of the introduced imidazole substituent. The ¹³C

NMR spectrum (see Supporting Information, Figure S3.6) supported this proposed product identity; for example the chemical shift for substituted C-6 appeared at 50 ppm, shifted downfield from 32 ppm in the brominated starting material. No trace of the starting material brominated carbon remains in the product spectrum. The highest DS of 6-IMCA obtained, as indicated by ^1H NMR analysis, is 0.74. Thus, the reaction efficiency of imidazole substitution is close to that of 1-methylimidazole substitution, in spite of the fact that no charge is being generated. 6-IMCA exhibits good solubility in common organic solvents including DMSO and DMF, whereas it is insoluble in water, presumably due to the lack of cationic charge in 6-IMCA. Spectroscopic evidence and the good solvent solubility of 6-IMCA support the notion that crosslinking has not occurred.



Scheme 3.2. Reaction scheme for the conversion of cellulose to a zwitterionic cellulose derivative.

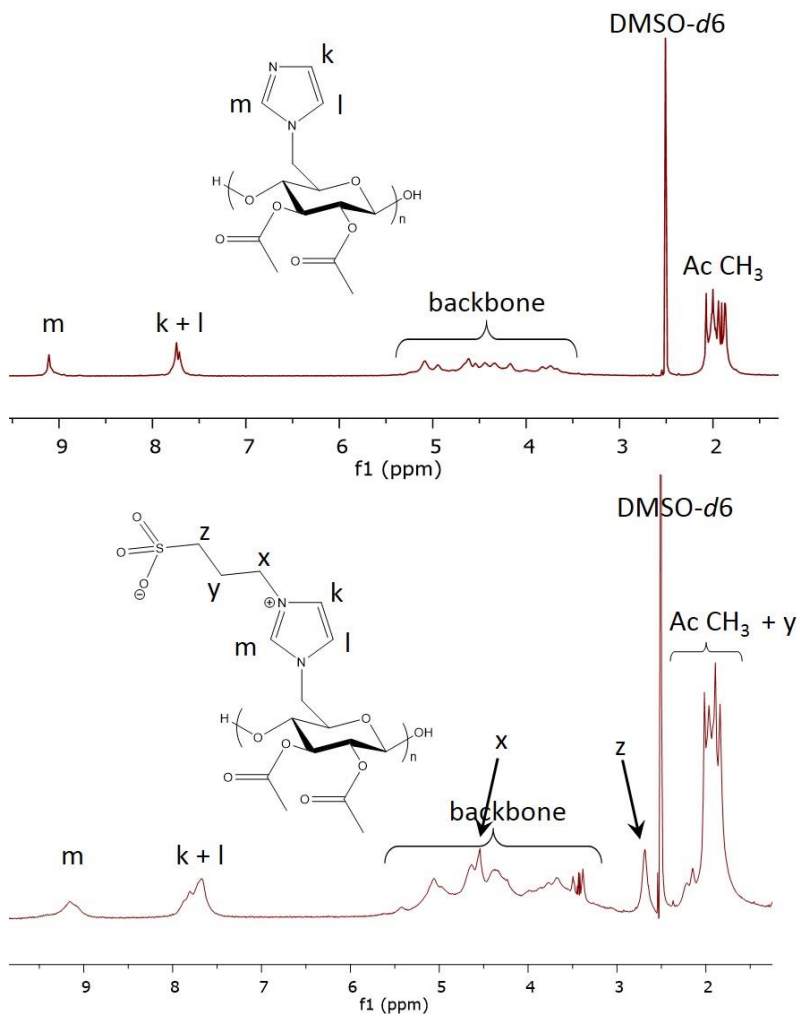


Figure 3.8. ¹H NMR spectra of 6-imidazolyl-6-deoxy-2,3-di-*O*-acetyl-cellulose (6-IMCA) and 6-(1-sulfonic propyl-3-imidazolyl)-6-deoxy-2,3-di-*O*-acetyl-cellulose (6-SPrIMCA).

With the successful synthesis of un-crosslinked 6-IMCA, we wished to investigate whether the remaining basic nitrogen of the 6-IMCA imidazole substituents could be exploited to provide access to zwitterionic derivatives. Imidazoles have previously been used for preparing zwitterionic polymers.⁴⁹ Thus, we attempted reaction of 6-IMCA with an electrophile that would generate negative charge by ring-opening reaction with the basic imidazole nitrogen, while simultaneously providing positive charge on nitrogen. As

Scheme 3.2 shows, 1,3-propane sultone (3 equiv per AGU) was employed as electrophile to react with 6-IMCA in DMSO at 70 °C. ¹H NMR spectroscopy (Figure 3.8) confirms successful formation of the targeted poly(zwitterion), 6-SPrIMCA. Nucleophilic attack of the remaining basic imidazole 3-nitrogen upon the sultone creates a positive charge at the imidazolium atom, while at the same time an accompanying negative charge is created by the tethered sulfate leaving group. The resonances at 8-10 ppm are due to the aromatic protons of the imidazolium substituent. New resonances around 2.2, 2.6 and 4.6 ppm belong to the protons of the 3-sulfopropyl group, and the protons of the 3-sulfopropyl group were assigned according to HSQC spectrum (Figure S7) and a previously published paper.⁴⁹ The DS(3-sulfopropyl) calculated from the ¹H NMR spectrum is 0.43. As is common for zwitterionic polymers, this zwitterionic cellulose derivative exhibits poor solubility in water or organic solvents. The potential utility of the zwitterionic cellulose derivative for various applications such as antifouling coatings or immunomodulatory agents will be explored in future work.

3.5 Conclusions

An efficient method has been developed for synthesizing cationic cellulose esters from 6-bromo-2,3-di-*O*-acetyl-cellulose by regioselective substitution at C-6, affording cationic cellulose derivatives, 6-pyridinio-2,3-di-*O*-acetyl-cellulose and 6-(1-methyl-3-imidazolium)-2,3-di-*O*-acetyl-cellulose, with high DS values. These cationic cellulose derivatives exhibit surprisingly high thermal stability and good water solubility. Based upon surface plasmon resonance experiments, these polysaccharide-based ionomers are found to be capable of binding irreversibly with a hydrophilic and anionic surface.

Availability of these families of cationic cellulose derivatives will accelerate structure-property relationship studies, i.e. for biomedical applications including complexation of poly(nucleic acids) for delivery to cell nuclei, delivery of anionic drugs, and epithelial tight junction opening for oral protein delivery. In addition, 6-imidazolyl-6-deoxy-2,3-di-*O*-acetyl-cellulose was prepared by reacting 6-bromo-2,3-di-*O*-acetyl-cellulose with imidazole, and was further functionalized by 1,3-propane sultone for generating a new zwitterionic cellulose derivative, 6-(1-(3-sulfopropyl)-3-imidazolyl)-6-deoxy-2,3-di-*O*-acetyl-cellulose. This route to new zwitterionic cellulose derivatives may be of particular value, and their possible uses are of special interest to us.

Pyridinium and imidazolium compounds are important families of organic compounds, comprising a large and diverse number of derivatives.^{50,51} The success of regio- and chemoselective pyridine and 1-methylimidazole substitutions points the way to broader exploration of other pyridinium and imidazolium derivatives of cellulose and other polysaccharides to generate a family of cationic *N*-heterocyclic polysaccharide derivatives. It will be useful to study other interesting properties of the cationic *N*-heterocyclic cellulose derivatives such as morphology and ion conductivity to gain structure/property relationship understanding, and reveal their potential for specific uses. In order to apply these cationic materials in biomedical and pharmaceutical areas, it is of particular interest for us to investigate the interactions between the cationic cellulose derivatives and biomolecules such as nucleic acids or certain anionic proteins, as well as cellular toxicity and antimicrobial activity. Moreover, while the reaction conversions obtained were gratifyingly high in most cases, we will further explore methods of enhancing synthesis of

these cationic and zwitterionic derivatives so as to obtain quantitative or near-quantitative conversions, thereby obtaining polymers of well defined structure and lacking potential alkylating agents, so as to enhance potential utility for biomedical applications.

3.6 Supporting information

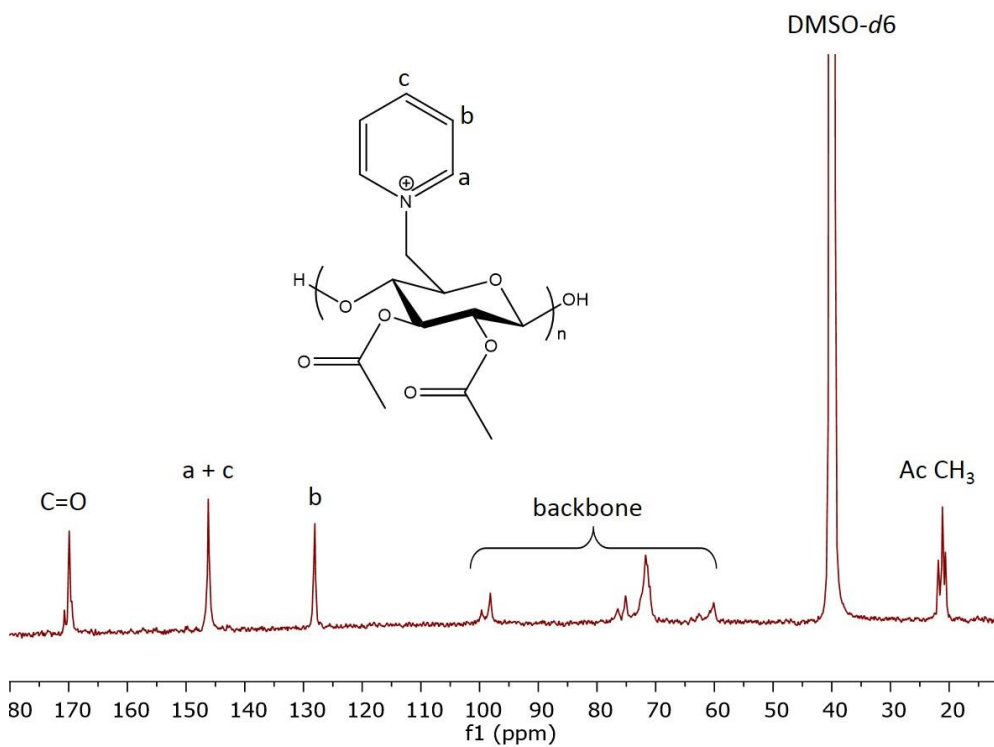


Figure S3.1. ^{13}C NMR spectrum of 6-pyridinio-6-deoxy-2,3-di-*O*-acetyl-cellulose (6-PyrCA).

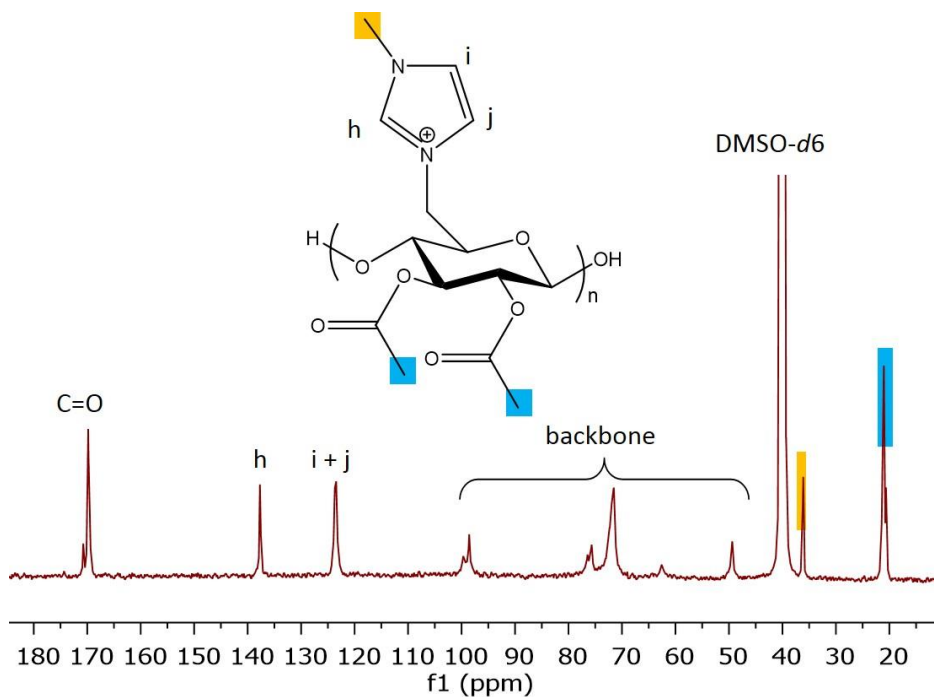


Figure S3.2. ^{13}C NMR spectrum of 6-(1-methyl-3-imidazolyl)-6-deoxy-2,3-di-*O*-acetylcellulose (6-MeIMCA).

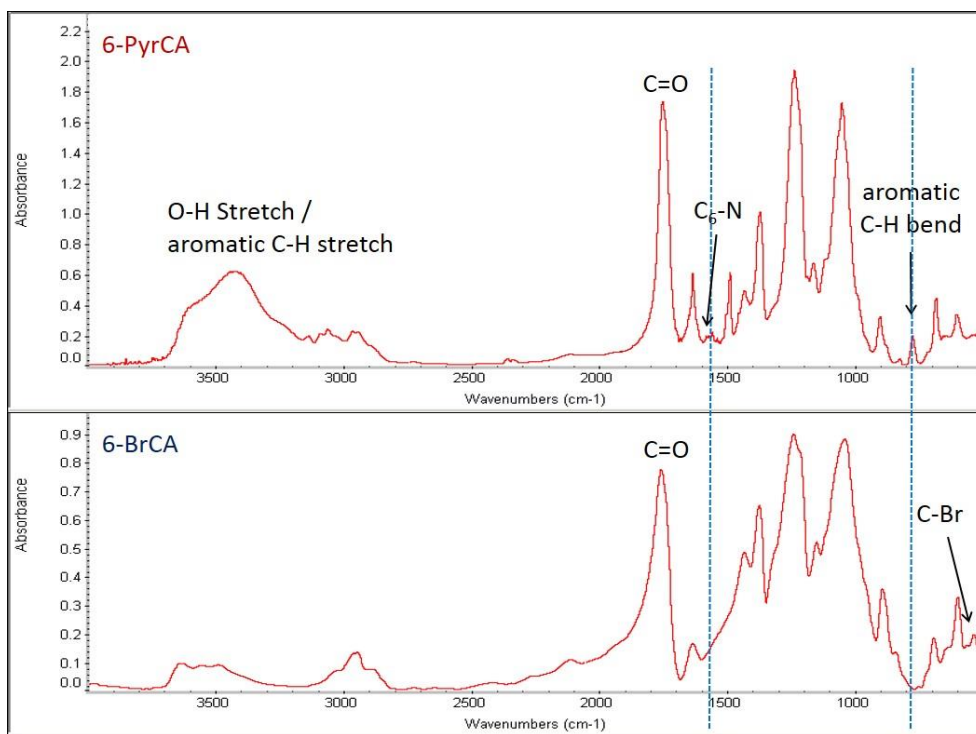


Figure S3.3. FTIR spectra of 6-pyridinio-6-deoxy-2,3-di-*O*-acetyl-cellulose (6-PyrCA) and 6-bromo-6-deoxy-2,3-di-*O*-acetyl-cellulose (6-BrCA).

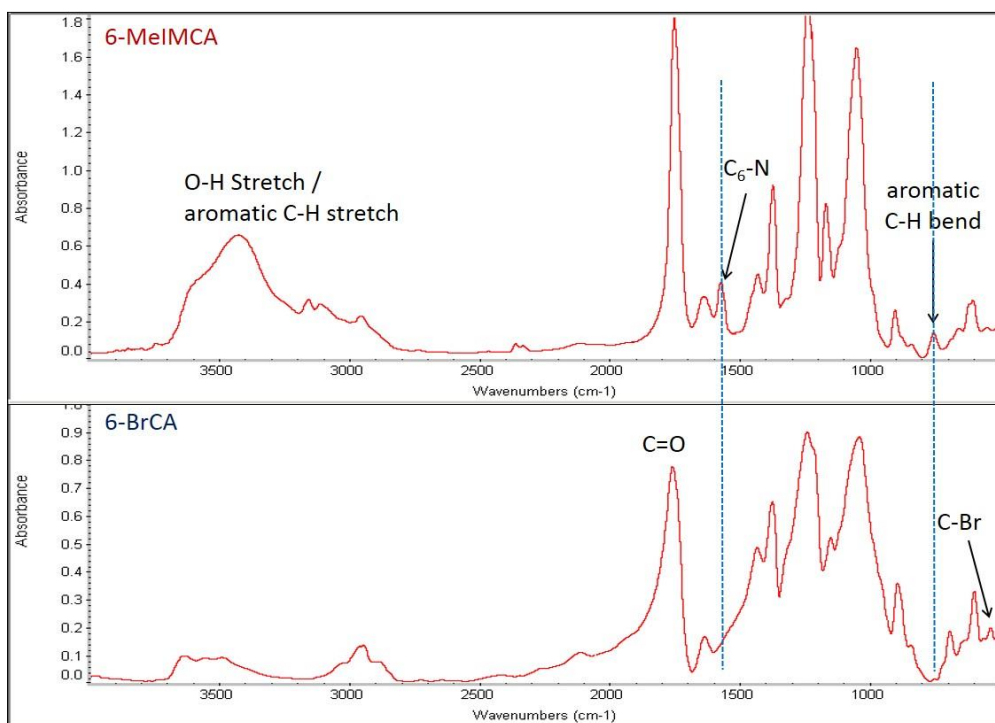


Figure S3.4. FTIR spectra of 6-(1-methyl-3-imidazolyl)-6-deoxy-2,3-di-*O*-acetyl-cellulose and 6-bromo-6-deoxy-2,3-di-*O*-acetyl-cellulose (6-BrCA).

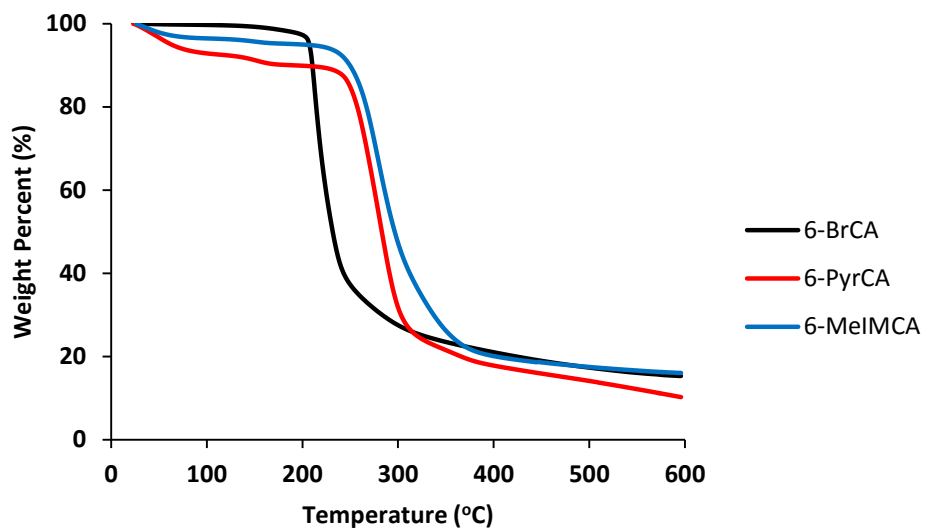


Figure S3.5. Thermal stability of 6-bromo-6-deoxy-2,3-di-*O*-acetyl-cellulose (6-BrCA), 6-pyridinio-6-deoxy-2,3-di-*O*-acetyl-cellulose (6-PyrCA) and 6-(1-methyl-3-imidazolyl)-6-deoxy-2,3-di-*O*-acetyl-cellulose (6-MeIMCA).

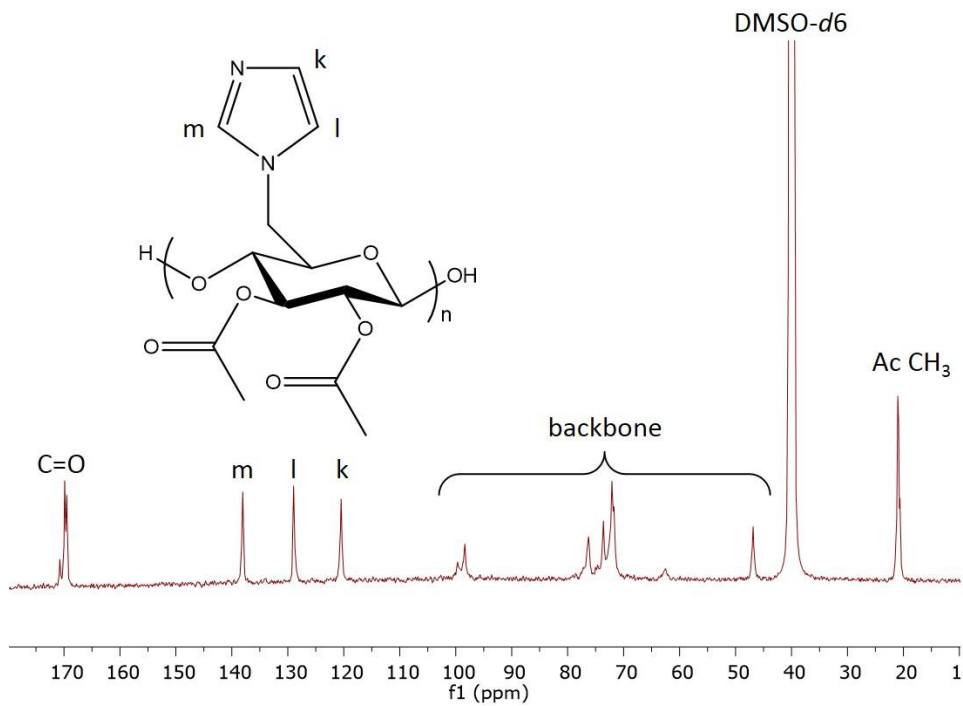


Figure S3.6. ¹³C NMR spectrum of 6-imidazolyl-6-deoxy-2,3-di-*O*-acetyl-cellulose (6-IMCA).

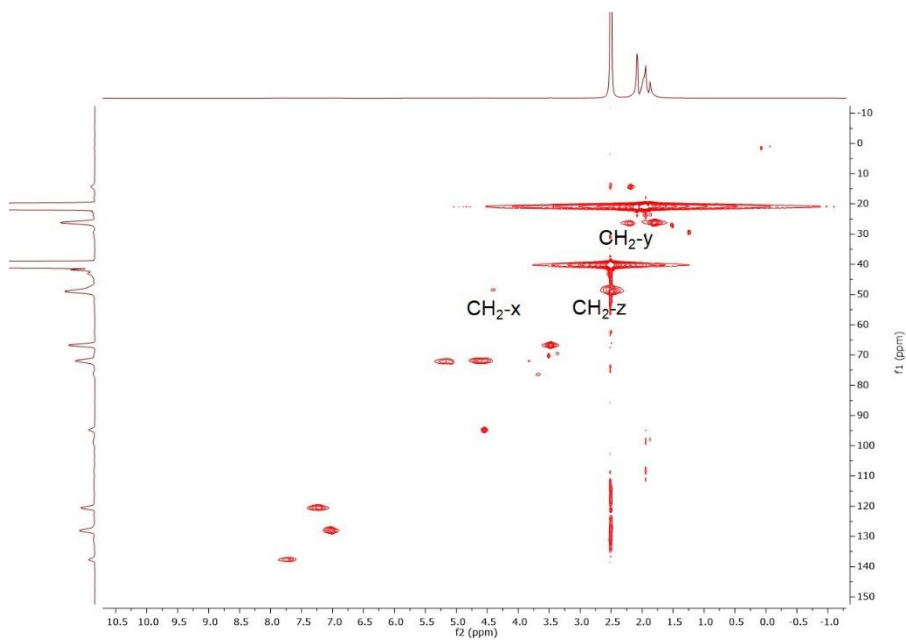


Figure S3.7. HSQC spectrum of 6-(1-sulfonic propyl-3-imidazolyl)-6-deoxy-2,3-di-*O*-acetyl-cellulose (6-SPrIMCA).

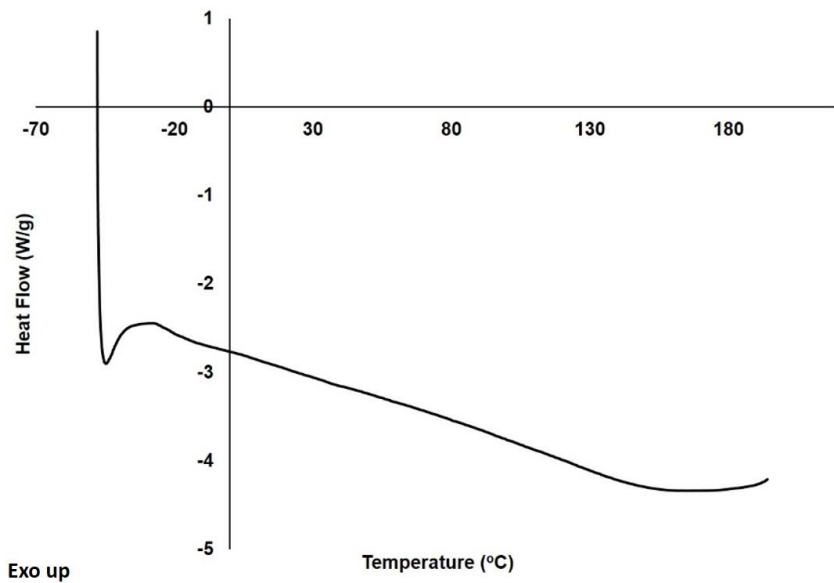


Figure S3.8. DSC thermogram of 6-pyridinio-6-deoxy-2,3-di-*O*-acetyl-cellulose (6-PyrCA).

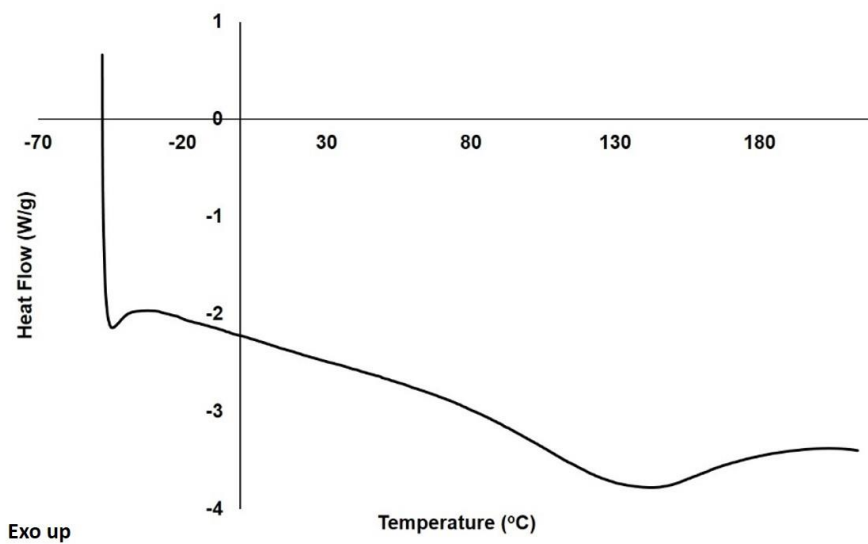


Figure S3.9. DSC thermogram of 6-(1-methyl-3-imidazolyl)-6-deoxy-2,3-di-*O*-acetylcellulose (6-MeIMCA).

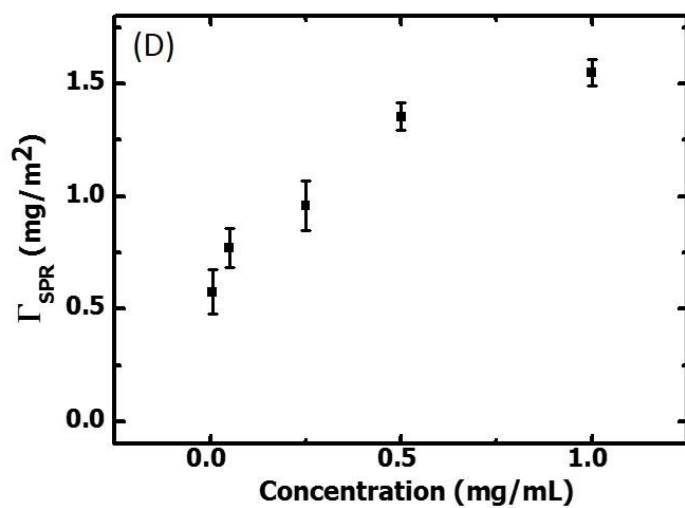
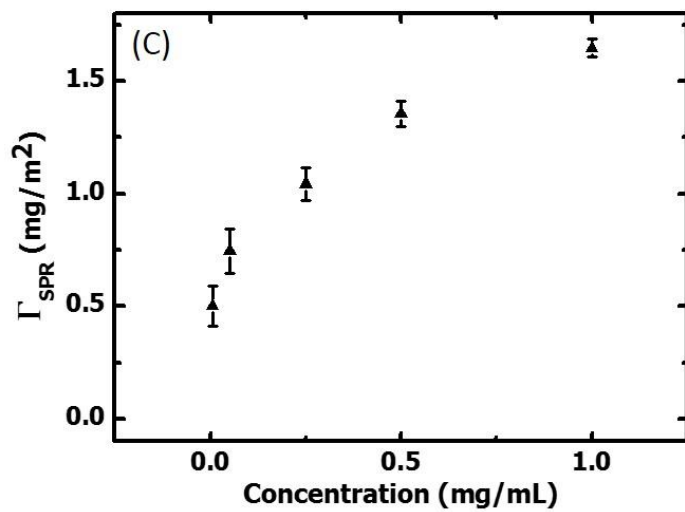


Figure S3.10. Surface vs. bulk concentrations for (C) 6-PyrCA and (D) 6-MeIMCA adsorption onto bare gold surfaces at 20 °C.

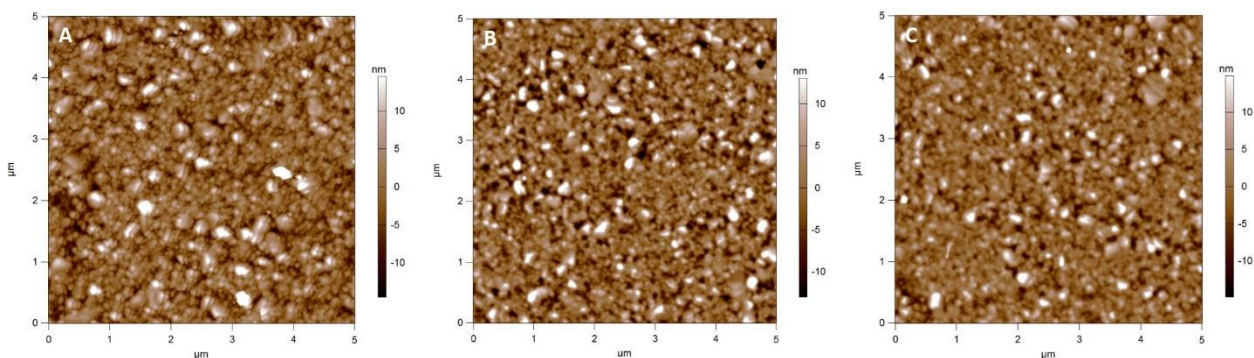


Figure S3.11. AFM height images ($5\ \mu\text{m} \times 5\ \mu\text{m}$) of (A) SAM-COOH coated SPR sensor, and (B) 1 mg/mL 6-PyrCA and (C) 1 mg/mL 6-MeIMCA adsorbed onto SAM-COOH surfaces. RMS roughnesses for the images are (A) $\sim 4.8\ \text{nm}$, (B) $\sim 4.8\ \text{nm}$, and (C) $\sim 4.5\ \text{nm}$.

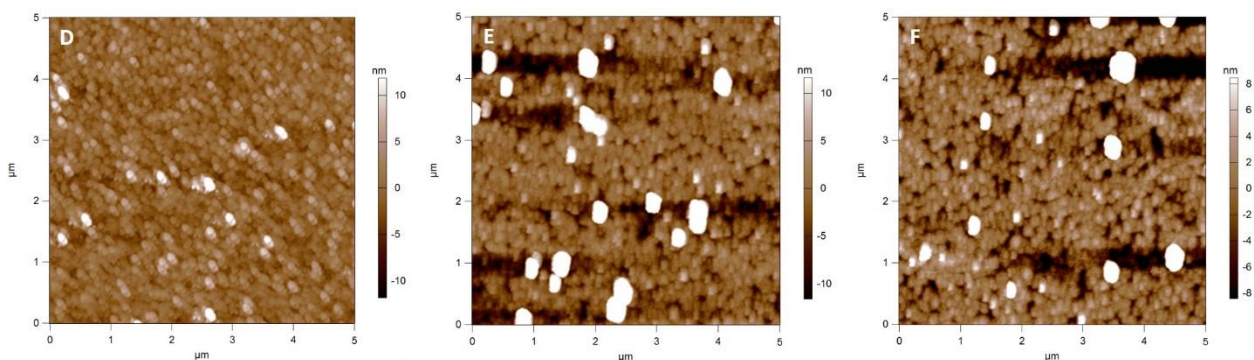


Figure S3.12. AFM height images ($5\ \mu\text{m} \times 5\ \mu\text{m}$) of (D) bare gold SPR sensor, and (E) 1 mg/mL 6-PyrCA and (F) 1 mg/mL 6-MeIMCA adsorbed onto bare gold surfaces. RMS roughnesses for the images are (D) $\sim 2.5\ \text{nm}$, (E) $\sim 8.5\ \text{nm}$, and (F) $\sim 6.9\ \text{nm}$.

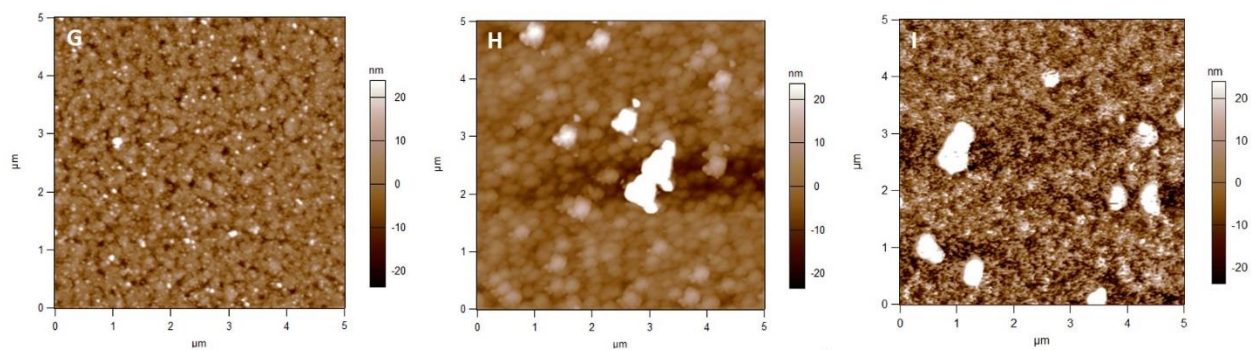


Figure S3.13. AFM height images ($5 \mu\text{m} \times 5 \mu\text{m}$) of (G) SAM-CH₃ coated SPR sensor, and (H) 1 mg/mL 6-PyrCA ($\Gamma_{\text{SPR}} \sim 0.9 \text{ mg} \cdot \text{m}^{-2}$) and (I) 1 mg/mL 6-MeIMCA ($\Gamma_{\text{SPR}} \sim 0.74 \text{ mg} \cdot \text{m}^{-2}$) adsorbed onto SAM-CH₃ surfaces. RMS roughnesses for the images are (G) ~ 5.4 nm, (H) ~ 9.4 nm, and (I) ~ 11.9 nm.

Table S3.1. pKa values of triethylamine, pyridine and 1-methylimidazole

Compound	pKa
triethylamine	11
pyridine	5.2
1-methylimidazole	7.4

Table S3.2. Effect of equiv (MeIM) on reaction with 6-bromo-6-deoxy-2,3-di-*O*-acetyl-cellulose

Equivalent / AGU	DS(MeIM⁺)
10	0.74
20	0.79
30	0.79
40	0.79

Table S3.3. Static water contact angles (θ) of the different surfaces (bare gold, SAM-COOH and SAM-CH₃) before and after 6-PyrCA or 6-MeIMCA adsorption

Surface	θ (deg)
bare gold	73 ± 2
6-PyrCA-bare gold	49 ± 1
6-MeIMCA-bare gold	47 ± 2
SAM-COOH	62 ± 1
6-PyrCA-SAM-COOH	50 ± 1
6-MeIMCA-SAM-COOH	49 ± 1
SAM-CH ₃	82 ± 2
6-PyrCA-SAM-CH ₃	52 ± 2
6-MeIMCA-SAM-CH ₃	59 ± 2

Method: a contact angle measurement system, assembled by a stage (Technical Manufacturing Corporation), a camera (SANYO) and an analyzer (FTA200 Dynamic Contact Angle Analyzer), was employed to measure the wettabilities of different surfaces, using the sessile drop method. All the measurements were performed with at least three drops per surface, and an average value was calculated.

3.7 Acknowledgement

We gratefully acknowledge the Institute for Critical Technologies and Applied Science (ICTAS), Macromolecules and Interfaces Institute (MII) and Department of Sustainable

Biomaterials at Virginia Tech for their financial, facilities, and educational support. We thank the USDA for partial support of this work through grant No. 2011-67009-20090.

3.8 References

1. Dubin, P.; Bock, J.; Davies, R. M.; Schulz, D. N.; Thies, C. *Macromolecular Complexes in Chemistry and Biology*; Springer-Verlag: Berlin, **1994**.
2. Oosawa, F. *Polyelectrolytes*; Marcel-Dekker: New York, **1971**.
3. Mortimer, D. A. Synthetic polyelectrolytes-a review. *Polym. Int.* **1991**, *25*, 29–41.
4. Lowe, A. B.; McCormick, C. L. Synthesis and solution properties of zwitterionic polymers. *Chem. Rev.* **2002**, *102*, 4177–4189.
5. Mi, L.; Jiang, S. Integrated antimicrobial and nonfouling zwitterionic polymers. *Angew. Chem. Int. Ed.* **2014**, *53*, 1746–1754.
6. Neurath, A. R.; Strick, N.; Li, Y. Y. Anti-HIV-1 activity of anionic polymers: a comparative study of candidate microbicides. *BMC Infect. Dis.* **2002**, *2*, 27–37.
7. Kobayashi, J.; Kikuchi, A.; Sakai, K.; Okano, T. Cross-linked thermoresponsive anionic polymer-grafted surfaces to separate bioactive basic peptides. *Anal. Chem.* **2003**, *75*, 3244–3249.
8. Scranton, A. B.; Rangarajan, B.; Klier, J. Biomedical applications of polyelectrolytes. *Adv. Polym. Sci.* **1995**, *122*, 1–54.
9. Hemp, S. T.; Allen, M. H.; Green, M. D.; Long, T. E. Phosphonium-containing polyelectrolytes for nonviral gene delivery. *Biomacromolecules* **2012**, *13*, 231–238.

10. Samal, S. K.; Dash, M.; Vlierberghe, S. V.; Kaplan, D. L.; Chiellini, E.; van Blitterswijk, C.; Moronid, L.; Dubruel, P. Cationic polymers and their therapeutic potential. *Chem. Soc. Rev.* **2012**, *41*, 7147–7194.
11. Thanou, M.; Verhoef, J. C.; Junginger, H.E. Oral drug absorption enhancement by chitosan and its derivatives. *Adv. Drug Deliv. Rev.* **2001**, *52*, 117–126.
12. Lai, W. F.; Lin, M. C. Nucleic acid delivery with chitosan and its derivatives. *J. Controlled Release* **2009**, *134*, 158–168.
13. Kotzé, A. F.; de Leeuw, B. J.; Lueßen, H. L.; de Boer, A. G.; Verhoef, J. C.; Junginger, H. E. Chitosan for enhanced intestinal permeability: prospects for derivatives soluble in neutral and basic environments. *Int. J. Pharm.* **1997**, *159*, 243–253.
14. Cobb, B. A.; Kasper, D. L. Microreview: zwitterionic capsular polysaccharides: The new MHCII-dependent antigens. *Cell. Microbiol.* **2005**, *7*, 1398–1403.
15. Mazmanian, S. K.; Kasper, D. L. The love-hate relationship between bacterial polysaccharides and the host immune system. *Nat. Rev. Immunol.* **2006**, *6*, 849–858.
16. Avci, F. Y.; Kasper, D. L. How bacterial carbohydrates influence the adaptive immune system. *Annu. Rev. Immunol.* **2010**, *28*, 107–130.
17. Gallorini, S.; Berti, F.; Mancuso, G.; Cozzi, R.; Tortoli, M.; Volpini, G.; Telford, J. L.; Beninati, C.; Maione, D.; Wack, A. Toll-like receptor 2 dependent immunogenicity of glycoconjugate vaccines containing chemically derived zwitterionic polysaccharides. *Proc. Natl. Acad. Sci. U.S.A.* **2009**, *106*, 17481–17486.
18. Meng, C.; Peng, X.; Shi, X.; Wang, H.; Guo, Y. Effects of a chemically derived homo zwitterionic polysaccharide on immune activation in mice. *Acta Biochim. Biophys. Sin* **2009**, *41*, 737–744.

19. Abdulmir, A. S.; Hafidh, R. R.; Abubaker, F. In vitro immunogenic and immunostimulatory effects of zwitterionized 23-valent pneumococcal polysaccharide vaccine compared with nonzwitterionized vaccine. *Curr. Ther. Res. Clin. Exp.* **2010**, *71*, 60–77.
20. de Silva, R. A.; Wang, Q.; Chidley, T.; Appulage, D. K.; Andreana, P. R. Immunological response from an entirely carbohydrate antigen: design of synthetic vaccines based on Tn-PS A1 conjugates. *J. Am. Chem. Soc.* **2009**, *131*, 9622–9623.
21. Achur, R. N.; Valiyaveetil, M.; Gowda, D. C. The Low sulfated chondroitin sulfate proteoglycans of human placenta have sulfate group-clustered domains that can efficiently bind plasmodium falciparum-infected erythrocytes. *J. Biol. Chem.* **2003**, *278*, 11705–11713.
22. Liu, C.; Baumann, H. Exclusive and complete introduction of amino groups and their *N*-sulfo and *N*-carboxymethyl groups into the 6-position of cellulose without the use of protecting groups. *Carbohydr. Res.* **2005**, *340*, 2229–2235.
23. Marks, J. A. *Synthesis and Applications of Cellulose Derivatives for Drug Delivery*; Macromolecular Science and Engineering (Vol. Doctor of Philosophy): Virginia Polytechnic Institute and State University, **2015**.
24. Zhang, R.; Liu, S.; Edgar, K. J. Regioselective synthesis of cationic 6-deoxy-6-(*N,N,N*-trialkylammonio)curdlan derivatives. *Carbohydr. Polym.* **2016**, *136*, 474–484.
25. Fox, S. C.; Edgar, K. J. Synthesis of regioselectively brominated cellulose esters and 6-cyano-6-deoxycellulose esters. *Cellulose* **2011**, *18*, 1305–1314.

26. Fox, S. C.; Edgar, K. J. Staudinger reduction chemistry of cellulose: Synthesis of selectively *O*-acylated 6-amino-6-deoxy-cellulose. *Biomacromolecules* **2012**, *13*, 992–1001.
27. Furuhashi, K.; Koganei, K.; Chang, H. S.; Aoki, N.; Sakamoto, M. Dissolution of cellulose in lithium bromide-organic solvent systems and homogeneous bromination of cellulose with *N*-bromosuccinimide-triphenylphosphine in lithium bromide-*N,N*-dimethylacetamide. *Carbohydr. Res.* **1992**, *230*, 165–177.
28. Heinze, T.; Pfeiffer, K. Studies on the synthesis and characterization of carboxymethylcellulose. *Die Angew. Makromol. Chem.* **1999**, *266*, 37–45.
29. Alder, R. W. Strain effects on amine basicities. *Chem. Rev.* **1989**, *89*, 1215–1223.
30. Zhang, R.; Edgar, K. J. Synthesis of curdlan derivatives regioselectively modified at C-6: *O*-(*N*)-Acylated 6-amino-6-deoxycurdlan. *Carbohydr. Polym.* **2014**, *105*, 161–168.
31. Pereira, J. M.; Edgar, K. J. Regioselective synthesis of 6-amino- and 6-amido-6-deoxypullulans. *Cellulose* **2014**, *21*, 2379–2396.
32. Zheng, X.; Gandour, R. Edgar, K. J. Probing the mechanism of TBAF-catalyzed deacylation of cellulose esters. *Biomacromolecules* **2013**, *14*, 1388–1394.
33. Pearson, R. G. Equilibrium constants, oxidation potentials, and nucleophilicity in S_N2 displacements. *J. Org. Chem.* **1987**, *52*, 2131–2136.
34. Carey, F. A.; Sundberg, R. J. *Advanced Organic Chemistry, Part A: Structure and Mechanisms*; 5th ed.; Springer: US, **2007**.
35. Sorgi, K. L. *Encyclopedia of Reagents for Organic Synthesis*; John Wiley & Sons: New York, **2001**.

36. Appukkuttan, V. K.; Dupont, A.; Denis-Quanquin, S.; Andraud, C.; Monnereau C. Mild and efficient bromination of poly(hydroxyethyl acrylate) and its use towards ionic-liquid containing polymers. *Polym. Chem.* **2012**, *3*, 2723–2726.
37. von Hofmann, A. W. Beitrage zur Kenntnis der flüchtigen organischen Basen. *Annalen der Chemie und Pharmacie* **1851**, *78*, 253–286.
38. de Feijter, J. A.; Benjamins, J.; Veer, F. A. Ellipsometry as a tool to study the adsorption behavior of synthetic and biopolymers at the air-water interface. *Biopolymers* **1978**, *17*, 1759–1772.
39. Terada, E.; Samoshina, Y.; Nylander, T.; Lindman, B. Adsorption of cationic cellulose derivatives/anionic surfactant complexes onto solid surfaces. I. Silica surfaces *Langmuir* **2004**, *20*, 1753–1762.
40. Kawaguchi, T.; Nakahara, H.; Fukuda, K. Monomolecular and multimolecular films of cellulose Esters with various alkyl chains. *Thin Solid Films* **1985**, *133*, 29–38.
41. Dobrynin, A. V.; Deshkovski, A.; Rubinstein, M. Adsorption of polyelectrolytes at oppositely charged surfaces. *Macromolecules* **2001**, *34*, 3421–3436.
42. Fears, K. P.; Creager, S. E.; Latour, R. A. Determination of the surface pK of carboxylic- and amine-terminated alkanethiols using surface plasmon resonance spectroscopy. *Langmuir* **2008**, *24*, 837–843.
43. Ulman, A.; Eilers, J. E.; Tillman, N. Packing and molecular orientation of alkanethiol monolayers on gold surfaces. *Langmuir* **1989**, *5*, 1147–1152.
44. Zhao, J.; Luo, L.; Yang, X.; Wang, E.; Dong, S. Determination of surface pKa of SAM using an electrochemical titration method. *Electroanalysis* **1999**, *11*, 1108–1111.

45. Vezenov, D. V.; Noy, A.; Rozsnyai, L. F.; Lieber, C. M. Force titrations and ionization state sensitive imaging of functional groups in aqueous solutions by chemical force microscopy. *J. Am. Chem. Soc.* **1997**, *119*, 2006–2015.
46. Mohan, T.; Niegelhell, K.; Zarth, C. S. P.; Kargl, R.; Köstler, S.; Ribitsch, V.; Heinze, T.; Spirk, S.; Stana-Kleinschek, K. Triggering protein adsorption on tailored cationic cellulose surfaces. *Biomacromolecules* **2014**, *15*, 3931–3941.
47. Mohan, T.; Zarth, C. S. P.; Doliška, A.; Kargl, R.; Grießer, T.; Spirk, S.; Heinze, T.; Stana-Kleinschek, K. *Carbohydr. Polym.* **2013**, *92*, 1046–1053.
48. Liu, Z.; Choi, H.; Gatenholm, P.; Esker, A. R. Quartz crystal microbalance with dissipation monitoring and surface plasmon resonance studies of carboxymethyl cellulose adsorption onto regenerated cellulose surfaces. *Langmuir* **2011**, *27*, 8718–8728.
49. Vasantha, V. A.; Jana, S.; Parthiban, A.; Vancso, J. G. Water swelling, brine soluble imidazole based zwitterionic polymers-synthesis and study of reversible UCST behaviour and gel–sol transitions. *Chem. Commun.* **2014**, *50*, 46–48.
50. Movassaghi, M.; Hill, M. D.; Ahmad, O. K. Direct synthesis of pyridine derivatives. *J. Am. Chem. Soc.* **2007**, *129*, 10096–10097.
51. Sundberg, R. J.; Martin, R. B. Interactions of histidine and other imidazole derivatives with transition metal ions in chemical and biological systems. *Chem. Rev.* **1974**, *74*, 471–517.

Chapter 4. Water-soluble Co-polyelectrolytes by Selective Modification of Cellulose Esters

Liu, S.; Edgar, K. J. *Carbohydrate Polymers* **2017**, *162*, 1–9. Used permission of Elsevier, 2017

4.1 Abstract

Cellulose-based materials are well-suited for biomedical uses, because of their abundance, renewable nature, biodegradability, and relatively low cost. However, the set of commercially available cellulose esters and ethers is limited in number and diversity, and contains no cationically charged cellulose esters. Herein we report a simple, efficient strategy for synthesizing cationic, water-soluble co-polyelectrolytes from commercial, hydrophobic, renewable-based cellulose esters. Cellulose acetate (degree of substitution (DS) 1.78, CA320S), was the exemplary starting material for preparing these cationic polyelectrolytes by a reaction sequence of phosphine-catalyzed bromination and subsequent displacement by an aromatic amine, affording high reaction conversions. We show that these modification techniques can be carried out with essentially complete regio- and chemoselectivity, proceeding in the presence of multiple ester groups, yet preserving those groups. Availability of these novel polysaccharide-based electrolytes starting from uncharged, commercial, inexpensive cellulose esters may open up multiple new application areas, including in several aspects of gene or drug delivery.

4.2 Introduction

Polysaccharides, one of the most abundant and diverse families of natural polymers, exhibit an incredibly wide range of natural functions including structural reinforcement¹, energy storage², modification of aqueous rheology³, and communication⁴. Native cellulose is a homopolymer ($\rightarrow 4\text{-}\beta\text{-D-Glcp-1}\rightarrow$) of the monosaccharide D-glucopyranose, without branching or substituents.⁵ Its derivatives dominate commercial uses and sales of polysaccharide derivatives.⁶ Application of native cellulose as a sustainable material is impeded by its insolubility in common solvents including water, poor dimensional stability, and lack of thermoplasticity. To increase its functionality and utility, researchers have tailored the chemical and physical properties of cellulose derivatives using a variety of chemical modification techniques, resulting in a relatively small number of commercial derivatives. Hundreds of millions of kilograms of cellulose derivatives are sold annually and used for numerous applications including coatings, optical films, pharmaceuticals, and composite materials.⁷

Esters of cellulose, including cellulose nitrate and its organic esters, have been among its most important and useful derivatives.^{6,8} More recently, the small set of cellulose organic esters that could be synthesized practically given the limitations of conventional esterification has been expanded⁹⁻¹⁶, assisted by the development of cellulose solvents¹⁷⁻¹⁹. Regioselective ester synthesis has afforded access to new structures and properties, e.g. through selective protection and deprotection²⁰⁻³⁰, oxidation at the primary alcohol groups³¹⁻³⁵, and Staudinger reactions^{36,37}. In 1992, Furuhashi et al. reported a simple and powerful method for regioselective halogenation at the C-6 position³⁸ by dissolving cellulose in

DMAc/lithium bromide, then adding triphenylphosphine (Ph₃P) and N-bromosuccinimide (NBS). An advantage versus frequently-described cellulose tosylation is that Furuhata bromination is virtually quantitative and completely selective for C-6, in contrast with a significant amount of off-target reaction with tosylation.³⁹⁻⁴³ 6-Deoxy-6-bromocellulose has proven to be a versatile intermediate for further modification of cellulose. Thiols can effectively displace the 6-bromide, thereby regioselectively attaching different pendent functional groups, such as carboxylic acids to form anionic cellulose derivatives⁴⁴ or reaction with sodium sulfite can afford water-soluble 6-sulfonate derivatives⁴⁵.

Cationic cellulose derivatives have recently received increasing attention, since they are capable of binding electrostatically with anionic biomolecules including nucleic acids and certain proteins to produce therapeutically useful polyelectrolyte complexes.⁴⁶ Compared to synthetic cationic polymers, cationic cellulose derivatives may in some cases be more attractive candidates for therapeutic uses because they frequently are more biocompatible and biodegradable, and have low immunogenicity.⁴⁷ Recently we have prepared cationic derivatives of cellulose and other glucans that possess free 6-OH groups by reacting trialkylamines with 6-bromo-6-deoxyglucans, for example 6-bromo-6-deoxy-2,3-*O*-diacetyl-cellulose, which is generated from native cellulose by Furuhata bromination and *in situ* peracylation.⁴⁸ However, we found that such nucleophilic bromide displacements by trialkylamines are quite difficult to drive to high reaction conversion, possibly due to developing charge-charge repulsion in the increasingly cationic product.⁴⁸⁻⁵⁰ We have also observed that aromatic amines (e.g., pyridine and 1-methylimidazole) are more efficient nucleophiles in such displacement reactions, affording high DS values of the cationic

substituents.⁴⁹ These cationic cellulose derivatives exhibit surprisingly high thermal stability and good water solubility, and are capable of binding irreversibly to hydrophilic and anionic surfaces. However, all of these cationic cellulose ionomers synthesized using phosphine-catalyzed bromination and aromatic amine displacements were derived from low degree of polymerization (DP) microcrystalline cellulose (MCC). MCC is popular for cellulose solution methods, since its solutions are less viscous and more easily managed than those that result from high DP dissolving pulp. However, this low starting DP (DP < 100) restricts the utility of its derivatives for plastics and other applications where high DP (DP > 100) is needed. Also, since 100% conversion of the 6-bromo groups of 6-bromo-6-deoxycellulose to cationic substituents is very difficult to achieve, the products still contain 6-bromide residues, which could be alkylating sites *in vivo* (reacting for example with endogenous proteins and peptides) and therefore could lead to polymer toxicity.

Thus, there could be considerable advantage if one could start with high DP commercial esters, so long as they contain substantial DS of residual 6-OH groups. Such starting materials could in theory afford quantitative conversion of the resulting 6-bromo groups to, e.g., ammonio substituents (since positive charges would be on average more widely separated), and provide water- and organic-soluble, high DP products useful in a wider variety of applications. However, there was considerable reason to be concerned about whether bromination of such derivatives would be effective. Would the simultaneous presence in the brominated cellulose esters of alkyl halides and hydroxyl groups lead to crosslinking via bromide displacement? Would the ester groups lead to undesired side

reactions (e.g. deacylation catalyzed by the trialkylamine base)? Would the products have sufficient DS of ammonio groups to afford the desired properties?

We hypothesize that Furuhashi bromination of cellulose esters containing a sufficient concentration of free 6-OH groups will afford selectively, partially brominated 6-bromo-6-deoxy cellulose ester derivatives. We further hypothesize that displacement of these 6-bromo groups by tertiary amines will afford, in high conversion, 6-ammonio-6-deoxycellulose ester polyelectrolytes that will have high DP, and good solubility in both water and organic solvents. In this work, we attempt to confirm these hypotheses by applying phosphine-catalyzed bromination and subsequent aromatic amine displacements to commercial cellulose esters, in order to prepare cellulose-based sustainable materials for advanced technologies. We selected a commercial cellulose acetate with high DS(OH), cellulose acetate (DS(Ac) 1.78, *vide infra*), as substrate for our planned phosphine-catalyzed bromination. We report attempts to functionalize the resulting derivative by azide and aromatic amine displacements to prepare cellulose-based *N*-containing copolymers, including polyelectrolytes.

4.3 Materials and methods

4.3.1 Materials

Cellulose acetate (CA320S, DS(Ac) 1.78, DS(6-OH) 0.49 (measured using perpropionylated sample by ^1H nuclear magnetic resonance (NMR)), DP = 191 (measured by SEC), Eastman Chemical Company) was dried under vacuum at 50 °C overnight before use. *N*-Bromosuccinimide (NBS, 99%, Acros) was recrystallized from boiling water

and dried for two days under reduced pressure over anhydrous calcium chloride. 4-(Dimethylamino)pyridine (DMAP, Sigma-Aldrich), triphenylphosphine (Ph₃P, Sigma-Aldrich), sodium azide (NaN₃, Fisher), pyridine (anhydrous, 99+%, AcroSeal), imidazole (99+%, Sigma-Aldrich), 1-methylimidazole (99+%, Sigma-Aldrich), methyl iodide (Sigma-Aldrich), and potassium bromide (KBr, Sigma-Aldrich) were used as received. Methanol, ethanol and *N*-methyl-2-pyrrolidone (NMP) were from Fisher Scientific, Pittsburgh, PA and used as received. *N,N*-Dimethylacetamide (DMAc, Fisher), propionic anhydride (Sigma-Aldrich), and dimethyl sulfoxide (DMSO, Acros) were kept over 4 Å molecular sieves under dry nitrogen until use. Regenerated cellulose dialysis tubing (3500 g/mol molecular weight cut-off (MWCO)) was purchased from Fisher and used as received.

4.3.2 Measurements

¹H and ¹³C NMR spectra were obtained on a Bruker AVANCE II 500 MHz spectrometer in DMSO-*d*₆ at room temperature or 50 °C. Infrared spectroscopic analyses of samples as pressed KBr pellets were obtained on a Thermo Electron Nicolet 8700 instrument using 64 scans and 4 cm⁻¹ resolution. Size exclusion chromatography (SEC) was performed on Agilent 1260 Infinity MultiDetector SEC using DMAc with 0.05 M LiCl as the mobile phase (50 °C) with 3 PLgel 10 μm mixed-B 300 × 7.5 mm columns in series. Data acquisition and analysis was conducted using Astra 6 software (Wyatt Technology Corporation, Goleta, CA). Monodisperse polystyrene standard (M_w ~ 21k, polydispersity index (PDI) ~ 1.02) was run first in every sample series for the purpose of calibration and confirmation. Carbon, nitrogen, and bromine contents were determined by Micro Analysis

Inc. using a Perkin Elmer 2400 II analyzer. Carbon and nitrogen contents were measured by flask combustion followed by ion chromatography, and bromine content was determined with a thermal conductivity detector. Zeta potentials (Zetasizer NanoZS, Malvern Instruments) were measured at 25 °C. DS values were determined by means of ¹H NMR spectroscopy, according to the following equations, respectively.

$$DS_{Ac} = \frac{7I_{Ac-CH_3}}{3I_{cellulose\ backbone}}$$

$$DS_{Pyr^+} = \frac{7I_{CH-ring}}{5I_{cellulose\ backbone}}$$

$$DS_{MeIM^+} = \frac{7}{\frac{3I_{cellulose\ backbone+N-CH_3}}{I_{CH-ring}} - 3}$$

$$DS_{IM} = \frac{7I_{CH-ring}}{3I_{cellulose\ backbone}}$$

4.3.3 Perpropionylation of CA320S

Cellulose acetate (CA320S) was propionylated for easier NMR analysis using methods first described by the Heinze group and adapted from previous studies^{15,51,52}. 4-(Dimethylamino)pyridine (15 mg) and propionic anhydride (4 mL) were added to a solution of CA320S (300 mg) in pyridine (4 mL) at 80 °C and stirred for 24 h, then the cooled reaction solution was added slowly to ethanol. The precipitated product was collected by filtration and was washed several times with ethanol. The crude product was redissolved in chloroform (5 mL), reprecipitated into ethanol (150 mL), and washed several

times with ethanol. The resulting material was dried under vacuum to yield the perpropionylated CA320S.

4.3.4 Regioselective bromination of CA320S

In a 100 mL three-necked round-bottom flask, 1.00 g CA320S (4.22 mmol) was dissolved in 40 mL of DMAc. Ph₃P (3 equiv per AGU, 12.66 mmol, 3.32 g) and NBS (3 equiv per AGU, 12.66 mmol, 2.25 g) were separately dissolved in 10 mL portions of DMAc. The Ph₃P solution was added dropwise to the CA320S solution, followed by the dropwise addition of the NBS solution. The resulting solution was heated to 70 °C under nitrogen for 1 h while stirring. It was then cooled and added slowly to 1 L of a 50:50 (v/v) mixture of methanol and deionized water to precipitate the product, followed by filtration. The precipitate was then twice redissolved in acetone, followed by precipitation in ethanol, then was dried overnight in a vacuum oven at 50 °C, affording (6-bromo-6-deoxy)-*co*-(6-*O*-acetyl)-CA 320S (6-BrCA320S) (992 mg, 3.59 mmol). Yield: 85%. ¹³C NMR (500 MHz, CDCl₃): 21.06 (O-(C=O)-CH₃), 33.52 (C-6-Br), 62.87 (C-6'-O-Ac) 71.84-78.46 (C-2, C-3, C-4 and C-5), 100.09 (C-1), 103.47 (C-1'), 170.85 (O-(C=O)-CH₃). Elemental analysis: %C 42.13, %H 4.69, %N None Found, %Br 14.21 (Theoretical: (DS(Br) 0.49) %C 41.69, %H 6.44 %, N 0 %, Br 14.18); DS by elemental analysis: DS(Br) 0.49.

4.3.5 Synthesis of (6-azido-6-deoxy)-*co*-(6-*O*-acetyl)-CA320S (6-N₃CA320S)

In a 100 mL three-necked round-bottom flask, 250 mg 6-BrCA320S (0.9 mmol) was dissolved in 10 mL of DMSO. Sodium azide (3 equiv per AGU, 2.7 mmol, 176 mg) was added to the flask. The solution was heated to 80 °C and stirred at that temperature for 24

h under nitrogen. The cooled solution was then transferred to dialysis tubing. After 3 days of dialysis against ethanol and 3 days of dialysis against deionized water, the solution was freeze-dried to yield 6-N₃CA320S (207 mg, 0.79 mmol). Yield: 87%. ¹³C NMR (500 MHz, DMSO-*d*₆): 21.02 (O-(C=O)-CH₃), 50.41 (C-6-Br), 62.86 (C-6'-O-Ac), 77.00-81.00 (C-2, C-3, C-4 and C-5), 99.75 (C-1), 103.05 (C-1'), 169.86 (O-(C=O)-CH₃). Elemental analysis: %C 45.13, %H 5.30, %N 7.86, %Br None Found (Theoretical: (DS(N₃) 0.49) %C 44.70, %H 6.90, %N 7.99, %Br 0). DS by elemental analysis: DS(N₃) 0.49.

4.3.6 Synthesis of (6-pyridinio-6-deoxy)-*co*-(6-*O*-acetyl)-CA320S (6-PyrCA320S)

In a 100 mL three-necked round-bottom flask, 250 mg 6-BrCA320S (0.9 mmol) was dissolved in 10 mL of DMSO. Pyridine (1.42 g, 18 mmol, 20 equiv per AGU) was added to the flask. The solution was heated to 80 °C and stirred at that temperature for 48 h under nitrogen. The cooled solution was then transferred to dialysis tubing. After dialysis (3 days against ethanol, then 3 days against deionized water), the solution was freeze-dried to yield 6-PyrCA320S (243 mg, 0.80 mmol). Yield: 89%. ¹H NMR (500 MHz, DMSO-*d*₆): 1.84-2.07 (O-(C=O)-CH₃), 3.00-6.00 (cellulose backbone), 8.22 (N-CH=CH-CH), 8.67 (N-CH=CH-CH), 8.95 (N-CH=CH-CH); ¹³C NMR (500 MHz, DMSO-*d*₆): 20.65 (O-(C=O)-CH₃), 60.98 (C-6), 62.85 (C-6'), 71.00-77.00 (C-2, C-3, C-4 and C-5), 99.73 (C-1), 103.16 (C-1'), 128.26 (N-CH=CH-CH), 146.41 (N-CH=CH-CH and N-CH=CH-CH), 169.86 (O-(C=O)-CH₃). DS by ¹H NMR: DS(Pyr⁺) 0.41, DS(Ac) 1.82. Elemental analysis: %C 44.09, %H 4.91, %N 1.91, %Br 8.62 (Theoretical: (DS(Pyr⁺) 0.49) %C 45.65, %H 6.41, %N 2.21, %Br 12.44). DS by elemental analysis: DS(Pyr⁺) 0.42.

4.3.7 Synthesis of (6-(1-methyl-3-imidazolio)-6-deoxy)-co-(6-O-acetyl)-CA320S (6-MeIMCA320S)

6-BrCA320S (250 mg, 0.9 mmol) was dissolved in 10 mL of DMSO in a 100 mL three-necked round-bottom flask. 1-Methylimidazole (1.47 g, 18 mmol, 20 equiv per AGU) was added to the flask. The solution was heated to 80 °C and stirred at that temperature for 48 h under nitrogen. The cooled solution was transferred to dialysis tubing. After dialysis (3 days against ethanol, then 3 days against deionized water), the solution was freeze-dried to yield 6-MeIMCA320S (255 mg, 0.81 mmol). Yield: 90%. ¹H NMR (500 MHz, DMSO-*d*₆): 1.86-2.07 (O-(C=O)-CH₃), 3.00-6.00 (cellulose backbone and N-CH₃), 7.69-7.82 (N-CH=CH-N-CH₃ and N-CH=CH-N-CH₃), 9.14 (N=CH-N-CH₃); ¹³C NMR (500 MHz, DMSO-*d*₆): 20.64 (O-(C=O)-CH₃), 36.23 (N-CH₃), 49.55 (C-6), 63.01 (C-6'), 71.00-80.00 (C-2, C-3, C-4 and C-5), 99.80 (C-1), 103.57 (C-1'), 123.50 (N-CH=CH-N-CH₃), 123.70 (N-CH=CH-N-CH₃), 137.69 (N=CH-N-CH₃), 169.82 (O-(C=O)-CH₃). DS by ¹H NMR: DS(MeIM⁺) 0.46, DS(Ac) 1.70. Elemental analysis: %C 44.28, %H 5.32, %N 4.19, %Br 6.63 (Theoretical: (DS(MeIM⁺) 0.49) %C 47.53, %H 6.54, %N 4.34, %Br 12.39). DS by elemental analysis: DS(MeIM⁺) 0.47.

4.3.8 One pot synthesis of 6-MeIMCA320S

CA320S (1.00 g, 4.22 mmol) was dissolved in 40 mL of DMAc in a 100 mL three-necked round-bottom flask. Ph₃P (3.32 g, 12.66 mmol, 3 equiv per AGU) and NBS (2.25 g, 12.66 mmol, 3 equiv per AGU) were separately dissolved in 10 mL portions of DMAc. The Ph₃P solution was added dropwise to the CA320S solution, followed by the dropwise addition of the NBS solution. The resulting solution was heated to 70 °C under nitrogen for 1 h

while stirring. 1-Methylimidazole (20 equiv per AGU) was added to the flask. The solution was heated to 80 °C and stirred at that temperature for 48 h under nitrogen. The cooled solution was transferred to dialysis tubing. After dialysis (3 days against ethanol, then 3 days against deionized water), the solution was freeze-dried to yield 6-MeIMCA 320S (990 mg, 3.19 mmol). Yield: 88%. ¹H NMR (500 MHz, DMSO-*d*₆): 1.86-2.07 (O-(C=O)-CH₃), 3.00-6.00 (cellulose backbone and N-CH₃), 7.69-7.82 (N-CH=CH-N-CH₃ and N-CH=CH-N-CH₃), 9.14 (N=CH-N-CH₃); ¹³C NMR (500 MHz, DMSO-*d*₆): 20.66 (O-(C=O)-CH₃), 36.27 (N-CH₃), 49.59 (C-6), 63.04 (C-6'), 71.00-80.00 (C-2, C-3, C-4 and C-5), 99.80 (C-1), 103.57 (C-1'), 123.68 (N-CH=CH-N-CH₃ and N-CH=CH-N-CH₃), 138.50 (N=CH-N-CH₃), 170.86 (O-(C=O)-CH₃). DS by ¹H NMR: DS(MeIM⁺) 0.41, DS(Ac) 1.70.

4.3.9 Synthesis of (6-imidazolyl-6-deoxy)-*co*-(6-*O*-acetyl)-CA320S (6-IMCA320S) and quaternization of 6-IMCA320S

In a 100 mL three-necked round-bottom flask, 6-BrCA320S (250 mg, 0.9 mmol) was dissolved in 10 mL of DMSO. Imidazole (1.84 g, 30 equiv per AGU) was added to the flask and dissolved. The solution was heated to 80 °C and held at that temperature for 48 h under nitrogen with stirring. The cooled reaction solution was added to dialysis tubing, followed by dialysis (3 days against ethanol, then 3 days against deionized water). The retentate was finally dried under vacuum overnight to yield 6-IMCA320S (192 mg, 0.71 mmol). Yield: 79%. ¹H NMR (500 MHz, DMSO-*d*₆): 1.70-2.30 (O-(C=O)-CH₃), 3.00-6.00 (cellulose backbone), 7.60-7.80 (N-CH=CH-N and N-CH=CH-N), 8.80-9.10 (N-CH=N); ¹³C NMR (500 MHz, DMSO-*d*₆): 21.03 (O-(C=O)-CH₃), 46.90 (C-6), 62.88 (C-CH=N);

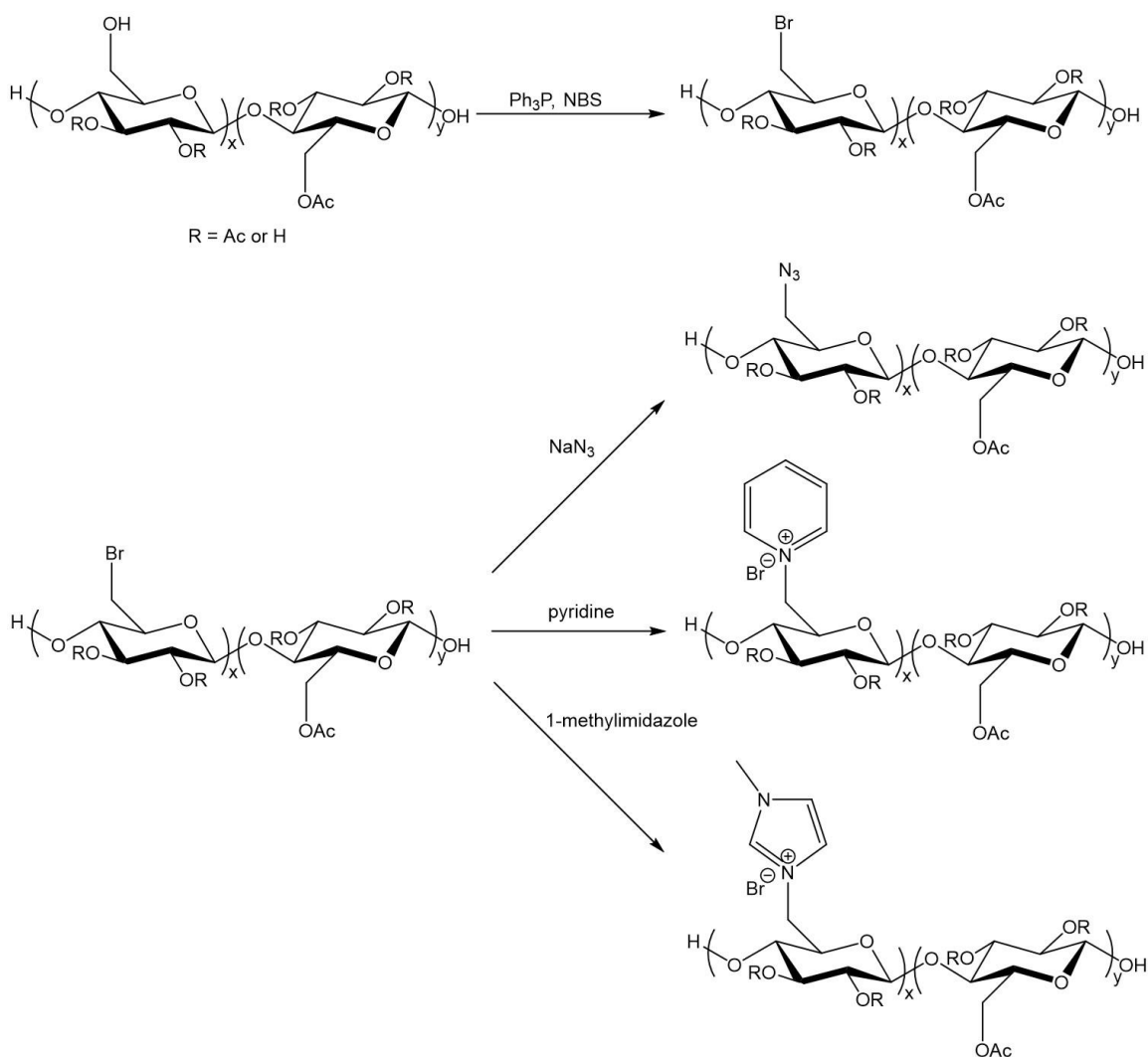
6'), 71.00-77.00 (C-2, C-3, C-4 and C-5), 99.72 (C-1), 103.17 (C-1'), 120.50 (N-CH=CH-N), 128.78 (N-CH=CH-N), 138.35 (N-CH=N), 169.89 (O-(C=O)-CH₃). DS by ¹H NMR: DS(IM) 0.49, DS(Ac) 1.77. Elemental analysis: %C 49.41, %H 5.63, %N 4.82, %Br None Found (Theoretical: (DS(IM) 0.49) %C 49.35, %H 7.51, %N 5.18 %Br 0). DS by elemental analysis: DS(IM) 0.49.

In a 25 mL round-bottom flask, 6-IMCA320S (100 mg, 0.37 mmol) was dissolved in 10 mL of NMP. Methyl iodide (10 equiv per AGU) was added to the flask. The solution was heated to 50 °C and held at that temperature for 48 h under reflux with stirring. The cooled reaction solution was added to dialysis tubing, followed by dialysis (3 days against ethanol, then 3 days against deionized water). The retentate was finally dried under vacuum overnight to yield 6-MeIMCA320S (101 mg, 0.32 mmol). Yield: 86%. ¹H NMR (500 MHz, DMSO-*d*₆): 1.86-2.07 (O-(C=O)-CH₃), 3.00-6.00 (cellulose backbone and N-CH₃), 7.69-7.82 (N-CH=CH-N-CH₃ and N-CH=CH-N-CH₃), 9.14 (N=CH-N-CH₃); ¹³C NMR (500 MHz, DMSO-*d*₆): 20.56 (O-(C=O)-CH₃), 36.17 (N-CH₃), 49.49 (C-6), 63.08 (C-6'), 71.00-80.00 (C-2, C-3, C-4 and C-5), 99.83 (C-1), 103.58 (C-1'), 123.82 (N-CH=CH-N-CH₃ and N-CH=CH-N-CH₃), 138.58 (N=CH-N-CH₃), 170.94 (O-(C=O)-CH₃). DS by ¹H NMR: DS(*N*-methyl) 0.39, DS(Ac) 1.70.

4.4 Results and discussion

In this work, a commercial cellulose acetate (CA320S) was selected as starting material because it has relatively high molecular weight and, most crucially, contains a high DS(OH). Because cellulose ester synthesis typically involves peracetylation followed by

back-hydrolysis to the desired DS(acyl), CA 320S should have a relatively high DS(6-OH) (since the primary alcohol acetate has wider approach angles and therefore should be hydrolyzed most rapidly). In order to measure the acetyl content at each position, CA320S was perpropionylated by reacting with propionic anhydride in the presence of pyridine and DMAP. The acetyl singlets in the ^1H NMR spectrum were readily assigned based on HMBC and other NMR methods¹⁵, and thus readily quantified by the ratios of their integrals to that of the backbone protons. By this method (Figure S1), DS(Ac) for CA 320S calculated is 1.78, which is consistent with previous reports (Zheng, Gandour & Edgar, 2013a). DS(6-Pr) calculated from ^1H NMR is 0.49. Therefore, DS(6-Ac) is 0.51 and DS(6-OH) is 0.49 (see Table S4.1 for other positional DS data by this method).



Scheme 4.1. Reaction scheme for conversions of CA320S to 6-N₃CA320S, 6-PyrCA320S and 6-MeIMCA320S.

4.4.1 6-BrCA320S

We attempted to brominate CA320S using a procedure adapted from Furuhashi et al.³⁸, reacting with Ph₃P and NBS in DMAc at 70 °C for 1 h (Scheme 4.1). The product ¹³C NMR spectrum (Figure 4.1) provides confirmation that the desired C-6 bromination has cleanly occurred. A new resonance appears at 37 ppm, consistent with bromo-substituted

C-6³⁶. Based on previous reports^{49,50}, the resonance at 63 ppm is from 6-carbons bearing acetyl groups. Resonances at 130 and 135 ppm indicate that the product contains small proportions of Ph₃P and its oxide; as in our previous studies, it was difficult to completely remove phosphine impurities from the initial brominated product.^{36,43} Satisfyingly, DS(Br) calculated from elemental analysis was 0.49. Since the DS(6-OH) of CA320S was measured as 0.49 by integration of the 6-propionate methyl in the perpropionylated product, C-6 bromination is quantitative. The resulting 6-BrCA320S exhibits good solubility in commonly used organic solvents such as DMAc, DMSO or DMF, indicating that little or none of the feared crosslinking reaction had taken place. The ability to carry out the desired bromination cleanly and quantitatively on a cellulose ester was a promising start.

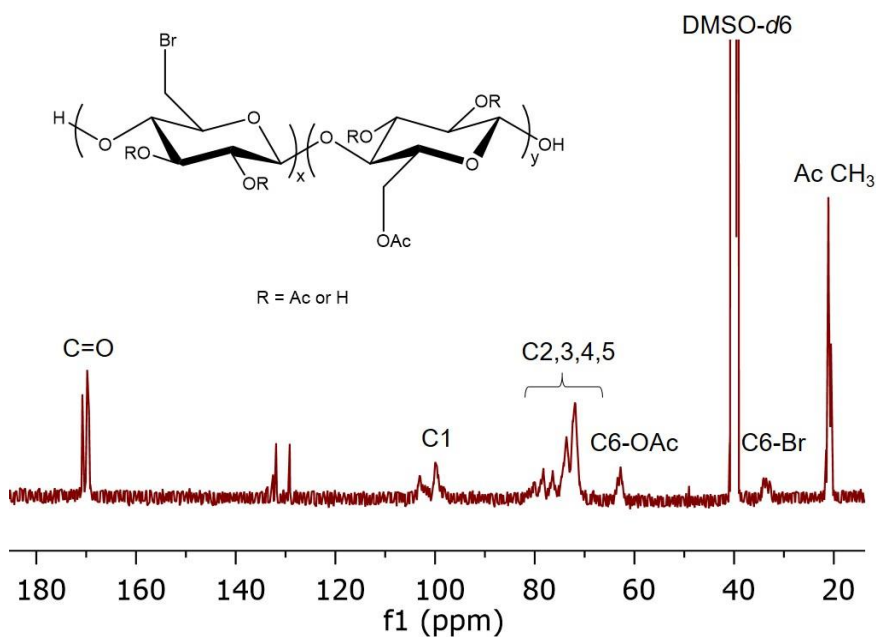


Figure 4.1. ¹³C NMR spectrum of 6-BrCA320S.

4.4.2 Azide displacement

The key remaining questions were whether the 6-bromo substituents of 6-BrCA320S were sufficiently susceptible to nucleophilic displacement, and whether the reaction would be free of side reactions like base-catalyzed deacylation. We first explored displacement by the highly nucleophilic azide. The Edgar and Kaplan groups, for example, have previously demonstrated that bromide displacement by azide was efficient on 6-bromo-6-deoxypolysaccharide derivatives of native cellulose, amylose, pullulan, and curdlan.^{36,39,42,43} In addition, azide is a useful handle for click chemistry⁵³ or Staudinger ligations⁵⁴, permitting complex and useful polysaccharide functionalization. In the event, reaction of 6-BrCA320S with NaN₃ in DMSO at 80 °C for 24 h (Scheme 4.1) was successful. By ¹³C NMR (Figure S4.2), the C-Br peak at 37 ppm was absent in the product, while a new peak at 50 ppm was assigned as the C-N₃ resonance. The product FTIR spectrum (Figure S4.3) is conclusive, with a strong azide absorption at 2110 cm⁻¹ and a carbonyl absorption from the ester at 1760 cm⁻¹, supporting successful azide displacement without apparent loss of ester groups. The absorption at 3500 cm⁻¹ results from the unreacted (as expected) secondary OH groups at C-2 and C-3, and possibly from trace moisture in the sample. Elemental analysis indicated DS(N₃) 0.49, with no bromine content found, supporting quantitative overall conversion of the original 6-OH groups to 6-N₃ groups. Successful synthesis of azido-substituted cellulose ester co-polymers creates a gateway to a panoply of useful, regioselectively functionalized cellulose-based amines and amides⁴³.

4.4.3 Cationic copolymer electrolytes (6-PyrCA320S and 6-MeIMCA320S) derived from 6-BrCA320S

We first tested our hypothesis that the lower DS(Br) of 6-BrCA320S would permit more complete displacement by aromatic amines by reacting pyridine with 6-BrCA320S in DMSO at 80 °C for 48 h (Scheme 4.1). In the product ^{13}C NMR spectrum (Figure S4.4), the peak for 6-bromide at 37 ppm was absent, while the new peak at 61 ppm is consistent with pyridinio-substituted C-6. The ^1H NMR spectrum also supported product identification as 6-PyrCA320S (Figure 4.2); new resonances at 8-10 ppm are assigned to the aromatic protons of the added pyridinium substituent. DS(Pyr $^+$) calculated from ^1H NMR is 0.41, implying that the reaction conversion is 84%. The conversion is indeed higher than from pyridine displacement on 6-bromo-6-deoxy MCC (75%)⁴⁹. Still incomplete conversion may result from the fact that pyridine is a weak base and thus not a very good nucleophile for $\text{S}_{\text{N}}2$ displacement. Pyridine acting as a base could in theory have catalyzed deacetylation of some cellulose ester groups. However, DS(Ac) was measured by ^1H NMR to be 1.75 (vs. the starting CA 320S DS(Ac) of 1.78), indicating that little or no deacetylation occurred during phosphine-catalyzed bromination and pyridine displacement.

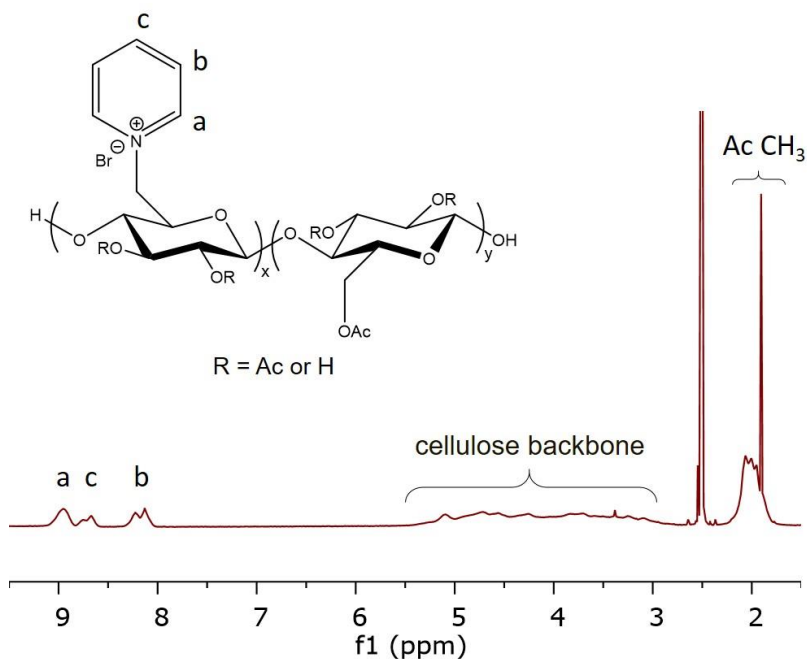


Figure 4.2. ^1H NMR spectrum for 6-PyrCA320S.

In order to improve the conversion, we explored displacement by the more basic and nucleophilic 1-methylimidazole. Reaction of 6-BrCA320S with 1-methylimidazole in DMSO at 80 °C for 48 h (Scheme 4.1) afforded a product whose ^{13}C NMR spectrum (Figure S4.5) shows a new resonance for the imidazolium-substituted C-6 around 50 ppm; no trace of the brominated carbon (37 ppm) remains. The product ^1H NMR spectrum (Figure 4.3) shows new resonances at 7.5 - 9.5 ppm, assigned to the aromatic protons of the 1-methylimidazolium substituent, and a sharp and strong peak at 4 ppm from the protons of the *N*-methyl group. DS(MeIM $^+$) calculated from ^1H NMR is 0.46, implying that the reaction conversion is 94%. This is improved vs. pyridine displacement (84%), consistent with the higher nucleophilicity of the imidazole, leaving very little covalently bonded bromide in the product. It is also improved vs. that observed from fully 6-

brominated MCC (83%), consistent with the hypothesis that developing charge density (higher in 6-BrMCC) limits conversion⁴⁹. The DS(Ac) of 6-MeIMCA320S calculated from ¹H NMR is 1.70, again indicating that there is no significant deacetylation during the reaction.

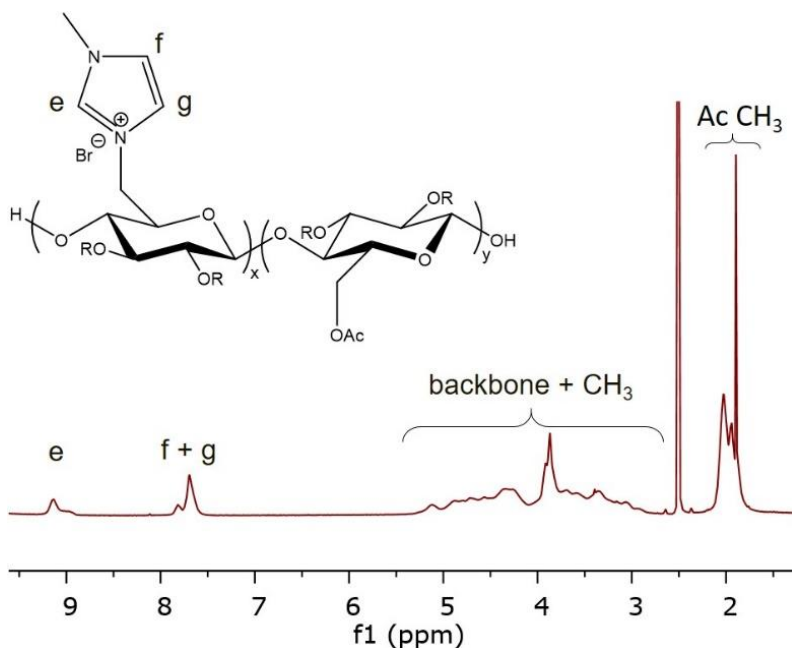


Figure 4.3. ¹H NMR spectrum for 6-MeIMCA320S.

4.4.4 One-Pot synthesis of 6-MeIMCA320S

Having achieved a high degree of conversion to a cationic polyelectrolyte using 1-methylimidazole as nucleophile, we wondered whether bromination and aromatic amine displacement could be carried out in one pot without isolation of the intermediate in order to enhance efficiency. To test this possibility, CA320S was first reacted with NBS and Ph₃P in DMAc (70 °C, 1 h). Then 1-methylimidazole was added to this solution, and temperature was increased to 80 °C for 48 h. The ¹³C NMR spectrum (Figure 4.4) of the

product isolated from this one-pot sequence had a new resonance for the imidazolium-substituted C-6 around 50 ppm, with no trace of the brominated carbon (37 ppm). Both ^1H and ^{13}C NMR spectra were essentially identical to those of the product from “2-pot” synthesis, indicating that the one-pot reaction was successful. DS(MeIM $^+$) calculated from ^1H NMR spectrum of the one-pot sequence product was 0.41, slightly lower conversion (84%) than in the 2-pot sequence.

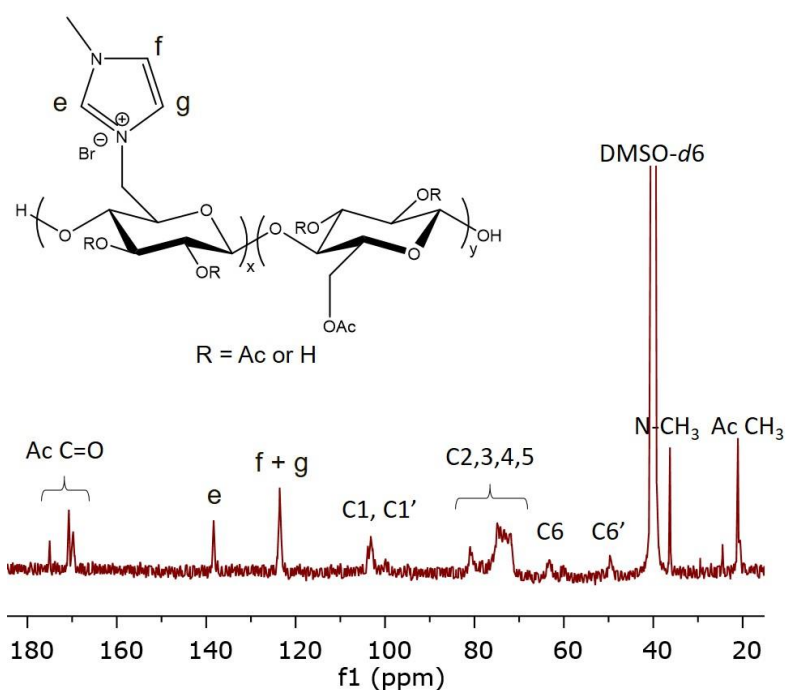


Figure 4.4. ^{13}C NMR spectrum for one-pot synthesized 6-MeIMCA320S.

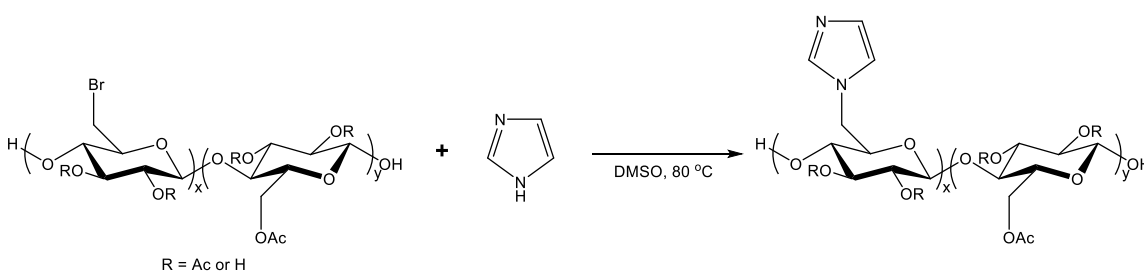
4.4.5 6-IMCA320S and quaternization of 6-IMCA320S

Successful 1-methylimidazole displacement at rather high conversion was encouraging, but conversion was still short of 100%. This was perhaps due to random instances along the CA-320S chain where multiple successive monosaccharides had free 6-OH groups,

thus resulting in charge repulsion between the eventual neighboring cationic groups. On the other hand, displacement by azide, since it did not generate charged groups, was quantitative. Therefore, it was of particular interest for us to study the reaction between 6-BrCA320S and imidazole itself, since such displacement would create no charge and thus might be expected to occur in quantitative fashion, eliminating all 6-bromide groups. Note that, unlike 1-alkylimidazoles, imidazole contains two nucleophilic nitrogen atoms. If imidazole can be efficiently appended to C-6 of cellulose via S_N2 bromide displacement, the other basic nitrogen of imidazole could then be used as a nucleophile for incorporation of other interesting functional groups. In particular, we could generate cationic charge e.g. by methylation, or zwitterionic derivatives by reaction, e.g., with propane sultone⁴⁹, and these derivatives would not possess any undesirably reactive alkyl bromide groups. It has also been demonstrated that the imidazole group can be involved in metal-ligand interactions with metal ions, e.g. zinc ions.⁵⁵

There was some concern that reaction with difunctional imidazole could cause cross-linking by further reaction of the second nucleophilic nitrogen with 6-bromo-6-deoxy substituents on other cellulose chains. To avoid such crosslinking, excess imidazole was employed to react with 6-BrCA in DMSO (80 °C, 48 h, Scheme 4.2). The product ¹³C NMR spectrum (Figure S4.6) confirmed the desired product identity; for example, the imidazole-substituted C-6 appeared at 48 ppm, shifted downfield from 32 ppm in the brominated starting material. No trace of the starting material brominated carbon remains in the product spectrum. ¹H NMR spectroscopy (Figure 4.5) also supported product identity as 6-IMCA320S; new peaks at 8-10 ppm are assigned to the aromatic protons of the

incorporated imidazole substituent. Elemental analysis indicated no residual bromine in the product, confirming quantitative nucleophilic displacement by imidazole (DS(IM) 0.49, confirmed by ^1H NMR). 6-IMCA exhibits good solubility in common organic solvents including DMSO and DMF, whereas the uncharged polymer is insoluble in water. This good solvent solubility along with the spectroscopic evidence support the notion that no cross-linking has occurred during 6-IMCA synthesis.



Scheme 4.2. Reaction scheme for conversion of 6-BrCA320S to 6-IMCA320S.

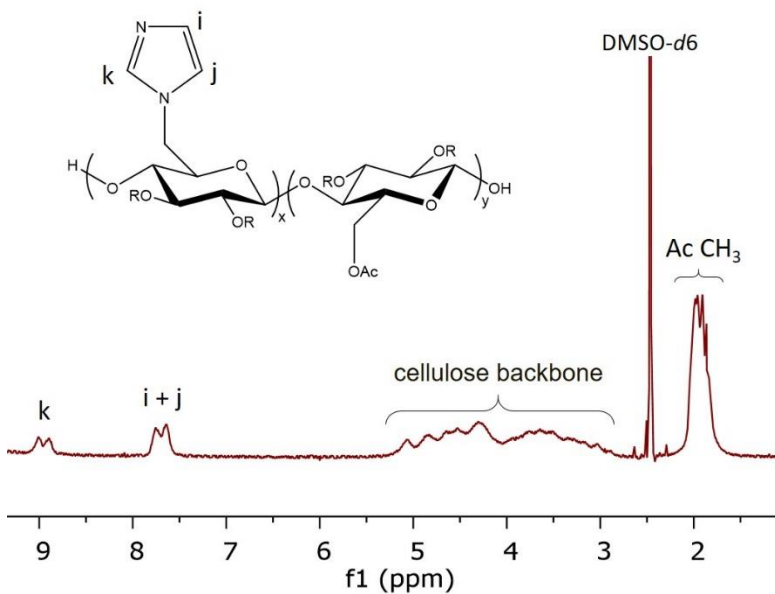
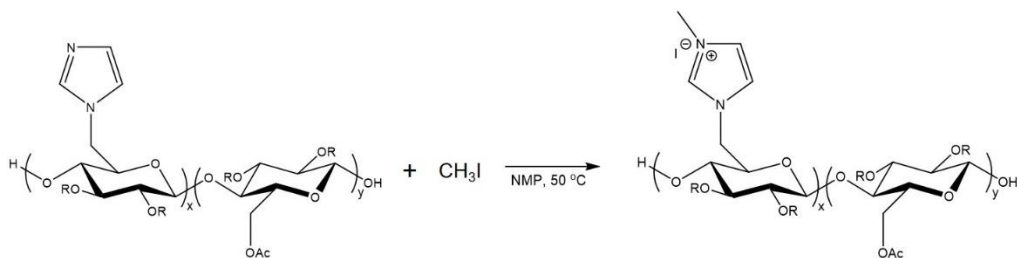


Figure 4.5. ^1H NMR spectrum of 6-IMCA320S.

Next, we used the fully converted, bromide-free imidazolyl derivative for further polyelectrolyte preparation. We wished to investigate whether the remaining basic nitrogen of the 6-IMCA imidazole substituents could be exploited to provide access to bromide-free polyelectrolyte. As Scheme 4.3 shows, methyl iodide (10 equiv/AGU) was employed as electrophile to react with 6-IMCA in NMP at 50 °C. ¹H NMR spectroscopy (Figure S4.7) confirms successful formation of the targeted cationic ionomer, 6-MeIMCA. Nucleophilic attack of the remaining basic imidazole 3-nitrogen upon methyl iodide creates a positive charge at the imidazolium atom. The resonances at 8-10 ppm are due to the aromatic protons of the imidazolium substituent, while the resonance around 3.8 ppm indicates imidazolium *N*-methyl, confirming successful conversion to the targeted cationic derivative. DS(*N*-methyl) calculated by ¹H NMR is 0.39. ¹³C NMR spectroscopy (Figure S4.8) also shows a new resonance at 37 ppm which we assign to the methyl group appended to the cationic nitrogen atom of imidazole. Based on ¹H NMR and FTIR spectroscopy (Figure S4.9), it appears that the quaternization reaction does not greatly affect the acetyl groups of CA320S. DS(Ac) 1.70 calculated by ¹H NMR (supported by the strong carbonyl absorbance at ca. 1750 cm⁻¹ in the FTIR spectrum) means that there is no significant loss of ester groups of cellulose esters during imidazole displacement and quaternization by methyl iodide.



Scheme 4.3. Quaternization of 6-IMCA320S with methyl iodide.

4.4.6 Water solubility and zeta potential of 6-PyrCA320S and 6-MeIMCA320S

Having successfully prepared cationic cellulose-based polyelectrolytes from a commercial cellulose ester (CA320S), an important question was whether these amphiphilic polyelectrolytes would have sufficient water solubility for the anticipated biomedical applications. We found that relatively concentrated (50 mg/mL) aqueous solutions could be prepared from either 6-PyrCA320S or 6-MeIMCA320S, in addition to their good organic solubility in DMF and DMSO. It is interesting to note that 6-PyrCA320S and 6-MeIMCA320S are more water soluble than pyridine ($DS(\text{pyridinio}) = 0.71$) or 1-methylimidazole ($DS(\text{methylimidazolio}) = 0.79$) substituted cellulose acetate (acetylated at the C-2/3 positions) derived from MCC⁴⁹, in spite of the overall lower charge density of the CA 320S-based polymers. Improved solubility could be due in part to the reduced stereoregularity of the CA 320S derivatives (leading to less tendency to crystallize or self-associate), and could also be influenced by fact that CA320S retains some hydrophilic hydroxyl groups at C-2 and C-3.

Since the cationic polyelectrolytes are very soluble in water, we measured zeta (ζ)-potentials for aqueous solutions (0.1 mg/mL) of our polyelectrolytes to confirm the

expected charge. Zeta potential measurement is a simple but powerful tool to prove the successful preparation of cationic cellulose ionomers by phosphine-catalyzed bromination and subsequent aromatic amine displacement, and to affirm polyelectrolyte nature prior to testing in biomedical and other potential uses. The zeta-potential values for 6-PyrCA 320S and 6-MeIMCA320S solutions were $+ 52.43 \pm 1.16$ mV and $+ 52.68 \pm 0.19$ mV, respectively, consistent with the proposed polyelectrolyte structures.

4.5 Conclusions

A simple and efficient (high yields and conversions) strategy has been developed for preparing renewable-based copolymers containing useful leaving groups at C-6 by PPh₃/NBS bromination of commercial cellulose esters, with complete regio- and chemoselectivity. We show that displacement of these new C-6 bromides to afford uncharged products (6-azide, 6-imidazolyl) is quantitative, providing derivatives with high promise for introduction of amine or amide (azide) or cationic/zwitterionic (6-imidazolyl) functional groups to form derivatives that contain no residual 6-bromide and will therefore be devoid of toxicity therefrom. The 6-bromo-6-deoxy copolymers are also useful precursors to cationic polyelectrolytes, demonstrated for 6-BrCA320S by nucleophilic displacement with aromatic amines including pyridine and 1-methylimidazole. These polyelectrolytes exhibit very good solubility in water. Note that it should be possible to eliminate the (for some purposes) undesired residual 6-Br substituents by polishing reaction with a neutral nucleophile, such as imidazole or a thiol. Moreover, we demonstrated that neutral 6-IMCA320S, prepared by imidazole displacement reaction of 6-BrCA320S in quantitative conversion and high yield, provides an efficient pathway to

bromide-free polyelectrolytes, by quaternization of the other imidazole nitrogen with methyl iodide.

It is perhaps surprising and certainly satisfying that such halogenation and displacement reactions can be carried out in the presence of somewhat labile groups like acetate esters. Further, it is gratifying that these methods provide access to what promises to be a wide variety of novel cationic and zwitterionic polysaccharide ester derivatives, in a few steps from readily available commercial polymers. Availability of these polysaccharide-based electrolytes will accelerate structure-property relationship studies for a variety of emerging uses including complexation of poly(nucleic acids) for delivery to cell nuclei, delivery of anionic drugs, and epithelial tight junction opening for oral protein delivery. The ability to prepare neutral 6-IMCA320S by related, quantitative displacement reactions of 6-BrCA320S provides access to other interesting applications requiring zwitterionic polyelectrolytes (e.g. antifouling applications), by reaction with propane sultone or related reagents. The simple methodology for preparing water-soluble (and amphiphilic) derivatives from relatively hydrophobic cellulose esters is especially notable, and valuable. In order to apply these cationic polyelectrolytes to biomedical and pharmaceutical application areas, it will be of particular interest for us to investigate the interactions between the cationic cellulose derivatives and biomolecules such as nucleic acids or certain anionic proteins, as well as their cellular toxicity and antimicrobial activity.

4.6 Supporting information

Table S4.1. Degree of Substitutions (DSs) of Perpropionylated CA320S.

	DS(Pr)	DS(Ac)
6-	0.49	0.56
2,3-	0.91	1.22

*Measured by ^1H NMR

Table S4.2. SEC Data for CA320S, 6-BrCA320S and 6-N₃CA320S.

	M _n (kDa)	M _w (kDa)	PDI (M _w /M _n)
CA320S	29.6	45.3	1.53
6-BrCA320S	158.5	166.2	1.05
6-N₃CA320S	95.9	102.8	1.07

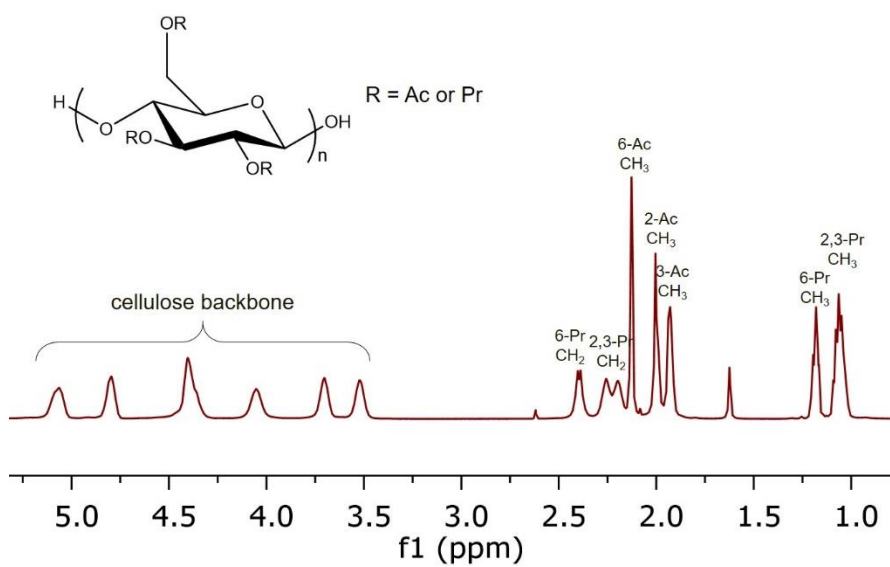


Figure S4.1. ¹H NMR spectrum of perpropionylated CA320S.

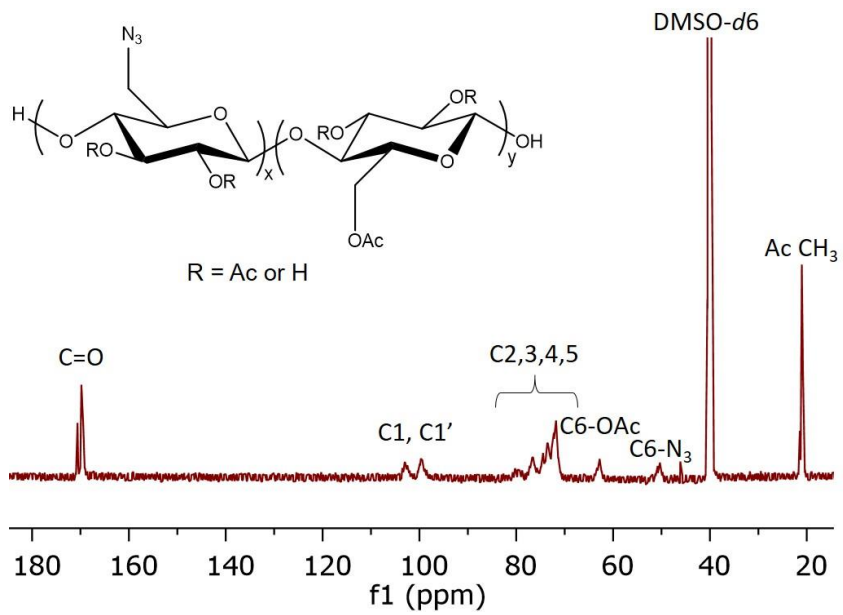


Figure S4.2. ¹³C NMR spectrum of 6-N₃CA320S.

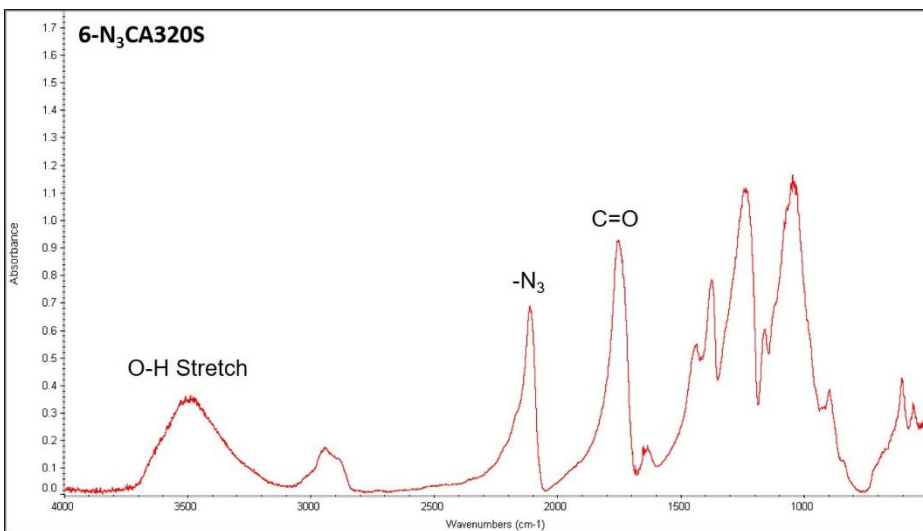


Figure S4.3. FTIR Spectrum of 6-N₃CA320S.

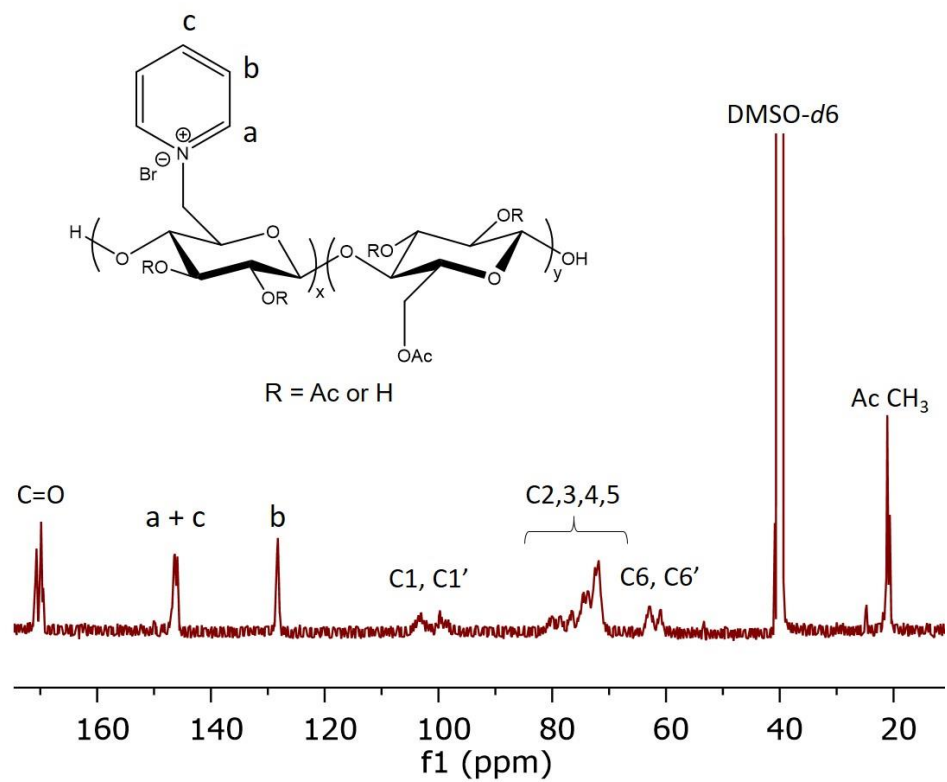


Figure S4.4. ¹³C NMR spectrum of 6-PyrCA320S.

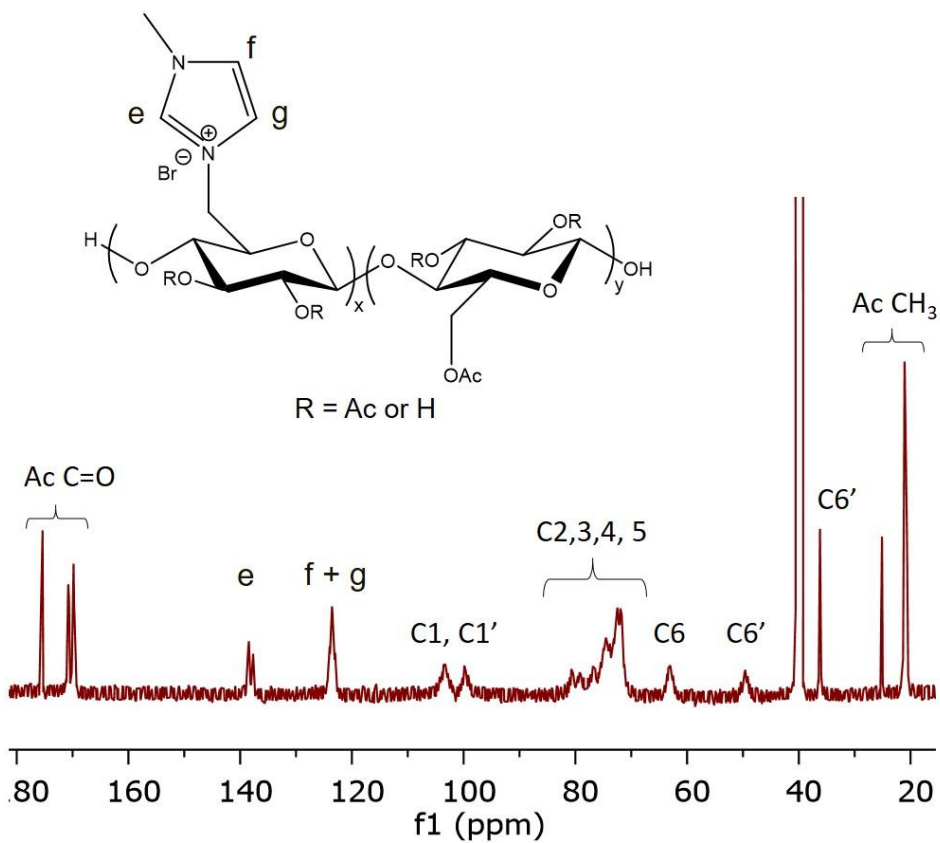


Figure S4.5. ^{13}C NMR spectrum of 6-MeIMCA320S.

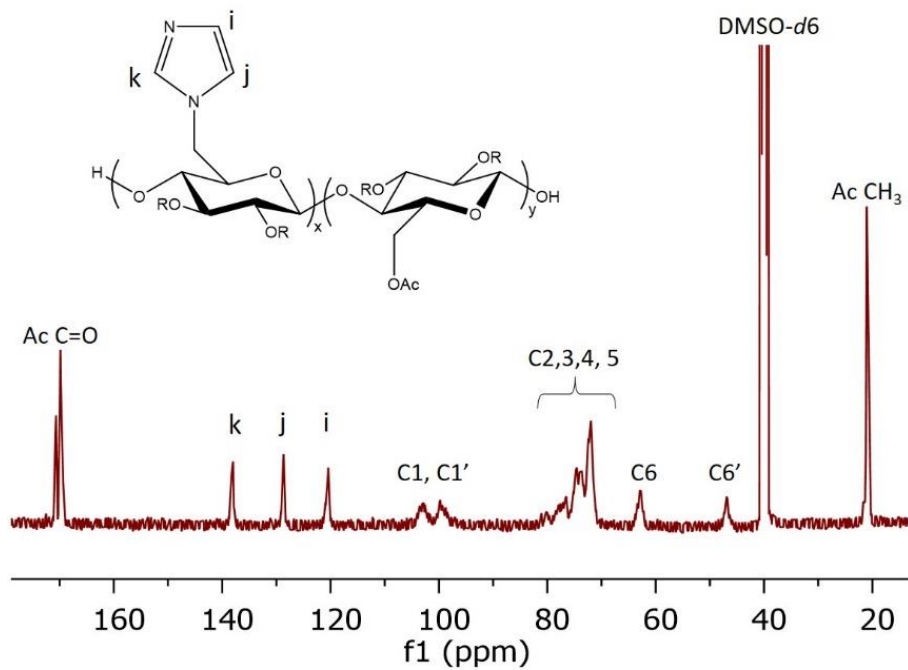


Figure S4.6. ¹³C NMR spectrum of 6-IMCA320S.

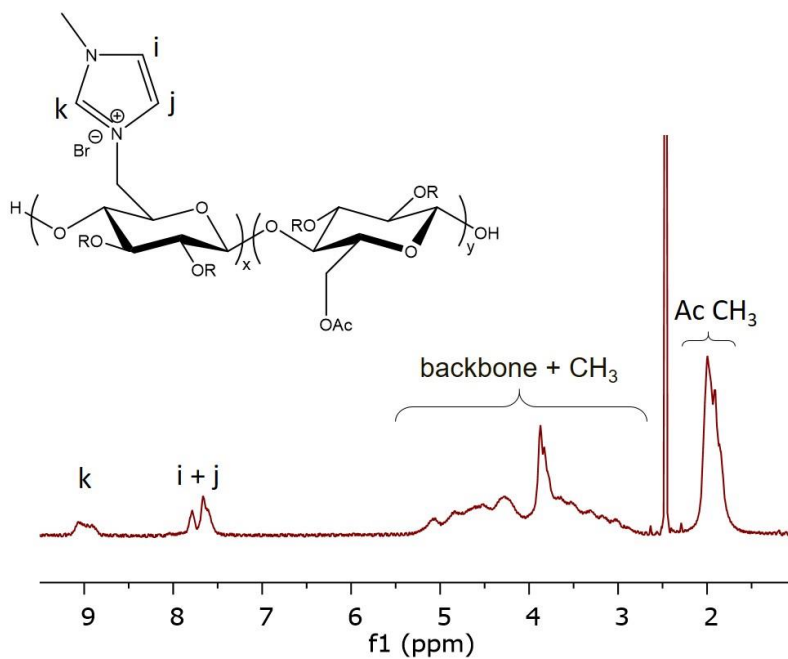


Figure S4.7. ^1H NMR spectrum of 6-IMCA320S quaternized with methyl iodide.

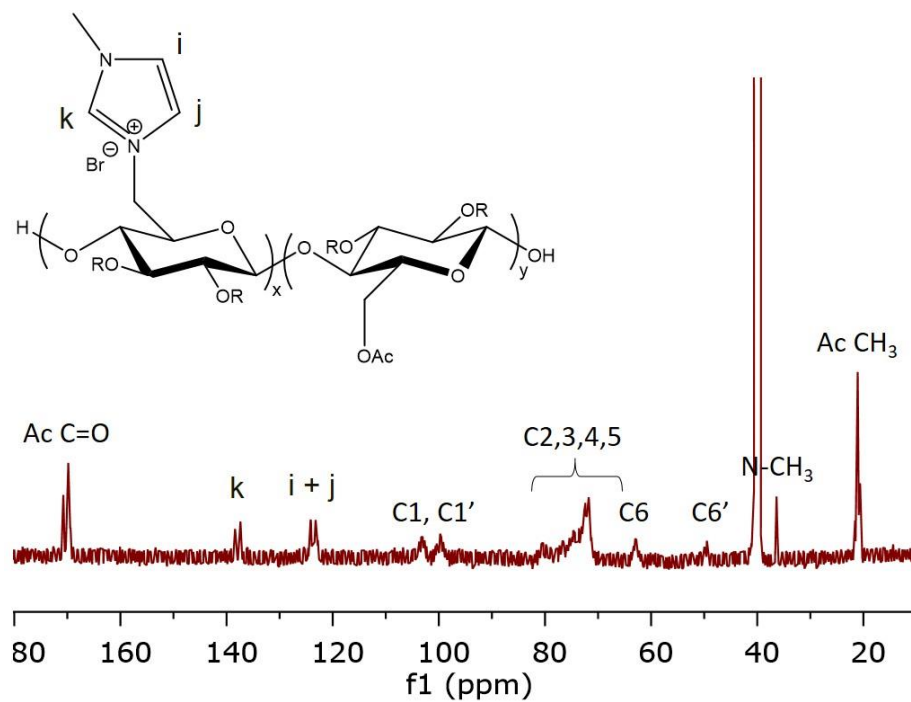


Figure S4.8. ^{13}C NMR spectrum of 6-IMCA320S quaternized with methyl iodide.

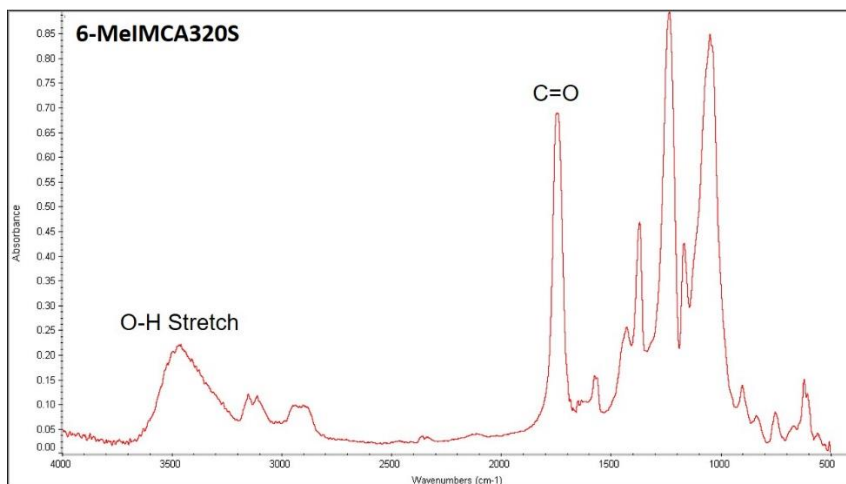


Figure S4.9. FTIR spectrum of 6-IMCA320S quaternized with methyl iodide.

4.7 Acknowledgements

We thank the Eastman Chemical Company for their kind donation of the cellulose esters used in this work. We gratefully acknowledge the Institute for Critical Technologies and Applied Science (ICTAS), Macromolecules Innovation Institute (MII) and Department of Sustainable Biomaterials at Virginia Tech for their financial, facilities, and educational support. We thank the USDA for partial support of this work through grant No. 2011-67009-20090. We also thank Shreya Choudhury of Virginia Tech for her SEC analyses.

4.8 References

1. Caffall, K. H.; Mohnen, D. The structure, function and biosynthesis of plant cell wall pectic polysaccharides. *Carbohydr. Res.* **2009**, *344*, 1879–1900.
2. Slock, J. A.; Stahly, D. P. Polysaccharides that may serve as a carbon and energy storage compound for sporulation in bacillus cereus. *J. Bacteriol.* **1974**, *120*, 399–406.
3. Lapasin, R.; Prici, S. *Rheology of Industrial Polysaccharides: Theory and Applications*. Springer: New York, **1995**.
4. Sakurai, K.; Shinkai, S. Molecular recognition of adenine, cytosine, and uracil in a single-stranded RNA by a natural polysaccharide: Schizophyllan. *J. Am. Chem. Soc.* **2000**, *122*, 4520–4521.
5. Dubin, P.; Bock, J.; Davies, R. M.; Schulz, D. N.; Thies, C. *Macromolecular Complexes in Chemistry and Biology*; Springer-Verlag: Berlin, **1994**.
6. Edgar, K. J.; Buchanan, C. M.; Debenham, J. S.; Rundquist, P. A.; Seiler, B. D.; Shelton, M. C.; Tindall, D. Advances in cellulose esters performance and application. *Prog. Polym. Sci.* **2001**, *26*, 1605–1688.

7. Heinze, T. *Polysaccharides I: Structure, Characterisation and Use*; Springer: Berlin, **2005**.
8. Klemm, D.; Heublein, B.; Fink, H. P.; Bohn, A. Cellulose: fascinating biopolymer and sustainable raw material. *Angew. Chem., Int. Ed.* **2005**, *44*, 3358–3393.
9. Fox, S. C.; Li, B.; Xu, D.; Edgar, K. J. Regioselective esterification and etherification of cellulose: A review. *Biomacromolecules* **2011**, *12*, 1956–1972.
10. Dong, Y.; Edgar, K. J. Imparting functional variety to cellulose ethers via olefin cross-metathesis. *Polym. Chem.* **2015**, *6*, 3816–3827.
11. Meng, X.; Matson, J. B.; Edgar, K. J. Olefin cross-metathesis as a source of polysaccharide derivatives: Cellulose ω -carboxyalkanoates. *Biomacromolecules* **2014**, *15*, 177–187.
12. Meng, X.; Matson, J. B.; Edgar, K. J. Olefin cross-metathesis: a mild, modular approach to functionalize cellulose esters. *Polym. Chem.* **2014**, *5*, 7021–7033.
13. Xu, D.; Edgar, K. J. TBAF and cellulose esters: Unexpected deacylation with unexpected regioselectivity. *Biomacromolecules* **2012**, *13*, 299–303.
14. Zhang, R.; Zheng, X.; Kuang, J.; Edgar, K. J. Glycan ester deacylation by TBAOH or TBAF: Regioselectivity vs. polysaccharide structure. *Carbohydr. Polym.* **2014**, *113*, 159–165.
15. Zheng, X.; Gandour, R. D.; Edgar, K. J. Probing the mechanism of TBAF-catalyzed deacylation of cellulose esters. *Biomacromolecules* **2013**, *14*, 1388–1394.
16. Zheng, X.; Gandour, R. D.; Edgar, K. J. TBAF-catalyzed deacylation of cellulose esters: reaction scope and influence of reaction parameters. *Carbohydr. Polym.* **2013**, *98*, 692–698.

17. Dawsey, T. R.; McCormick, C. L. The lithium chloride/dimethylacetamine solvent for cellulose *J. Macromol. Sci. Polymer Rev.* **1990**, *30*, 405–440.
18. Östlund, Å.; Lundberg, D.; Nordstierna, L.; Holmberg, K.; Nydén, M. Dissolution and gelation of cellulose in TBAF/DMSO solutions: The roles of fluoride ions and water. *Biomacromolecules*, **2009**, *10*, 2401–2407.
19. Zhu, S.; Wu, Y.; Chen, Q.; Yu, Z.; Wang, C.; Jin, S.; Ding, Y.; Wu, G. Dissolution of cellulose with ionic liquids and its application: A mini-review. *Green Chem.* **2006**, *8*, 325–327.
20. Gomez, J. A. C.; Eler, U.; Klemm, D. 4-Methoxy substituted trityl groups in 6-*O* protection of cellulose: homogeneous synthesis, characterization, detritylation. *Macromol. Chem. Phys.* **1996**, *197*, 953–964.
21. Hall, D. M.; Horne, J. R. Model compounds of cellulose: trityl ethers substituted exclusively at C-6 primary hydroxyls. *J. Appl. Polym. Sci.*, **1973**, *17*, 2891–2896.
22. Hearon, W. M.; Hiatt, G. D.; Fordyce, C. R. Cellulose trityl ether. *J. Am. Chem. Soc.* **1943**, *65*, 2449–2452.
23. Heinze, T.; Röttig, K.; Nehls, I. Synthesis of 2,3-*O*-carboxymethylcellulose. *Macromol. Rapid Commun.* **1994**, *15*, 311–317.
24. Heinze, T.; Pfeifer, A.; Sarbova, V.; Koschella, A. 3-*O*-Propyl cellulose: Cellulose ether with exceptionally low flocculation temperature. *Polym. Bull.* **2011**, *66*, 1219–1229.
25. Helferich, B.; Köster, H. Äther des triphenyl-carbinols mit cellulose und stärke. *Ber. Dtsch. Chem. Ges. B* **1924**, *57*, 587–591.
26. Honeyman, J. Reactions of Cellulose. Part I. *J. Chem. Soc.* **1947**, 168–173.

27. Klemm, D.; Stein, A. Silylated cellulose materials in design of supramolecular structures of ultrathin cellulose films. *J. Macromol. Sci., Part A: Pure Appl. Chem.* **1995**, *32*, 899–904.
28. Koschella, A.; Heinze, T.; Klemm, D. First synthesis of 3-*O*-functionalized cellulose ethers via 2,6-di-*O*-protected silyl cellulose. *Macromol. Biosci.* **2001**, *1*, 49–54.
29. Koschella, A.; Fenn, D.; Heinze, T. Water soluble 3-mono-*O*-ethyl cellulose: synthesis and characterization. *Polym. Bull.* **2006**, *57*, 33–41.
30. Yin, X.; Koschella, A.; Heinze, T. Regioselectively oxidized 3-*O*-alkyl ethers of cellulose: synthesis and characterization. *React. Funct. Polym.* **2009**, *69*, 341–346.
31. Bragd, P. L.; van Bekkum, H.; Besemer, A. C. TEMPO-mediated oxidation of polysaccharides: survey of methods and applications. *Top. Catal.* **2004**, *27*, 49–66.
32. Fukuzumi, H.; Saito, T.; Iwata, T.; Kumamoto, Y.; Isogai, A. Transparent and high gas barrier films of cellulose nanofibers prepared by TEMPO-mediated oxidation. *Biomacromolecules* **2009**, *10*, 162–165.
33. Isogai, A.; Kato, Y. Preparation of polyuronic acid from cellulose by TEMPO-mediated oxidation. *Cellulose* **1998**, *5*, 153–164.
34. Saito, T.; Isogai, A. TEMPO-mediated oxidation of native cellulose. The effect of oxidation conditions on chemical and crystal structures of the water-insoluble fractions. *Biomacromolecules* **2004**, *5*, 1983–1989.
35. Saito, T.; Kimura, S.; Nishiyama, Y.; Isogai, A. Cellulose nanofibers prepared by TEMPO-mediated oxidation of native cellulose. *Biomacromolecules* **2007**, *8*, 2485–2491.

36. Fox, S. C.; Edgar, K. J. Staudinger reduction chemistry of cellulose: Synthesis of selectively *O*-acylated 6-amino-6-deoxy-cellulose. *Biomacromolecules* **2012**, *13*, 992–1001.
37. Liu, S.; Edgar, K. J. Staudinger reactions for selective functionalization of polysaccharides: A review. *Biomacromolecules* **2015**, *16*, 2556–2571.
38. Furuhata, K.; Koganei, K.; Chang, H.-S.; Aoki, N.; Sakamoto, M. Dissolution of cellulose in lithium bromide-organic solvent systems and homogeneous bromination of cellulose with *N*-bromosuccinimide-triphenylphosphine in lithium bromide-*N,N*-dimethylacetamide. *Carbohydr. Res.* **1992**, *230*, 165–177.
39. Cimecioglu, A. L.; Ball, D. H.; Kaplan, D. L.; Huang, S. H. Preparation of amylose derivatives selectively modified at C-6. 6-Amino-6-deoxyamylose. *Macromolecules* **1994**, *27*, 2917–2922.
40. Gericke, M.; Schaller, J.; Liebert, T.; Fardim, P.; Meister, F.; Heinze, T. Studies on the tosylation of cellulose in mixtures of ionic liquids and a co-solvent. *Carbohydr. Polym.* **2012**, *89*, 526–536.
41. Koschella, A.; Heinze, T. Unconventional cellulose products by fluorination of tosyl cellulose. *Macromol. Symp.* **2003**, *197*, 243–254.
42. Pereira, J. M.; Edgar, K. J. Regioselective synthesis of 6-amino or 6-amido-6-deoxypullulans. *Cellulose* **2014**, *21*, 2379–2396.
43. Zhang, R.; Edgar, K. J. Synthesis of curdlan derivatives regioselectively modified at C-6: *O*-(*N*)-acylated 6-amino-6-deoxycurdlan. *Carbohydr. Polym.* **2014**, *105*, 161–168.

44. Aoki, N.; Furuhashi, K. I.; Saegusa, Y.; Nakamura, S.; Sakamoto, M. Reaction of 6-bromo-6-deoxycellulose with thiols in lithium bromide-*N,N*-dimethylacetamide. *J. Appl. Polym. Sci.* **1996**, *61*, 1173–1185.
45. Furuhashi, K.-i.; Ikeda, H. Ionic cellulose derivatives: Synthesis of sodium 6-deoxycellulose-6-sulfonate with high degree of substitution. *React. Funct. Polym.* **1999**, *42*, 103–109.
46. Scranton, A. B.; Rangarajan, B.; Klier, J. Biomedical applications of polyelectrolytes. *Adv. Polym. Sci.* **1995**, *122*, 1–54.
47. Samal, S. K.; Dash, M.; Van Vlierberghe, S.; Kaplan, D. L.; Chiellini, E.; van Blitterswijk, C.; Moroni, L.; Dubruel, P. Cationic polymers and their therapeutic potential. *Chem. Soc. Rev.* **2012**, *41*, 7147–7194.
48. Marks, J. A.; Fox, S. C.; Edgar, K. J. Cellulosic polyelectrolytes: Synthetic pathways to regioselectively substituted ammonium and phosphonium derivatives. *Cellulose* **2016**, *23*, 1687–1704.
49. Liu, S.; Liu, J.; Esker, A. R.; Edgar, K. J. An efficient, regioselective pathway to cationic and zwitterionic *N*-heterocyclic cellulose ionomers. *Biomacromolecules* **2016**, *17*, 503–513.
50. Zhang, R.; Liu, S.; Edgar, K. J. Regioselective synthesis of cationic 6-deoxy-6-(*N,N*, *N*-trialkylammonio)curdlan derivatives. *Carbohydr. Polym.* **2016**, *136*, 474–484.
51. Liebert, T.; Hussain, M. A.; Heinze, T. Structure determination of cellulose esters via subsequent functionalization and NMR spectroscopy. *Macromol. Symp.* **2005**, *223*, 79–91.

52. Xu, D.; Li, B.; Tate, C.; Edgar, K. J. Studies on regioselective acylation of cellulose with bulky acid chlorides. *Cellulose* **2011**, *18*, 405–419.
53. Liebert, T.; Hänsch, C.; Heinze, T. Click chemistry with polysaccharides. *Macromol. Rapid Commun.* **2006**, *27*, 208–213.
54. Gattás-Asfura, K. M.; Stabler, C. L. Chemoselective cross-linking and functionalization of alginate via Staudinger ligation. *Biomacromolecules* **2009**, *10*, 3122–3129.
55. Mozhdehi, D.; Ayala, S.; Cromwell, O. R.; Guan, Z. Self-healing multiphase polymers via dynamic metal-ligand interactions. *J. Am. Chem. Soc.* **2014**, *136*, 16128–16131.

Chapter 5. Selective Synthesis of Curdlan ω -Carboxyamides by Staudinger Ylide Nucleophilic Ring-opening

5.1 Abstract

Chemoselective modification of polysaccharides is a significant challenge, and regioselective modification is even more difficult, due to the low and similar reactivity of the various polysaccharide hydroxyl groups directly linked to the main polymer chain. Bromination of glycans that possess free 6-OH groups is exceptional in that regard, giving regiospecific, high-yield access to 6-bromo-6-deoxyglycans. Herein we report a simple and efficient pathway for synthesizing 6- ω -carboxyalkanamido-6-deoxy-containing polysaccharide derivatives in a sequence starting from 6-bromo-6-deoxycurdlan, via azide displacement, then conversion of the azide to the iminophosphorane ylide by triphenylphosphine (Ph₃P). We take advantage of the nucleophilicity of the iminophosphorane nitrogen by subsequent regioselective ring-opening reactions of cyclic anhydrides. These reactions of curdlan, a useful polysaccharide for food and biomedical applications, were essentially completely regio- and chemo-selective, proceeding under mild conditions in the presence of ester groups, yet preserving those groups. These interesting polysaccharide-based materials have pendant carboxyls attached through a hydrocarbon tether and hydrolytically stable amide linkage; as such they are promising for

diverse application areas, including aqueous dispersions for coatings, adhesives, and other consumer products, as well as for amorphous solid dispersions and oral drug delivery.

5.2 Introduction

Carboxyl-containing polysaccharides are useful in many applications, being based on abundant, renewable, often biodegradable, and diverse polysaccharides. Pendent carboxyl groups impart pH responsiveness to the polymer, and can enhance specific interactions with small molecules, enable dissolution or dispersion in water, and stabilize the polysaccharide itself or other molecules with which it associates against aggregation, due to the polyelectrolytic nature of the carboxylated polysaccharide. Despite their utility, there are not many effective methods for making carboxylated polysaccharides. Existing methods include direct oxidation of polysaccharides that contain unsubstituted C-6 primary hydroxyls,¹⁻³ reaction with chloroacetic acid to form carboxymethyl derivatives,⁴ cross-metathesis to introduce carboxyl terminal substituents,^{5,6} and ring opening of cyclic anhydrides by polysaccharide hydroxyls.^{7,8} Each has limitations; C-6 oxidation for example gives no flexibility with regard to length of the tether to the polysaccharide chain, and is limited to a maximum degree of substitution (DS) of 1.0. Carboxymethylation is very useful; carboxymethylcellulose (CMC) has the largest markets among cellulose ethers, including in detergent applications.⁹ However it is quite difficult to achieve high carboxymethyl DS (above ca. 1.5)¹⁰, due to developing repulsion between the appended carboxymethyl groups and approaching chloroacetate electrophiles, both of which are anionic under standard CMC reaction conditions. Ring opening of cyclic anhydrides by *O*-centered nucleophiles is more flexible (though limited by the stability of the needed

anhydrides, with adipic anhydride being the practical maximum ring size), but affords hydrolytically labile ester linkages.¹¹ In this way cellulose succinates have been prepared by ring-opening of succinic anhydride by cellulose or cellulose esters with or without an organic base catalyst,^{7,12} while the commercial enteric polymer cellulose acetate phthalate has been produced by base-catalyzed reaction of cellulose acetate with phthalic anhydride.¹³ These hydrolytically labile ester linkages might be adequate to survive their brief (ca. 4-6 h) exposure to neutral pH in the gastrointestinal tract as part of drug delivery systems, but are not stable enough to survive longer term exposure to alkaline pH, as in paint dispersions or other consumer products. Thus new, more flexible approaches are needed, that tether the carboxyl to the polysaccharide by more hydrolytically robust links.

The bacterial exopolysaccharide curdlan is of particular interest because of its low oral toxicity, good solubility and rheological properties.¹⁴ Curdlan is a linear, neutral glucan with (1→3)- β -glucosidic linkages, without branching or substituents. The primary 6-OH is the most reactive hydroxyl group due to its better accessibility. Curdlan is soluble in alkaline media, though insoluble in water, and has enhanced solubility in organic solvents compared to many other natural polysaccharides.¹⁵ This solubility facilitates curdlan chemical reactions and processing. In recent years, curdlan and its derivatives have been investigated for biomedical or therapeutic uses, in part due to curdlan's low toxicity.¹⁶ Therefore non-toxic, relatively soluble curdlan was a sensible starting point for our work.

In spite of the challenges that (generally poorly reactive) polysaccharides present to chemo- and regioselective modification, some progress has been made lately.¹⁷⁻²³ Perhaps the most

selective reaction of polysaccharides that possess unsubstituted, primary C-6 hydroxyls is bromination using triphenylphosphine and *N*-bromosuccinimide (NBS), discovered by the Furuhashi group.^{24,25} This reaction appears to be essentially perfectly selective within the limitations of spectroscopic methods, and hydrolysis to monosaccharides and chromatographic analysis confirms the absence of off-target bromination products.²⁴ Several groups have leveraged this selective 6-bromination as a path for synthesis of regioselective C-6 amination of polysaccharides including cellulose^{20,26-28} and amylose²⁹. Our group has exploited 6-bromo-6-deoxycurdlan, prepared by Furuhashi bromination, through azide displacement followed by Staudinger reduction of the azide, or direct amine displacements of the 6-bromide, for regioselective synthesis of a series of 6-deoxy-6-(azido/amino/amido/ammonium) curdlan derivatives.^{30,31} Indeed, the full range of amine, ammonium, and amide types are accessible in this way, and include promising candidates for biomedical and pharmaceutical applications.

The iminophosphorane ylide that results from PPh₃ reduction of 6-azido-6-deoxy polysaccharides, including curdlan, has a highly nucleophilic, negatively charged nitrogen atom. Having proven that these curdlan ylides could be successfully acylated, alkylated with alkyl iodides, and reacted to aldehydes to form imines (which could be reduced to secondary amines), we realized that they might also be sufficiently good nucleophiles to effectively ring-open cyclic carboxylic acid anhydrides. We hypothesized that such ring opening would be successful and selective, and that the products would be curdlan 6- ω -carboxyalkanamides, where the carboxyl-containing chain was appended by a hydrolytically stable amide linkage. We further hypothesized that such derivatives could

be highly valuable as amorphous solid dispersion (ASD) polymers, for enhancing solubility and oral bioavailability of otherwise poorly soluble drugs.^{32,33} The potential for these target curdlan 6- ω -carboxyalkanamides as stable, carboxyl-containing, amphiphilic polymers for ASD is exciting, especially since they could likely be tailored to have high glass transition temperatures (T_g), desired solubility parameters, and other key ASD properties. They are also materials of interest beyond ASD; the likely hydrolytic stability of the amide linkage means that the tether to the key carboxyl group, which would provide the pH responsiveness, water-dispersibility, and specific interactions with other molecules, would remain intact across a broad pH range. Therefore we could anticipate utility in higher pH dispersions such as those typically used in aqueous coating and adhesive formulations, to cite two examples. These characteristics could provide broad utility in demanding applications. Furthermore, success at the iminophosphorane/ring-opening strategy could have impact far beyond curdlan derivatives.

Herein, we describe our attempts to realize a simple and efficient strategy for synthesizing ω -carboxyalkanamide-substituted polysaccharide derivatives from curdlan esters by reacting iminophosphorane ylides with cyclic anhydrides. We fully characterize the products of these attempts, report their interesting physical properties, and describe initial screening as ASD polymers by crystallization inhibition experiments.

5.3 Materials and methods

5.3.1 Materials

Curdlan (degree of polymerization (DP) = 421, measured by size exclusion chromatography of the per(phenylcarbamate) derivative) was obtained from Wako Chemicals and dried under vacuum at 40 °C overnight prior to use. Lithium bromide (LiBr, laboratory grade, Fisher) was dried under vacuum at 125 °C. *N*-Bromosuccinimide (NBS, 99%, Acros) was recrystallized from boiling water and dried for two days under reduced pressure over anhydrous calcium chloride. *N,N*-Dimethylacetamide (DMAc, reagent grade, Fisher) was stored over 4 Å molecular sieves. Pyridine (anhydrous, 99%, AcroSeal), 4-dimethylaminopyridine (DMAP, Acros), triphenylphosphine (Ph₃P, 99%, Acros), sodium azide (NaN₃, 99%, Acros), acetic anhydride (Ac₂O, 99+%, Sigma-Aldrich), succinic anhydride (99%, Sigma-Aldrich), glutaric anhydride (99%, Sigma-Aldrich), potassium bromide (KBr, Sigma-Aldrich), ethanol (HPLC grade, Fisher), molecular sieves (4 Å, Fisher) and regenerated cellulose dialysis tubing (MW 3500, Fisher) were used as received.

5.3.2 Measurements

¹H and ¹³C NMR spectra were obtained on a Bruker Avance II 500MHz spectrometer in DMSO-*d*₆ or DMF-*d*₇ at room temperature, employing 32, and 15,000 scans, respectively. Infrared spectra of samples as pressed KBr pellets were obtained on a Thermo Electron Nicolet 8700 instrument using 64 scans and 4 cm⁻¹ resolution. Size exclusion chromatography (SEC) was performed on Agilent 1260 Infinity MultiDetector SEC using DMAc with 0.05 M LiCl as the mobile phase (50 °C) with 3 PLgel 10 μm mixed-B 300 × 7.5 mm columns in series. Data acquisition and analysis were conducted using Astra 6 software (Wyatt Technology Corporation, Goleta, CA). Monodisperse polystyrene standard (M_w ~21k, polydispersity index (PDI) ~1.02) was run first in every sample series

for the purpose of calibration and confirmation. Carbon and nitrogen contents were determined by Micro Analysis Inc. using a Perkin Elmer 2400 II analyzer, while bromine content was determined with a thermal conductivity detector. DS values were determined by means of ^1H NMR spectroscopy, according to the following equations, respectively.

$$\text{DS}(\omega\text{-carboxysuccinamide}) = \frac{7I_{\text{SA-CH}_2}}{4}$$

$$\text{DS}(\omega\text{-carboxyglutaramide}) = \frac{7I_{\text{CH}_2}}{6} - 1$$

$$\text{DS}(\text{Ac}) = \frac{7I_{\text{CH}_3}}{3}$$

5.3.3 Synthesis of 6-bromo-6-deoxy-curdlan

The method for dissolving curdlan in DMAc/LiBr was adapted from one previously reported for cellulose dissolution.³⁴ Ph_3P (25.96 g, 4 equiv/AGU) and NBS (17.58 g, 4 equiv/AGU) were separately dissolved in 50 mL of dry DMAc each. The Ph_3P solution was added dropwise via a liquid addition funnel to curdlan (4.00 g, 24.69 mmol) solution in DMAc/LiBr, followed by addition of the NBS solution in similar fashion. The reaction solution was then heated at 70 °C for 1 h. The cooled mixture was added slowly to 1 L of a 50:50 mixture of methanol and deionized water and then filtered to recover the precipitate. The isolated product was redissolved in DMSO and re-precipitated in ethanol twice. The sample was dried under vacuum at 40 °C overnight to yield 6-bromo-6-deoxycurdlan (brown fine powder). ^{13}C NMR (DMSO-*d*₆): 103.3 (C-1), 85.0 (C-3), 74.6 (C-5), 73.6 (C-2), 70.0 (C-4), 34.5 (C-6-Br). Yield: 4.89 g, 21.67 mmol, 88%.

5.3.4 Syntheses of 6-azido-6-deoxy-curdlan and 6-azido-6-deoxy-2,4-di-*O*-acetyl-curdlan

The procedure was adapted from a previously reported method.³⁰ Briefly, in a 100 mL round-bottom flask, dry 6-bromo-6-deoxycurdlan (2.00 g, 8.88 mmol) was dissolved in 50 mL DMSO. Then NaN₃ (2.88 g, 5 equiv/AGU) was added to the solution. The resulting mixture was heated at 80 °C and stirred for 24 h under nitrogen. The solution was cooled to room temperature, then the product was precipitated by pouring into 300 mL of deionized water, then collected by filtration. The precipitate was re-dissolved in acetone, re-precipitated into deionized water, and again isolated by filtration. The sample was dried under vacuum (40 °C) overnight to yield 6-azido-6-deoxy-curdlan (brown powder). ¹³C NMR (DMSO-*d*₆): 103.3(C-1), 84.8 (C-3), 74.6 (C-5), 73.4 (C-2), 70.1 (C-4), 51.5 (C-6-N₃). Yield: 1.51g, 8.08 mmol, 91%.

Dry 6-azido-6-deoxycurdlan (1.00 g, 5.35 mmol), 4-dimethylaminopyridine (DMAP, 20 mg), pyridine (3.6 mL, 10 eq per AGU), and 20 eq per AGU of acetic anhydride (Ac₂O, 10.93 g, 107 mmol) were combined. The mixture was heated to 80 °C and held at that temperature for 24 h while stirring, then the product was precipitated by adding the solution slowly to 200 mL deionized water, and the resulting solid product was collected by filtration. The precipitate was re-dissolved in chloroform, re-precipitated into ethanol, and finally isolated by filtration. The product was washed with ethanol and water several times and then dried under vacuum (40 °C) overnight to yield 6-azido-6-deoxy-2,4-di-*O*-acetyl-curdlan (brown fine powder). ¹³C NMR (DMSO-*d*₆): 170.0 (C=O), 99.4 (C-1), 78.0 (C-3),

72.1(C-5), 71.1 (C-2), 68.5 (C-4), 50.5 (C-6-N₃), 20.6 (CH₃). Yield: 1.35 g, 5.03 mmol, 94%.

5.3.5 Synthesis of 6- ω -carboxypropionamido-6-deoxy-2,4-di-*O*-acetyl-curdlan

In a 100 mL round-bottom flask, 0.150 g 6-azido-6-deoxy-2,3-di-*O*-acetyl-curdlan was dissolved in 5 mL of anhydrous DMAc under dry nitrogen, and 1.11 g succinic anhydride (20 equiv/AGU) was added to the flask. In a separate flask, 0.290 g Ph₃P (2 equiv/AGU) was dissolved in 5 mL DMAc, after which the solution was added to the first flask. The reaction solution was stirred for 24 h at room temperature under dry nitrogen. Afterward, the solution was transferred to 3,500 MWCO dialysis tubing (prewet with water) that was then placed in a large beaker containing ethanol. The precipitate was isolated by filtration, washed with additional water, and dried in a vacuum oven at (40 °C) overnight to yield 6- ω -carboxypropionamido-6-deoxy-2,4-di-*O*-acetyl-curdlan (brown powder). ¹H NMR (DMSO-*d*₆): 3.3-5.5 (curdlan backbone), 2.7 (CH₂), 2.5-2.0 (CH₃). ¹³C NMR (DMSO-*d*₆): 160-180 (C=O), 103.2(C-1), 65-80 (C-2, C-3, C-4, C-5), 60.2 (C-6-amido), 30.3 (CH₂), 20.7 (CH₃). DS by ¹H NMR: DS(ω -carboxypropionamido) 0.85. Yield: 0.14 g, 0.41 mmol, 73%.

5.3.6 Synthesis of 6- ω -carboxybutyramido-6-deoxy-2,4-di-*O*-acetyl-curdlan

In a 100 mL round-bottom flask, 0.150 g 6-azido-6-deoxy-2,3-di-*O*-acetyl-curdlan was dissolved in 5 mL of anhydrous DMAc under dry nitrogen, and 1.26 g glutaric anhydride (20 equiv/AGU) was added to the flask. In a separate flask, 0.290 g Ph₃P (2 equiv/AGU) was dissolved in 5 mL DMAc, after which the solution was added to the first flask. The

reaction solution was stirred for 16 h at room temperature under dry nitrogen. Afterward, the solution was transferred to 3,500 MWCO dialysis tubing (prewet with water) that was then placed in a large beaker containing ethanol. The precipitate was isolated by filtration, washed with additional water, and dried in a vacuum oven at (40 °C) overnight to yield 6- ω -carboxybutyramido-6-deoxy-2,4-di-*O*-acetyl-curdlan (brown powder). ¹H NMR (DMSO-*d*₆): 3.3-5.5 (curdlan backbone), 2.5-1.5 (CH₂ and Ac CH₃). ¹³C NMR (DMSO-*d*₆): 160-180 (C=O), 103.2(C-1), 65-80 (C-2, C-3, C-4, C-5), 60.2 (C-6-amido), 34.3 (CH₂), 21.2 (CH₃). DS by ¹H NMR: DS(ω -carboxybutyramido) 0.85. Yield: 0.14 g, 0.40 mmol, 71%.

5.3.7 Nucleation induction time measurements

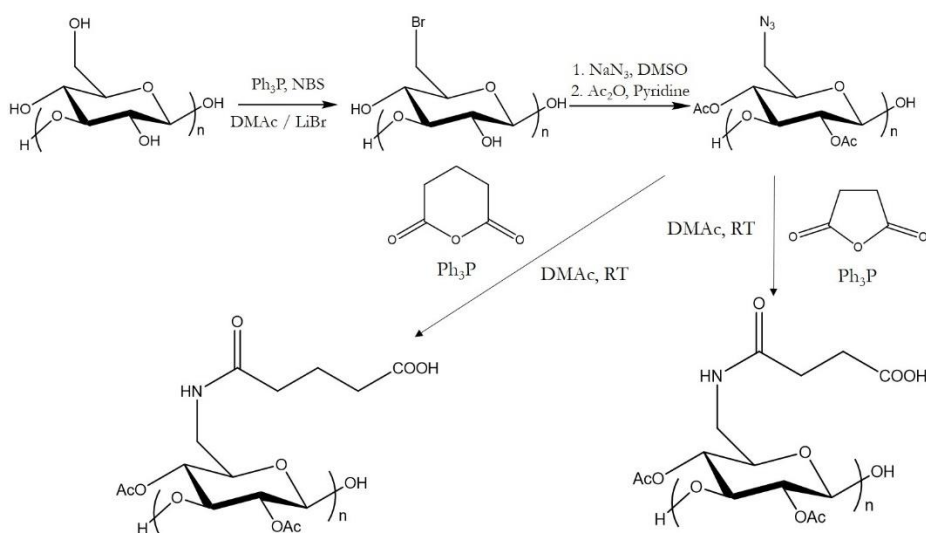
6- ω -Carboxypropionamido-6-deoxy-2,4-di-*O*-acetyl-curdlan and 6- ω -carboxybutyramido-6-deoxy-2,4-di-*O*-acetyl-curdlan were predissolved in THF, respectively, and sonicated for 60 minutes or until the polymer was fully dissolved. Next, the THF solution was added to pH 6.8 100 mM buffer, and the volume was adjusted to 5 μ g/mL polymer concentration, followed by sonication. The final solution had less than 1% THF. The 6- ω -carboxypropionamido-6-deoxy-2,4-di-*O*-acetyl-curdlan final solution had a cloudy appearance, but polymer agglomerates were not observed; while the 6- ω -carboxybutyramido-6-deoxy-2,4-di-*O*-acetyl-curdlan solution was completely transparent. Supersaturated solutions were generated by adding 150 μ g/mL of telaprevir stock solution in methanol (7 mg telaprevir/mL) to 47 mL buffer solution containing 5 μ g/mL predissolved polymer with a constant agitation of 300 rpm, and temperature controlled at 37 °C. The experimental nucleation time is defined as the sum of the time for critical

nucleus formation and growth to a detectable size. The nucleation time was determined using an SI Photonics UV/vis spectrometer (Tucson, Arizona) coupled to a fiber optic probe (path length 5 mm). Measurements were recorded every 1 min at two wavelengths: the maximum UV absorbance wavelength of telaprevir (270 nm) and a non-absorbing wavelength (370 nm) to account for changes in scattering. The point at which the apparent telaprevir concentration dropped was defined as the induction time with 5% statistical significance.

5.4 Results and discussion

The regioselectivity of this approach is set by the selectivity of the Furuata bromination, and the chemoselectivity is aided by the mild nature of the conversion of the azide to iminophosphorane ylide using Staudinger reduction. As we showed in earlier work, curdlan was readily converted to 6-azido-6-deoxy-curdlan, and if desired to 6-azido-6-deoxy-2,4-di-*O*-acetyl-curdlan, with each step taking place with high regio- and chemoselectivity, and high yield (Scheme 5.1; from curdlan to azide 80% overall, and to the azide diester, 75% overall for the three steps). We have previously reported Staudinger reduction of curdlan 6-azides in the presence of alkanolic anhydrides (e.g., acetic anhydride) to afford the corresponding 6-*N*-amides (e.g., 6-acetamido-6-deoxy-2,4-di-*O*-acetylcurdlan).^{26,30} This gave us confidence that nucleophilic attack of the curdlan iminophosphorane upon a cyclic anhydride would be successful, affording an amidocarboxylate intermediate. However, one must keep in mind that these cyclic anhydrides are difunctional; therefore upon ring opening, the pendent carboxylate may also be reactive towards the cyclic anhydride reagent. Indeed, we experienced such issues in our previously reported syntheses of

cellulose adipates that involved ring opening of adipic anhydride by cellulose hydroxyl nucleophiles. We found that it was important not to let the cellulose adipate reaction go on too long, lest gelation occur. We hypothesized that such gelation was the result of formation of oligo(anhydride) side chains by additional ring opening reactions, and attack by a hydroxyl on another polysaccharide chain upon one of the anhydride linkages, thereby forming crosslinks (Scheme S5.1). We were concerned that similar issues could accompany reactions of curdlan iminophosphoranes with cyclic anhydrides.



Scheme 5.1. Conversion of curdlan to 6- ω -carboxyamido curdlans.

5.4.1 Synthesis of 6-azido-6-deoxycurdlan via 6-bromo-6-deoxycurdlan

DMAc/LiBr is useful for curdlan dissolution and chemical modification, since it is a reasonable curdlan solvent and is unreactive towards many common reagents. Use of LiBr instead of LiCl inhibits halogen exchange of the 6-bromo derivative prepared by Furuhata bromination (NBS/Ph₃P).²⁴ As we have shown previously, replacement of the curdlan primary hydroxyl by bromide is entirely regioselective (ca. 100%, DS(Br) = 1.0) as

indicated by ^{13}C NMR analysis, as a result of the fact that it involves two consecutive $\text{S}_{\text{N}}2$ displacements, which are severely disfavored at the secondary hydroxyl groups.¹⁵ Product spectra (^{13}C NMR and FTIR) and interpretation can be found in the Supporting Information.

Azide displacement of the 6-bromide of 6-bromo-6-deoxycurdans in DMSO proceeded in high yield (94%) as we have previously reported, to afford the 6-azido-6-deoxy derivative. Displacement was complete and selective according to both NMR (^{13}C spectrum shown in Figure 5.1A) and IR analyses. See the Supporting Information (Figures S5.3 and S5.4) for full description of characterization and peak assignments. Quantitative esterification of the secondary hydroxyl groups has likewise been previously reported; it can be carried out *in situ* or as a separate step, as was done here (see FTIR spectrum of 6-azido-6-deoxy-2,4-di-*O*-acetylcurdan to illustrate, Figure 5.1B).

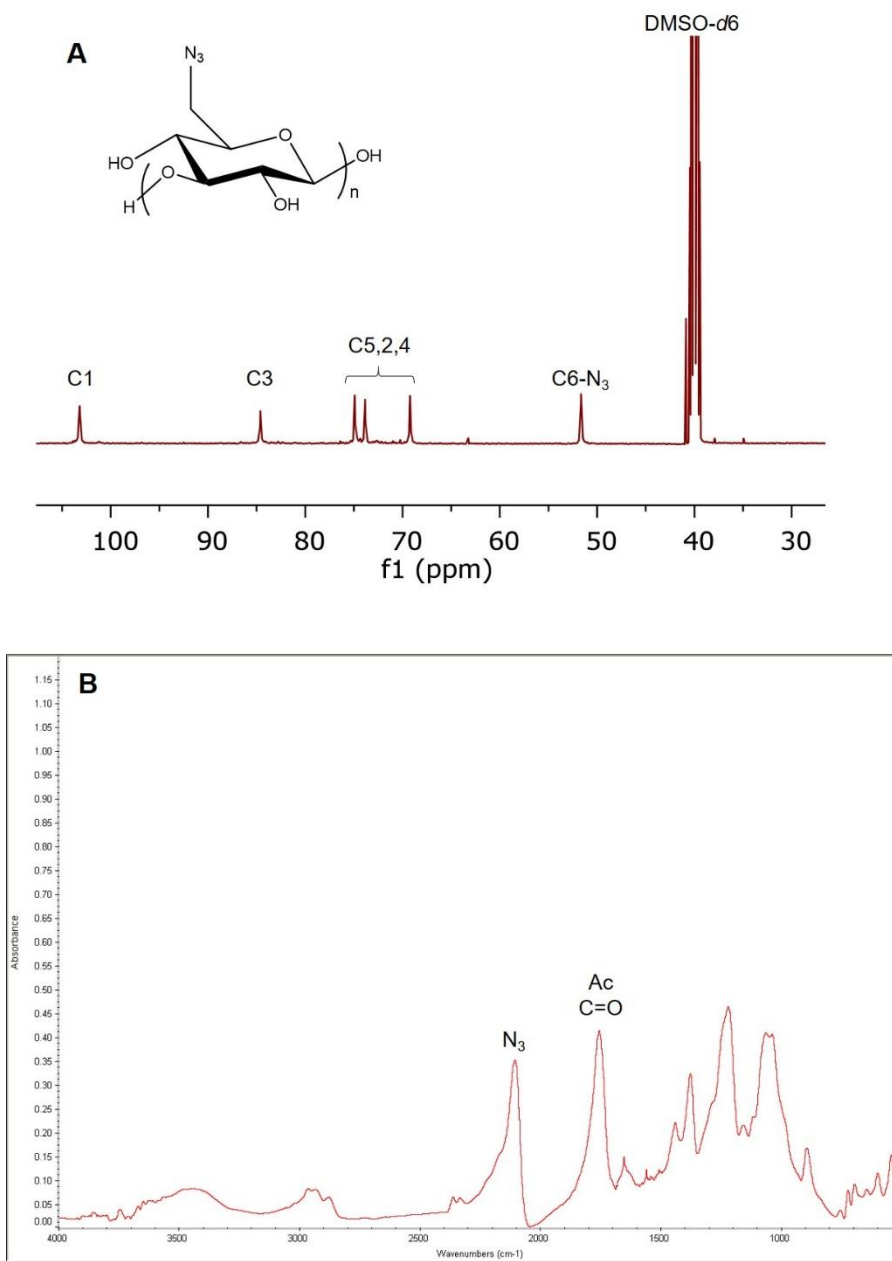


Figure 5.1. (A) ^{13}C NMR of 6-azido-6-deoxy-curdlan. (B) FTIR spectrum of 6-azido-6-deoxy-2,4-di-*O*-acetyl-curdlan.

5.4.2 Synthesis of 6- ω -carboxypropionamido-6-deoxy-2,4-di-*O*-acetyl-curdlan

Staudinger reduction (Ph_3P , H_2O , room temperature) is a remarkably useful, mild method for reducing azides to amines.³⁵ Our previous work indicated that Staudinger reduction of polysaccharide azides to amines is sufficiently mild to preserve ester bonds against reduction.²⁶ We have also found that the Staudinger reduction to the iminophosphorane can occur in the presence of anhydrides, without interference, and that the ylide so generated then reacts smoothly with monofunctional anhydrides (e.g., acetic anhydride) to form amides. In this work, 6-azido-6-deoxy-2,4-di-*O*-acetyl-curdlan was first reacted with the difunctional cyclic anhydride succinic anhydride and Ph_3P in DMAc at room temperature for 24 h. The ^{13}C NMR (Figure 5.2) spectrum of the product confirmed that the starting azide C- N_3 peak at 51 ppm had disappeared, while a new peak at 61 ppm was assigned as the resonance of C-6 bearing the new amide carbonyl. In further confirmation, by comparing with the ^{13}C NMR spectrum for 6-azido-6-deoxy-2,3-di-*O*-acetyl-curdlan, three carbonyl resonances appeared in the range of 160-180 ppm: Ac C=O 164 ppm, amide C=O 166 ppm, and carboxyl C=O 167 ppm, while two resonances at ca. 30 ppm are assigned to the succinamide methylenes. In the product ^1H NMR spectrum (Figure 5.3), the resonance around 2.7 ppm is attributed to the two succinamide methylene groups, while the resonance between 2.0 and 2.5 ppm is from the acetyl methyl groups at C-2 and C-4. The product FTIR spectrum (Figure S5.5) displayed a strong amide absorption at 1650 cm^{-1} and an ester carbonyl absorption at 1760 cm^{-1} , supporting successful ring-opening reaction without apparent loss of acetyl groups. The absorption at 3500 cm^{-1} provides further support, resulting from the ω -carboxyl acid group generated by succinic anhydride ring-opening. The ratio of the ^1H NMR integrations of the amide methylenes vs. the curdlan backbone

revealed that the product had DS(ω -carboxypropionamido) 0.85 and DS(Ac) 1.98, showing that the ring opening reaction occurs with high conversion and with no more than minimal loss of ester groups. This is particularly important, since acyl migration is a known complication of Staudinger reactions in the presence of ester groups²⁶; this result indicates that reaction of the ylide with the cyclic anhydride is sufficiently fast and favored to compete successfully with acetyl migration (intra- or intermolecular) from an ester group. Resonances in the range of 120 - 140 ppm were assigned to residual Ph₃P and Ph₃P→O.^{12,21} Our attempts to completely remove P-containing impurities were not fully successful. As we and many others have previously reported²⁸, residues of Ph₃P and its oxide are very difficult to remove from polysaccharide Staudinger ylide products, for which chromatographic purification is impractical. Nonetheless, the product has good solubility in commonly used organic solvents such as DMAc and DMSO. Taken together, the characterization data show conclusively that the product was the desired 6- ω -carboxypropionamido-6-deoxy-2,4-di-*O*-acetyl-curdlan.

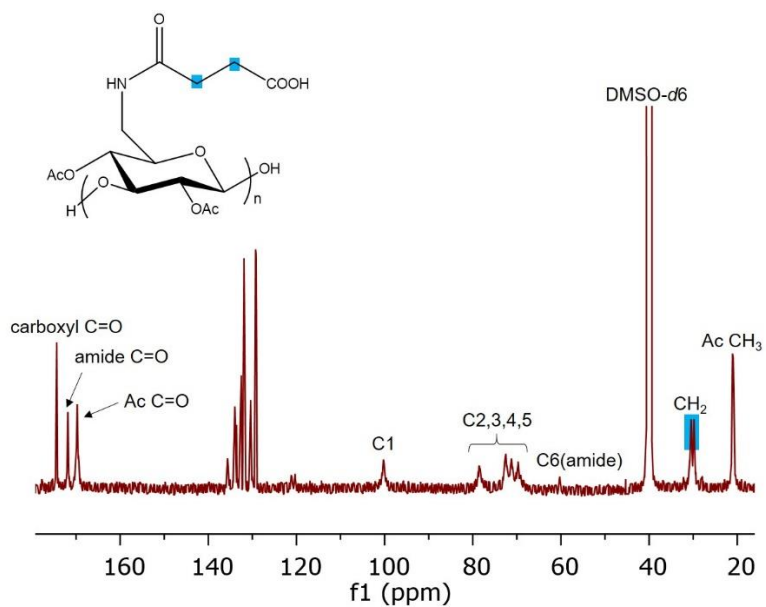


Figure 5.2. ^{13}C NMR spectrum of 6- ω -carboxypropionamido-6-deoxy-2,4-di-*O*-acetylcurdlan.

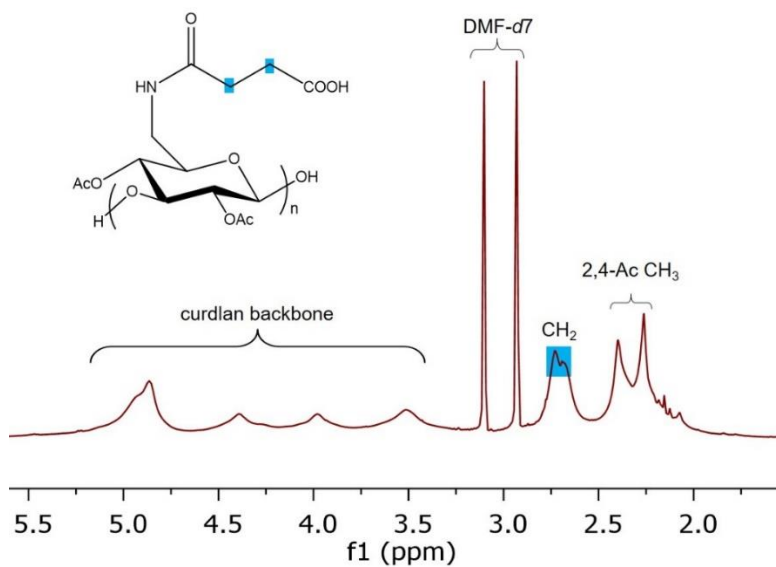


Figure 5.3. ^1H NMR spectrum of 6- ω -carboxypropionamido-6-deoxy-2,4-di-*O*-acetylcurdlan.

5.4.3 Synthesis of 6- ω -carboxybutyramido-6-deoxy-2,4-di-*O*-acetyl-curdlan

Having successfully demonstrated the ring-opening strategy with succinic anhydride, we wished to explore the impact of the tether length upon product properties and of anhydride ring size upon reactivity. For this purpose, 6-azido-6-deoxy-2,4-di-*O*-acetyl-curdlan was reacted with glutaric anhydride, possessing a 6-membered ring. Reaction of the ylide generated in the presence of the anhydride using Ph₃P in DMAc for 24 h afforded a white solid product after isolation by dialysis. As the product ¹³C NMR (Figure 5.4) spectrum shows, the 6-C-N₃ peak at 51 ppm was absent in the product, while a peak at 61 ppm was assigned as the the new amide carbonyl appended to the C-6 nitrogen. Three carbonyl resonances appear in the ¹³C NMR spectrum, which we assign to the amide (166 ppm), carboxyl (168 ppm) and two overlapping resonances for the acetyl groups (164 ppm). Resonances between 120 and 140 ppm are attributed to residual Ph₃P and Ph₃P→O. In this case, we tried dialysis, precipitation and re-dialysis, in order to obtain product free of phosphine and phosphine oxide impurities, but the product still contains small amounts of these impurities. FTIR analysis of the product (Figure 5.5) revealed the expected carboxamide absorption at 1650 cm⁻¹, a broad absorption at 3500 cm⁻¹ resulting from the carboxylic acid OH and amide NH (and likely also from contaminating 6-NH₂, see below), and a strong ester carbonyl absorption at 1760 cm⁻¹. Taken together, these infrared features support the hypothesis that the ring-opening reaction was successful with no substantial loss of ester groups. The product ¹H NMR spectrum (Figure S5.6) shows multiple resonances in the 1.5-2.5 ppm range that we attribute to the three methylene groups of the C-6 appended ω -carboxybutyramide chain, and the acetyls at C-2 and C-4. DS(ω -

carboxybutyramide) measured by ^1H NMR integration was 0.85, indicating high ring opening conversion; we suspect that conversion does not reach 100% due to competitive side reaction of the ylide with adventitious water. As with the succinic anhydride product, the ω -carboxyglutaramide product is soluble in organic solvents and in pH 6.8 buffer at the level of 16.2 mg/mL.

We carried out a kinetic study of the ylide reaction with glutaric anhydride, in order to monitor and limit any chain extension during the reaction that would occur by reaction of the initially formed ω -carboxybutyramide anion with glutaric anhydride, forming an oligoanhydride chain (see Figure S5.6A). As Figure S5.6B shows, over 24 h, the DS(ω -carboxybutyramide) value does not exceed 1.0, suggesting that there is no apparent chain extension within this reaction time. We also attempted the reaction of the iminophosphorane from 6-azido-6-deoxy-2,4-di-*O*-acetyl-curdlan with adipic anhydride. In this case, gelation was observed during the reaction. Adipic anhydride is relatively reactive due to its less favored seven-membered ring size, and so is prone to homopolymerization. This can lead to formation of poly(adipic anhydride), which we have postulated is capable of reacting in multiple sites along the polyanhydride chain with a polysaccharide OH group (or iminophosphorane ylide in this case), thereby forming crosslinks (Scheme S5.1), as we have discussed in previous work⁸.

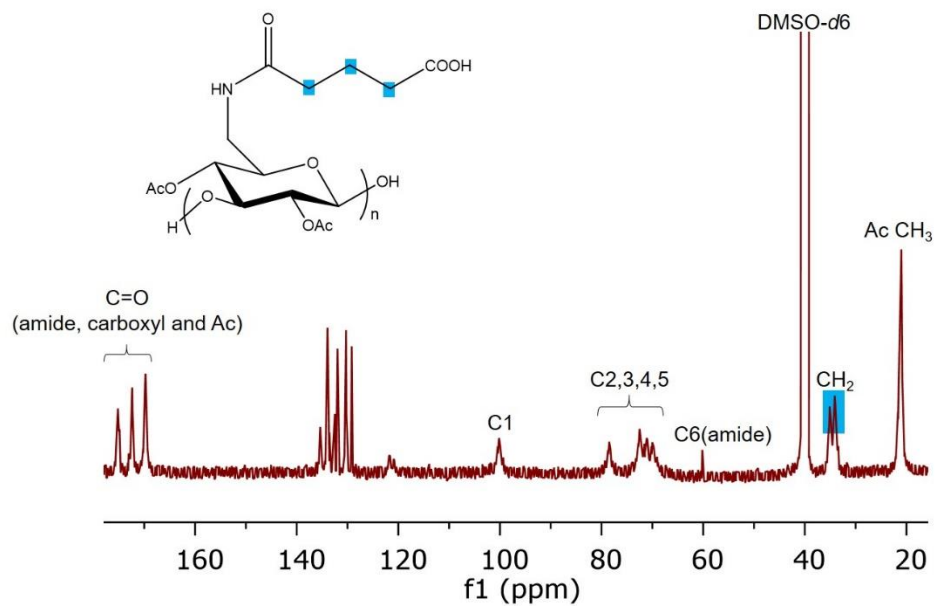


Figure 5.4. ^{13}C NMR spectrum of 6- ω -carboxybutyramido-6-deoxy-2,4-di-*O*-acetyl-curdlan.

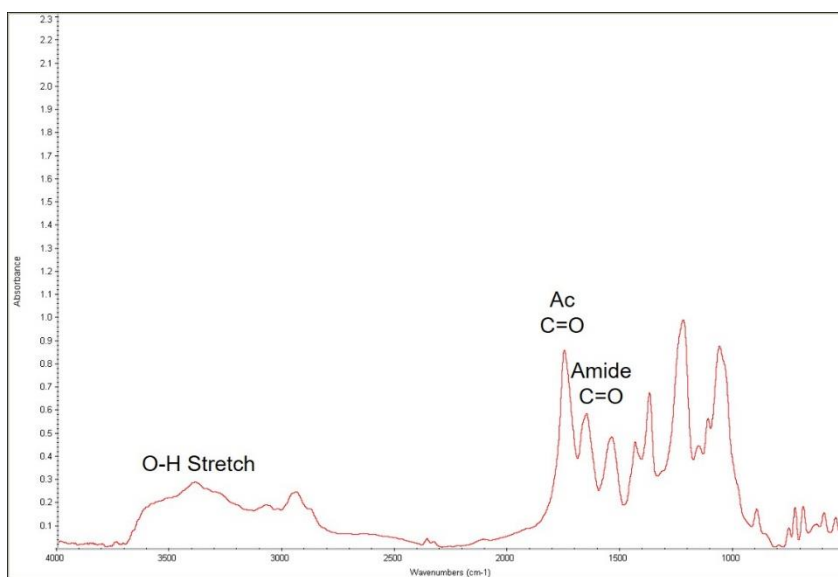


Figure 5.5. FTIR spectrum of 6- ω -carboxybutyramido-6-deoxy-2,4-di-*O*-acetyl-curdlan.

5.4.4 Crystallization inhibition properties of 6- ω -carboxypropionamido-6-deoxy-2,4-di-*O*-acetyl-curdlan and 6- ω -carboxybutyramido-6-deoxy-2,4-di-*O*-acetyl-curdlan

The crystallization inhibition properties of several cellulose ethers and esters designed and synthesized for that purpose by the Taylor and Edgar groups have been studied,^{6,31} and several derivatives have been demonstrated to be promising for ASD applications. Herein, we explored the performance of our curdlan derivatives, which differ from previous ASD candidate polymers from our labs in that they are based on curdlan vs. cellulose, include an amide linkage instead of an ether or ester linkage, and are also entirely regioselectively substituted (vs. the relatively random substitution patterns of previously investigated polymers).

Telaprevir, a protease inhibitor for the treatment of hepatitis C, was used as the model poorly soluble drug (MP 246 °C, solubility in water 4.7 $\mu\text{g}/\text{mL}$). The polymers explored include carboxylic acid substituents, based on our previous studies that showed clearly that carboxylate groups are highly effective at promoting crystallization inhibition among a number of polysaccharide-based polymers bearing various chemical groups.³¹ The only difference between the two polymers used in this study is the length of the hydrocarbon tether to the ω -carboxy group: two methylenes for 6- ω -carboxypropionamido-6-deoxy-2,4-di-*O*-acetyl-curdlan vs. three methylenes for 6- ω -carboxybutyramido-6-deoxy-2,4-di-*O*-acetyl-curdlan. The degrees of substitution were kept constant to facilitate comparison of variations in nucleation time as a function of hydrocarbon chain length. As Figures 5.6A and 5.6B show that, while 6- ω -carboxypropionamido-6-deoxy-2,4-di-*O*-acetyl-curdlan is

only slightly effective, not reaching statistical significance, 6- ω -carboxybutyramido-6-deoxy-2,4-di-*O*-acetyl-curdlan significantly increases nucleation induction times. These results agree with our previous observations about the importance of maintaining a hydrophilic/hydrophobic balance to create effective polymers. We have previously observed good performance by cellulose esters including adipate (four carbons) and suberate (six carbons).³¹ It is interesting that the stereoregularity of 6- ω -carboxybutyramido-6-deoxy-2,4-di-*O*-acetyl-curdlan does not seem to impair its ability to inhibit telaprevir crystallization.

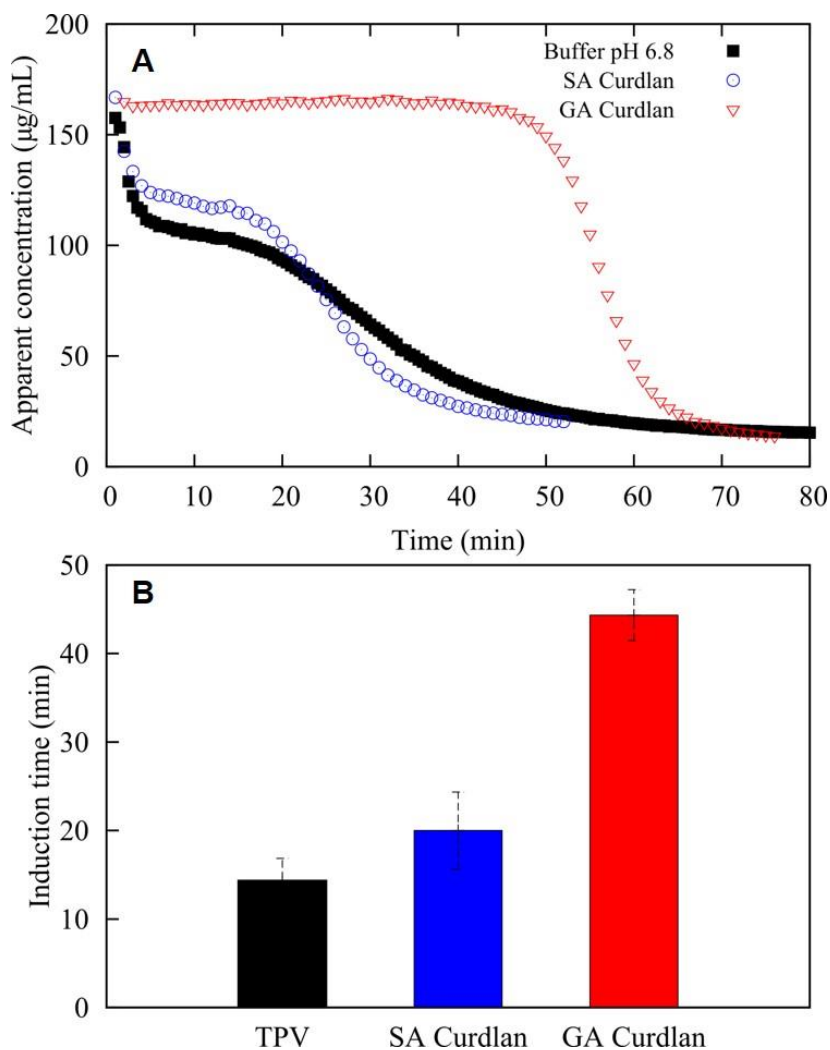


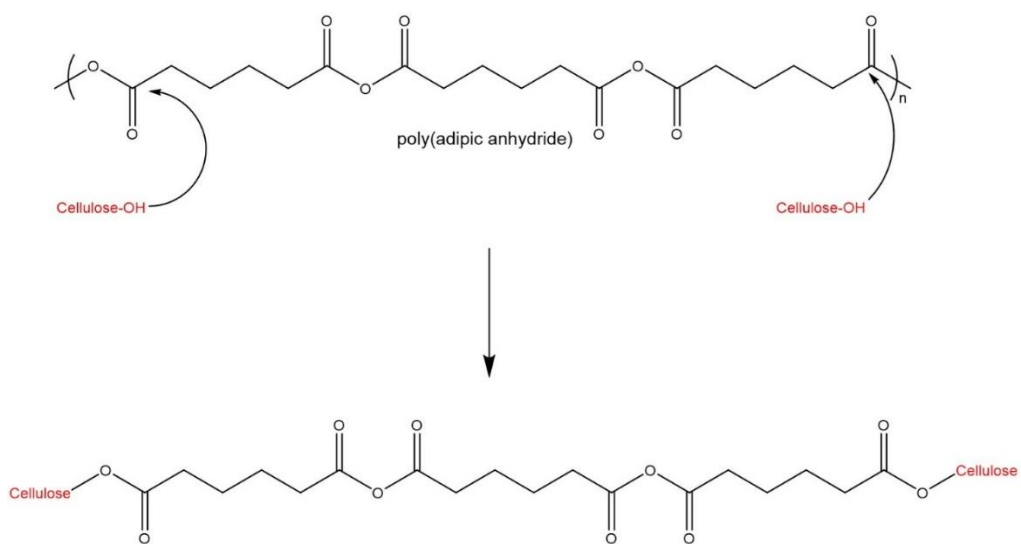
Figure 5.6. (A) Change in apparent concentration as a function of time for supersaturated solutions containing 5 $\mu\text{g/ml}$ polymer and 150 $\mu\text{g/ml}$ telaprevir. (B) Nucleation induction times in the absence and presence of curdlan ω -carboxyamides. (SA Curdlan: 6- ω -carboxypropionamido-6-deoxy-2,4-di-*O*-acetyl-curdlan, GA Curdlan: 6- ω -carboxybutyramido-6-deoxy-2,4-di-*O*-acetyl-curdlan).

5.5 Conclusions

We have developed a simple and useful route for synthesis of regioselectively substituted carboxyl-containing curdlan derivatives. 6-Azido-6-deoxy-2,4-di-*O*-acetylcurdlan was used to generate the corresponding 6-aminophosphorane ylide by chemoselective Staudinger reduction. This ylide smoothly reacted with cyclic anhydrides at room temperature, opening the anhydride ring to create a new amide linkage and generating an ω -carboxyalkanoyl substituent appended to the C-6 nitrogen, all in high reaction conversion. More importantly, it was demonstrated that these modification techniques can be carried out with essentially complete regio- and chemo-selectivity, proceeding in the presence of ester groups, yet preserving those groups. The resulting products possess durable amide linkages that should be much more stable towards hydrolysis than ester linkages.

This phosphine-triggered ring-opening reaction is exciting in terms of the potential to greatly expand the synthetic routes to curdlan carboxyamides and other polysaccharide derivatives beyond traditional methods. This new method will provide access to a broad variety of available polysaccharides with durable amide linkages and terminal carboxy groups, including those that are promising for drug delivery applications, such as ASD, and for waterborne coatings. In addition, it is of particular interest for us to investigate structure–property–performance relationships for a series of polymers with desired functionality created by this novel method for drug-delivery polymeric matrices and for other emerging technologies.

5.6 Supporting information



Scheme S5.1. Gelation mechanism for cellulose reacting with adipic anhydride.

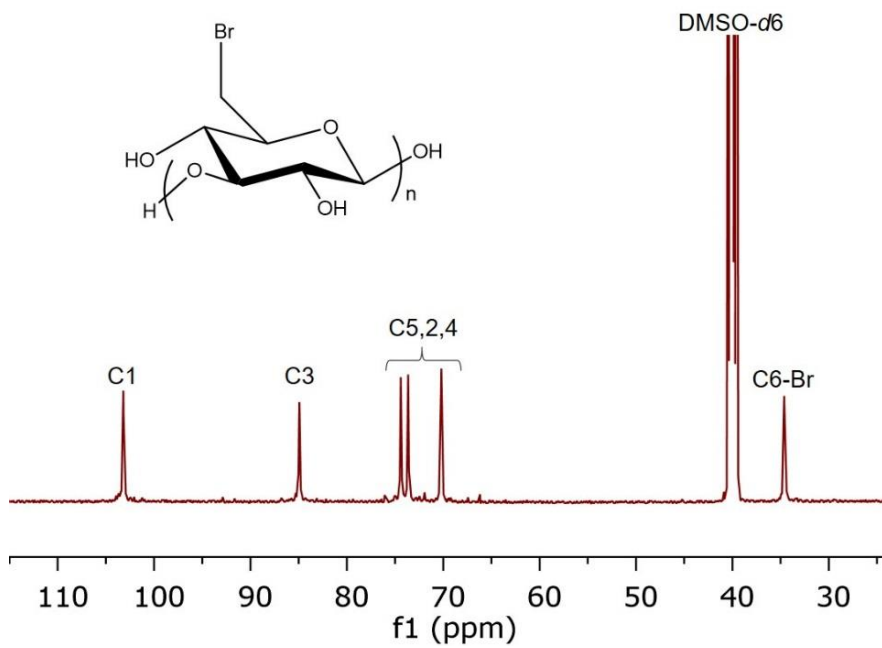


Figure S5.1. ^{13}C NMR spectrum of 6-bromo-6-deoxy-curdlan.

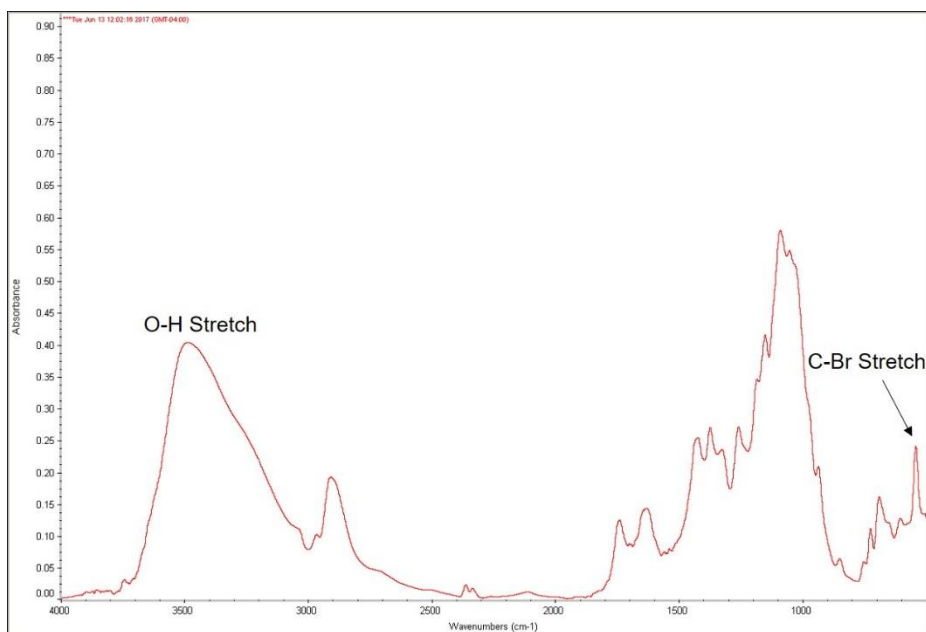


Figure S5.2. FTIR spectrum of 6-bromo-6-deoxy-curdlan.

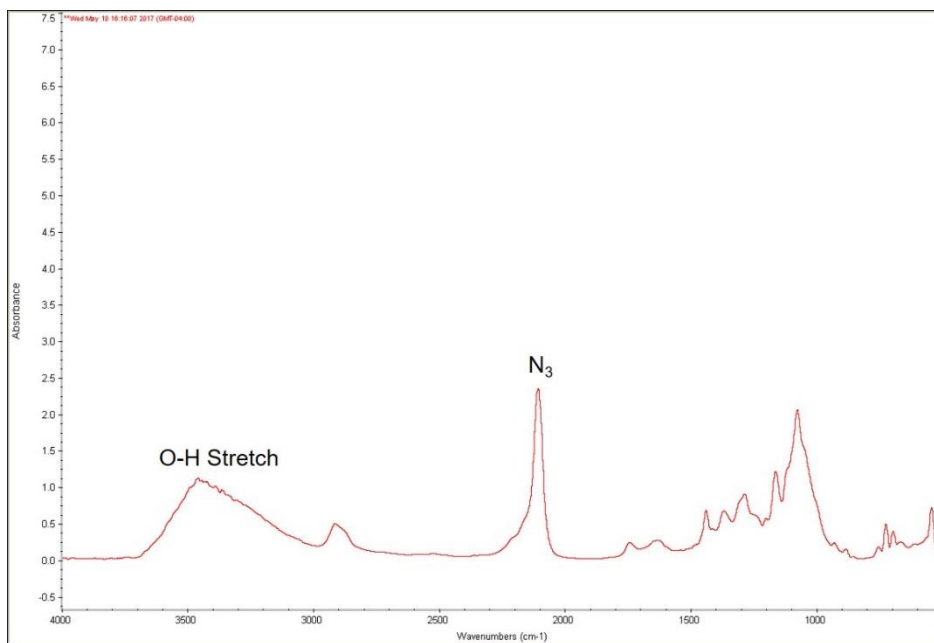


Figure S5.3. FTIR spectrum of 6-azido-6-deoxy-curdlan.

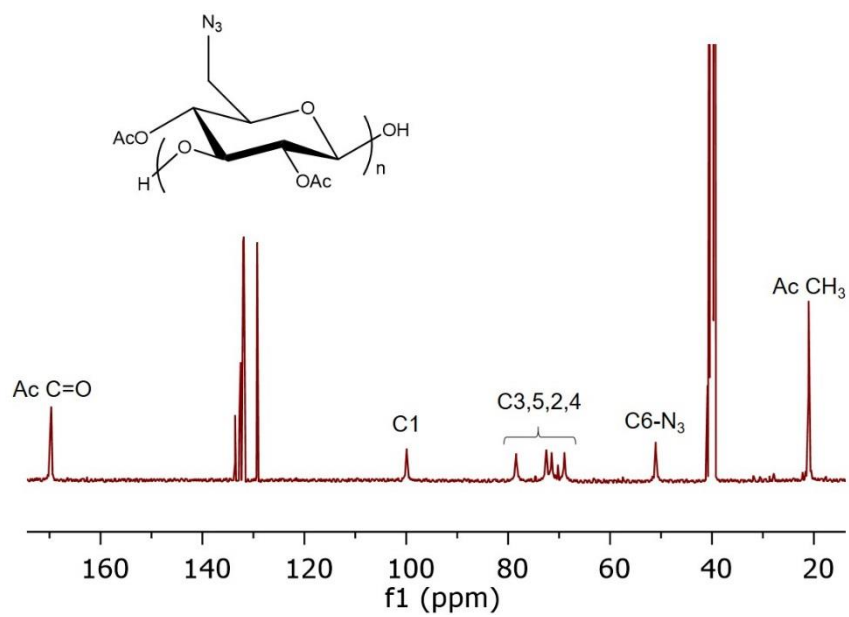


Figure S5.4. ¹³C NMR spectrum of 6-azido-6-deoxy-2,4-di-O-acetyl-curdlan.

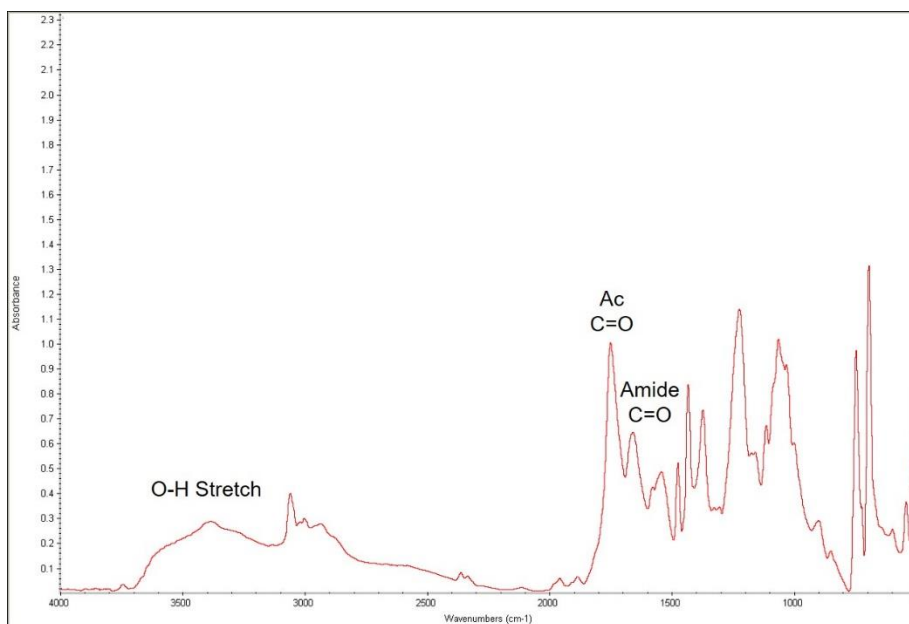


Figure S5.5. FTIR spectrum of 6- ω -carboxypropionamido-6-deoxy-2,4-di-*O*-acetylcurdlan.

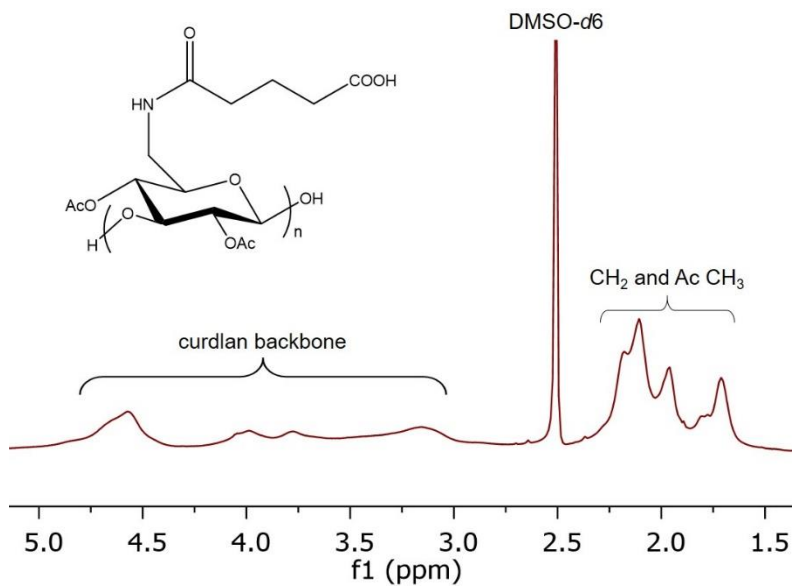
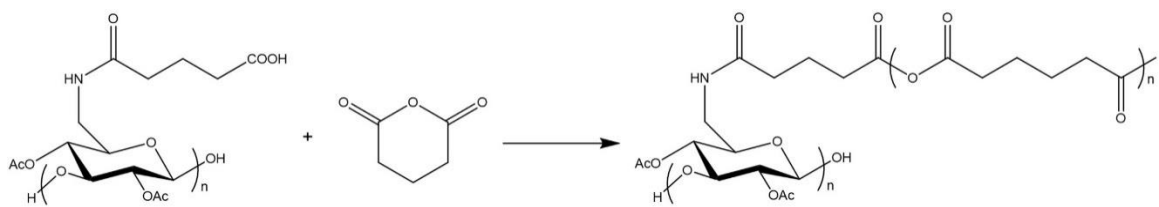


Figure S5.6. ^1H NMR spectrum of 6- ω -carboxybutyramido-6-deoxy-2,4-di-*O*-acetylcurdlan.

(A)



(B)

Time (hours)	DS
1	0.11
3	0.28
9	0.61
20	0.80
24	0.85

Figure S5.6. (A) Hypothetical chain extension mechanism by reacting 6- ω -carboxybutyramido-6-deoxy-2,4-di-*O*-acetyl-curdlan with additional glutaric anhydride.

(B) Kinetic study for conversion of 6-azido-6-deoxy-2,4-di-*O*-acetyl-curdlan to 6- ω -carboxybutyramido-6-deoxy-2,4-di-*O*-acetyl-curdlan.

Synthesis of 6-bromo-6-deoxy-curdlan

In the event, we brominated curdlan by reacting with NBS and PPh₃ in DMAc/LiBr at 70 °C for 1 h. The product ¹³C NMR spectrum (Figure S5.1) shows that distinct single resonances for C-1 to C-5 of the curdlan backbone appear in a range of 65 and 105 ppm, while the strong peak for C-6 upon substitution by bromine is around 34 ppm, implying that the bromination on curdlan worked well. In addition, there is no resonance observed at 60 ppm which belongs to the original C-6-OH of native curdlan, suggesting that the bromination reaction was quantitative.

Syntheses of 6-azido-6-deoxy-curdlan and 6-azido-6-deoxy-2,4-di-*O*-acetyl-curdlan

We carried out azide displacement reaction by reacting 6-bromo-6-deoxy-curdlan with NaN₃ in DMSO at 80 °C for 24 h (Scheme 5.1), resulting in 6-azido-6-deoxy-curdlan. NMR and FTIR were employed for determining the structure of product and confirming its regioselectivity. FTIR spectrum for the product (Figure S5.3) shows that there is a strong N₃ stretching absorption around 2100 cm⁻¹, indicating successful incorporation of azide group with curdlan backbone. The product ¹³C NMR spectrum (Figure 5.2) indicates that the C-6 chemical shift appears at 51 ppm, while the C-6 resonance substitution by bromine at 34 ppm disappears. ¹³C NMR and FTIR spectra suggest that in this work, azide displacement was highly chemo- and region-selective and its conversion was quantitative.

In order to prevent side reactions from next step modifications, we need to esterify the free hydroxyl groups at C-2 and C-4 of 6-azido-6-deoxy-curdlan. It was simple and straightforward to convert pure 6-azido-6-deoxycurdlan to its peracetylated derivatives. In

this work, 6-azido-6-deoxy-curdlan was reacted with acetic anhydride in the presence of pyridine and DMAP at 80 °C for 24 h (Scheme 5.1) to fully esterify the free 2- and 4-hydroxyls. As the product ¹³C NMR spectrum (Figure S5.4) shows the 2,4-diacetate carbonyl peaks appear around 170 ppm, and the methyl resonance is at 20 ppm. The FTIR spectrum (Figure 5.1B) shows a strong ester carbonyl stretch around 1750 cm⁻¹.

5.7 Acknowledgements

We gratefully acknowledge the Institute for Critical Technology and Applied Science (ICTAS), Macromolecules Innovation Institute (MII) and Department of Sustainable Biomaterials at Virginia Tech for their financial, facilities, and educational support. We thank the USDA for partial support of this work through grant No. 2011-67009-20090.

5.8 References

1. de Nooy, A.E.J.; Besemer, A.C.; van Bekkum, H.; van Dijk, J.A.P.P.; Smit, J.A.M. TEMPO-mediated oxidation of pullulan and influence of ionic strength and linear charge density on the dimensions of the obtained polyelectrolyte chains. *Macromolecules* **1996**, *29*, 6541–6547.
2. Tamura, N.; Wada, M.; Isogai, A. TEMPO-mediated oxidation of (1→3)-β-D-glucans. *Carbohydr. Polym.* **2009**, *77*, 300–305.
3. Pereira, J.; Mahoney, M.; Edgar, K. J. Synthesis of amphiphilic 6-carboxypullulan ethers. *Carbohydr. Polym.* **2014**, *100*, 65–73.

4. Posey-Dowty, J. D.; Watterson, T. L.; Wilson, A. K.; Edgar, K. J.; Shelton, M. C.; Lingerfelt, L. R. Zero-order release formulations using a novel cellulose ester. *Cellulose* **2007**, *14*, 79–83.
5. McCormick, C. L.; Dawsey, T. R. Preparation of cellulose derivatives via ring-opening reactions with cyclic reagents in lithium chloride/*N,N*-dimethylacetamide. *Macromolecules* **1990**, *23*, 3606–3610.
6. Liu, H.; Kar, N.; Edgar, K. J. Direct synthesis of cellulose adipate derivatives using adipic anhydride. *Cellulose* **2012**, *19*, 1279–1293.
7. Hollabaugh, C. B.; Burt, L. H.; Walsh, A. P. Carboxymethylcellulose. Uses and applications. *Ind. Eng. Chem.* **1945**, *37*, 943–947.
8. Heinze, T.; Koschella, A. Carboxymethyl ethers of cellulose and starch—a review. *Macromol. Symp.* **2005**, *223*, 13–39.
9. Edgar, K. J. Cellulose esters in waterborne coatings. *Polymers Paint Colour Journal* **1993**, *83*, 564–571.
10. Liu, C. F.; Sun, R. C.; Zhang, A. P.; Ren, J. L.; Wang, X. A.; Qin, M. H.; Chao, Z. N.; Luo, W. Homogeneous modification of sugarcane bagasse cellulose with succinic anhydride using a ionic liquid as reaction medium. *Carbohydr. Res.* **2007**, *342*, 919–926.
11. Malm, C. J.; Fordyce, C. R. Cellulose esters of dibasic organic acids. *Ind. Eng. Chem.* **1940**, *32*, 405–408.
12. Zhang, R.; Edgar, K. J. Properties, chemistry, and applications of the bioactive polysaccharide curdlan. *Biomacromolecules* **2014**, *15*, 1079–1096.

13. Harada, T.; Masada, M.; Hidaka, H.; Takada, M. Production of firm, resilient gel-forming polysaccharide in natural medium by a mutant of *Alcaligenes faecalis* var. *myxogenes* 10C3. *Hakko Kogaku Zasshi* **1966**, *44*, 20–24.
14. Spicer, E. F.; Goldenthal, E. I.; Ikeda, T. A toxicological assessment of curdlan. *Food and Chemical Toxicology* **1999**, *37*, 455–479.
15. Fox, S. C.; Li, B.; Xu, D.; Edgar, K. J. Regioselective esterification and etherification of cellulose: A review. *Biomacromolecules* **2011**, *12*, 1956–1972.
16. Nakagawa, A.; Ishizu, C.; Sarbova, V.; Koschella, A.; Takano, T.; Heinze, T.; Kamitakahara, H. 2-*O*-Methyl- and 3,6-di-*O*-methylcellulose from natural cellulose: synthesis and structure characterization. *Biomacromolecules* **2012**, *13*, 2760–2768.
17. Zheng, X.; Gandour, R. D.; Edgar, K. J. Probing the mechanism of TBAF-catalyzed deacylation of cellulose esters. *Biomacromolecules* **2013**, *14*, 1388–1394.
18. Liu, C.; Baumann, H. Exclusive and complete introduction of amino groups and their *N*-sulfo and *N*-carboxymethyl groups into the 6-position of cellulose without the use of protecting groups. *Carbohydr. Res.* **2002**, *337*, 1297–1307.
19. Zheng, X.; Xu, D.; Edgar, K. J. Cellulose levulinate: A protecting group for cellulose that can be selectively removed in the presence of other ester groups. *Cellulose* **2015**, *22*, 301–311.
20. Liu, S.; Liu, J.; Esker, A. R.; Edgar, K. J. An efficient, regioselective pathway to cationic and zwitterionic *N*-heterocyclic cellulose ionomers. *Biomacromolecules* **2016**, *17*, 503–513.
21. Liu, S.; Edgar, K. J. Water-soluble co-polyelectrolytes by selective modification of cellulose esters *Carbohydr. Polym.* **2017**, *162*, 1–9.

22. Furuhashi K.-i.; Koganei, K.; Chang, H.-S.; Aoki, N.; Sakamoto, M. Dissolution of cellulose in lithium bromide-organic solvent systems and homogeneous bromination of cellulose with *N*-bromosuccinimide-triphenylphosphine in lithium bromide-*N,N*-dimethylacetamide. *Carbohydr. Res.* **1992**, *230*, 165–177.
23. Tseng, H.; Furuhashi, K.-i.; Sakamoto, M. Bromination of regenerated chitin with *N*-bromosuccinimide and triphenylphosphine under homogeneous conditions in lithium bromide-*N,N*-dimethylacetamide. *Carbohydr. Res.* **1995**, *270*, 149–161.
24. Fox, S. C.; Edgar, K. J. Staudinger reduction chemistry of cellulose: Synthesis of selectively *O*-acylated 6-amino-6-deoxy-cellulose. *Biomacromolecules* **2012**, *13*, 992–1001.
25. Heinze, T.; Koschella, A.; Brackhagen, M.; Engelhardt, J.; Nachtkamp, K. Studies on non-natural deoxyammonium cellulose. *Macromol. Symp.* **2006**, *244*, 74–82.
26. Matsui, Y.; Ishikawa, J.; Kamitakahara, H.; Takano, T.; Nakatsubo, F. Facile synthesis of 6-amino-6-deoxycellulose. *Carbohydr. Res.* **2005**, *340*, 1403–1406.
27. Cimecioglu, A. L.; Ball, D. H.; Kaplan, D. L.; Huang, S. H. Preparation of amylose derivatives selectively modified at C-6. 6-Amino-6-deoxyamylose. *Macromolecules* **1994**, *27*, 2917–2922.
28. Zhang, R.; Edgar, K. J. Synthesis of curdlan derivatives regioselectively modified at C-6: *O*-(*N*)-acylated 6-amino-6-deoxycurdlan. *Carbohydr. Polym.* **2014**, *105*, 161–168.
29. Zhang, R.; Liu, S.; Edgar, K. J. Regioselective synthesis of cationic 6-deoxy-6-(*N,N,N*-trialkylammonio) curdlan derivatives. *Carbohydr. Polym.* **2016**, *136*, 474–484.
30. Liu, S.; Edgar, K. J. Staudinger reactions for selective functionalization of polysaccharides: A review. *Biomacromolecules* **2015**, *16*, 2556–2571.

31. Mosquera-Giraldo, L. I.; Borca, C. H.; Meng, X.; Edgar, K. J. Slipchenko, L. V.; Taylor, L.S. Mechanistic design of chemically diverse polymers with applications in oral drug delivery. *Biomacromolecules* **2016**, *17*, 3659–3671.
32. Liu, H.; Ilevbare, G. A.; Cherniawski, B. P.; Ritchie, E. T.; Taylor, L. S.; Edgar, K. J. Synthesis and structure-property evaluation of cellulose ω -carboxyesters for amorphous solid dispersions. *Carbohydr. Polym.* **2014**, *100*, 116–125.
33. Scriven, E. F. V.; Turnbull, K. Azides: Their preparation and synthetic uses. *Chemical Reviews* **1988**, *88*, 297–368.
34. Edgar, K. J.; Arnold, K. M.; Blount, W. W.; Lawniczak, J. E.; Lowman, D. W. Synthesis and properties of cellulose acetoacetates. *Macromolecules* **1995**, *28*, 4122–4128.

Chapter 6. Efficient Synthesis of Secondary Amines by Reductive Amination of Curdlan Staudinger Ylides

Zhang, R.; Liu, S.; Edgar, K. J. *Carbohydrate Polymers* **2017**, *171*, 1–8. Used permission of Elsevier, 2017

6.1 Abstract

Staudinger-related reactions between azides and phosphines are important in organic chemistry due to their chemoselectivity, high efficiency, and mild reaction conditions. Staudinger reduction of azides affords highly reactive iminophosphorane ylides; the reactivity of the negatively charged ylide nitrogen atom has not previously been fully explored in polysaccharide chemistry. Curdlan, a natural, biocompatible and bioactive β -1,3-glucan with low toxicity, has remarkable potential in biomedical and pharmaceutical applications. Herein we describe a new method for preparation of regioselectively iminated/aminated curdlan derivatives via a Staudinger ylide. 6-Azido-6-deoxy-2,4-di-*O*-acyl-curdlan was treated with triphenylphosphine to generate the highly nucleophilic iminophosphorane intermediate which afforded: i) 6-imino curdlans by reaction with several aromatic aldehydes, and ii) 6-monoalkylamino curdlans by reductive amination using these aldehydes and NaBH₃CN. This new chemistry combined with our previous results makes available valuable primary, secondary, and tertiary amines, quaternary ammonio derivatives, and amides, all with complete C-6 regioselectivity for the *N*-substitution.

6.2 Introduction

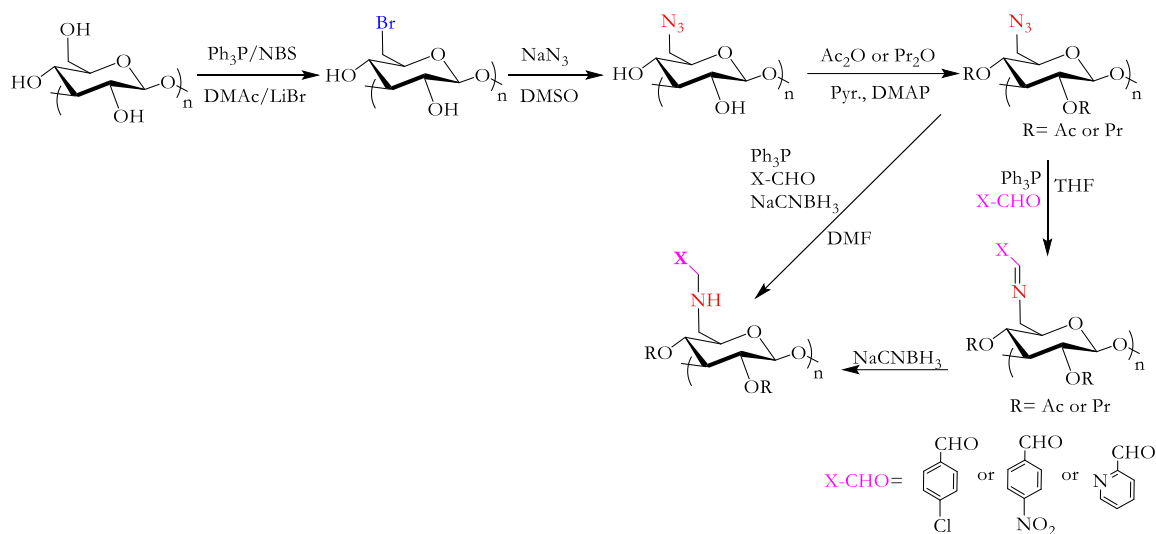
Natural polysaccharides are remarkably abundant, diverse materials that have many important functions in living organisms. These sustainable polymers are underutilized, with only a few being used to create functional derivatives to serve society (albeit in important ways). In order to effectively utilize polysaccharides, we need to understand the fundamental relationship between structure and properties, and we need better methods for selective modification of natural polysaccharides. Curdlan, an extracellular bacterial polysaccharide, is of significant interest due to its valuable rheological properties and inherent bioactivity. The simple homopolymeric, unbranched and uncharged structure of the (1,3)- β -D-glucan curdlan can be elaborated using a range of chemical modifications, such as esterification¹, carboxymethylation², phosphorylation³, sulfation^{4,5} and TEMPO oxidization^{6,7}. Our laboratory has developed a series of regioselective C-6 modifications of curdlan to synthesize 6-deoxy-6-(bromo/azido/amino/amido/ammonium) derivatives that are promising candidates for biomedical and pharmaceutical applications.⁸⁻¹⁰ We have observed that the iminophosphorane intermediate generated during Staudinger reduction of 6-azido-6-deoxycurdlan is highly nucleophilic, in accord with the previous work of Bertozzi^{11,12} and others. 6-Azido-6-deoxycurdlan is an efficient ylide precursor that upon treatment with triphenylphosphine at ambient temperature forms a phosphazide, which in turn loses nitrogen gas to form the desired iminophosphorane.

Iminophosphoranes are organic compounds of general composition $R_3P=NR$ that possess a highly polarized P=N bond and are best described as resonance hybrids of the two

extreme forms A and B (Figure S6.1).¹³ Staudinger reaction of a phosphine ($R_3P:$) with an organic azide is by far the most widely used method to synthesize iminophosphoranes. Although Staudinger and Meyers¹⁴ prepared the first aza-Wittig reagent $Ph_3P=NPh$ in 1919, the chemistry of iminophosphoranes was not heavily explored until three decades later. Since then, aza-Wittig reaction between iminophosphoranes and aldehydes has become a powerful tool in small molecule organic synthetic strategies due to the absence of metal catalysts, mild reaction conditions, and relatively high yield of the product imine. Small molecule iminophosphoranes can also react with other carbonyl compounds, such as ketones, esters, thioesters, amides, and anhydrides, providing an effective method for construction of C-N bonds, including C=N double bonds.¹⁵ We have previously reported using iminophosphorane intermediates, generated by Staudinger reduction of azides, for synthesis of *O*-acylated 6-amido-(or 6-amino)-6-deoxy-cellulose¹⁶⁻¹⁸, -curdlan⁸, and -pullulan¹⁹ derivatives by *in situ* reaction of the ylide with water, or with excess carboxylic anhydride. The Heinze group has synthesized a class of 6-amino polysaccharide derivatives by an alternate route, using 6-tosylate as the precursor.^{20,21}

Isolated small molecule imines from iminophosphorane-aldehyde condensations can be further reduced by borohydride to produce amines; this is known as indirect reductive amination. In direct reductive amination, imine formation and reduction occur sequentially in one pot, so the imine must be reduced much faster than the carbonyl group of the aldehyde reagent. Therefore the more selective reducing agent $NaCNBH_3$ is preferred for the direct process; in the indirect process its selectivity vs. ester reduction can also be

useful.²² There appear to be no previous reports in polysaccharide chemistry of reductive amination between an aldehyde and a polysaccharide iminophosphorane intermediate formed by Staudinger reaction. We hypothesize that the curdlan-based 6-iminophosphorane intermediate generated during the Staudinger reduction may be a sufficiently reactive nucleophile to undergo reductive amination with aldehydes, in the presence of a borohydride reductant, thereby providing a regioselective and chemoselective route to 6-monoalkylamino-6-deoxy-curdlans. Success in this endeavor would complement our recent efforts^{8,10,16-19,23}, together affording access to an exceptionally broad array of amines (primary, secondary, tertiary, quaternary ammonium) and amides from either 6-bromo- or 6-azido-6-deoxycurdlan. This synthetic capability would enable flexible structure-property studies with regard to cationic curdlan derivatives, afford useful intermediates for pro-drug synthesis, and feed many other potential applications. Herein we report our attempts to prepare a family of 6-monoalkylamino curdlans by reacting 6-azido-6-deoxy-2,4-di-*O*-acyl-curdlan with Ph₃P and aldehydes (Scheme 6.1).



Scheme 6.1. Synthetic scheme for 6-aminated curdlan derivatives via Staudinger ylide.

6.3 Materials and methods

6.3.1 Materials

Curdlan (DP ~ 500) was obtained from Wako Chemicals and dried under vacuum at 40 °C overnight prior to use. Lithium bromide (LiBr, laboratory grade, Fisher) was dried under vacuum at 125 °C. *N*-Bromosuccinimide (NBS, 99%, Acros) was recrystallized from boiling water and dried for two days under reduced pressure over anhydrous calcium chloride. *N,N*-Dimethylacetamide (DMAc, reagent grade, Fisher) and *N,N*-dimethylformamide (DMF, HPLC grade, Fisher) were stored over 4 Å molecular sieves. Tetrahydrofuran (THF, 99.8%, extra dry, stabilized, AcroSeal®), *N*-methyl-2-pyrrolidone (NMP, 99.5%, extra dry, AcroSeal®), pyridine (Pyr, anhydrous, 99%, AcroSeal®), benzaldehyde (PhCHO, purified by redistillation, ≥ 99.5%, Aldrich), 4-nitrobenzaldehyde (NO₂PhCHO, 98%, Aldrich), 4-chlorobenzaldehyde (4-ClPhCHO, 98%, Aldrich), 2-

pyridinecarboxaldehyde (Pyr-2-CHO, 99%, Aldrich), 4-dimethylaminopyridine (DMAP, Acros), triphenylphosphine (Ph₃P, 99%, Acros), sodium azide (NaN₃, 99%, Alfa Aesar), sodium hydroxide (NaOH, reagent grade, 97%, Sigma-Aldrich), sodium cyanoborohydride (NaBH₃CN, reagent grade, 95%, Aldrich), acetic anhydride (Ac₂O, 99+%, Sigma-Aldrich), propionic anhydride (Pr₂O, 97% Sigma-Aldrich), *n*-butyric anhydride (Bu₂O, 98%, Acros), ethanol (HPLC grade, Fisher), molecular sieves (4 Å, Fisher) and regenerated cellulose dialysis tubing (MW 3500, Fisher) were used as received.

6.3.2 Measurements

¹H, ¹³C and HSQC NMR spectra were obtained on a Bruker Avance II 500MHz spectrometer in CDCl₃, DMSO-*d*₆, DMF-*d*₇, or D₂O at room temperature or 50 °C, employing 32, 15,000 and 19,000 scans, respectively. Infrared spectroscopic analyses of samples as pressed KBr pellets were obtained on a Thermo Electron Nicolet 8700 instrument using 64 scans and 4 cm⁻¹ resolution. Carbon and nitrogen contents were determined by Micro Analysis Inc. using a Perkin Elmer 2400 II analyzer.

6.3.3 Synthesis of 6-bromo-6-deoxycurdlan in DMAc/LiBr

The procedure was adapted from a previously reported method.⁸ Dried curdlan (4.00 g, 24.7 mmol AGU) was dissolved in DMAc (110 mL) and LiBr (36.00 g, 42.4 mmol). Separate solutions of Ph₃P (25.96 g, 4 eq per AGU) and NBS (17.58 g, 4 eq per AGU), each in dry DMAc (50 mL), were added dropwise, sequentially, to the curdlan solution. The reaction solution was then heated at 70 °C for 1 h. The mixture was added slowly to 1 L of a 50:50 mixture of methanol and deionized water and then filtered to recover the

precipitate. The isolated sample was washed with ethanol twice and then dried under vacuum (40 °C) overnight to yield 6-bromo-6-deoxycurdlan. ^{13}C NMR (DMSO- d_6): δ 103.2 (C-1), 84.9 (C-3), 74.4 (C-5), 73.6 (C-2), 70.1 (C-4), 34.6 (C-6-Br). Yield: 86%.

6.3.4 Synthesis of 6-azido-6-deoxycurdlan

The procedure was adapted from one reported earlier.⁸ Briefly, dry 6-bromo-6-deoxycurdlan (1.00 g, 4.44 mmol) was dissolved in DMSO (25 mL). Then NaN_3 (1.44 g, 5 eq per AGU) was added to the solution. The resulting mixture was heated at 80 °C for 24 h under nitrogen. The product was isolated by pouring into 300 mL of deionized water and collected by filtration. The precipitate was re-dissolved in acetone, re-precipitated into deionized water, and again isolated by filtration. The sample was dried under vacuum (40 °C) overnight to yield 6-azido-6-deoxycurdlan. ^{13}C NMR (DMSO- d_6): δ 103.4 (C-1), 84.9 (C-3), 74.9 (C-5), 73.9 (C-2), 69.4 (C-4), 51.7 (C-6- N_3). Yield: 92%.

6.3.5 Synthesis of 6-azido-6-deoxy-2,4-di-*O*-acyl-curdlan

The procedure was adapted from one reported earlier.⁸ Dry 6-azido-6-deoxycurdlan (1.00 g, 5.35 mmol), 4-dimethylaminopyridine (DMAP, 20 mg), pyridine (3.6 mL, 10 eq per AGU), and 20 eq per AGU of carboxylic anhydride (Ac_2O , 10.1 mL; Pr_2O , 13.8 mL) were combined. The mixture was stirred at 80 °C for 24 h, then cooled and added slowly to 200 mL deionized water to precipitate the product, which was recovered by filtration, re-dissolved in chloroform, re-precipitated into ethanol, and finally isolated by filtration. The

product was washed with ethanol and water several times and then dried under vacuum (40 °C) overnight.

6-Azido-6-deoxy-2,4-di-*O*-acetyl-curdlan: ¹H NMR (CDCl₃) (Figure S6.2a): δ 4.7 (H-5), 4.6 (H-5), 4.3 (H-1), 3.7 (H-6), 3.5 (H-6'), 3.3 (H-3), 3.1 (H-2), 2.2-1.9 (CH₃-acetate). Yield: 91%.

6-Azido-6-deoxy-2,4-di-*O*-propionyl-curdlan: ¹H NMR (CDCl₃) (Figure S6.2b): δ 4.7 (H-5), 4.6 (H-5), 4.3 (H-1), 3.7 (H-6), 3.5 (H-6'), 3.3 (H-3), 3.1 (H-2), 2.6-2.0 (CH₂-propionate), 1.3-1.0 (CH₃-propionate). Yield: 90%.

6.3.6 Syntheses of (6-amino-*N*-benzylidene/4-nitrobenzylidene

/4-chlorobenzylidene/2-pyridinylmethylene)-6-deoxy-2,4-di-O-acetyl-curdlangs

Dry 6-azido-6-deoxy-2,4-di-*O*-acetyl-curdlan (0.25 g, 0.92 mmol) was dissolved in 15 mL of THF or DMAc in a 50 mL flask with molecular sieves. Then Ph₃P (2 eq per AGU) and 30 eq per AGU of aldehyde (PhCHO (2.94 g), 4-NO₂PhCHO (4.17 g), 4-ClPhCHO (3.88 g), or Pyr-2-CHO (2.96 g)) were added to the flask. The solution was stirred under nitrogen at room temperature for 24 h. The solution was transferred to 3,500 g/mol molecular weight cutoff (MWCO) dialysis tubing that was then placed in a large beaker containing ethanol. After three to five days of dialysis, the precipitate formed within the tubing was isolated

by filtration and then dried under vacuum (40 °C) overnight. The DS_{imine} values were determined according to the following equation by ¹H NMR.

$$DS_{\text{imine}} = \frac{7 \times I_{H,\text{aromatic}+H,7}}{6 \times I_{H,\text{AGU}}}$$

I = integral, *H*_{aromatic} = aromatic protons, *H*_{AGU} = curdlan backbone protons

6-Amino-*N*-benzylidene-6-deoxy-2,4-di-*O*-acetyl-curdlan: ¹H NMR (CDCl₃): δ 8.2 (H-7), 7.7 (H-9, 13), 7.5 (H-10~12), 5.2-3.2 (curdlan backbone protons H-1~6), 2.2-1.8 (CH₃-acetate); ¹³C NMR (CDCl₃): δ 169 (C=O-acetate), 162 (N=C-7), 145-125 (aromatic carbons C-8~13), 100 (C-1), 82-68 (C-2~5), 62 (C-6-N), 20 (CH₃-acetate). Yield: 90%. Elemental analysis: %C 57.25, %H 5.38, %N 4.40 (theoretical (DS 1.0) %C 61.26, %H 5.71, %N 4.20); DS_{imine, EA} = 0.93.

6-Amino-*N*-4-nitrobenzylidene-6-deoxy-2,4-di-*O*-acetyl-curdlan: ¹H NMR (CDCl₃): δ 8.3 (H-10, 12), 7.9 (H-7, 9, 13), 4.9-3.4 (curdlan backbone protons H-1~6), 2.2-1.8 (CH₃-acetate). ¹³C NMR (DMSO-*d*₆): δ 170 (C=O-acetate), 162 (C-7=N), 150-120 (aromatic protons C-8~13), 100 (C-1), 82-68 (C-2~5), 60 (C-6-N), 21 (CH₃-acetate). Yield: 81%.

6-Amino-*N*-4-chlorobenzylidene-6-deoxy-2,4-di-*O*-acetyl-curdlan: ¹H NMR (CDCl₃): δ 8.1 (H-7), 7.6 (H-9, 13), 7.4 (H-10, 12), 5.0-3.3 (curdlan backbone protons H-

1~6), 2.3-1.8 (CH₃-acetate). ¹³C NMR (CDCl₃): δ 21 (CH₃-acetate), 61 (C-6-N), 70-105 (curdlan backbone carbons), 125-145 (aromatic carbons), 162 (C-7=N), 169 (C=O-acetate).

Yield: 87%.

6-Amino-*N*-2-pyridinylmethylene-6-deoxy-2,4-di-*O*-acetyl-curdlan: ¹H NMR (CDCl₃): δ 7.5 (H-10, 11, 12), 7.7 (H-9, 13), 8.2 (H-7), 5.2-3.2 (curdlan backbone protons H-1~6), 2.2-1.8 (CH₃-acetate). ¹³C NMR (CDCl₃): δ 21 (CH₃-acetate), 61(C-6-N), 70-105 (curdlan backbone carbons), 120-160 (aromatic carbons), 164 (C-7=N), 169 (C=O-acetate). Yield: 84%.

6.3.7 Synthesis of 6-amino-*N*-benzyl-6-deoxy-2,4-di-*O*-acetyl-curdlan

Dry 6-amino-*N*-benzylidene-6-deoxy-2,4-di-*O*-acetyl-curdlan (0.1 g, 0.30 mmol) was dissolved in 10 mL of THF in a 50 mL flask. Then NaBH₃CN (0.19 g, 3.0 mmol, 5 eq per AGU) was added to the flask. The solution was stirred at ambient temperature (ca. 23°C) for 24 h. The mixture was added to 100 mL of ethanol. The precipitate was isolated by filtration and washed with ethanol, then dried under vacuum (40 °C) overnight. The DS_{amine} values were determined according to the following equation by ¹H NMR. Elemental analysis: %C 56.46, %H 5.45, %N 4.78 (theoretical (DS 1.0) %C 60.89, %H 6.27, %N 4.18); DS_{imine, EA}=0.35.

$$DS_{\text{amine}} = 1 - \frac{5 \times I_{\text{H},7}}{I_{\text{H},\text{aromatic}}}$$

6-Amino-*N*-benzyl-6-deoxy-2,4-di-*O*-acetyl-curdlan: ¹H NMR (CDCl₃): δ 8.2 (H-7), 7.7 (H-9, 9', 13, 13'), 7.5 (H-10~12, 10'~12'), 4.8-3.2 (curdlan backbone protons H-1~6 & H-7'), 2.2-1.8 (CH₃-acetate).

6.3.8 Synthesis of 6-amino-*N*-benzyl-6-deoxy-2,4-di-*O*-acetyl-curdlan by one-pot

reductive amination via Staudinger ylide

Dry 6-azido-6-deoxy-2,4-di-*O*-acetyl-curdlan (0.25 g, 0.92 mmol) was dissolved in 15 mL of DMF in a 50 mL flask containing molecular sieves (2 g, 4 Å). Then Ph₃P (2 eq per AGU), PhCHO (2.82 mL, 30 eq per AGU), and NaBH₃CN (0.23 g, 10 eq per AGU) were added to the flask. The solution was stirred under nitrogen at ambient temperature for 24 h. The solution was transferred to 3,500 g/mol MWCO dialysis tubing and dialyzed against ethanol for at least three days; the ethanol was replaced daily. The precipitate formed within the tubing was isolated by filtration and then dried under vacuum (40 °C) overnight. The DS_{amine} values were determined according to the following equation by ¹H NMR.

$$DS_{\text{amine}} = \left(\frac{5 \times I_{\text{H,AGU+H,7}}}{I_{\text{H,aromatic}}} - 7 \right) / 2$$

6-Amino-*N*-benzyl-6-deoxy-2,4-di-*O*-acetyl-curdlan: ¹H NMR (CDCl₃): δ 7.8-7.2 (aromatic protons H-9~13), 5.1-2.8 (curdlan backbone protons H-1~6 & H-7). Yield: 69%.

6.3.9 Synthesis of 6-amino-*N*-benzyl-6-deoxycurdlan by one-pot reductive amination via Staudinger ylide

Dry 6-azido-6-deoxycurdlan (0.25 g, 1.34 mmol) was dissolved in 15 mL of THF in a 50 mL flask containing molecular sieves (2 g, 4 Å). Then Ph₃P (2 eq per AGU), PhCHO (2.82 mL, 30 eq per AGU), and NaBH₃CN (3.36 g, 40 eq per AGU) were added to the flask. The clear solution was stirred under nitrogen at ambient temperature for 24 h. The solution was transferred to 3,500 g/mol MWCO dialysis tubing and dialyzed against ethanol for at least three days; the ethanol was replaced daily. The precipitate formed within the tubing was isolated by filtration and then dried under vacuum (40 °C) overnight. The DS_{amine} values were determined according to the following equation by ¹H NMR.

$$DS_{\text{amine}} = \left(\frac{5 \times I_{\text{H,AGU+H,7}}}{I_{\text{H,aromatic}}} - 7 \right) / 2$$

6-Amino-*N*-benzyl-6-deoxycurdlan: ¹H NMR (CDCl₃): δ 7.6-7.3 (aromatic protons H-9~13), 5.1-2.8 (curdlan backbone protons H-1~6 & H-7). Yield: 75%.

6.4 Results and discussion

6.4.1 Synthesis of 6-amino-*N*-benzylidene-6-deoxy-2,4-di-*O*-acyl-curdlan

The Furuhashi bromination and iminophosphorane ylide-based approaches previously reported by our laboratory provided ready access to many 6-amino-, 6-ammonio-, and 6-amido-6-deoxy curdlan derivatives, but could not provide access to secondary amines. Secondary amines can be challenging to synthesize, since alkylation of a primary amine precursor frequently affords a mixture of the corresponding secondary and tertiary amines, and quaternary ammonium, due to insufficiently differentiated starting material and product reactivity.²⁴ We felt that a reductive amination protocol, previously unreported from polysaccharide-linked Staudinger ylides, could be an effective approach to these secondary amines. Herein, we prepared a family of 6-monoalkylamino curdlan derivatives by reacting 6-azido-6-deoxy-2,4-di-*O*-acyl-curdlan with Ph₃P and aldehydes (Scheme 6.1). In the event, we found that treating 2,4-*O*-acetyl-6-azido-6-deoxycurdlan in THF with triphenylphosphine at ambient temperature to form the iminophosphorane ylide as we had before, but this time in the presence of benzaldehyde as electrophile, afforded 6-amino-*N*-benzylidene-6-deoxy-2,4-di-*O*-acetyl-curdlan; product identity was confirmed by FTIR and ¹H/¹³C NMR spectroscopy as described in detail below. FTIR analysis (Fig. S6.10) showed a characteristic imino C=N stretch at 1671 cm⁻¹ as well as aromatic C-H bend at 762 cm⁻¹ and 701 cm⁻¹, indicating successful amino-*N*-benzylidene introduction. No azido N₃ stretch was observed around 2100 cm⁻¹. Conversion to the imine appeared to be high but incomplete under these conditions, as indicated by ¹H NMR integration, so we sought to optimize the reaction conditions to enhance conversion. We explored the effects of changing solvent (DMAc vs. THF), temperature (RT vs. 50 °C), reaction time (24 h vs. 36 h) and benzaldehyde molar excess (20 vs. 30 equiv. per AGU). As can be seen from Table

S6.1 entries 1 and 2, reaction in THF gave slightly higher DS_{imine} than in DMAc. Extending the reaction time by 12 h did not enhance conversion as might have been expected; instead, DS_{imine} decreased from 0.89 (entry 1) to 0.73 (entry 3). We feel that the most logical explanation is hydrolysis of the initially formed imine due to the presence of adventitious water. Note that, even when azide reduction is complete as it appears to be here, there are two potential sources of an unsubstituted 6-amino-6-deoxy byproduct (that is, 6-amino-6-deoxy-2,4-di-*O*-acetyl-curdlan). This product can arise by hydrolysis of the imine product (from co-product water, or adventitious water), or alternatively by protonation of the intermediate iminophosphorane ylide by water (as in the intentional synthesis of the primary amine by running the Staudinger reduction in water as solvent or co-solvent).^{8,16,19} Increasing either the excess of PhCHO (entry 4) or the reaction temperature (entry 5) afforded slightly increased DS (DS_{imine} 0.91), approaching full conversion (DS_{Br} of the starting 6-bromo product was 0.95). Due to the potential for degradation and instability of imino derivatives at higher temperatures, we applied the reaction conditions of entry 4 for the following imine syntheses.

¹³C NMR was useful for characterizing the 6-amino-*N*-benzylidene-6-deoxy-2,4-di-*O*-acetyl-curdlan product (Figure 6.1); resonances in the range of δ 126-137 ppm were assigned to the aromatic carbons of the phenyl ring. Additionally, signals at δ 62 and 162 ppm were assigned to the $\underline{\text{C}}_6\text{-N}$ and $\text{N}=\underline{\text{C}}_7$ respectively. Diagnostic features of the ¹H NMR spectrum (Figure S6.3) included the aromatic proton resonances at δ 7.5 ppm ($\text{H}_{10,11,12}$) and δ 7.7 ppm ($\text{H}_{9,13}$) as well as the imino proton signal at δ 8.2 ppm (H_7) from the $\underline{\text{H}}\text{-C}_7=\text{N}$ moiety. DS_{imine} values were calculated by the ratio of the integral of protons H_{7-13} to that

of curdlan backbone protons ($H_{1-6/6'}$) and are summarized in Table 6.1. Our previous work indicated that the Staudinger reaction (Ph_3P) to reduce the curdlan azide to amine is sufficiently mild to preserve ester bonds against reduction⁸; we confirmed that they were also stable during imine formation by the presence in the product 1H NMR spectrum of singlets from of acetyl groups around δ 2.0 ppm, integration of which indicated full 2, 4-*O*-substitution (DS_{Ac} 2.0). However, there were some small peaks evident close to the imino aromatic signals as well as the apparent aldehyde proton signal at δ 10.0 ppm and the carbonyl carbon signal at δ 192.0 ppm, attributed to a residual benzaldehyde impurity; this is likely to be the result of imide hydrolysis rather than or in addition to failure to separate excess benzaldehyde from the product by dialysis. In order to increase the DS and avoid the accompanying hydrolysis by co-product or adventitious water, we hypothesized that inclusion of molecular sieves in the reaction mixture would capture any water present, thereby minimizing imine hydrolysis. When molecular sieves were so used, benzaldehyde signals were absent in the products, as evidenced by the 1H NMR spectra (Figure 6.2) with complete imine substitution (DS_{imine} 1.0), confirming our hypothesis and providing a highly efficient route to the regioselectively substituted imines.

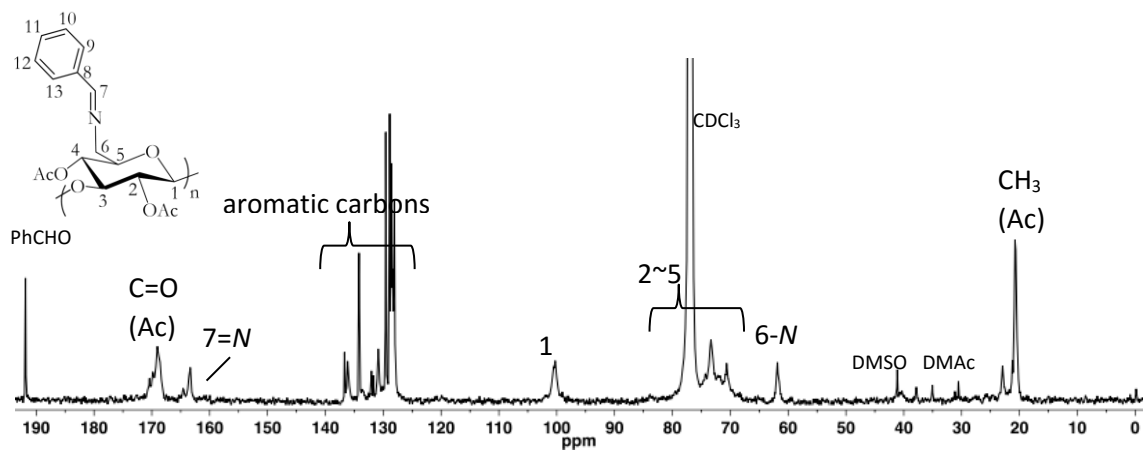


Figure 6.1. ^{13}C NMR spectrum of 6-amino-*N*-benzylidene-6-deoxy-2,4-di-*O*-acetylcurdlan performed in CDCl_3 at RT (30 equiv. PhCHO/AGU, THF, RT, 24 h, $\text{DS}_{\text{imine}} = 0.91$).

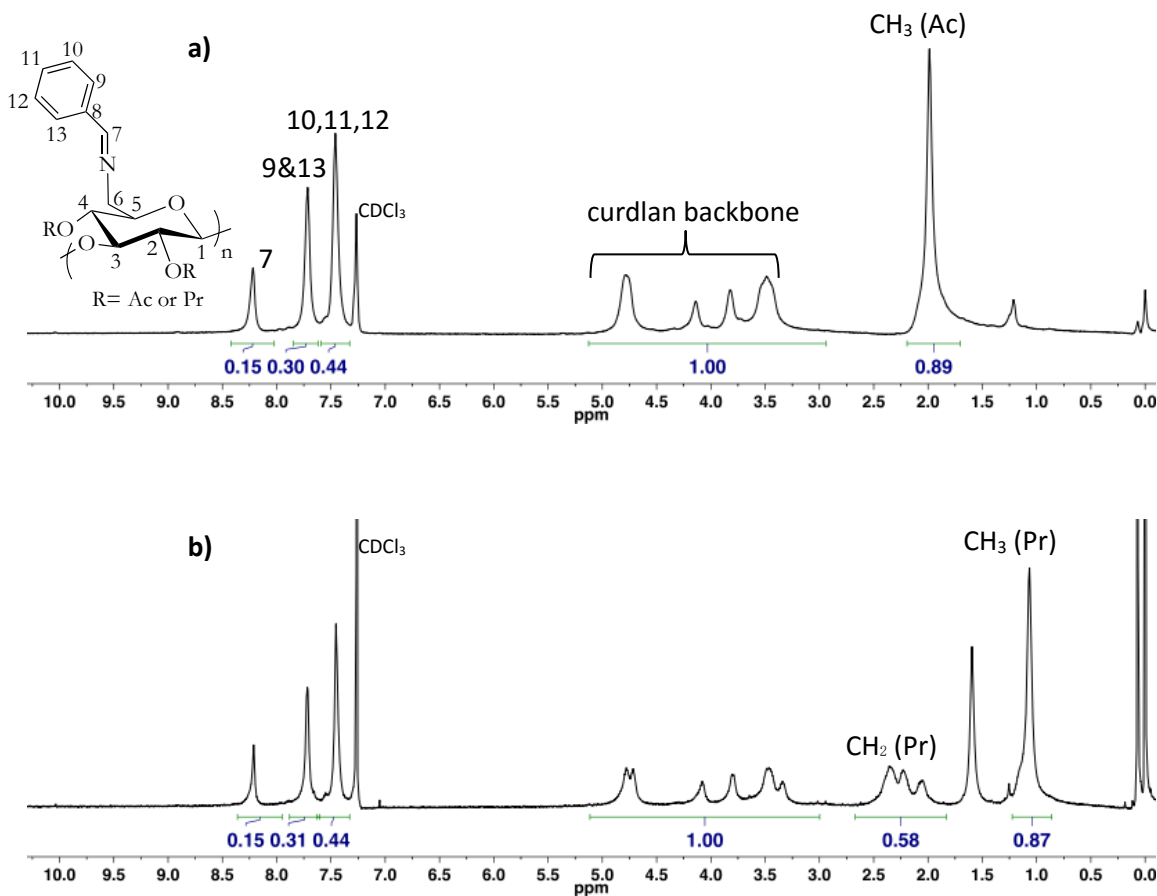
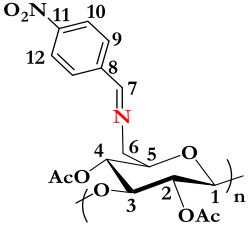
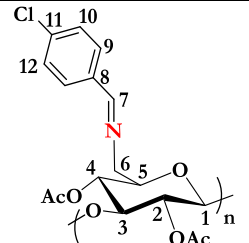
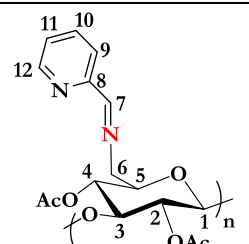


Figure 6.2. ^1H NMR spectra (performed in CDCl_3 at RT) of **(a)** 6-amino-*N*-benzylidene-6-deoxy-2,4-di-*O*-acetyl-curdlan and **(b)** 6-amino-*N*-benzylidene-6-deoxy-2,4-di-*O*-propionyl-curdlan (30 equiv. PhCHO/AGU , THF, RT, 24 h, molecular sieves, $\text{DS}_{\text{imine}} = 1.0$ (conversion 100%).

In order to explore the breadth of applicability of this 6-deoxy-6-iminocurdlan synthetic method, three other aldehydes (4- NO_2PhCHO , 4- ClPhCHO and 2-PyrCHO) were reacted with 6-azido-6-deoxycurdlan under otherwise identical reaction conditions (Scheme 6.1). ^{13}C NMR spectroscopy (Figures S6.7-6.9) helped to confirm product structures.

Resonances in the range of δ 120-160 ppm were assigned to the aromatic carbons, while peaks around 60 ppm (imino-substituted C6) and 162 ppm (imine carbon, C7) confirmed successful curdlan aryl imine formation. The imines were also characterized by ^1H NMR spectroscopy (Figure S6.4). In each case, curdlan backbone proton resonances fell within δ 5.0-3.0 ppm while aromatic ring and H-C=N-R protons resonated in the range of δ 8.7-7.4 ppm. ^1H and ^{13}C NMR spectra indicated that the isolated imine products were free of azide or brominated impurities within the sensitivities of the techniques. Table 6.1 summarizes the chemical structure, DS_{imine} , product yield, and chemical shift assignments of the imino analogs. Degrees of substitution of the imino products were determined as $\text{DS}_{\text{ClPh-imine}}$ 0.63, $\text{DS}_{\text{Pyr-imine}}$ 0.76 and $\text{DS}_{\text{NO}_2\text{Ph-imine}}$ 0.77, respectively. The apparent incomplete imine formation could rather be due to partial hydrolysis of the initially formed imine (each derivative has a more electron poor, thus more reactive imine moiety than that of the *N*-benzylidene-6-amino derivative).

Table 6.1. ^1H NMR chemical shift assignments for aromatic ring and imine protons, DS_{imine} values, and yields of 6-deoxy-6-imino-curdans.

Imine structure	Aldehyde used	^1H NMR assignment		DS_{imine}	Yield (%)
		proton	(ppm)		
	4- O_2NPhCHO	10.12	8.3	0.77	81
		7.9.13	7.9		
	4-ClPhCHO	7	8.1	0.63	87
		9.13	7.6		
		10.12	7.4		
	Pyr-2-CHO	12	8.6	0.76	84
		7.9	8.3-8.2		
		10.11	7.7-7.9		

6.4.2 Borohydride reduction of 6-amino-*N*-benzylidene-6-deoxy-2,4-di-*O*-acetylcurdlan

We selected sodium cyanoborohydride for initial experiments on reduction of the imine to secondary amine, since it is known to be less reactive towards ester groups than

NaBH₄.^{22,25-27} Therefore we treated 2,4-di-*O*-acetyl-(6-amino-*N*-benzylidene)-6-deoxycurdlan (DS_{imine} 1.0) with different molar ratios of NaBH₃CN to attempt imine to amine reduction. As clearly indicated by ¹H NMR spectra and integration (Figure S6.5), the amine product was obtained but with DS_{amine} only 0.18 (Table 6.2, entry 1), far lower than the starting DS_{imine} 1.0. We could increase amine DS to 0.38 (Table 6.2, entry 2) by increasing reaction time from 5 h to 24 h, indicating that incomplete reduction was at least part of the problem. On the other hand, increasing the NaBH₃CN molar excess had essentially no effect on DS_{amine}, which leveled off at around 0.4 (Table 6.2, entry 3-5).

Table 6.2. Substitution achieved (DS_{amine}) vs. NaBH₃CN imine reduction conditions.*

Entry	NaBH ₃ CN (eq/AGU)	Solvent	Temp. (°C)	Time (h)	DS _{amine}
1	2	THF	RT	5	0.15
2				24	0.38
3	5			0.41	
4	10			0.38	
5	20			0.42	

*Isolated 6-amino-*N*-benzylidene-6-deoxy 2,4-di-*O*-acetyl-curdlan (DS_{imine} 1.0) used as starting material.

6.4.3 One-pot reductive amination via Staudinger ylide

We initially explored the two-step process for conversion of iminophosphorane to secondary amine (imine formation, followed by separate reduction) in order to make sure we understood each step and the influence of reaction conditions on each. We hoped however that ultimately a one-pot process of imine formation and reduction would be successful, as is commonly employed in small molecule chemistry.²⁸⁻³⁰ We hypothesized that a one-pot method, by avoiding isolation of the hydrolytically sensitive imine, would provide improved overall selectivity and efficiency. Our one-pot reductive amination started by generating a Staudinger iminophosphorane from the corresponding azide in the presence of molecular sieves, then reacting with excess aldehyde in the presence of sodium cyanoborohydride, by a method in which all reagents (2,4-*O*-acetyl-6-azido-6-deoxycurdlan, Ph₃P, PhCHO, NaBH₃CN) were present from the beginning in various solvent systems. We investigated the influence of solvent upon the reduction; reduction proceeded in common organic solvents including THF, NMP and DMF (Table 6.3, entry 1-3). The DS_{amine} value reached 0.5 when the reduction was carried out in DMF, while DS 0.27 and 0.31 were achieved in THF and NMP, respectively. We also noted that DS_{amine} obtained was much higher (0.89) when 6-azido-6-deoxycurdlan, lacking the ester moieties at O-2 and O-4, was used as starting material (Table 6.3, entry 4). 6-Azido-6-deoxycurdlan has better solubility than its acetylated analog in THF solvent, which may influence reduction conversion. The electron withdrawing ester moieties may also influence the rate of ylide attack upon the aldehyde, and the stability of the intermediate ylide to hydrolysis, both of which could negatively influence DS_{amine}. Figure 6.3 clearly shows the broad aromatic protons in the range of δ 7.5 - 7.3 ppm with disappearance of the imino proton at

δ 8.2 ppm, indicating high conversion to *N*-benzylidene-6-amino-6-deoxycurdlan. We note that the spectrum also shows a small amount of residual PPh₃ and/or triphenyl phosphine oxide (7.6 – 8.0 ppm). It is well understood that it can be difficult to remove such residues, especially from polymeric products; our previous work has demonstrated that they are typically removed in subsequent steps.^{8,16} In addition, the FTIR spectrum (Figure S6.11) demonstrated a significant absorption at 3200 - 3600 cm⁻¹, assigned to N-H stretch of the amine product. This confirmed our hypothesis that hydrolytic instability of the imine had been the limiting factor in the two-pot, imine isolation approach, and provided a far more efficient route from 6-azido-6-deoxycurdlan to the corresponding 6-(benzylamino)-6-deoxycurdlan derivative.

Table 6.3. Substitution achieved (DS_{amine}) by one-pot reductive amination of the Staudinger ylide.*

Entry	NaBH ₃ CN (eq/AGU)	Solvent	Temp. (°C)	Time (h)	DS _{amine}
1	10	THF	RT	24	0.27
2		NMP			0.31
3		DMF			0.50
4	THF	0.89			

*2,4-Di-*O*-acetyl-6-azido-6-deoxycurdlan used as starting material (entries 1-3) except entry 4 (used 6-azido-6-deoxycurdlan), with Ph₃P (2 eq/AGU), PhCHO (30 eq/AGU).

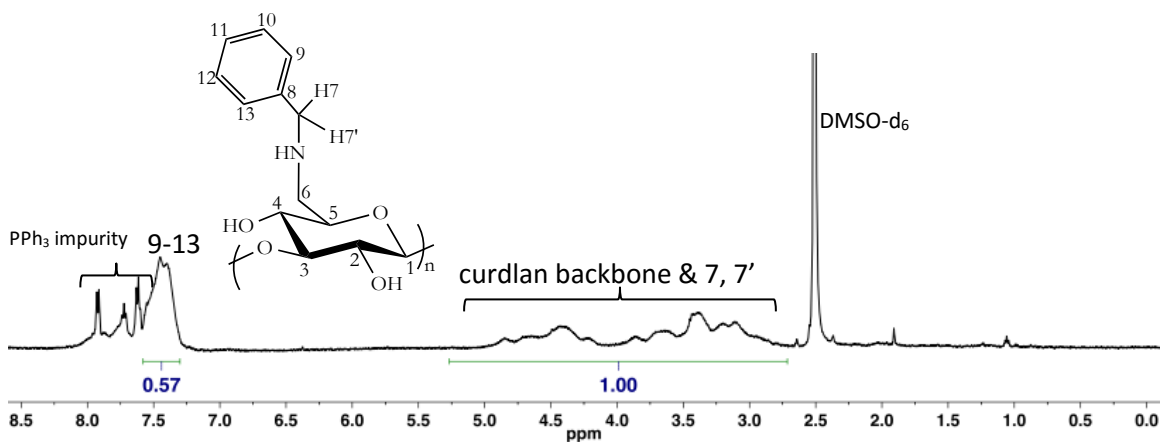


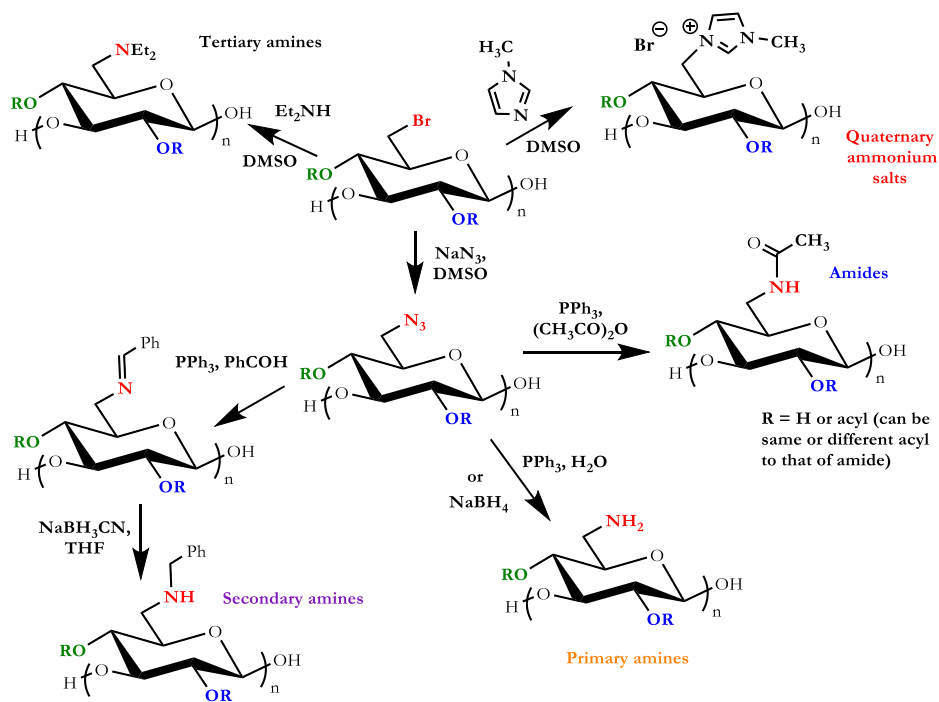
Figure 6.3. ^1H NMR spectrum (performed in DMSO- d_6 at RT) of 6-amino-*N*-benzyl-6-deoxycurdlan (Table S6.1, entry 4).

6.5 Conclusions

We have developed methods for further exploitation of the nucleophilic Staudinger ylide (iminophosphorane intermediate) obtained by reduction of 6-azido-6-deoxycurdlans for the synthesis of 6-aminated curdlans, specifically by reductive amination. By adding aldehydes and/or sodium cyanoborohydride, a series of imino- and amino-curdlans was produced with high chemoselectivity, providing a new strategy for regioselective incorporation of a range of monoalkylamino pendants at C-6 of curdlan.

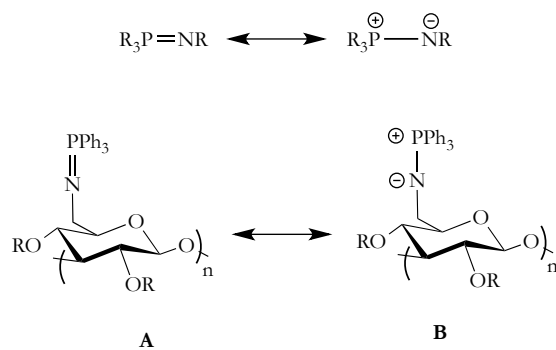
The success and selectivity of these approaches complement synthetic strategies previously developed in our lab for preparing families of regioselectively aminated curdlan derivatives, now providing access to a very broad variety of amines (primary, secondary, and tertiary

amines, and quaternary ammonio derivatives) and amides (with amide acyl moieties the same as those appended to the OH groups as esters, different from those moieties, or with only amides and no esters present, whichever is preferred). All of these amino, ammonio, and amido curdlans are prepared from 6-bromo- or 6-azido-6-deoxycurdlan (Scheme 6.2) with very high degrees of chemo- and regioselectivity. This set of complementary synthetic methods opens doors to a wide variety of potentially useful aminated/amidated polymers for use biomedical, pharmaceutical, and other fields, and should of course be applicable to other polysaccharides, for example other glucans with unencumbered C-6 OH groups. We will continue to explore new ways to exploit the nucleophilic Staudinger ylide for regio- and chemoselective synthesis of substituted, functional, and useful polysaccharide derivatives.



Scheme 6.2. Example syntheses of curdlan derivatives regioselectively aminated/amidated at C-6.

6.6 Supporting information



Scheme S6.1. Depictions of general iminophosphorane structure, and structure of curdlan iminophosphorane generated by Staudinger reaction.

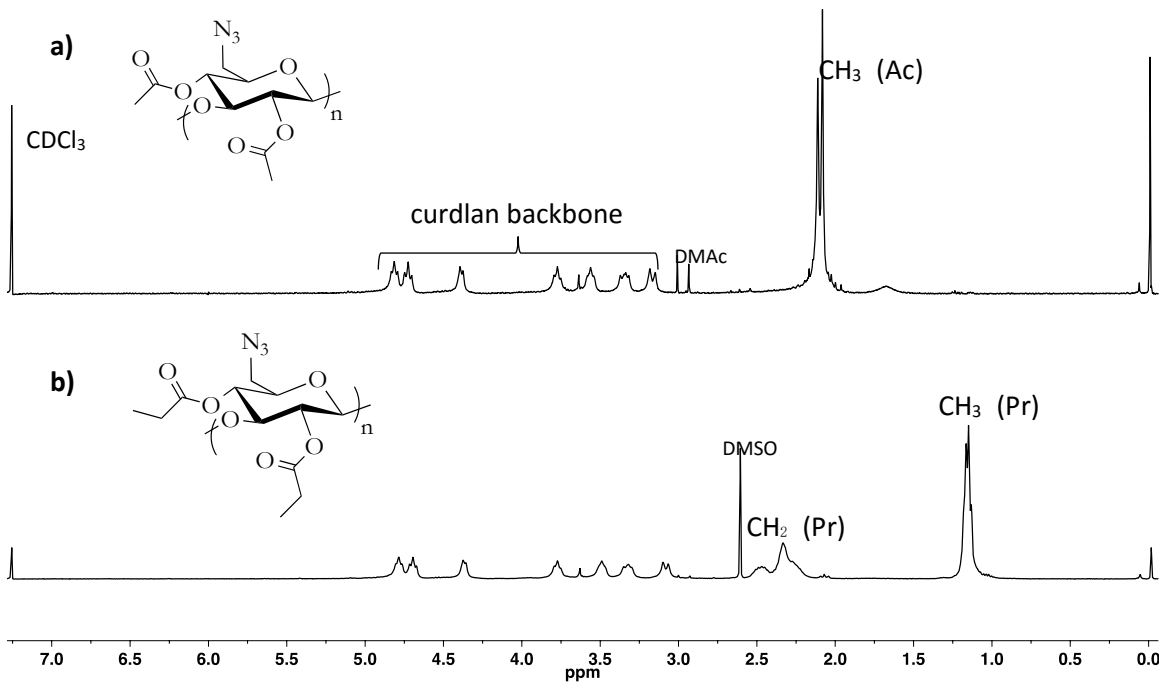


Figure S6.2. ^1H NMR spectra ($\text{DS}_{\text{ester}} = 2.0$) of: **(a)** 6-azido-6-deoxy-2,4-di-*O*-acetyl-curdlan and **(b)** 6-azido-6-deoxy-2,4-di-*O*-propionyl-curdlan.

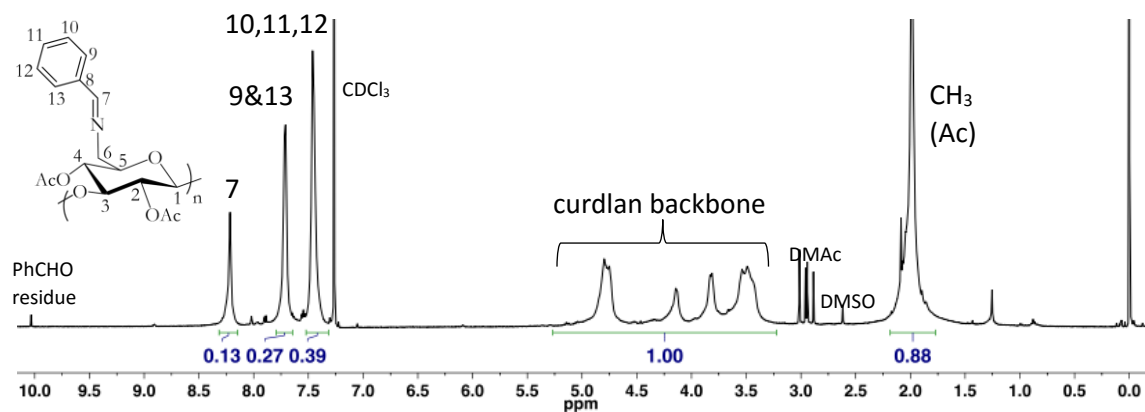


Figure S6.3. ¹H NMR of 2,4-Di-O-acetyl-(6-amino-N-benzylidene)-6-deoxycurdlan performed in CDCl₃ at RT (30 equiv. PhCHO/AGU, THF, RT, 24 h, DS_{imine} = 0.91).

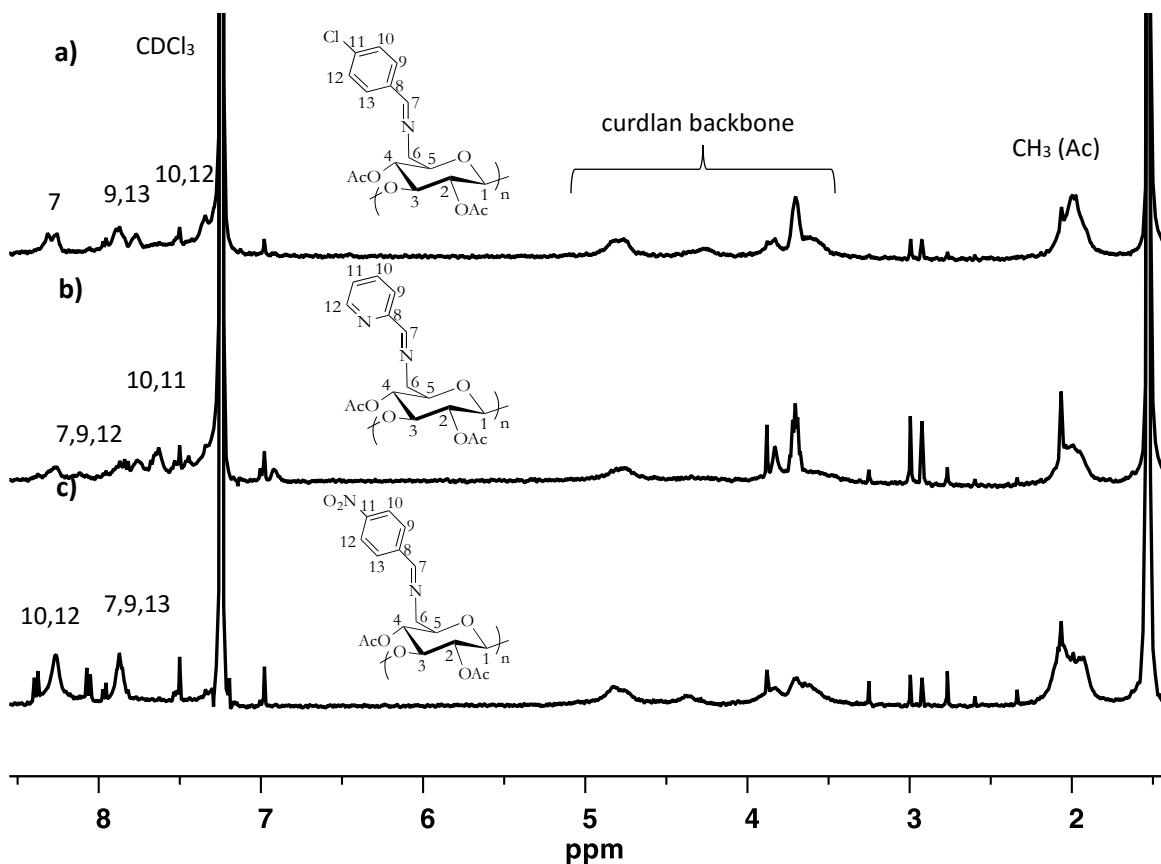


Figure S6.4. ^1H NMR spectra of (a) 2,4-di-*O*-acetyl-(6-amino-*N*-4-chlorobenzylidene)-6-deoxycurdlan and (b) 2,4-di-*O*-acetyl-(6-amino-*N*-2-pyridinidylmethylene)-6-deoxycurdlan (c) 2,4-di-*O*-acetyl-(6-amino-*N*-4-nitrobenzylidene)-6-deoxycurdlan (30 equiv. aldehyde/AGU, THF, RT, 24 h, molecular sieves).

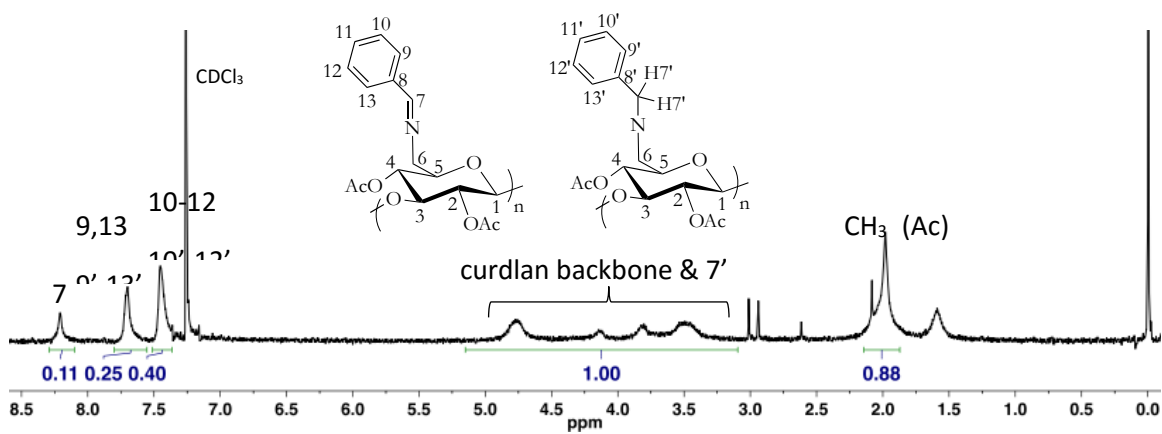


Figure S6.5. ^1H NMR (in CDCl_3) spectrum of 2,4-di-O-acetyl-(6-amino-N-benzylidene)-6-deoxycurdlan reduced by NaBH_3CN (Table 6.2, entry 1).

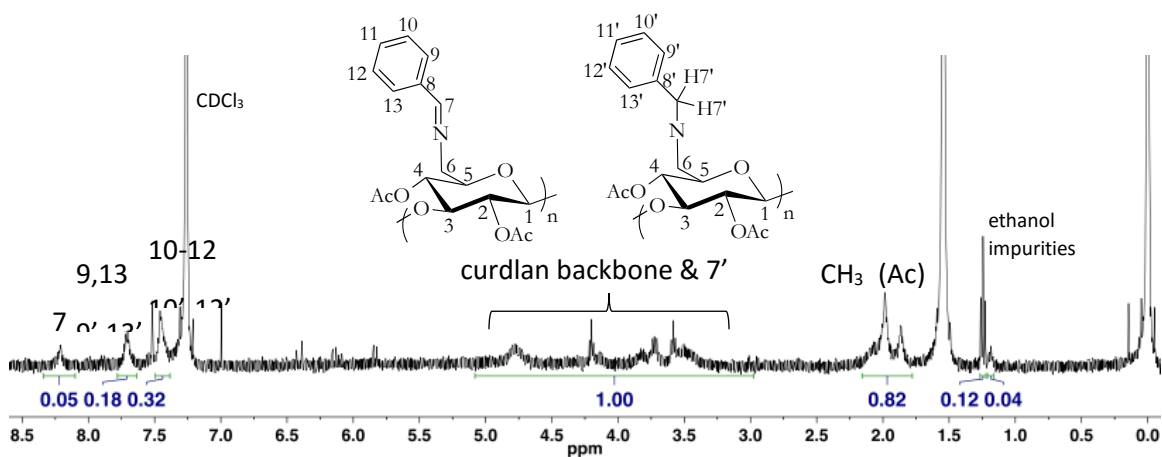


Figure S6.6. ¹H NMR (in DMSO-d₆) spectrum of 2,4-di-*O*-acetyl-(6-amino-*N*-benzylidene)-6-deoxycurdlan prepared by one-pot method (Table 6.2, entry 8).

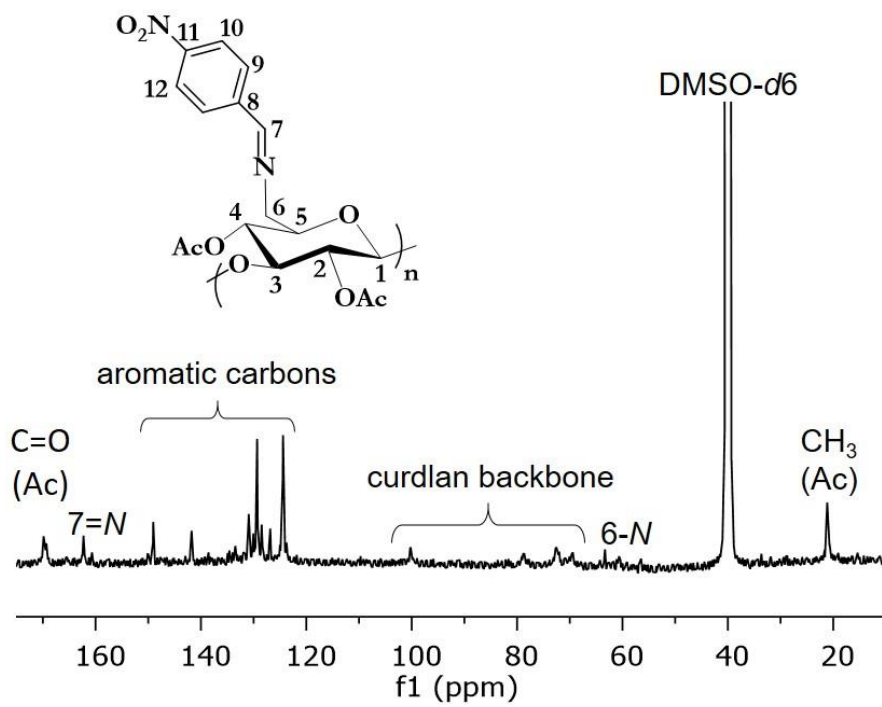


Figure S6.7. ^{13}C NMR (in DMSO- d_6) spectrum of 2,4-di-*O*-acetyl-(6-amino-*N*-4-nitrobenzylidene)-6-deoxycurdlan.

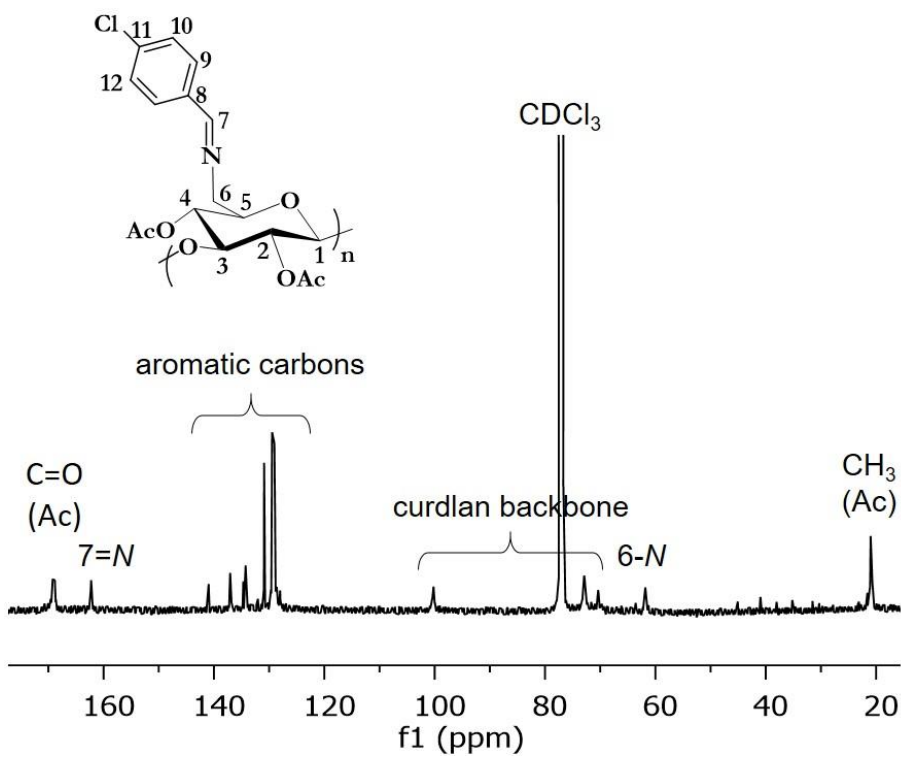


Figure S6.8. ^{13}C NMR (in CDCl_3) spectrum of 2,4-di-*O*-acetyl-(6-amino-*N*-4-chlorobenzylidene)-6-deoxycurdlan.

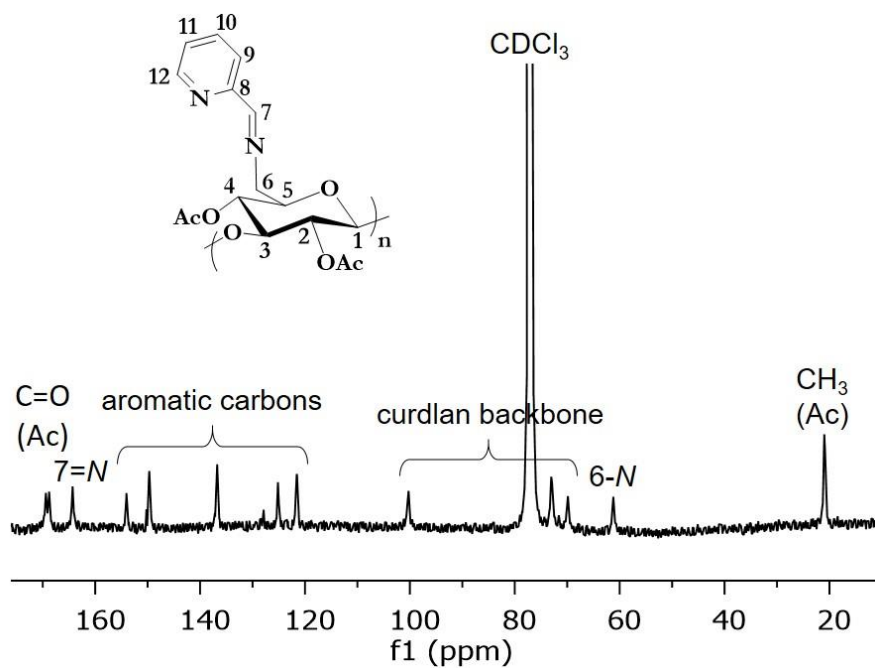


Figure S6.9. ^{13}C NMR (in CDCl_3) spectrum of 2,4-di-O-acetyl-(6-amino-N-2-pyridinylmethylene)-6-deoxycurdlan.

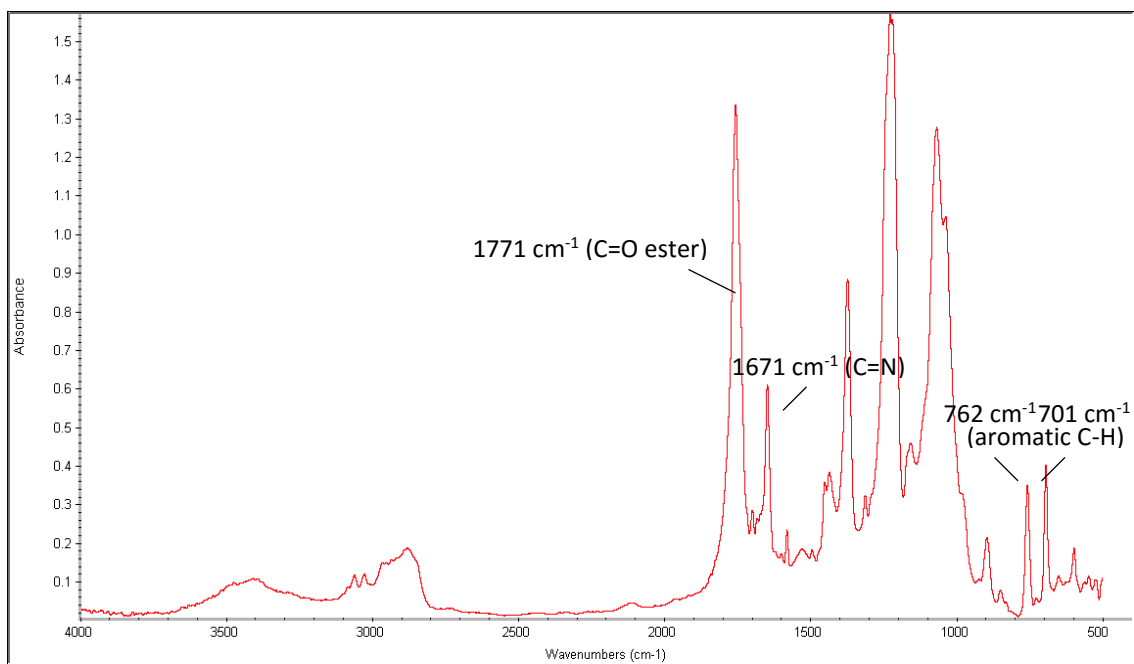


Figure S6.10. FTIR spectrum of 2,4-di-*O*-acetyl-(6-amino-*N*-benzylidene)-6-deoxycurdlan (2 equiv. Ph₃P, 30 equiv. PhCHO/AGU, THF, RT, 24 h, molecular sieves, DS_{imine} = 1.0).

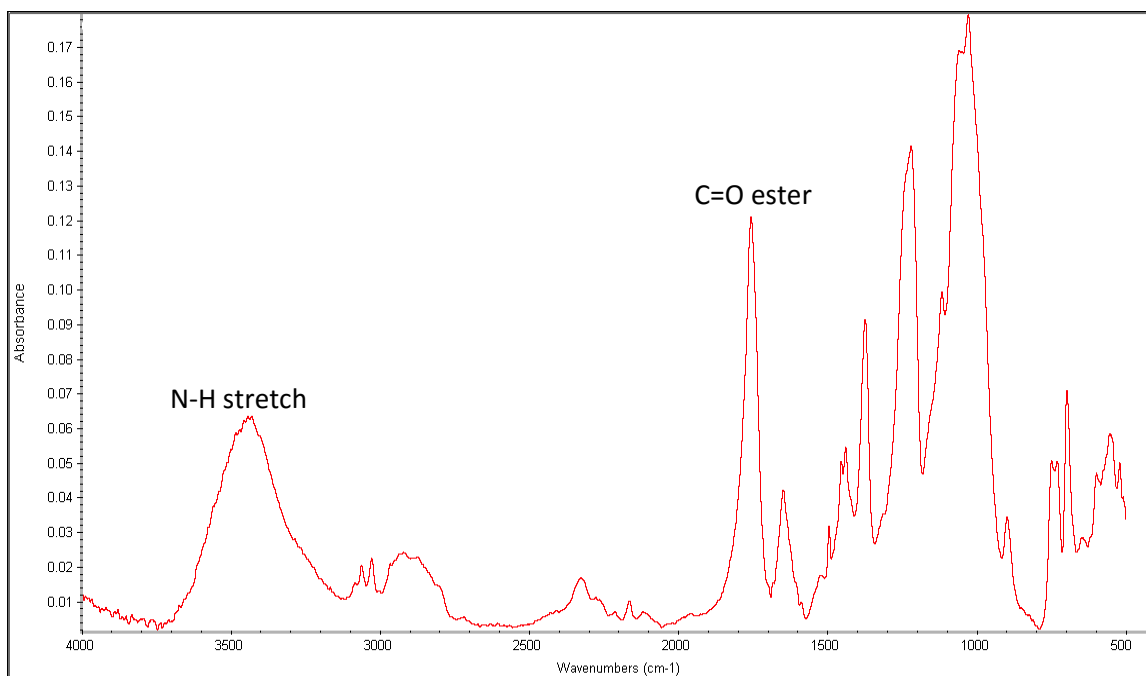


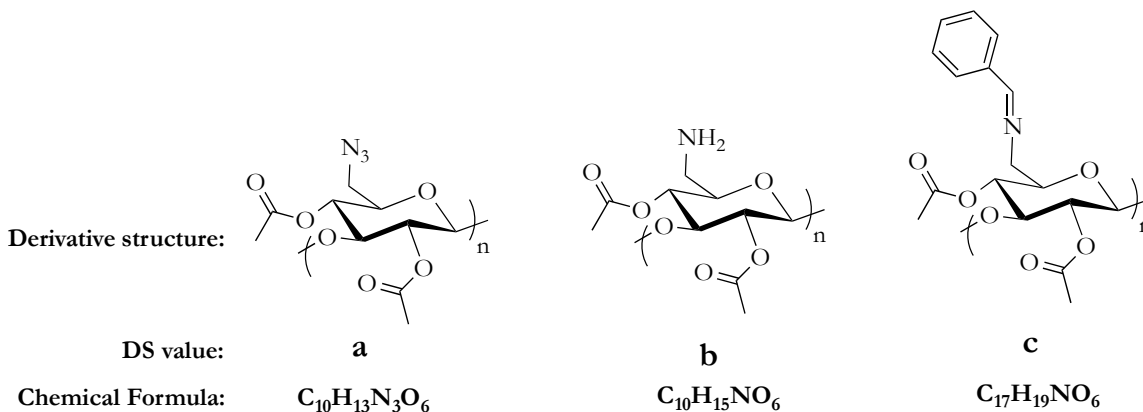
Figure S6.11. FTIR spectrum of 2,4-di-*O*-acetyl-(6-amino-*N*-benzyl)-6-deoxycurdlan (one-pot reductive amination, 2 equiv. Ph₃P, 30 equiv. PhCHO/AGU, 40 equiv. NaBH₃CN, DMF, RT, 24 h).

Table S6.1. Substitution achieved (DS_{imine}) vs. conditions for the synthesis of 2,4-di-*O*-acetyl-(6-amino-*N*-benzylidene)-6-deoxycurdlan by conversion of 6-azido-6-deoxy-2,4-*O*-acetyl-curdlan (DS_{azide} 1.0) with benzaldehyde.

Entry	PhCHO (eq/AGU)	Temp. (°C)	Time (h)	Solvent	DS_{imine}
1	20	RT	24	THF	0.89
2	20	RT	24	DMAc	0.83
3	20	RT	36	THF	0.73
4	30	RT	24	THF	0.91
5	20	50	24	THF	0.91

DS calculation for 2,4-di-*O*-acetyl-(6-amino-*N*-benzylidene)-6-deoxycurdlan from elemental analysis

We made the calculations based on the assumption that the curdlan derivative comprises benzylidene substituted monosaccharide **c**, as well as (potentially) unreacted azido- (**a**) and amino-substituted (**b**) monosaccharides.



$$\frac{12 \times (10a + 10b + 17c)}{14 \times (3a + b + c)} = \frac{57.25}{4.4} \dots\dots\dots(1) \dots\dots\dots \text{C/N weight ratio}$$

$$\frac{14 \times (3a + b + c)}{1 \times (13a + 15b + 19c)} = \frac{4.4}{5.38} \dots\dots\dots(2) \dots\dots\dots \text{N/H weight ratio}$$

$$a + b + c = 1 \dots\dots\dots(3) \dots\dots\dots \text{DS}_{\text{total}} \text{ is } 1$$

Solving equations (1), (2), and (3) above for **c** by MATLAB, we can calculate that **c** = ca. 0.933, which means that the DS(benzylidene) value of 2,4-di-*O*-acetyl-(6-amino-*N*-benzylidene)-6-deoxycurdlan is 0.93.

6.7 Acknowledgements

We thank the Institute for Critical Technologies and Applied Science (ICTAS), the Macromolecules Innovation Institute (MII), and the Department of Sustainable Biomaterials (SBIO) at Virginia Tech for their financial, facilities and educational support. We thank the USDA for partial support of this work through grant No. 2011-67009-20090.

6.8 References

1. Marubayashi, H.; Yukinaka, K.; Enomoto-Rogers, Y.; Takemura, A.; Iwata, T. Curdlan ester derivatives: Synthesis, structure, and properties. *Carbohydr. Polym.* **2014**, *103*, 427–433.
2. Jin, Y.; Zhang, H.; Yin, Y.; Nishinari, K. Comparison of curdlan and its carboxymethylated derivative by means of rheology, DSC, and AFM. *Carbohydr. Res.* **2006**, *341*, 90–99.
3. Suflet, D. M.; Nicolescu, A.; Popescu, I.; Chitanu, G. C. Phosphorylated polysaccharides. 3. Synthesis of phosphorylated curdlan and its polyelectrolyte behaviour compared with other phosphorylated polysaccharides. *Carbohydr. Polym.* **2011**, *84*, 1176–1181.
4. Osawa, Z.; Morota, T.; Hatanaka, K.; Akaike, T.; Matsuzaki, K.; Nakashima, H.; Yamamoto, N.; Suzuki, E.; Miyano, H.; Mimura, T.; Kaneko, Y. Synthesis of sulfated derivatives of curdlan and their anti-HIV activity. *Carbohydr. Polym.* **1993**, *21*, 283–288.

5. Meng, M; Matson, J. B.; Edgar, K. J. Olefin cross-metathesis as a source of polysaccharide derivatives: Cellulose ω -carboxyalkanoates. *Biomacromolecules* **2014**, *15*, 177–187.
6. Dong, Y.; Mosquera-Giraldo, L. I.; Taylor, L. S.; Egar, K. J. Amphiphilic cellulose ethers designed for amorphous solid dispersion via olefin cross-metathesis. *Biomacromolecules* **2016**, *17*, 454–465.
7. Yoshida, T.; Hatanaka, K.; Uryu, T.; Kaneko, Y.; Suzuki, E.; Miyano, H.; Mimura, T.; Yoshida, O.; Yamamoto, N. Synthesis and structural analysis of curdlan sulfate with a potent inhibitory effect in vitro of AIDS virus infection. *Macromolecules* **1990**, *23*, 3717–3712.
8. Delattre, C.; Rios, L.; Laroche, C.; Le, N. H. T.; Lecerf, D.; Picton, L.; Yves Berthon, J.; Michaud, P. Production and characterization of new families of polyglucuronic acids from TEMPO-NaOCl oxidation of curdlan. *Int. J. Biol. Macromol.* **2009**, *45*, 458–462.
9. Tamura, N.; Hirota, M.; Saito, T.; Isogai, A. Oxidation of curdlan and other polysaccharides by 4-acetamide-TEMPO/NaClO/NaClO₂ under acid conditions. *Carbohydr. Polym.* **2010**, *81*, 592–598.
10. Zhang, R.; Edgar, K. J. Synthesis of curdlan derivatives regioselectively modified at C-6: *O*-(*N*)-Acylated 6-amino-6-deoxycurdlan. *Carbohydr. Polym.* **2014**, *105*, 161–168.
11. Zhang, R.; Edgar, K. J. Water-soluble aminocurdlan derivatives by chemoselective azide reduction using NaBH₄. *Carbohydr. Polym.* **2015**, *122*, 84–92.
12. Zhang, R.; Liu, S.; Edgar, K. J. Regioselective synthesis of cationic 6-deoxy-6-(*N,N,N*-trialkylammonio)curdlan derivatives. *Carbohydr. Polym.* **2016**, *136*, 474–484.

13. Saxon, E.; Armstrong, J. I.; Bertozzi, C. R. A “traceless” Staudinger ligation for the chemoselective synthesis of amide bonds. *Org. Lett.* **2000**, *2*, 2141–2143.
14. Saxon, E.; Bertozzi, C. R. Cell surface engineering by a modified Staudinger reaction. *Science* **2000**, *287*, 2007–2010.
15. García-Álvarez, J.; García-Garrido, S. E.; Cadierno, V. Iminophosphorane–phosphines: Versatile ligands for homogeneous catalysis. *J. Organomet. Chem.* **2014**, *751*, 792–808.
16. Staudinger, H.; Meyer, J. New organic compounds of phosphorus. II. Phosphazines. *Helv. Chim. Acta* **1919**, *2*, 619–635.
17. Palacios, F.; Alonso, C.; Aparicio, D.; Rubiales, G.; de los Santos, J. M. The aza-Wittig reaction. An efficient tool for the construction of carbon-nitrogen double bonds. *Tetrahedron* **2007**, *63*, 523–575.
18. Fox, S. C.; Edgar, K. J. Staudinger reduction chemistry of cellulose: Synthesis of selectively O-acylated 6-amino-6-deoxy-cellulose. *Biomacromolecules* **2012**, *13*, 992–1001.
19. Liu, S.; Liu, J.; Esker, A. R.; Edgar, K. J. An efficient, regioselective pathway to cationic and zwitterionic *N*-heterocyclic cellulose ionomers. *Biomacromolecules* **2016**, *17*, 503–513.
20. Marks, J. A.; Fox, S. C.; Edgar, K. J. Cellulosic polyelectrolytes: Synthetic pathways to regioselectively substituted ammonium and phosphonium derivatives. *Cellulose* **2016**, *23*, 1687–1704.
21. Pereira, J. M.; Edgar, K. J. Regioselective synthesis of 6-amino- and 6-amido-6-deoxypullulans. *Cellulose* **2014**, *21*, 2379–2396.

22. Genco, T.; Zemljic, L. F.; Bracic, M.; Stana-Kleinschek, K.; Heinze, T. Physicochemical properties and bioactivity of a novel class of cellulosics: 6-Deoxy-6-amino cellulose sulfate. *Macromol. Chem. Phys.* **2012**, *213*, 539–548.
23. Heinze, T.; Koschella, A.; Magdaleno-Maiza, L.; Ulrich, A. S. Nucleophilic displacement reactions on tosyl cellulose by chiral amines. *Polym. Bull.* **2001**, *46*, 7–13.
24. Lane, C. F. Sodium cyanoborohydride, a highly selective reducing agent for organic functional groups. *Synthesis* **1975**, 135–146.
25. Liu, S.; Edgar, K. J. Water-soluble co-polyelectrolytes by selective modification of cellulose esters. *Carbohydr. Polym.* **2017**, *162*, 1–9.
26. Salvatore, R. A.; Yoon, C. H.; Jung, K. W. Synthesis of secondary amines. *Tetrahedron* **2001**, *57*, 7758–7811.
27. Boechat, N.; da Costa, J. C. S.; de Souza Mendonca, J.; de Oliveira, P. S. M.; Vinícius Nora De Souza, M. A simple reduction of methyl aromatic esters to alcohols using sodium borohydride–methanol system. *Tet. Lett.* **2004**, *45*, 6021–6022.
28. Borch, R. F.; Bernstein, M. D.; Durst, H. D. Cyanohydridoborate anion as a selective reducing agent. *J. Am. Chem. Soc.* **1971**, *93*, 2897–2904.
29. Das, D.; Roy, S.; Das, P. K. Efficient and simple NaBH₄ reduction of esters at cationic micellar surface. *Org. Lett.* **2004**, *6*, 4133–4136.
30. Abdel-Magid, A. F.; Carson, K. G.; Harris, B. D.; Maryanoff, C. A.; Shah, R. D. Reductive amination of aldehydes and ketones with sodium triacetoxyborohydride. Studies on direct and indirect reductive amination procedures¹. *J. Org. Chem.* **1996**, *61*, 3849–3862.

31. Goldstein, S. W.; Cross, A. V. Solvent-free reductive amination: An organic chemistry experiment. *J. Chem. Educ.* **2015**, *92*, 1214–1216.
32. Sato, S.; Sakamoto, T.; Miyazawa, E.; Kikugawa, Y. One-pot reductive amination of aldehydes and ketones with α -picoline-borane in methanol, in water, and in neat conditions. *Tetrahedron* **2004**, *60*, 7899–7906.

Chapter 7. Summary and Future Work

Polysaccharide-based polyelectrolytes including cationic, zwitterionic and carboxyl-containing derivatives, have great potential for biomedical applications including drug and gene delivery and tight junction opening. For instance, cationic polymers are capable of binding electrostatically with anionic biomolecules such as nucleic acids and certain basic proteins, resulting in polyelectrolyte complexes for gene and drug delivery and other therapeutic applications.¹ Cationic polysaccharides may in some cases be more attractive candidates for therapeutic uses than synthetic cationic polymers, due to their greater biocompatibility and biodegradability, and low immunogenicity.² However, relatively few practical methods have been reported for their preparation. A simple and efficient method is needed for synthesizing polyelectrolytes from abundant and inexpensive polysaccharides.

My doctoral research work in this dissertation presents an extensive study on the synthesis of a series of polyelectrolytes derivatives substituted at the less hindered C-6 position for potential biomedical applications such as tight junction opening and drug delivery.

7.1 Syntheses of 6-pyridinio-6-deoxy-2,3-di-*O*-acetyl-cellulose (6-PyrCA), 6-(1-methyl-3-imidazolium)-6-deoxy-2,3-di-*O*-acetyl-cellulose (6-MeIMCA) and 6-(1-(3-sulfopropyl)-3-imidazolium)-6-deoxy-2,3-di-*O*-acetyl-cellulose (6-SPrIMCA).

It has been demonstrated by Furuhashi³ that bromination of cellulose with NBS and Ph₃P in DMAc/LiBr is completely regioselective at the C-6 position, resulting in 6-bromo-6-

deoxy-cellulose with quantitative conversion. Based upon Furuhashi bromination, we developed a simple, efficient route for synthesizing cationic polysaccharides by reaction of 6-bromo-6-deoxycellulose like 6-bromo-6-deoxy-2,3-di-*O*-acetyl-cellulose (6-BrCA) with pyridine or 1-methylimidazole at the C-6 position in DMSO, DMF or DMAc, resulting in 6-PyrCA and 6-MeIMCA, respectively, with high degrees of substitution. We have found that these permanently cationic polysaccharide derivatives dissolve readily in water, and exhibit surprisingly high thermal stability. Based upon surface plasmon resonance studies, these polysaccharide-based ionomers have been demonstrated to be capable of binding strongly and irreversibly with a hydrophilic and anionic surface, mainly by electrostatic interaction. Availability of these cationic cellulose derivatives will enable structure-property relationship studies, which can be used in biomedical areas such as complexation of poly(nucleic acids) for delivery to cell nuclei, anionic drug delivery, and tight junction opening for oral protein delivery. In addition, we further extended this chemistry, and successfully prepared a zwitterionic cellulose derivative: neutral 6-IMCA was synthesized by reacting 6-BrCA with imidazole, and was further functionalized by 1,3-propane sultone, affording a new zwitterionic cellulose derivative, 6-SPrIMCA.

7.2 Syntheses of water-soluble co-polyelectrolytes from commercial cellulose esters by selective modification

We prepared cellulose-based sustainable materials for advanced technologies, by applying Furuhashi bromination and subsequent aromatic amine displacements to cellulose acetate 320S (CA320S, DS(Ac) 1.78), which is a commercial cellulose ester with relatively low acetyl content, for generating renewable-based copolymers such as polyelectrolytes. We

brominated CA320S with Ph₃P and NBS in DMAc at 70 °C for 1 h, confirming by NMR spectroscopy and elemental analysis that the C-6 bromination is quantitative. We further demonstrated that displacement of these new C-6 bromides to result in uncharged products such as 6-azido-6-deoxycellulose and 6-imidazo-6-deoxycellulose is quantitative. The 6-bromo-6-deoxy copolymers are also useful precursors to cationic polyelectrolytes, and we have demonstrated that 6-bromo-6-deoxy CA320S (6-BrCA320S) was region- and chemo-selectively reacted with aromatic amines including pyridine and 1-methylimidazole by nucleophilic displacement, generating the corresponding cationic derivatives. These high DP polyelectrolytes exhibit very good solubility in water, despite the fact that they bear only ca. one positive charge for every two monosaccharides.

In addition, we demonstrated that bromination and aromatic amine displacement could be carried out in one pot rather than in two sequential reactions, in order to improve efficiency. CA320S was first reacted with NBS and Ph₃P in DMAc at 70 °C for 1 h, and then 1-methylimidazole was added to this solution with temperature increased to 80 °C for 48 h. Consequently, both ¹H and ¹³C NMR spectra indicate that the one-pot reaction was successful and exhibited conversion similar to that of the 2-pot sequence. Moreover, in order to eliminate all covalently-bonded bromide for some purposes, we created an efficient pathway to bromide-free polyelectrolytes prepared by methyl iodide quaternization with neutral 6-IMCA320S, synthesized by imidazole displacement reaction of 6-BrCA320S in quantitative conversion.

7.3 Syntheses of carboxyl-containing curdlan derivatives via regioselective ring-opening modifications

We developed a simple, practical route for synthesizing carboxyl-containing polysaccharide derivatives from curdlan esters via regioselective ring-opening reactions in the presence of Ph_3P . Curdlan was regioselectively and quantitatively brominated in DMAc/LiBr in the presence of NBS and Ph_3P , resulting in 6-bromo-6-deoxy-curdlan. The brominated intermediate was further modified with NaN_3 and acetic anhydride to displace the bromo groups at C-6 with azide groups for generating 6-azido-6-deoxy-2,4-di-*O*-acetyl-curdlan. Based on the previous studies for modifying polysaccharides via Staudinger reduction, 6-azido-6-deoxy curdlan acetate was reacted with cyclic anhydride including succinic anhydride and glutaric anhydride catalyzed by Ph_3P , and these ring-opening reactions lead to carboxyl-containing curdlan derivatives: 6- ω -carboxypropionamido-6-deoxy-2,4-di-*O*-acetyl-curdlan and 6- ω -carboxybutyramido-6-deoxy-2,4-di-*O*-acetyl-curdlan. More importantly, compared to other techniques for preparing carboxyl-containing polysaccharides, this synthetic route can guarantee essentially complete regio- and chemo-selectivity, and the resulting products possess amide linkages that are hydrolytically stable under all but forcing conditions, thereby ensuring retention of the pH-responsive ω -carboxyl group, for example under any imaginable physiological conditions or at the pH of latex coating dispersions (ca. pH 8-9). These new polysaccharide-based materials from abundant and inexpensive curdlan are promising for application areas including amorphous solid dispersion for oral drug delivery, coatings, or other aqueous dispersions.

7.4 Syntheses of iminated and aminated curdlan derivatives from a Staudinger ylide

We developed a new method for regioselective incorporation of a variety of monoalkylamino pendants at C-6 of curdlan, affording imino- and amino-curdlan derivatives. By reactions with aldehydes and/or sodium cyanoborohydride, a series of imino- and amino-curdlans was obtained with high chemoselectivity, and result in families of regioselectively aminated curdlan derivatives. We have demonstrated that the Staudinger ylide provides an access to a variety of aminated polymers including amines (primary, secondary, and tertiary amines), quaternary ammonio derivatives, and amides. A broad range of aminated/amidated polymers have a wide variety of potential uses in biomedical, pharmaceutical, and other areas, and the preparation method should be applicable to other polysaccharides with unencumbered C-6 OH groups.

7.5 Proposed future work

Novel polysaccharide-based polyelectrolytes with valuable properties as described above have potential for biomedical and pharmaceutical applications. However, some issues still have to be addressed, in order to widely use these polymers in biomedical areas.

Cationic *N*-heterocyclic cellulose derivatives are attractive candidates to interact with proteins for tight junction opening applications. Although we have prepared cellulose ammonium salts with high DS by pyridine or 1-methylimidazole displacement, still there were bromides present after reaction. Thiolated polymers have been demonstrated to improve mucoadhesive properties and permeation-enhancing properties for tight junction opening.^{4,5} Therefore, the substitution reactions of those cationic *N*-heterocyclic cellulose

derivatives with thiols can eliminate residual bromides and thereby further enhance paracellular transportation efficiency. In addition, we will further improve methods for synthesis of zwitterionic derivatives, in order to reach quantitative or near quantitative conversion and enhance potential utility for biomedical applications.

It will be also important to investigate other interesting properties of the cationic *N*-heterocyclic cellulose derivatives such as morphology and ion conductivity for specific applications. In order to use these cationic materials in biomedical and pharmaceutical areas, it is interesting to study the interactions between the cationic cellulose derivatives and biomolecules such as nucleic acids or certain anionic proteins. Cellular toxicity and antimicrobial activity should be studied.

Carboxyl-containing derivatives were produced by ring-opening reactions catalyzed by Ph_3P , but the residual arylphosphorus impurities including Ph_3P and $\text{Ph}_3\text{P}=\text{O}$ were extremely difficult to remove. It has been reported that trimethyl phosphine (PMe_3) can be employed as a reductant in carbohydrate chemistry for efficiently reducing the azide to amine in organic solvents like THF in the presence of NaOH, providing a clean product without phosphine-containing residual reagent and its oxide byproduct.^{6,7} It is worthwhile to attempt PMe_3 in the reduction of azide-functionalized polysaccharides, and optimize reaction conditions to improve conversion.

Finally, work in our group has proven that iminophosphorane-containing polysaccharide derivatives can be versatile intermediates for further modification. In addition to the

reductive amination reaction with aldehydes for synthesizing 6-imino- and 6-monoalkylamino curdlans, we will also be looking for other subsequent possibilities. It is worthwhile to attempt to react Staudinger ylide with some other carbonyl compounds such as ketones, amides, esters and thioesters,⁸ which may afford a wide range of acyclic and heterocyclic functionalities on polysaccharide backbone.

7.6 References

1. Scranton, A. B.; Rangarajan, B.; Klier, J. Biomedical applications of polyelectrolytes. *Adv. Polym. Sci.* **1995**, *122*, 1–54.
2. Samal, S. K.; Dash, M.; Van Vlierberghe, S.; Kaplan, D. L.; Chiellini, E.; van Blitterswijk, C.; Moroni, L.; Dubruel, P. Cationic polymers and their therapeutic potential. *Chem. Soc. Rev.* **2012**, *41*, 7147–7194.
3. Furuhata, K.; Koganei, K.; Chang, H. S.; Aoki, N.; Sakamoto, M. Dissolution of cellulose in lithium bromide-organic solvent systems and homogeneous bromination of cellulose with *N*-bromosuccinimide-triphenylphosphine in lithium bromide-*N,N*-dimethylacetamide. *Carbohydr. Res.* **1992**, *230*, 165–177.
4. Bhalekar, M. R.; Bargaje, R. V.; Upadhaya, P. G.; Madgulkar, A. R.; Kshirsagar, S. J. Formulation of mucoadhesive gastric retentive drug delivery using thiolated xyloglucan. *Carbohydr. Polym.* **2016**, *136*, 537–542.
5. Kast, C. E.; Bernkop-Schnürch, A. Thiolated polymers-thiomers: Development and in vitro evaluation of chitosan-thioglycolic acid conjugates. *Biomaterials* **2001**, *22*, 2345–2352.

6. Noti, C.; de Paz, J. L.; Polito, L.; Seeberger, P. H. Preparation and use of microarrays containing synthetic heparin oligosaccharides for the rapid analysis of heparin-protein interactions. *Chem. Eur. J.* **2006**, *12*, 8664–8686;
7. Zong, C.; Venot, A.; Dhamale, O.; Boons, G.-J. Fluorous supported modular synthesis of heparan sulfate oligosaccharides. *Org. Lett.* **2013**, *15*, 342–345.
8. Palacios, F.; Alonso, C.; Aparicio, D.; Rubiales, G.; de los Santos, J. M. The aza-Wittig reaction: An efficient tool for the construction of carbon–nitrogen double bonds. *Tetrahedron* **2007**, *63*, 523–575.